中華民國核醫學學會 2026 年會暨國際學術研討會

NMTSR 2026

Nuclear Medicine Theranostics
Advancing with Sustainability and Resilience

核醫療診合一，永續韌性前行

Nov. 07 SAT → 高雄榮總國際會議中心





主辦單位 / 中華民國核醫學學會 高雄榮民總醫院 亞東紀念醫院 國家原子能科技研究院

協辦單位 / 台灣神經內分泌腫瘤病友關懷協會 台灣血脂衛教協會 台灣甲狀腺醫護衛教暨健康促進協會

CONTENTS

目錄

歡迎詞 3

大會組織 4

議程　主會場：第一會議室 5

議程　第二會議室 6

議程　第三會議室 7

議程　第四會議室 8

午餐研討會 9

會場導覽　國際會議中心 1F 10

路線指引　第七、第八會議室 11

急診大樓 6F 平面圖 12

路線指引　住院醫師考試考場 13

大會接駁車 14

接駁車上下車地點 15

交通資訊 16

講者介紹 17

- 第一會議室 17
- 第二會議室 31
- 第三會議室 43
- 第四會議室 52

口頭論文摘要 54

壁報論文索引 74

壁報論文摘要 79

贊助廠商 223

WELCOME MESSAGE

歡迎詞



2026核醫年會主席　諶鴻遠主任

各位尊敬的來賓，包括來自世界各地的專家學者、同業人士和朋友們，大家好！

歡迎各位蒞臨在高雄舉辦的2026年台灣核醫學學會年會。鴻遠謹代表大會及籌備處熱烈歡迎各位參加我們的年度盛會。我們深感榮幸，感謝各位尊貴的賓客、專家演講嘉賓以及所有遠道而來的朋友們。距離上次在高雄舉辦年會已過十年，非常高興能再次在高雄舉辦這場盛會。2026年TSNM年會的主軸是「核醫療診合一：永續發展與韌性（NMTSR）」。會議議程涵蓋多個主題：精準腫瘤診療學進展、神經和心血管分子影像學新知、新型放射核種藥物研發、人工智慧革新核醫學等核醫診療整合的最新進展。

眾所周知，近年來核醫領域發展迅速。這些進展得益於標靶腫瘤研究、新型放射性配體（可用於測量神經退化性疾病和心血管疾病之變化）、人工智慧以及新一代影像儀器的進步。透過本次會議的共同討論，相信與會者必能收獲滿溢，在未來核醫工作能有幫助。在此我們特別感謝來自美國、歐洲和日本的幾位特邀嘉賓，他們將在大會分享新的創見，可以激發我們學識交流，並探討可能之創新方案。同時，我們也衷心感謝台灣主掌衛生福利的官員和立法委員蒞會致詞，以表達他們對核醫學發展和永續性的支持。最後，我們向所有來賓為本次會議帶來活力和熱情致以最誠摯的謝意。

Dear distinguished guests from everywhere including local and international experts and industries or friends and welcome to the Taiwanese Society of Nuclear Medicine (TSNM) 2026 conference at Kaohsiung. On behalf of the organizing team, it is our absolute pleasure to welcome you to our annual gathering. We are deeply honored by the presence of our distinguished guests, expert speakers, and all of you who traveled to be here today. It’s been 10 years since last time the conference being held at Kaohsiung and at this moment we are more than glad to host all of you here to this meeting. The main theme for 2026 TSNM conference is “Nuclear Medicine Theranostics, advancing with Sustainability and Resilience (NMTSR)”. The meeting program covers several topics: updates of nuclear medicine theranostics in precision oncology, neuro- and cardiovascular molecular imaging, novel radiopharmaceutical development, revolutionized nuclear medicine via AI, etc. As you know our nuclear medicine filed has greatly moved at breakneck speed during these days. It has been driven by advances in targeted oncology, novel radioligands allowing to measure neurodegenerative and cardiovascular disease, AI and also next generation detector. Through the collaborative discussions at this conference, we believe that all participants will gain valuable insights that will be helpful in their future work in nuclear medicine. We specially thank several invited speakers overseas from United States, Europe, and Japan to share with us new ideas, spark meaningful connections, and explore innovative solutions. Also we greatly appreciate that our Taiwanese healthcare officials and lawmakers presented to the meeting expressing their support for nuclear medicine advancing and sustainability. Finally, we’d like to show our profound gratitude to everyone bringing your energy and enthusiasm to this meeting.

Daniel Hueng-Yuan Shen, M.D., PhD.

TSNM 2026 Conference President

ORGANIZATION

大會組織

主辦單位	中華民國核醫學學會、高雄榮民總醫院、亞東紀念醫院、國家原子能科技研究院
協辦單位	台灣甲狀腺醫護衛教暨健保促進協會、台灣血脂衛教協會、台灣神經內分泌腫瘤病友關懷協會
理事長	**吳彥雯**
大會主席	**諶鴻遠**

指導委員

王安美	王秀珊	王美惠	何恭之	吳彥雯	李哲皓	林立凡	林宜瀞
林昆儒	洪光威	胡蓮欣	張文議	張宇捷	張晉銓	張婉柔	張雁翔
曹勤和	陳世欣	陳志成	陳宜伶	陳怡潔	陳惠萍	陳傳霖	陳義丰
曾能泉	曾敬仁	程紹智	黃文盛	黃玉儀	黃奕琿	黃莆蓉	黃潔宜
楊邦宏	路景竹	樊修秀	樊裕明	蔡世傳	鄭媚方	鄭雯文	蕭穎聰
諶鴻遠	龔瑞英						

論文評選組

總編輯	鄭媚方						
執行秘書	陳建榮						
口頭論文	吳駿一	柯紀綸	陳宏杰	黃蜂運	黃潔宜	葉信顯	詹勝傑
	劉豐源						
壁報論文	林立凡	王秀珊	邱創新	高嘉鴻	黃蜂運	汪姍瑩	陳昱宏
	王昱豐	蔡世傳	柯冠吟	陳惠萍	李佩瑛	倪于晴	吳駿一
	葉信顯	李昕迪	邱南津	曾敬仁	何恭之	陳世欣	曾能泉
	龔瑞英	李哲皓	林可瀚	胡蓮欣	張文議	楊邦宏	劉嘉儒
	鄭媚方	黃潔宜	劉建助	柯紀綸	陳怡潔	黃奕琿	詹勝傑
	蕭穎聰	陳傳霖	王安美	詹宏彬	陳宜伶	陳毓雯	陳宏杰

秘書處

秘書長	汪姍瑩
副秘書長	劉嘉儒、陳建榮、吳駿一
秘書	石采庭、蕭晴

大會工作團隊

王文婷	石采庭	吳京育	吳忠順	李岳	李姿瑩	林雯君	林琇屏
邱宇莉	俞長青	陳宥銘	陳幸鈴	張春梅	楊月桂	楊玉芳	楊宜純
蔡富任	蕭晴	簡慧敏	曾文正	蘇詩琪			

PROGRAM 議程

主會場：第一會議室

門診大樓 1 樓

時間	演講題目	講者	座長
08:20~09:00	會員報到		
09:00~09:15	**開幕致詞**	高雄榮民總醫院 國家原子能科技研究院 2026年會主席 中華民國核醫學學會	**陳以書 副院長** **高梓木 院長** **諶鴻遠 主任** **吳彥雯 理事長**
09:15~09:30	Current Status and Industry Perspective of Radiopharmaceuticals in Nuclear Medicine	**劉韋博 處長** 財團法人生物技術開發中心	諶鴻遠 年會主席 中華民國核醫學學會 樊裕明 副院長 耕莘醫院
09:30~10:00	Shaping the future of cancer treatment with radioligand therapy	**Prof. Ken Herrmann** University Hospital Essen, Germany	諶鴻遠 年會主席 中華民國核醫學學會 黃玉儀 副理事長 中華民國核醫學學會
10:00~10:30	PSMA PET use for management of prostate cancer and Theranostics	**Prof. Sean P. Collins** University of South Florida, USA	諶鴻遠 年會主席 中華民國核醫學學會 高潘福 教授 中山醫學大學附設醫院
10:30~10:45	BREAK		
10:45~11:15	Cardiac PET/SPECT explain angina	**Prof. Nils Johnson** University of Texas, Houston, USA	洪光威 副院長 彰濱秀傳紀念醫院 顏若芳 副教授 台大醫院
11:15~11:45	Classification of tau status with machine learning models	**方佑華 副教授** 阿拉巴馬大學伯明罕分校	吳彥雯 理事長 中華民國核醫學學會 鄭澄意 教授 三軍總醫院
11:45~12:15	PET Visualization of Canonical Pathologies in Neurodegenerative Dementias	**Prof. Makoto Higuchi** National Institutes for Quantum Science and Technology, Japan	蕭穎聰 教授 長庚大學 張瓊之 醫師 高雄長庚紀念醫院
12:15~12:30	會員大會		
12:30~13:30	LUNCH 午餐研討會地點見第 9 頁		
13:30~13:55	Targeted Alpha Therapy Using Cyclotron-Produced Astatine 211	**Prof. Tadashi Watabe** University of Osaka, Japan	諶鴻遠 年會主席 中華民國核醫學學會 陳傳霖 副理事長 中華民國核醫學學會
13:55~14:20	胃腸胰神經內分泌腫瘤診療指引之國際比較與台灣共識：從SSTR-PET/CT影像判讀到PRRT治療定位	**黃文冠 副教授** 林口長庚紀念醫院	陳彥仰 主任 高雄長庚紀念醫院 張晉銓 主任 高雄醫學大學附設中和紀念醫院
14:20~14:45	Efficacy and Safety of PRRT: a multicenter retrospectives study in Taiwan (TAILOR-NET)	**柯冠吟 主任** 台大醫院癌醫中心分院	蔡世傳 教授 台中榮民總醫院 鄭媚方 主任 台大醫院
14:45~15:00	BREAK		
15:00~15:25	Overcoming Diversity: Innovative Initiatives of Radio-Theranostics after the Fukushima Nuclear Disaster	**Prof. Shunichi Yamashita** Fukushima Medical University, Japan	吳彥雯 理事長 中華民國核醫學學會 諶鴻遠 年會主席 中華民國核醫學學會
15:25~15:50	Unraveling global theranostic clinical trials: Building Taiwan readiness and resilience 解構跨國核醫診療臨床試驗：推動台灣整備與韌性發展	**劉穎芯 技術專員** PSI CRO	黃玉儀 副理事長 中華民國核醫學學會 邱南津 主任 成大醫院
15:50~16:15	Dosimetry in Radioligand Therapy: Advances and Clinical Applications 放射配體治療（RLT）的劑量學：進展與臨床應用	**蔡惠予 教授** 國立清華大學	曾敬仁 主任 新北市立土城醫院 吳東信 教授 國立陽明交通大學
16:15~16:40	Redefining Alpha therapy in mCRPC: from Xofigo to PSMA-targeted next-generation therapies	**黃玉儀 副理事長** 中華民國核醫學學會	曾能泉 主任 童綜合醫院 路景竹 醫師 台大醫院
16:40~17:00	健保給付Cabozatinib 為2線放射碘無效甲狀腺癌之治療	**陳義丰 主任** 三軍總醫院	邱宇莉 醫師 高雄榮民總醫院 姚珊汎 主任 耕莘醫院

PROGRAM 議程

第二會議室

門診大樓 1 樓

時間	演講題目	講者	座長
08:20~09:00	會員報到		
10:20~10:45	Deep learning for diagnostic & prognostic SPECT MPI: from image segmentation to image classification	**Prof. Laurent RIOU** INSERM, France	吳彥雯 理事長 中華民國核醫學學會 陳遠光 主任 新光醫院
10:45~11:10	SMART on FHIR	**林昆儒 教授** 林口長庚紀念醫院	陳志成 教授 國立陽明交通大學 吳明哲 主任 台北馬偕紀念醫院
11:10~11:35	AI在核醫報告的應用	**韓紹禮 醫師** 高雄秀傳紀念醫院 **李碧芳 副教授** 彰化基督教醫院	高嘉鴻 主任 中國醫藥大學附設醫院 曹勤和 主任 台北馬偕紀念醫院
11:35~12:00	AI在核醫影像的應用	**胡蓮欣 主任** 台北榮民總醫院	何恭之 教授 林口長庚紀念醫院 李昕迪 主任 屏東榮民總醫院
12:30~13:30	LUNCH 午餐研討會地點見第 9 頁		
13:30~13:55	Cardiac Sympathetic Denervation and Atrial Fibrillation in Diabetic Patients Assessed by I-123 MIBG Imaging: The Modulatory Role of Cholesterol	**邱百誼 主任** 彰化秀傳紀念醫院	黃文盛 教授 彰濱秀傳紀念醫院 李碧芳 副教授 彰化基督教醫院
13:55~14:20	AI-Powered Automated Quantification of Cardia MIBG Scintigraphy with Phantom based HMR Standardization	**蕭穎聰 教授** 長庚大學	陳世欣 主任 林口長庚紀念醫院 翁瑞鴻 主任 中山醫學大學附設醫院
14:20~14:45	PET-enabled Amyloid-Targeting Therapy for Alzheimer’s Disease: Trials Overview and Case Sharing 正子賦能阿茲海默症類澱粉蛋白標靶治療：臨床試驗總覽及病例分享	**周美鵑 醫師** 高雄醫學大學附設中和紀念醫院	梁志光 副教授 高雄榮民總醫院 胡璟 醫師 高雄榮民總醫院
14:45~15:10	Evaluating Late-Onset Depression Using Nuclear Scintigraphy	**蔡佳芬 醫師** 振興醫院	葉信顯 副教授 國防醫學大學 韓登宇 主任 臺北市立聯合醫院中興院區
15:10~15:30	BREAK		
	Appropriate Use Criteria, Standardized Reporting, and Case Sharing		
15:30~16:00	Seeing Through the Plaque: What Every Nuclear Physician Needs to Know About Amyloid PET	**劉嘉儒 副秘書長** 中華民國核醫學學會	汪姍瑩 秘書長 中華民國核醫學學會 李哲皓 醫師 台北榮民總醫院
16:00~16:30	Appropriate Use Criteria, Standardized Reporting, and Case Sharing of SSTR PET	**李岳 醫師** 三軍總醫院	林立凡 主任 三軍總醫院 陳毓雯 主任 高雄醫學大學附設中和紀念醫院
16:30~17:00	PSMA PET (18F-flotufolastat)正子影像判讀與臨床經驗分享	**林宜瀞 主任** 台中榮民總醫院	張雁翔 主任 高雄長庚紀念醫院 柯冠吟 主任 台大醫院癌醫中心分院

PROGRAM 議程

第三會議室

門診大樓 1 樓

時間	演講題目	講者	座長
08:20~09:00	會員報到		
09:10~09:50	Precision Theranostics:Innovations and Radioiodinated Pharmaceuticals in Targeted Cancer Therapy	**田育彰 教授** 高雄醫學大學	王安美 技術主任 台北馬偕紀念醫院
09:50~10:30	大型語言模型於醫學檢驗之應用	**陳柏志 主任** 高雄醫學大學附設中和紀念醫院	王安美 技術主任 台北馬偕紀念醫院
10:30~10:50	BREAK		
10:50~11:30	Vibe Coding於教學及流程改善之實現	**陳柏志 主任** 高雄醫學大學附設中和紀念醫院	王安美 技術主任 台北馬偕紀念醫院
11:30~12:10	RIA的trouble shooting	**王安美 技術主任** 台北馬偕紀念醫院	陳宜伶 醫事放射師 高雄醫學大學附設中和紀念醫院
12:30~13:30	Lunch Symposium 午餐研討會地點見第 9 頁		
13:30~14:10	Auto QC for SPECT/CT and PET/CT at MD Anderson Cancer Center	**潘亭壽 教授** University of Texas, USA	洪光威 副院長 彰濱秀傳紀念醫院 黃莆蓉 醫事放射師 台中榮民總醫院
14:10~14:50	From Quantitative Imaging to Personalized Therapy: The Evolving Role of Nuclear Medicine 從影像量化到個人化治療：核醫角色的演進	**施宜伶 跨產品整合方案經理** GE Healthcare	俞長青 醫事放射師 高雄榮民總醫院 張嘉容 醫事放射師 台北榮民總醫院
14:50~15:10	BREAK		
15:10~16:00	Theranostics 團隊：角色分工、核心能力與跨團隊合作	**詹宏彬 醫師** 高雄榮民總醫院	楊邦宏 副理事長 中華民國核醫學學會 陳建榮 副秘書長 中華民國核醫學學會
16:00~16:20	論文寫作及研究分享：如何找題目	**杜高瑩 醫事放射師** 台北馬偕紀念醫院	黃奕琿 技術長 台大醫院 王秀珊 技術長 三軍總醫院
16:20~16:40	論文寫作及研究分享：投稿與寫作技巧	**龔瑞英 醫事放射師** 台中榮民總醫院	黃奕琿 技術長 台大醫院 王秀珊 技術長 三軍總醫院
16:40~17:00	論文寫作及研究分享：研究計畫準備工作	**陳惠萍 副主任** 台東基督教醫院	黃奕琿 技術長 台大醫院 王秀珊 技術長 三軍總醫院

PROGRAM 議程

第四會議室

門診大樓 1 樓

時間	演講題目	講者	座長
08:20~09:00	會員報到		
10:30~10:50	BREAK		
10:50~11:30	口頭論文-臨床組	OC-1、OC-2、OC-3、OC-4	劉豐源 醫師 林口長庚紀念醫院 黃潔宜 醫師 臺大醫院
11:30~12:10	口頭論文-基礎組	OB-1、OB-2、OB-3、OB-4、OB-5	吳駿一 教授 國立陽明交通大學 葉信顯 副教授 國防醫學大學
12:30~13:30	Lunch Symposium 午餐研討會地點見第 9 頁		
13:30~14:10	口頭論文-臨床組	OC-5、OC-6、OC-7、OC-8、OC-9	陳宏杰 醫師 高雄長庚紀念醫院 詹勝傑 醫師 花蓮慈濟醫院
14:10~14:50	口頭論文-基礎組	OB-6、OB-7、OB-8、OB-9	黃蜂運 副教授 中臺科技大學 柯紀綸 醫師 台大醫院
14:50~15:10	BREAK		
15:10~15:30	PSMA and SSTR-Targeted Theranostics: A Practical Perspective and Experience	**Dr. Dheeratama Siripongsatian** Chulabhorn Hospital, Thailand	黃文盛 教授 彰濱秀傳紀念醫院 莊佩儒 醫師 台大醫院
15:30~15:50	Building Sustainable PSMA Theranostic Radiopharmaceuticals in Thailand: Eight Years from Tc-99m SPECT to Ac-225 Alpha Therapy	**Dr. Shuichi Shiratori** Faculty of Medicine Siriraj Hospital, Mahidol University	黃文盛 教授 彰濱秀傳紀念醫院 莊佩儒 醫師 台大醫院
16:00~17:00	第11屆第5次理監事會議		

LUNCH SYMPOSIUM

午餐研討會

2026.11.07（六）12:30 – 13:30　四場同時進行，請依報名場次前往

1F 第三會議室 高雄榮總國際會議中心 1F

諾華 午餐會議

12:30–13:30

From PSMAfore to Clinical Practice: Optimizing Patient Selection and Treatment Experience with ^{177}Lu-PSMA in mCRPC

SPEAKER	MODERATOR
曾敬仁 主任 土城長庚	**林宜瀞 主任** 台中榮總

1F 第四會議室 高雄榮總國際會議中心 1F

艾拉倫 午餐會議

12:30–13:30

From Red Flags to Nuclear Diagnosis: Clinical Experience and Integrated Diagnostic Approach in ATTR-CM

SPEAKER	MODERATOR
吳彥雯 理事長 核醫學會	**樊裕明 副院長** 耕莘醫院

6F 第七會議室 急診大樓 6F

輝瑞 午餐會議

12:30–13:30

Beyond Positive and Negative: Practical Challenges and Future Directions of PYP Imaging in ATTR-CM

SPEAKER	MODERATOR
紀雅閔 醫師 高醫附醫	**胡蓮欣 主任** 台北榮總

6F 第八會議室 急診大樓 6F

普瑞默 午餐會議

12:30–13:30

RLT Landscape of US and Europe and Experience Sharing of KCGMH

SPEAKER	MODERATOR
Dr. Jean-Luc 張雁翔 主任 高雄長庚	**諶鴻遠 主任** 高雄榮總

怎麼走

1F **第三、第四會議室**（國際會議中心 1 樓）
與主會場同層，位於第一會議室後方（見第 10 頁會場導覽）。

6F **第七、第八會議室**（急診大樓 6 樓）
由主會場 Eposter 旁搭 25／26 號電梯至 2F，經走廊往急診大樓，再搭 37／38 號電梯至 6F（逐步照片見第 11 頁路線指引）。

VENUE　會場資訊

會場導覽

高雄榮總 國際會議中心 1F｜2026.11.07（六）

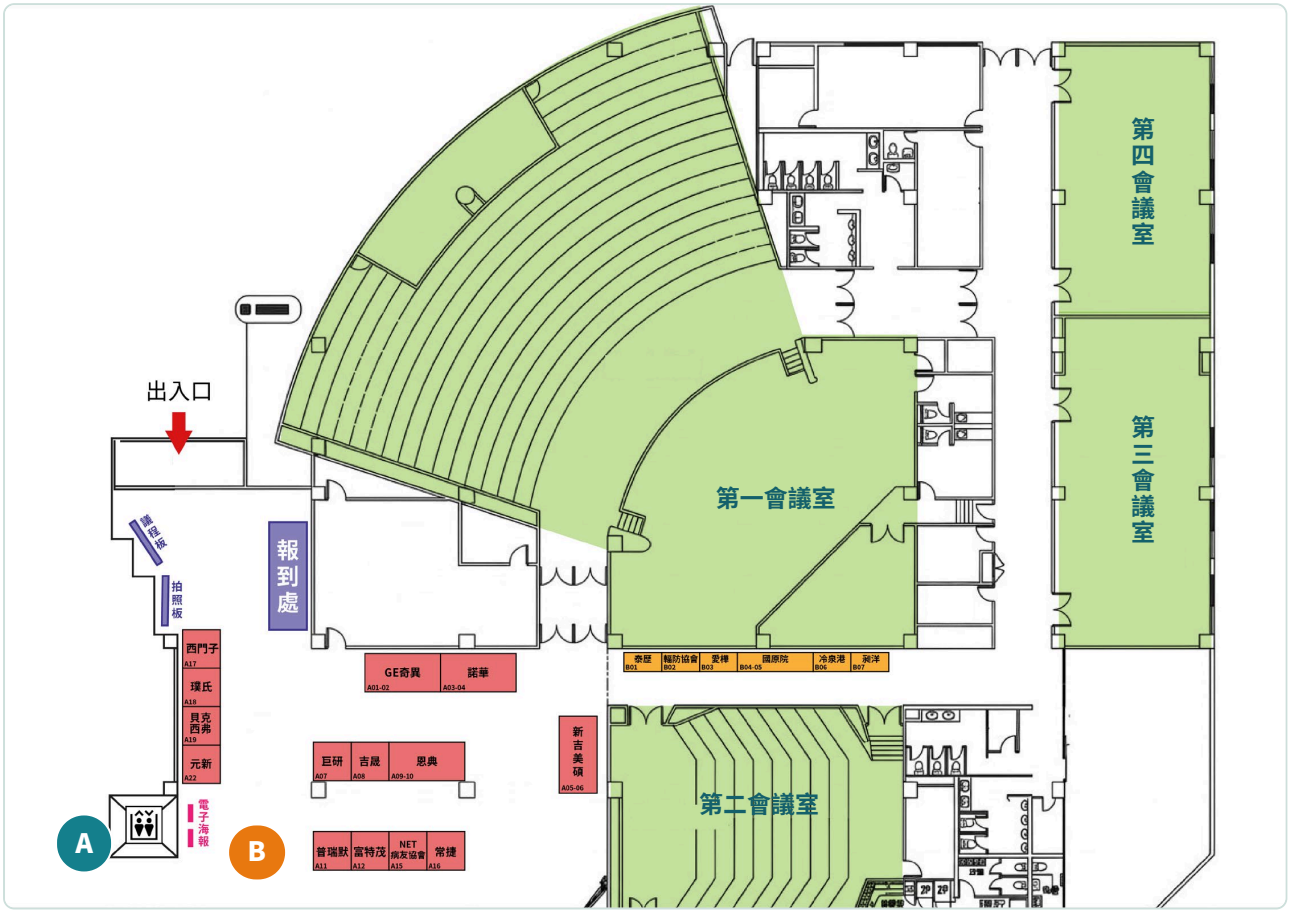

B ↓　往美食廣場・核醫科

目的地索引

	地點	位置／出發點	路線
	報到處	1F 大門入口進來即是	本頁
	第一～第四會議室	1F 國際會議中心	本頁
A	第七、第八會議室（午餐研討會）	急診大樓 6F｜由 A 搭 25／26 號電梯	第 11–12 頁
B	美食廣場	由 B 往前直走（與往核醫科同方向）	第 13 頁
B	核醫科會議室（住院醫師考試考場）	由 B（A11／A22 中間通道）出發	第 13 頁

ROUTE　路線指引

第七、第八會議室 路線指引

午餐研討會｜急診大樓 6F｜由 1F 主會場出發

1F 25／26 號電梯 ▶ 2F 往急診大樓 ▶ 37／38 號電梯 ▶ 6F 第七、第八會議室



1F

主會場 Eposter 旁，搭 25／26 號電梯至 2F



2F

出電梯後右轉（→），直行到底



2F

沿走廊直行（右側為耳鼻喉科）



2F

走到底右轉（→），往急診大樓方向



2F

第一個岔路左轉（←），勿往高齡醫學大樓



2F

看到電梯標誌後右轉（→）



2F

搭 37／38 號電梯至 6F



6F

出電梯左轉（←），即抵第七、第八會議室

沿途設有指示立牌，請依箭頭前往。回程：搭 37／38 號電梯至 2F，循原路返回 1F 主會場。

VENUE　會場資訊

急診大樓 6F　第七、第八會議室

午餐研討會 12:30–13:30

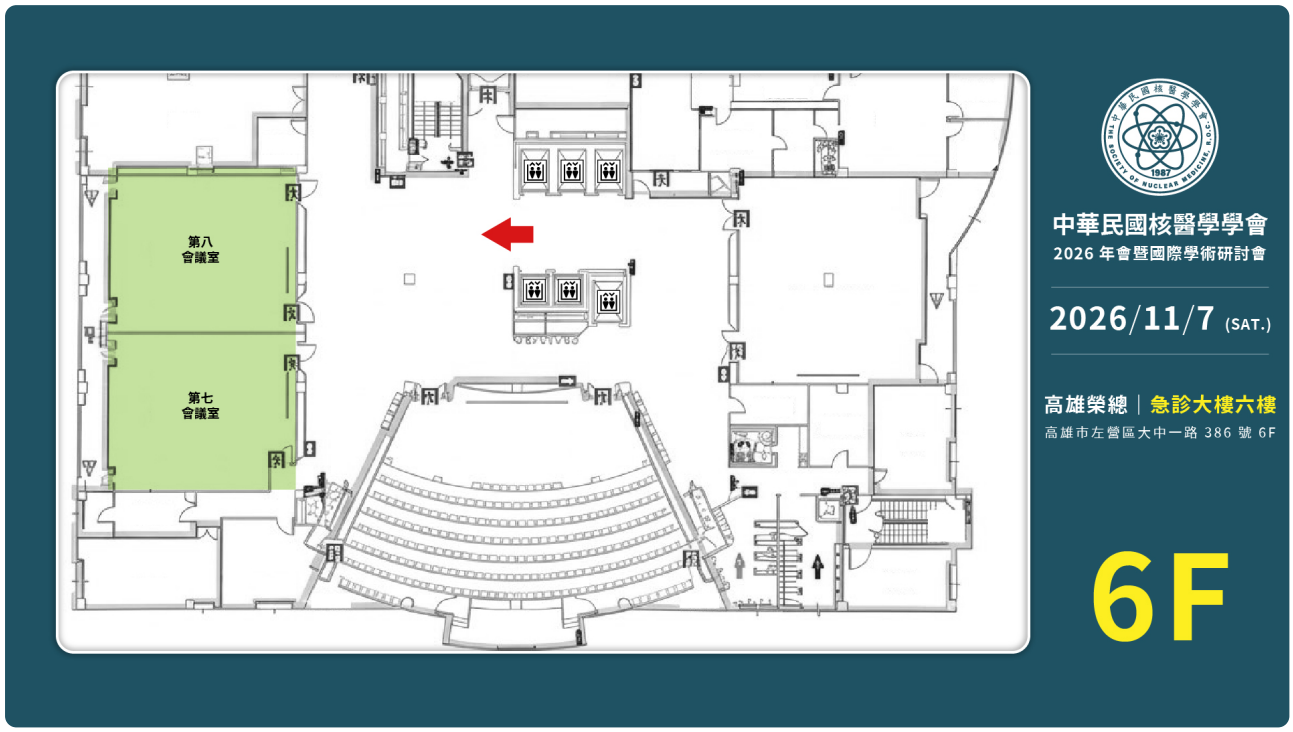

搭 37／38 號電梯到 6F，出電梯後左轉（←），即抵第七、第八會議室。

從主會場怎麼來：見第 11 頁路線指引。

回程：搭 37／38 號電梯至 2F，循原路回到 1F 主會場。

ROUTE　路線指引

第一年住院醫師考試 考場路線

考試時間 14:00–15:00｜考場：高雄榮總 核醫科會議室

A11／A22 通道出發 ▶ 直走到底 70–80 M ▶ 左轉直行約 50 M ▶ 核醫科（右側）



B ↓　由此出發往核醫科

出發　**從 1F 會場 A11 與 A22 攤位中間的通道（地圖左下 B 處）出發，往前直走。**

美食廣場也是同一方向：由此通道往前直走。



1　直走到底，約 70–80 M



2　走到底左轉（←），直行約 50 M（左側為大象山）



3　經過星巴克（右側），繼續往前，核醫科在右方



4　抵達核醫科大門，考場為核醫科會議室

沿途設有指示立牌，請依箭頭前往；請預留步行時間，提早抵達考場。回程：原路返回，走到底右轉（→）後直行到底，即回到 1F 主會場。

SHUTTLE BUS　交通資訊

大會接駁車

高鐵左營站／城市商旅真愛館 ↔ 高雄榮總

時刻表　Shuttle Bus Schedule｜2026.11.07（六）

	發車時間	上車地點	下車地點
上午	08:10	城市商旅真愛館	高雄榮總
	09:20	高鐵左營站	高雄榮總
	10:00	高鐵左營站	高雄榮總
	10:40	高鐵左營站	高雄榮總
	11:20	高鐵左營站	高雄榮總
	11:30–12:30　司機午餐休息，暫停發車		
下午	13:00	高雄榮總	高鐵左營站
	13:40	高雄榮總	高鐵左營站
	14:00	高鐵左營站	高雄榮總
	14:30	高雄榮總	高鐵左營站
	15:00	高雄榮總	高鐵左營站
	15:40	高雄榮總	高鐵左營站
	16:30	高雄榮總	城市商旅真愛館
	17:10	高雄榮總	城市商旅真愛館
	17:30–18:30　司機晚餐休息，暫停發車		
晚上	19:30	城市商旅真愛館	高鐵左營站
	20:40	城市商旅真愛館	高鐵左營站

每班車依表定時間發車，座位有限，額滿後恕無法搭乘，敬請改搭下一班次。

SHUTTLE BUS　交通資訊

接駁車上下車地點

班次時間見第 14 頁時刻表



高鐵左營站　上車處

新光三越高雄左營店（彩虹市集）門口

搭高鐵抵達左營站後，往 **2 號出口**（新光三越高雄左營店方向）出站，即達上車處。
台鐵新左營站旅客：先到台鐵大廳，再往高鐵大廳 2 號出口出站。

去程 09:20、10:00、10:40、11:20、14:00 發車



高雄榮總　上／下車處

門診大樓門口

去程在門診大樓門口下車；回程請至門診大樓門口候車。

回程 13:00、13:40、14:30、15:00、15:40、16:30、17:10 發車



城市商旅真愛館　上／下車處

飯店門口

於飯店大門口上下車。

08:10、19:30、20:40 由飯店發車；16:30、17:10 回程抵達飯店

每班車依表定時間發車，座位有限，額滿後恕無法搭乘，敬請改搭下一班次。

ACCESS 交通資訊

交通資訊

高雄榮民總醫院

高鐵	高鐵左營站出口(高鐵路)(1)下車地點為榮總路榮總側門站：3路、紅35路、紅50至本院(2)下車地點為民族路新莊高中站：90民族幹線(3)下車地點為大中路榮總站：8025、E11路
台鐵	高雄火車站 前站出口(建國路)，搭 28線、72A線、72B線 (下車地點：大中路榮總站) 新左營火車站出口(高鐵路)(1)下車地點為榮總路榮總側門站：3路、紅35路、紅50至本院(2)下車地點為民族路新莊高中站：90民族幹線(3)下車地點為大中路榮總站：8025、E11路
捷運	捷運凹子底站 轉乘24B、紅35路至本院(下車地點：榮總路 榮總側門站) 捷運生態園區站 轉乘紅35路、紅50路至本院(下車地點：榮總路榮總側門站)
開車	國道1號（中山高）鼎金系統交流道 左營（右側）下 大中路（右轉）→ 本院 醫療大樓 鼎金系統交流道 左營(右側) 下 大中路 → (右轉) 榮總路 → 本院門/急診大樓 國道3號（南二高）→ 接 東西向10號快速道路 往西(高雄方向)鼎金系統交流道 左營（右側）下 大中路（右轉）→ 本院 醫療大樓 鼎金系統交流道 左營(右側) 下 大中路 → (右轉) 榮總路 → 本院門/急診大樓
公車 大中路 榮總站	高雄客運24A線：圓照寺－捷運巨蛋站；高雄客運24B線：楠梓－鹽埕；南台灣客運28線：加昌站－火車站；台灣愛巴士72A線：金獅湖站－中正高工；台灣愛巴士72B線：金獅湖站－中正高工(延駛正勤社區)；高雄客運E11線(鳳山高鐵城市快線)：鳳山－台鐵新左營站；高雄客運旗美國道10號(旗美國道快捷)：美濃站－高鐵左營站；8021 鳳山－彌陀；8025 高雄－六龜；8028 美濃－高雄；8032 高雄－甲仙；就醫公車 H12：桃源－榮總－高醫 (週二、四行駛，國定假日、例假日停駛)；就醫公車 H21：那瑪夏－榮總－高醫 (週一、三、五行駛，國定假日、例假日停駛)
公車 榮總路 榮總側門站	台灣愛巴士紅35路：金獅湖站－高雄捷運凹子底站；港都客運38：左營南站－榮總；港都客運39線：左營南站－榮總；南台灣客運紅50路：捷運生態園區站－捷運左營站；南台灣客運紅3路：高鐵左營站－榮總－凹子底公園
公車 民族路 新莊高中站	南台灣客運90民族幹線：高鐵左營站－捷運三多商圈站；8023 高雄－旗山；8040 岡山－高雄；8041B 鳳山－岡山；8041C 鳳山－-茄萣；高南雙城快線(8046) 高雄火車站－台一線－台南火車站 (8046A沒有經過榮總民族路 新莊高中站)；8049鳳山－崗山頭
無障礙	復康巴士（伊甸社會福利基金會）預約專線：(07) 360-1160 (伊甸社會福利基金會)；臨時叫車專線：(07) 360-1165傳真：(07) 360-1175（限無法電話聯絡者使用）。



講者介紹

09:15–09:30　第一會議室

Current Status and Industry Perspective of Radiopharmaceuticals in Nuclear Medicine

座長　諶鴻遠 年會主席（中華民國核醫學學會）、樊裕明 副院長（耕莘醫院）

摘要

The radiopharmaceutical landscape has evolved from conventional diagnostic imaging into a targeted oncological therapeutic pillar, driven largely by the clinical validation of theranostics and radioligand therapies (RLTs). The global market, valued at approximately $8B USD, is experiencing structural shifts across funding, manufacturing, and supply networks. However, the biggest hurdle for radiopharmaceuticals is the physics and logistics. The industry is facing acute scaling pain because its assets are radioactive and decay rapidly. The future of nuclear medicine rests on transforming this fragile "just-in-time" model into an industrialized, scalable supply chain that can deliver precision radiotherapy to any patient, anywhere in the world.

講者



劉韋博
Weber Liu

處長
財團法人生物技術開發中心產業發展處

現職	財團法人生物技術開發中心　處長
學歷	國立台灣大學　分子醫學研究所（2007） 國立台灣大學　EMBA 財務金融所（2015）
經歷	世福細胞醫學科技(股)公司　副總 瑪旺幹細胞醫學生物科技(股)公司　執行長 財團法人生物技術開發中心　副研究員 三軍總醫院　臨床醫檢師
專長	生醫產業科技管理、細胞治療營運管理、品質系統與臨床試驗
特殊成就	八仙塵爆期間與日本 JTEC 公司完成首例台日國際細胞治療合作，救治重度傷燙傷病患

講者介紹

09:30–10:00 第一會議室

Shaping the future of cancer treatment with radioligand therapy

座長 諶鴻遠 年會主席（中華民國核醫學學會）、黃玉儀 副理事長（中華民國核醫學學會）

摘要

Radioligand therapy (RLT) is emerging as a transformative approach in precision oncology, delivering targeted radiation directly to cancer cells while minimizing damage to healthy tissues. By combining molecular imaging and therapy, RLT enables personalized treatment based on tumor-specific targets, offering a true theranostic strategy. Clinical success in neuroendocrine tumors and prostate cancer has demonstrated the potential of RLT to improve patient outcomes and expand therapeutic options. Ongoing research is focused on earlier use of RLT, novel molecular targets, innovative radionuclides, and combination approaches with existing cancer therapies. As evidence continues to grow, multidisciplinary collaboration will be essential to integrate RLT into routine clinical practice. This presentation will review recent advances in radioligand therapy, discuss emerging clinical data, and explore future opportunities to reshape cancer care through precision-targeted treatment

講者



Ken Herrmann

MD

University Hospital Essen, Germany

現職 Professor of Nuclear Medicine / Director, Department of Nuclear Medicine, University Hospital Essen

學歷 Doctorate in Medicine (Dr. med.), Humboldt University of Berlin, Germany (2007)
Habilitation, Technical University of Munich, Germany (2010)
Executive MBA, University of Zürich, Switzerland (2011)

經歷 Director, Department of Nuclear Medicine, University Hospital Essen, Germany (since 2016)
Associate Professor and Director of Translational Research, UCLA, USA (2015–2021)
Section Editor, The Journal of Nuclear Medicine
From January 2027: Editor-in-Chief, The Journal of Nuclear Medicine

講者介紹

10:00–10:30 第一會議室

PSMA PET use for management of prostate cancer and Theranostics

座長 諶鴻遠 年會主席（中華民國核醫學學會）、高潘福 教授（中山醫學大學附設醫院）

摘要

PSMA PET imaging and theranostics have transform prostate cancer management by combining high-precision diagnostic scanning with targeted radiation therapy and radionuclide therapy. PSMA PET/CT improves detection of prostate cancer compared to conventional CT, MRI, or bone scans. PSMA PET/CT tracers like Flotufolastat-F18 (Posluma) identify dominant intraprostatic lesions, small-volume nodal recurrences and bone metastases even at low PSA levels. Currently available PSMA-PET tracers vary in their availability, modes of clearance and patterns of non-specific uptake. Results guide salvage radiotherapy or metastasis-directed therapy such as stereotactic body radiotherapy (SBRT) with minimal side effects. Positive findings allow for targeted radioligand therapy—such as Lutetium-177 (^{177}Lu-PSMA)—delivering localized radiation directly to cancer sites while sparing healthy tissue. Clinical trial data highlight high response rates in metastatic prostate cancer with improvement in clinically meaningful endpoints. Whether PSMA PET imaging can replace conventionally imaging in defining early surrogate endpoints for overall survival is under clinical investigation. This session is intended to guide clinicians on the potential utilization of PSMA-PET imaging in the rapidly changing management of prostate cancer.

講者



Sean P. Collins

MD, PhD

University of South Florida, USA

現職	Professor, Radiation Oncology, University of South Florida
學歷	Doctor of Medicine and Doctor of Philosophy in Biochemistry, University of Michigan, Ann Arbor, MI Residency: Radiation Oncology, Georgetown University Hospital, Washington DC
經歷	Professor Vice Chair of Faculty Affairs, Tampa General Hospital, Dept. of Radiation Oncology, University of South Florida, 2024-present Professor Director of Cyberknife Prostate Program, Medstar Georgetown University Hospital, Washington, DC, 2022-2024

講者介紹

10:45–11:15 第一會議室

Cardiac PET/SPECT explain angina

座長 洪光威 副院長（彰濱秀傳紀念醫院）、顏若芳 副教授（台大醫院）

摘要

Patients with angina provide a common clinical presentation due to a variety of distinct mechanisms. Distinguishing the different physiology abnormalities behind this symptom allows personalized therapy. Myocardial perfusion imaging using positron emission tomography (PET) or single photon emission computed tomography (SPECT) provides a foundational tool to achieve this goal. An insightful framework separates perfusion results into four categories, classified by transmural flow capacity and subendocardial perfusion (flow to the innermost layer of the heart muscle). Although each axis is a continuum, considering these two metrics as abnormal yields a 2x2 classification: (1) intact flow with reduced subendocardial perfusion, (2) reduced flow with intact subendocardial perfusion, (3) intact flow and subendocardial perfusion, and (4) reduced flow with reduced subendocardial perfusion. However, the relative frequency of each category is not equal. A classic perfusion defect reduces flow across all layers of the myocardium and yields the strongest association with clinical signs and symptoms of ischemia during vasodilator stress (moderate or severe angina with significant ST-segment changes). The next most common pattern produces intact transmural flow but with subendocardial hypoperfusion. Indeed, it accounts for the vast majority of ischemic responses. Isolated microvascular disease – a uniform reduction in perfusion without subendocardial imbalance – actually cases few patients to experience angina and ECG changes. Intriguingly, some patients with normal flow capacity and intact subendocardial perfusion also experience angina and ST-segment depression during vasodilator stress, a scenario that cannot be explained by ischemia. Cardiac PET/SPECT provides a unique roadmap for guiding diagnosis and therefore treatment.

講者



Nils Johnson

M.D.

University of Texas, Houston, USA

現職	Professor of Medicine, Department of Cardiology, University of Texas
學歷	2004 – Doctor of Medicine (M.D.), Columbia University, New York 2009 – Master of Science (M.S.), Northwestern University, Chicago
經歷	2010 to now – Cardiologist, University of Texas, Houston 2004 to 2010 – Internal medicine, cardiology, interventional cardiology, Northwestern University, Chicago

講者介紹

11:15–11:45　第一會議室

Classification of tau status with machine learning models

座長　吳彥雯 理事長（中華民國核醫學學會）、鄭澄意 教授（三軍總醫院）

摘要

隨著阿茲海默症精準醫療的發展，精確評估大腦內病理蛋白的累積狀態已成為臨床與研究的重要關鍵。本次演講將聚焦於「利用機器學習模型預測 Tau 蛋白狀態」。在 Amyloid beta 呈現陽性的阿茲海默症患者中，精確掌握 Tau 蛋白的病理變化，對於病情評估、個人化治療、藥物發展與預後追蹤至關重要。本研究運用機器學習演算法，整合分子造影與臨床相關特徵，建構出能有效分類 Tau 狀態的預測模型。這項方法不僅能提升診斷效率，也為阿茲海默症的早期病理剖析提供了一條可行的技術途徑。

講者



方佑華

副教授

阿拉巴馬大學伯明罕分校

現職	阿拉巴馬大學伯明罕分校　副教授
學歷	Case Western Reserve University　Biomedical Engineering（2009） 國立陽明大學　醫學工程所（2002） 國立交通大學　資訊科學系（2000）
經歷	國立成功大學醫學工程系　副教授 長庚大學電機系　助理教授 長庚醫院分子影像中心　助理研究員
專長	分子影像、影像定量分析、影像處理、人工智慧

講者介紹

11:45–12:15 第一會議室

PET Visualization of Canonical Pathologies in Neurodegenerative Dementias

座長 蕭穎聰 教授（長庚大學）、張瓊之 醫師（高雄長庚紀念醫院）

摘要

Neurodegenerative dementias are characterized by the accumulation of disease-associated protein aggregates in the brain. Alzheimer’ s disease (AD), dementia with Lewy bodies (DLB), and frontotemporal lobar degeneration (FTLD) are among the major causes of dementia, with amyloid-β (Aβ), tau, and α-synuclein constituting key pathological substrates. Positron emission tomography (PET) enables these molecular pathologies to be visualized and quantified in the living brain, providing a powerful translational bridge from basic research to clinical diagnosis and therapeutic development.

Following the development of Aβ PET, we have focused on PET imaging of tau pathology. We developed radioligands capable of detecting tau aggregates in experimental models and subsequently demonstrated their ability to visualize tau lesions in patients with AD and diverse non-AD tauopathies. These technologies are now being translated toward clinical applications, including global clinical development of tau PET as a diagnostic tool and its use as a pharmacodynamic biomarker for evaluating anti-tau therapies.

We have further extended this strategy to α-synuclein, a major pathological protein in DLB, Parkinson’ s disease, and related disorders. Through academia–industry collaboration, PET tracers have been developed that enable in vivo visualization of α-synuclein aggregates in patients. Such imaging may provide direct information on the distribution and progression of α-synuclein pathology and facilitate the development and evaluation of disease-modifying therapies targeting this protein.

Although PET provides highly specific spatial and quantitative information, its cost and throughput limit its widespread use. We are therefore using molecular PET as a reference standard for the development and validation of scalable blood biomarkers. Integration of PET and fluid biomarkers may ultimately enable a staged diagnostic framework, ranging from population-level screening to precise molecular characterization, and accelerate the realization of pathology-based diagnosis, prevention, and treatment of neurodegenerative dementias.

講者



Makoto Higuchi

MD, PhD

National Institutes for Quantum Science and Technology, Japan

現職	Director, Advanced Neuroimaging Center, Institute for Quantum Medical Science, National Institutes for Quantum Science and Technology
學歷	1993: Tohoku University School of Medicine, Sendai, Japan (M. D.) 1997: Tohoku University Graduate School of Medicine, Sendai, Japan (Ph. D. degree)
經歷	2024–Present: Director, Advanced Neuroimaging Center, Institute for Quantum Medical Science, QST 2023–Present: Professor (cross-appointed), Osaka Metropolitan University Graduate School of Medicine, Osaka, Japan 2019–2024: Department Head, Department of Functional Brain Imaging, NIRS/QST, Chiba, Japan 1999–2003: Postdoctoral Researcher, Center for Neurodegenerative Disease Research, University of Pennsylvania School of Medicine, USA

講者介紹

13:30–13:55　第一會議室

Targeted Alpha Therapy Using Cyclotron-Produced Astatine 211

座長　諶鴻遠 年會主席（中華民國核醫學學會）、陳傳霖 副理事長（中華民國核醫學學會）

摘要

Astatine-211 (^{211}At) is an alpha-particle-emitting radionuclide that can be produced using a cyclotron and has a relatively short half-life of 7.2 h, making it attractive for targeted alpha therapy. Alpha particles have a high linear energy transfer and a short tissue range, enabling potent and localized cytotoxic effects with limited irradiation of surrounding normal tissues. In addition, ^{211}At-based therapy may offer practical advantages over conventional beta-emitting radionuclide therapy, including the potential to avoid inpatient isolation in dedicated radiation-protected rooms.

We evaluated the safety and preliminary efficacy of [^{211}At]NaAt in patients with differentiated thyroid cancer refractory to conventional [^{131}I]NaI therapy (Watabe T, et al. J Nucl Med. 2025). A single intravenous administration of [^{211}At]NaAt was generally well tolerated, and some patients showed more than a 50% reduction in serum thyroglobulin levels, accompanied by decreased uptake on subsequent [^{131}I] imaging, suggesting meaningful biological and therapeutic activity.

We are also conducting a clinical trial of [^{211}At]PSMA-5 in patients with metastatic castration-resistant prostate cancer, with promising early safety and antitumor activity. Beyond these disease-specific approaches, we are developing ^{211}At-labeled agents targeting pan-tumor molecules, including LAT1, FAP, and EphA2. Together, these studies support cyclotron-produced ^{211}At as a versatile next-generation platform for targeted alpha therapy and theranostics across a broad spectrum of malignancies.

講者



Tadashi Watabe

MD, PhD／Professor

University of Osaka, Japan

現職　Associate Professor, Laboratory for Theranostics, Division of Clinical Translation, Institute for Radiation Sciences, the University of Osaka

學歷　2004 M.D. Faculty of Medicine, Osaka University
2013 Ph.D. Osaka University Graduate School of Medicine

經歷　2024.4- Associate Professor/Lecturer, Radiology, Osaka University Graduate School of Medicine
2017.5- Assistant Professor, Nuclear Medicine and Tracer Kinetics, Osaka University Graduate School of Medicine
2009-2013 Physician, Nuclear Medicine, Osaka University Hospital

講者介紹

13:55–14:20　第一會議室

胃腸胰神經內分泌腫瘤診療指引之國際比較與台灣共識：從SSTR-PET/CT影像判讀到PRRT治療定位

座長　陳彥仰 主任（高雄長庚紀念醫院）、張晉銓 主任（高雄醫學大學附設中和紀念醫院）

摘要

胃腸胰神經內分泌腫瘤（gastroenteropancreatic neuroendocrine tumor, GEP-NET）異質性高，NANETS、ENETS／ESMO、JNETS、CACA 與 NCCN 指引近年密集改版，共識與歧異並存。本課程以跨指引比較為主軸：病理端一致採世界衛生組織（WHO）分級，嚴格區分分化良好的 NET G3 與神經內分泌癌（neuroendocrine carcinoma, NEC）；影像端一致認定體抑素受體正子造影（somatostatin receptor PET/CT, SSTR-PET/CT）優於傳統 Octreoscan，並視分化程度加做去氧葡萄糖正子造影（FDG-PET/CT）作雙示蹤劑評估；歧異則見於血清標記定位、內視鏡切除門檻與肝轉移減積手術之腫瘤負荷門檻。治療聚焦核醫實務：NETTER-2 試驗已使鎦-177 標記 DOTATATE 之胜肽受體放射性核種治療（peptide receptor radionuclide therapy, PRRT）自二線前移為受體陽性、高增殖個案的第一線選項，並討論其與體抑素類似物及 CAPTEM 之排序。最後介紹台灣神經內分泌腫瘤學會（TNETS）共識七大主題之制定流程與投票機制，說明核醫在跨科團隊決策中的角色。

講者



黃文冠

副教授

林口長庚紀念醫院

現職	林口長庚紀念醫院內科部血液腫瘤科／長庚大學醫學院　主治醫師／副教授
學歷	瑞典 Karolinska Institutet　腫瘤病理學系（2020）
經歷	林口長庚紀念醫院醫學研究部　醫師科學家 長庚大學醫學院　助理教授 林口長庚紀念醫院內科部　住院醫師、血液腫瘤科研修醫師
專長	消化道癌症（胰臟癌、膽道癌、胃癌、大腸直腸癌）之全身性治療 神經內分泌腫瘤（neuroendocrine tumor, NET）之診斷、分期與治療決策 泌尿道腫瘤（攝護腺癌、膀胱癌、腎細胞癌）之全身性治療 轉譯研究：癌症代謝、腫瘤免疫微環境、DNA 損傷修復
特殊成就	台灣神經內分泌腫瘤學會（TNETS）「胃腸胰神經內分泌腫瘤診療共識」編輯委員（2025–2026） 發表學術論文 88 篇（其中 84 篇刊載於 JCR 收錄期刊）

講者介紹

14:20–14:45　第一會議室

Efficacy and Safety of PRRT: a multicenter retrospectives study in Taiwan (TAILOR-NET)

座長　蔡世傳 教授（台中榮民總醫院）、鄭媚方 主任（台大醫院）

摘要

Peptide receptor radionuclide therapy (PRRT) with ^{177}Lu-DOTATATE has emerged as an effective treatment for patients with unresectable or metastatic somatostatin receptor-positive neuroendocrine tumors (NETs). However, real-world data from Asian populations remain limited. This multicenter retrospective study aimed to evaluate the efficacy and safety of PRRT in Taiwanese patients with NETs.

講者

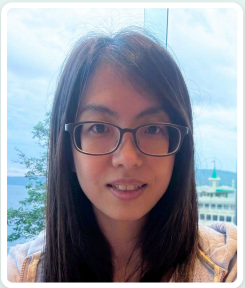

柯冠吟

主任

台大醫院癌醫中心分院

現職	台大癌醫分院核子醫學部　主任/主治醫師
學歷	台灣大學　醫學院臨床醫學研究所（2024）
經歷	臺大醫院核子醫學部　主治醫師 台大雲林分院核子醫學部　主治醫師
專長	核子醫學

講者介紹

15:00–15:25 第一會議室

Overcoming Diversity: Innovative Initiatives of Radio-Theranostics after the Fukushima Nuclear Disaster

座長 吳彥雯 理事長（中華民國核醫學學會）、諶鴻遠 年會主席（中華民國核醫學學會）

摘要

Fifteen years have passed since the accident at the Tokyo Electric Power Company (TEPCO) Fukushima Daiichi Nuclear Power Plant, which occurred in the wake of the Great East Japan Earthquake on March 11, 2011. During this time, those affected have endured hardship and inconvenience while living with anxiety and fear regarding radioactivity and radiation exposure. Since the accident, tremendous efforts have been made to promote understanding of radiation risks both domestically and internationally. Various initiatives—including accident response countermeasures such as plant decommissioning, treated water management, and interim and long-term storage of contaminated soils, as well as support for those affected and efforts to accelerate reconstruction—have been implemented as various national projects.

This presentation will introduce the actual situation of Fukushima after the accident and a new challenge of the global improvement of radiation emergency medicine with radiological protection at the standpoint of “Radiation and Health”. One of the reconstruction projects is the Fukushima Institute for Research, Education and Innovation (F-REI), which was newly established in April 2023 in Namie Town, Fukushima Prefecture. In particular, through the promotion of various projects aimed at the clinical implementation of “Radio-Theranostics”—a pioneering approach to drug discovery and medical treatment using radioisotopes—breakthroughs in Nuclear Medicine Diagnostics and Therapy in Japan are highly anticipated.

講者



Shunichi Yamashita

MD, PhD

Fukushima Medical University, Japan

現職	Vice President, Fukushima Medical University
學歷	Graduated from Nagasaki University School of Medicine in March 1978
經歷	Vice President, Fukushima Medical University (2011-now) Deputy Director, Field 4 Radiation Science and RI Drug Discovery, Fukushima Institute for Research, Education and Innovation (F-REI) (cross appointment 2023-now) Professor, Atomic Bomb Disease Institute, Nagasaki University (1990-2018) Radiation Scientist P5, dispatched to the WHO Headquarter in Geneva (2005-2006) Former President of the Japan Thyroid Association(2010-2014)

講者介紹

15:25–15:50　第一會議室

Unraveling global theranostic clinical trials: Building Taiwan readiness and resilience

解構跨國核醫診療臨床試驗：推動台灣整備與韌性發展

座長　黃玉儀 副理事長（中華民國核醫學學會）、邱南津 主任（成大醫院）

摘要

Driven by a rapidly expanding global pipeline, theranostic radiopharmaceuticals are transforming precision oncology. This presentation maps the global trial landscape and charts the patient journey from enrollment to treatment. To assess Taiwan's trial readiness, the presentation evaluates the site infrastructure, investigational product management, and key bottlenecks. Integrating clinical and industry perspectives, it offers actionable insights to overcome operational hurdles, while mapping strategic pathways to establish Taiwan as a resilient and competitive hub for theranostic clinical trials.

隨著全球研發項目快速擴增，診療合一放射性藥物正在改變精準癌症治療。本課程將介紹全球臨床試驗版圖，並解析病患從收案到治療的歷程。為評估台灣的臨床試驗整備度，內容將檢視試驗機構設施、試驗用藥管理與關鍵瓶頸。結合臨床與產業視角，本課程提出克服營運挑戰的建議，並建立長期韌性的策略，協助台灣成為具備韌性與競爭力的國際診療合一臨床試驗樞紐。

講者



劉穎芯

Cherry Lau

技術專員 Site Technology Specialist

PSI CRO

現職	PSI CRO (台灣璞氏健康發展有限公司)　Site Technology Specialist (技術專員)
學歷	香港理工大學　放射系
經歷	BC Cancer Vancouver; BC Cancer Research Centre　Clinical Trial Study Coordinator; Research Technologist Hong Kong Baptist Hospital – Nuclear Medicine and PET Centre　Radiographer Hong Kong Polytechnic University　Research Assistant
專長	Theranostics clinical trials; clinical and translational radiopharmaceuticals drug development, PET/CT examinations and reporting

講者介紹

15:50–16:15　第一會議室

Dosimetry in Radioligand Therapy: Advances and Clinical Applications
放射配體治療（RLT）的劑量學：進展與臨床應用

座長　曾敬仁 主任（新北市立土城醫院）、吳東信 教授（國立陽明交通大學）

摘要

放射配體治療（radioligand therapy, RLT）中，相同給藥活度下的腫瘤與正常器官吸收劑量，可能因放射性藥物的攝取、滯留、清除及組織質量不同而產生顯著差異。劑量學透過估算吸收劑量，為探討治療反應與毒性提供量化依據，並支持個人化治療策略的研究。

本演講以核醫科醫師的臨床需求為出發點，聚焦於 ^{177}Lu-PSMA 與 ^{177}Lu-DOTATATE，概述 RLT 劑量學的基本原理、近期進展及臨床應用。內容涵蓋給藥活度與吸收劑量的區別，以及由治療後定量 SPECT/CT、時間積分活度至吸收劑量估算的基本流程；並介紹簡化取像策略，說明其動力學假設、適用條件與估算不確定度。

臨床部分將回顧腫瘤吸收劑量與治療反應的相關研究，以及劑量導引治療的試驗進展，區分劑量—反應關聯與依劑量調整治療能否改善臨床結果的證據。同時討論腎臟、唾液腺與骨髓的劑量評估及其限制，說明不同藥物的劑量—效應關係與器官耐受劑量，須依其證據分別判讀，並結合器官功能、疾病負荷及既往治療進行整體評估。最後，將簡介本團隊正在進行的治療後影像與臨床資料整合工作，作為跨專業合作的實務例子。期望協助核醫科醫師掌握 RLT 劑量學的基本概念、現階段可支持的臨床判斷，以及仍待驗證的個人化治療用途。

講者

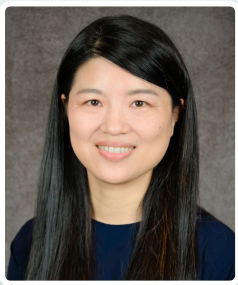

蔡惠予
教授
國立清華大學

現職	國立清華大學核子工程與科學研究所　教授
學歷	國立清華大學　原子科學系博士班
經歷	長庚大學醫學影像暨放射科學系　副教授 中山醫學大學醫學影像暨放射科學系　助理教授
專長	醫學物理、醫學輻射防護、保健物理、醫療曝露品質保證
特殊成就	榮獲原子能科技學術合作研究計畫「優良計劃」數次；榮獲第 12 屆原子能安全績優獎個人獎

講者介紹

16:15–16:40　第一會議室

Redefining Alpha therapy in mCRPC: from Xofigo to PSMA-targeted next-generation therapies

座長　曾能泉 主任（童綜合醫院）、路景竹 醫師（台大醫院）

摘要

Alpha 粒子具有高線性能量轉移與短射程特性，可在有限範圍內造成高密度 DNA 損傷。Ra-223 首先被證實 alpha 核種治療可改善骨轉移型 mCRPC 病人的存活，開啟臨床 alpha targeted radionuclide therapy(TRT)) 時代。隨 PSMA 標靶技術發展， Ac-225-PSMA 等標靶 alpha 核種治療將治療焦點由骨微環境進一步移至腫瘤細胞，並展現於 Lu-177-PSMA 治療後疾病中的潛力。然而，alpha 核種藥物開發仍面臨核種供應、放射化學、daughter recoil、劑量學、正常器官毒性、製造與法規等挑戰。未來發展重點除更強的 alpha 核種外，更需整合核種、配體、藥物動力學、影像、劑量學及治療時序，為 mCRPC 的 alpha 核種治療開創更有力的未來。

講者

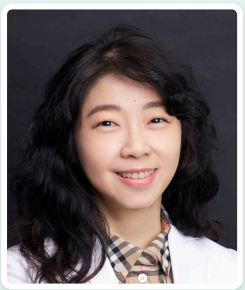

黃玉儀

副理事長

中華民國核醫學學會

現職　和信治癌醫院中心　主治醫師/主任
國立陽明交通大學　醫學系兼任講師

學歷　國立陽明交通大學　醫學系
國立政治大學　EMBA

經歷　Washington university, Mallinckrodt institute of radiology　visiting fellow

專長　核醫腫瘤學、核醫同位素腫瘤治療

講者介紹

16:40–17:00　第一會議室

健保給付Cabozatinib 為2線放射碘無效甲狀腺癌之治療

座長　邱宇莉 醫師（高雄榮民總醫院）、姚珊汎 主任（耕莘醫院）

摘要

針對放射性碘無效分化型甲狀腺癌（radioiodine-refractory differentiated thyroid cancer, RAIR-DTC），放射碘已無法有效治療病灶，導致患者預後較差，近年多重標靶治療的發展已大幅改變其治療策略。Cabozantinib 作為一種多重酪胺酸激酶抑制劑，已被證實可為接受過 VEGFR 標靶治療後仍發生疾病進展的患者帶來臨床效益。本次將討論 Cabozantinib 的作用機轉、適應症與臨床定位，並回顧重要臨床研究成果。此外，分享實際臨床個案，說明 Cabozantinib 對於 RAIR-DTC 患者的治療實務應用。

講者

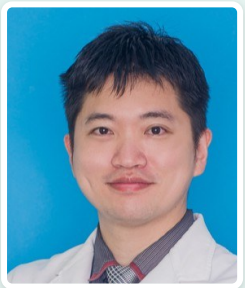

陳義丰

主任

三軍總醫院

現職	三軍總醫院核子醫學部(國防醫學院核子醫學科)　製藥科主任(講師)
學歷	國防醫學院　醫學系
專長	核子醫學、正子影像學、甲狀腺疾病放射碘治療、攝護腺癌同位素治療

講者介紹

10:20–10:45 第二會議室

Deep learning for diagnostic & prognostic SPECT MPI: from image segmentation to image classification

座長 吳彥雯 理事長（中華民國核醫學學會）、陳遠光 主任（新光醫院）

摘要

Cardiovascular diseases are the leading cause of death worldwide. Myocardial ischemia caused by coronary artery disease (CAD) and/or coronary microvascular dysfunction (CMVD) is the primary cause of cardiovascular mortality. Nuclear myocardial perfusion imaging using single-photon emission computed tomography (SPECT-MPI) is a non-invasive imaging modality that was initially validated against coronary angiography for the diagnosis of CAD. However, the underuse of SPECT-MPI for the diagnosis and management of chronic CAD is widely acknowledged. In addition, the major role of CMVD in cardiovascular mortality, regardless of the presence of CAD, is now well recognized, yet its non-invasive detection is not currently available in routine clinical practice. Overall, the presentation will provide an overview of currently developed artificial intelligence (AI) approaches aimed at automating and improving SPECT-MPI analysis for the management of chronic CAD and the detection of CMVD using SPECT-MPI. Special emphasis will be made on image segmentation and model robustness & generalizability issues as well as on the potential of dynamic SPECT-MPI acquisitions.

講者



Laurent RIOU

Research scientist, PhD

INSERM, France

現職	Inserm Researcher (CR Inserm), INSERM, U1039, Radiopharmaceutiques Biocliniques
學歷	2006: Accreditation to conduct Researches (HDR) 1999: PhD in Medical Sciences, Université Joseph Fourier, Grenoble, France
經歷	01/2003- Present : Inserm Researcher (CR Inserm) Post-doctoral experience, 09/1999 – 12/2002: Experimental Nuclear Cardiology Laboratory, University of Virginia, USA

講者介紹

10:45–11:10　第二會議室

SMART on FHIR

座長　陳志成 教授（國立陽明交通大學）、吳明哲 主任（台北馬偕紀念醫院）

摘要

SMART on FHIR 是建構於 HL7 FHIR 與 OAuth 2.0 之上的應用整合框架，讓 App 在 EHR／PACS 內帶著病人情境、以最小授權存取臨床資料。本演講以核醫需求為主軸：說明核醫工作流（開單、給藥、造影、定量、報告）如何對應 FHIR Resource 與 TW Core IG；解析 SMART App Launch 流程與 Scopes 安全機制；以阿茲海默症類澱粉蛋白 PET 治療決策系統（AID-AD）為例，分享核醫 AI 軟體從演算法驗證、流程整合到法規的開發經驗；並介紹林口長庚獲選衛福部「臺灣 50」之核醫放射藥物用藥治理系統，提出核醫科導入三步驟與常見陷阱。

講者



林昆儒

教授

林口長庚紀念醫院

現職	林口長庚紀念醫院核子醫學部　教授
學歷	長庚大學　臨床醫學研究所（2004）
經歷	基隆長庚紀念醫院核子醫學科　主任 台北長庚紀念醫院核子醫學科　主任
專長	分子影像，臨床研究，轉譯研究，醫學資訊，電腦程式開發，資訊安全
特殊成就	SMART on FHIR 作品獲選衛福部「Taiwan 50」

講者介紹

11:10–11:35　第二會議室

AI在核醫報告的應用

座長　高嘉鴻 主任（中國醫藥大學附設醫院）、曹勤和 主任（台北馬偕紀念醫院）

摘要

人工智慧在醫療領域的價值，不僅在於大型模型的效能，更在於能否解決真實臨床流程中的具體問題。本次演講將分享高雄秀傳紀念醫院從臨床痛點出發，運用生成式人工智慧與 Codex 協作開發醫療工具的實務經驗。其核心方法是由臨床醫師直接定義問題、判斷標準與安全邊界，再藉由人工智慧協助完成需求規格、程式原型、測試及反覆修正，縮短臨床構想與可操作系統之間的距離。

案例包括兒童髖關節發育不良及先天性肌性斜頸的跨平台結構化超音波報告工具；可進行六關節縱向追蹤、活動性與損傷分離及資料品質提示的 HEAD-US 系統；利用本機語意與模糊比對，從病歷片語提供候選診斷碼的改良式 ICD-10 工具；透過胸前視角影像辨識肩部理學檢查，經醫師確認後產生病歷文字的 POV_PE；以及運用雙鏡頭、聲音與流變特徵，協助分析 IDDSI 食物質地測試的多模態系統。

上述案例顯示，不同臨床應用其實可以共用「資料擷取、結構化、分析、品質閘控、人工覆核與系統輸出」的基本架構。人工智慧不應取代臨床判斷，而應協助量化、提示與整理資訊；當輸入品質不足時，系統必須停止輸出，而非產生看似完整但不可靠的答案。高雄秀傳的經驗說明，醫療 AI 導入可以從小型、高頻、可驗證的工作流程開始，先建立可操作原型，再逐步進行臨床驗證、資訊安全、系統介接與跨單位擴散。

講者



韓紹禮

醫師

高雄秀傳紀念醫院

共同主講：李碧芳 副教授

現職	高雄秀傳紀念醫院　主治醫師 樹人醫專　助理教授
學歷	國立中央大學　機械工程學系（2022）
經歷	彰化基督教醫院　主治醫師 國泰綜合醫院　主治醫師 汐止國泰綜合醫院　主治醫師
專長	復健醫學、老年醫學、醫療機器人
特殊成就	2024 年國家新創獎：倒尿機器人 2025 年 HTC 智慧眼鏡徵案大賽 Top 16

講者介紹

11:10–11:35　第二會議室

AI在核醫報告的應用

座長　高嘉鴻 主任（中國醫藥大學附設醫院）、曹勤和 主任（台北馬偕紀念醫院）

摘要

I. F-18 FDG PET/CT Lymphoma Structured Reporting Tool

Integrates Lugano staging, Deauville 5-point scoring, and Richter transformation red-flag clinical alerts (encompassing symptoms, organomegaly, lab abnormalities). Generates precise plain-text reports that eliminate software compatibility hurdles and optimize decision-making efficiency for molecular imaging.

II. Soft Tissue Tumor Ultrasound Structured Reporting Tool

Utilizes an 8-step guided workflow to automatically detect red-flag features (e.g., tumor size > 5 cm, deep location, aggressive margins, chaotic vascularity). Combines 50 automated diagnostic completions with 7 evidence-based management templates to enhance patient safety and report standardization.

III. Pediatric Torticollis Ultrasound Structured Reporting Tool

Divided into six evaluation modules covering onset, perinatal risk factors, family history, head tilt direction, and sternocleidomastoid (SCM) mass. Evaluates physical exam findings and screens for non-muscular red flags prior to specialized ultrasound. Automatically measures bilateral SCM thickness, evaluates qualitative characteristics, calculates thickness ratios, and generates editable reports.

IV. Developmental Dysplasia of the Hip (DDH) Ultrasound Structured Reporting Tool

Features a 6-module framework incorporating clinical indications, breech delivery risks, and associated torticollis. Evaluates Graf standard coronal view adequacy independently for left and right hips. If a view is inadequate, the system automatically locks alpha/beta angle inputs to prevent invalid measurements. Once validated, it calculates Graf classifications and dynamic stability to produce structured reports.

V. Local-First Hybrid Clinical Decision Support System for Outpatient ICD-10 Coding

Combines local Natural Language Processing (NLP) retrieval with cloud-based Large Language Model (LLM, such as ChatGPT) fallback mechanisms via a lightweight desktop interface running alongside the HIS. Normalizes and fuzzy-matches inputs locally, switching to the cloud LLM only when confidence falls below predefined thresholds. This architecture reduces cloud dependency and latency while boosting outpatient coding speed and accuracy.

講者



李碧芳

副教授

彰化基督教醫院

共同主講：韓紹禮 醫師

現職	彰化基督教醫院　講座主治醫師
學歷	高雄醫學大學　醫學研究所（2000）
經歷	財團法人醫藥品查驗中心　醫師審查員 A2 Healthcare Taiwan, A2TW　M.D. Medical Monitor 國立成功大學影像醫學科　Adjunct Associated Professor
專長	Nuclear Medicine、Medical Functional Image of Nuclear Medicine、Positron Emission Tomography (PET)、Radioimmunoassay (RIA)、Clinical trial、Research Ethics
特殊成就	2020: National Cheng Kung University and Hospital, Artificial Intelligence (AI) Smart health Proposal Challenge, Excellent work Award

講者介紹

11:35–12:00　第二會議室

AI在核醫影像的應用

座長　何恭之 教授（林口長庚紀念醫院）、李昕迪 主任（屏東榮民總醫院）

摘要

人工智慧（AI）正快速改變醫療與核醫學的樣貌。本演講將從基礎出發，介紹 AI 的基本概念與常用術語，並說明 AI 模型如何從資料收集、標註、訓練到驗證逐步建構而成。接著探討 AI 在核醫工作流程與影像上的潛在應用。最後將討論在這波 AI 浪潮中，核醫醫師應扮演的角色，以及如何善用 AI，同時維持專業判斷與病人安全。

講者



胡蓮欣

主任

台北榮民總醫院

現職	臺北榮民總醫院 核醫部　主治醫師 正子影像科科主任
學歷	慈濟大學　醫學系（2006）
經歷	美國洛杉磯西達賽奈醫學中心　博士後研究員 臺北榮民總醫院 核醫部　總住院醫師
專長	核醫影像診斷（正子/電腦斷層造影）、核醫心臟學（心肌灌注造影、心臟專用造影儀）、放射配體治療

講者介紹

13:30–13:55　第二會議室

Cardiac Sympathetic Denervation and Atrial Fibrillation in Diabetic Patients Assessed by I-123 MIBG Imaging: The Modulatory Role of Cholesterol

座長　黃文盛 教授（彰濱秀傳紀念醫院）、李碧芳 副教授（彰化基督教醫院）

摘要

Clinical trials on lipid-lowering medications have demonstrated a reduction in cardiovascular events, they have also suggested an increased risk of developing diabetes, particularly when cholesterol levels are aggressively reduced. Current guidelines tend to favor a “lower is better” approach to low-density lipoprotein cholesterol (LDL-C) control. However, systematic reviews indicate that for every 1 mmol/L increase in LDL-C, the risk of AF decreases by approximately 5%, suggesting potential risks associated with overly intensive cholesterol-lowering strategies that warrant further investigation.I-123 metaiodobenzylguanidine (MIBG) is a radiotracer used for imaging cardiac postganglionic sympathetic innervation. Reduced MIBG uptake has been used to detect sympathetic dysfunction in conditions such as heart failure and diabetes, making it a suitable tool for investigating whether AF in diabetic patients is associated with cardiac sympathetic nerve damage. This study first conducted a retrospective cross-sectional and longitudinal analysis using the Show Chwan Healthcare System database to examine the prevalence and incidence of diabetes, AF, and cholesterol levels. Preliminary findings suggest that lower cholesterol levels (both total cholesterol and LDL-C) are associated with a higher prevalence of AF, particularly among individuals taking lipid-lowering drugs. Furthermore, a prospective study was conducted involving 52 participants (21 diabetic patients without AF, 16 with both diabetes and AF, and 15 healthy controls) to compare plasma cholesterol levels, nerve conduction studies, and I-123 MIBG imaging. Results indicated that lower cholesterol levels (including TC and LDL-C) were significantly associated with a higher proportion of abnormal heart-to-mediastinum (H/M) ratios, reflecting impaired cardiac sympathetic innervation.

講者

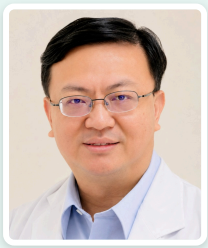

邱百誼

主任

彰化秀傳紀念醫院

現職	彰化秀傳紀念醫院/神經內科　主任
學歷	中山醫學大學　醫學研究所
經歷	中國醫藥大學附設醫院神經部　主治醫師 林新醫院神經內科　主治醫師 中華民國失智者照顧協會　理事長
專長	神經科學、脂質學

講者介紹

13:55–14:20　第二會議室

AI-Powered Automated Quantification of Cardia MIBG Scintigraphy with Phantom based HMR Standardization

座長　陳世欣 主任（林口長庚紀念醫院）、翁瑞鴻 主任（中山醫學大學附設醫院）

摘要

Cardiac ^{123}I-MIBG scintigraphy provides quantitative assessment of cardiac sympathetic innervation, but conventional heart-to-mediastinum ratio (HMR) measurement may be affected by operator variability and differences among imaging systems and collimators. We developed an AI-powered automated quantification approach using deep-learning-based segmentation to identify cardiac and mediastinal regions and calculate HMR with minimal user interaction. Phantom-based calibration was further incorporated to standardize HMR across different gamma-camera systems. By combining automated image analysis with physical system harmonization, this framework aims to improve reproducibility, reduce observer dependence, and facilitate more consistent clinical interpretation of cardiac MIBG scintigraphy across institutions and imaging platforms.

講者



蕭穎聰

教授

長庚大學

現職	長庚大學 醫學影像暨放射科學系　教授
學歷	紐約州立大學石溪分校 (SUNY Stony Brook)　電機系（2000）
經歷	長庚大學 人工智慧學士學位學程　合聘教授 長庚大學 醫學影像暨放射科學系　副教授 長庚大學 醫學影像暨放射科學系　助理教授
專長	醫學影像處理，腦神經影像處理與定量分析，正子影像診斷生物標誌之開發，人工智慧於醫學影像診斷之應用

講者介紹

14:20–14:45　第二會議室

PET-enabled Amyloid-Targeting Therapy for Alzheimer’ s Disease: Trials Overview and Case Sharing
正子賦能阿茲海默症類澱粉蛋白標靶治療：臨床試驗總覽及病例分享

座長　梁志光 副教授（高雄榮民總醫院）、胡瑨 醫師（高雄榮民總醫院）

摘要

The advent of anti-amyloid-beta monoclonal antibodies and positron emission tomography imaging marks a paradigm shift in Alzheimer's disease care from symptomatic management to disease-modifying interventions. This lecture will provide an overview of clinical trial evidence and real-world case sharing.

講者



周美鵑

醫師

高雄醫學大學附設中和紀念醫院

現職	尊德診所　主治醫師
學歷	高雄醫學大學　醫學系神經學科（2009） 高雄醫學大學　醫學系（1999）
經歷	高雄醫學大學附設中和紀念醫院神經部　主治醫師 高雄市立大同醫院神經科　主治醫師
專長	失智症及認知功能障礙、睡眠疾患、睡眠呼吸中止症

講者介紹

14:45–15:10　第二會議室

Evaluating Late-Onset Depression Using Nuclear Scintigraphy

座長　葉信顯 副教授（國防醫學大學）、韓登宇 主任（臺北市立聯合醫院中興院區）

摘要

晚發型憂鬱症（Late-Onset Depression, LOD）具有高度臨床異質性，部分患者可能伴隨潛在神經退化或腦血管病理。核子醫學影像提供由腦灌流、葡萄糖代謝至分子病理層次的 in vivo 評估工具。本演講將聚焦核子醫學影像在晚發型憂鬱症的臨床與研究應用，探討不同影像表現如何協助鑑別原發性憂鬱症與阿茲海默症、路易氏體失智症及其他神經退化疾病。同時回顧區域性灌流與代謝變化、病理蛋白沉積及多巴胺系統異常，作為預測治療反應、認知退化與疾病轉歸之影像生物標記的現有證據。期望從核子醫學觀點，探討功能性與分子影像在晚發型憂鬱症精準診斷、治療分層與預後評估中的角色與未來發展。

講者



蔡佳芬

醫師

振興醫院

現職	振興醫院　主治醫師
學歷	陽明交通大學　腦科所（2017）
經歷	台灣臨床失智症學會　理事 台灣老年精神醫學會　理事
專長	精神醫學，失智症
特殊成就	台北市醫師公會杏林獎

講者介紹

15:30–16:00 第二會議室

Seeing Through the Plaque: What Every Nuclear Physician Needs to Know About Amyloid PET

座長 汪姍瑩 秘書長（中華民國核醫學學會）、李哲皓 醫師（台北榮民總醫院）

摘要

With the arrival of disease-modifying therapies for Alzheimer’ s disease, amyloid PET has evolved from a diagnostic adjunct to a critical clinical gatekeeper. This continuing education session provides a comprehensive, practical roadmap for nuclear medicine physicians navigating this shifting landscape. We will review systematic visual interpretation criteria, address subtle borderlines and common diagnostic pitfalls, and explore the emerging role of semi-quantitative Centiloid scaling in therapy selection and monitoring. Attendees will gain actionable insights into optimizing reporting consistency and delivering high-impact clinical value in everyday neuroimaging practice.

講者



劉嘉儒

副秘書長

中華民國核醫學學會

現職	國立台灣大學醫學院附設醫院　主治醫師
學歷	國立台灣大學　醫學系
經歷	國立台灣大學醫學院附設醫院雲林分院　主任
專長	核子醫學、神經影像
特殊成就	2025 院內教學優異獎

講者介紹

16:00–16:30　第二會議室

Appropriate Use Criteria, Standardized Reporting, and Case Sharing of SSTR PET

座長　林立凡 主任（三軍總醫院）、陳毓雯 主任（高雄醫學大學附設中和紀念醫院）

摘要

體抑素受體正子電腦斷層掃描（SSTR PET）已成為神經內分泌腫瘤（NET）精準診斷與分期的核心影像工具。本次演講將著重於以下臨床實務面向：

1.適當使用準則：回顧國際最新指引，探討 SSTR PET 於初期診斷分期、復發評估及胜肽受體放射性核種治療（PRRT）篩選的最佳時機與效益。

2.標準化判讀與報告架構：介紹結構化報告原則與客觀評分系統，以提升跨專科團隊之溝通效率與診斷一致性。

3.臨床案例分享：透過典型病灶、潛在陷阱（pitfalls）及罕見案例，深入剖析影像特徵如何直接導引臨床治療決策。

期盼藉由指引規範與實務案例的整合，為核醫與臨床夥伴提供具實用價值的判讀與應用參考。

講者



李岳

醫師

三軍總醫院

現職	三軍總醫院核子醫學部　主治醫師
學歷	國防醫學大學　醫學系（2015）
經歷	三軍總醫院核子醫學部　總住院醫師
專長	核子醫學影像判讀、放射性核種治療、輻射災害防治、精準醫學、航空醫學、一般醫學教育、醫學人文教育
特殊成就	2025 年三軍總醫院 PBL 課程優良教師、2022 年三軍總醫院臨床研究論文獎 參與國內指引專書編撰　2024《Lu-177 標靶放射核種治療臨床核醫學與輻射安全建議》 2021《Radium-223 骨轉移標靶治療與輻射安全衛教建議》

講者介紹

16:30–17:00　第二會議室

PSMA PET (18F-flotufolastat)正子影像判讀與臨床經驗分享

座長　張雁翔 主任（高雄長庚紀念醫院）、柯冠吟 主任（台大醫院癌醫中心分院）

摘要

提供 Posluma (^{18}F-flotufolastat) 正子影像關於臨床使用時機，使用經驗，儀器配置，影像判讀與報告輸出等細節，比對科內使用 PET/CT 與 PET/MR 不同儀器間之間的差異，並提供影像案例進行討論。

講者



林宜瀞
Yi-Ching Lin
主任
台中榮民總醫院

現職	臺中榮民總醫院　主任醫師
學歷	中國醫藥大學　中醫學系雙主修
專長	核醫分子影像，核醫同位素治療
特殊成就	中華民國核醫學會歷任理監事

講者介紹

09:10–09:50　第三會議室

Precision Theranostics:Innovations and Radioiodinated Pharmaceuticals in Targeted Cancer Therapy

座長　王安美 技術主任（台北馬偕紀念醫院）

摘要

本報告聚焦於放射性同位素標定技術及其於臨床診療之應用。研究運用 Iodogen 塗層法、氯胺 T 法及同位素交換法，將放射性碘高效率標定於 anti-GPC3 單株抗體、阿拉伯半乳聚醣、脂碘油及 IMPY 等化合物，其中 Iodogen 法具約 85%–96.5%之高標記率及良好體外穩定性。在標靶放射免疫治療方面，放射性碘標記 anti-GPC3 抗體結合透明質酸奈米微胞，可針對 GPC3 過度表現之肝癌細胞，藉由輻射誘發 DNA 損傷並抑制修復機制，達到精準治療效果。此外，放射性碘標記阿拉伯糖結合 ASGPR 並搭配 ^{99m}Tc-Phytate，可應用於殘餘肝功能及肝癌進程評估；^{125}I-IMPY 則可用於神經母細胞瘤之細胞攝取與影像追蹤，展現放射性同位素技術於診斷、治療及疾病監測之多元應用潛力。

講者



田育彰

教授

高雄醫學大學

現職	高雄醫學大學　教授
學歷	中原大學　醫工系（2001）
經歷	高雄醫學大學　副教授 高雄醫學大學　助理教授 成功大學　博士後研究員
專長	醫學工程、藥物制放、蛋白質體、放射免疫

講者介紹

09:50–10:30、10:50–11:30　　第三會議室

大型語言模型於醫學檢驗之應用
Vibe Coding於教學及流程改善之實現

座長　王安美 技術主任（台北馬偕紀念醫院）

摘要

1.大型語言模型於醫學檢驗之應用:

探討大型語言模型（以 Claude AI 為例）在醫療領域的實務應用。內容涵蓋強大的數據分析與圖表視覺化（如肌酸酐標準化測驗分析、溶血退件率趨勢）、LOINC 編碼自動清理以及輔助撰寫學術短訊。

2. Vibe Coding 於教學及流程改善之實現:

「氛圍編程 (Vibe Coding)」，讓學員能以自然語言快速開發 PT/INR 計算機、eGFR 網頁及互動衛教遊戲。最後比較各大 AI 平台的自訂助理功能（如 Claude Projects），應用於 SOP 查詢與 ISO 15189 合規管理，強調「AI 是工具，專業才是關鍵」的核心理念。

講者



陳柏志

主任

高雄醫學大學附設中和紀念醫院

現職	高雄醫學大學附設中和紀念醫院　一般檢驗室主任
學歷	高雄醫學大學　醫學檢驗生物技術
經歷	高雄醫學大學附設中和紀念醫院檢驗醫學部　副主任/一般檢驗室主任 高雄醫學大學附設中和紀念醫院檢驗醫學部　品管暨教學室主任
專長	實驗室資訊、LOINC、生化免疫、血液鏡檢、實驗室認證/管理
特殊成就	IFBLS Scientific Network of Experts-Clinical Biochemistry

講者介紹

11:30–12:10　第三會議室

RIA的trouble shooting

座長　陳宜伶 醫事放射師（高雄醫學大學附設中和紀念醫院）

摘要

放射免疫分析（Radioimmunoassay, RIA）檢測結果易受到試劑、操作、儀器及反應條件等因素影響，當標準曲線、QC 或檢測結果出現異常時，快速且正確地判斷問題來源相當重要。本演講將介紹 RIA 常見異常狀況，包括標準曲線、Control、重複性及計數值異常，並說明其原因分析與排除方法。透過實際案例分享，建立系統化 Troubleshooting 流程，以提升檢驗品質、結果準確性及實驗室品質管理能力。

講者



王安美

技術主任

台北馬偕紀念醫院

現職	台北馬偕醫院核子醫學科　技術主任
學歷	大同大學　生物工程系　研究所(碩士)
經歷	馬偕護專　部定講師
專長	放射免疫分析

講者介紹

13:30–14:10 第三會議室

Auto QC for SPECT/CT and PET/CT at MD Anderson Cancer Center

座長 洪光威 副院長（彰濱秀傳紀念醫院）、黃莆蓉 醫事放射師（台中榮民總醫院）

摘要

Background

To ensure high-quality patient imaging, comprehensive quality assurance (QA) of SPECT/CT and PET/CT systems, including performance assessment, review, and documentation, is essential.

Purpose

We developed a novel Nuclear Medicine Quality Assurance (NMQA) server to automate QA data retrieval and integrated an AI deep-learning (AIDL) optical character recognition (OCR) system to automatically extract burn-in NEMA values from QA images. It can also parse QA data from PET and SPECT PDF reports and analyze CT QA data. The system compares QA measurements with predefined specifications, thereby improving the efficiency of QA review and facilitating longitudinal trending, centralized storage, and auditing of QA data.

Methods

The NMQA server was implemented in Python, with Structured Query Language (SQL) used to interact with a relational MySQL database. The database stores numerical QA results and pointers to the corresponding images, facilitating longitudinal trending of numerical measurements and review of QA images. The AIDL OCR system consists of two steps: region-of-interest extraction and character recognition. The NMQA server automatically retrieves, extracts, and analyzes daily QA data from SPECT, PET, and CT scanners.

Results

The NMQA server automatically retrieves QA data, extracts numerical QA measurements, and stores the results in a centralized database for trending and analysis. Its web-based interface facilitates efficient review of QA images and significantly reduces the time required for QA reviews. The AIDL OCR achieved 99.9% accuracy in recognizing numerical values. The web interface enables streamlined QA review on both computers and mobile devices, including iPhones.

Conclusions

The NMQA server significantly improves the efficiency of daily QA review while enabling longitudinal trending and analysis of QA measurements for quality assurance and continuous improvement. It also provides centralized documentation and auditing of QA data across SPECT/CT and PET/CT systems.

講者

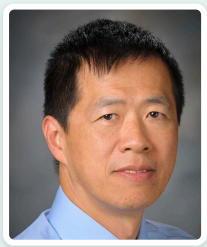

潘亭壽

Tinsu Pan

教授

University of Texas, USA

現職	The University of Texas, M.D. Anderson Cancer Center　Professor
學歷	The University of Michigan, Ann Arbor, Michigan　Electrical Engineering & Computer Sciences（1991）
經歷	GE healthcare, Applied Science Laboratory　CT Senior Scientist University of Massachusetts Medical Center　Post-doc, Instructor, Assistant Prof.
專長	Data-driven gated PET/CT, 4D CT and Cardiac CT
特殊成就	In 2019, my invention and publication of 4D-CT was selected as one of the 19 papers curated by Medical Physics on “Significant Advances in CT” Top 2% scientists in Top2PercentScientists.com.

講者介紹

14:10–14:50　第三會議室

From Quantitative Imaging to Personalized Therapy: The Evolving Role of Nuclear Medicine
從影像量化到個人化治療：核醫角色的演進

座長　俞長青 醫事放射師（高雄榮民總醫院）、張嘉容 醫事放射師（台北榮民總醫院）

摘要

核子醫學正從影像判讀逐步走向以量化數據支持臨床決策。從 SUV、SUVR 到 Amyloid PET 的定量，影像量化提供更客觀、標準化且可追蹤的評估方式；隨著 Theranostics 發展，量化的角色更進一步延伸至疾病負荷評估與個人化劑量學。

本演講將從 Amyloid PET 的定量、腫瘤負荷量化到 Theranostics dosimetry，探討定核醫影像如何從「看見疾病」進一步走向「量化疾病與治療」，支持未來更個人化的治療決策。

講者



施宜伶

跨產品整合方案經理 Integrated Solution Manager
GE Healthcare

現職	GE Healthcare　Integrated solution manager
學歷	台灣大學　醫學工程
專長	跨產品整合、分子影像、電腦斷層臨床應用

講者介紹

15:10–16:00　第三會議室

Theranostics 團隊：角色分工、核心能力與跨團隊合作

座長　楊邦宏 副理事長（中華民國核醫學學會）、陳建榮 副秘書長（中華民國核醫學學會）

摘要

本演講介紹診療整合團隊的角色分工，涵蓋醫師、護理師、藥師、放射師及輻射防護，說明病人選擇、影像判讀、治療規劃與療效追蹤等核心能力，並探討多專科共同決策與照護流程，促進跨團隊合作，提升治療品質與病人安全。

講者



詹宏彬

醫師

高雄榮民總醫院

現職	高雄榮民總醫院核醫科　主治醫師
學歷	國立中山大學　生物醫學
經歷	高雄榮民總醫院核醫科　總醫師
專長	核醫造影檢查，正子造影檢查，同位素治療

講者介紹

16:00–16:20　第三會議室

論文寫作及研究分享：如何找題目

座長　黃奕琿 技術長（台大醫院）、王秀珊 技術長（三軍總醫院）

摘要

醫事放射師除了常規的臨床作業外，對於提升自我專業能力，有某種特殊的壓力。通常最困難的不是如何寫專業報告或期刊論文, 而是如何踏出第一步: 怎麼找題目? 本課程就多年的臨床與教學的經驗, 來分享一些如何在日常工作中，發現並尋找出適合的研究題目.對有此需求的放射師們提供一個方向。

講者



杜高瑩

醫事放射師

台北馬偕紀念醫院

現職	馬偕紀念醫院核醫科　醫事放射師
學歷	陽明大學　放射醫學科學研究所
經歷	馬偕紀念醫院核醫科　技術主任 陽明大學放射學系　講師
專長	核醫造影技術, 醫學資訊系統

講者介紹

16:20–16:40　第三會議室

論文寫作及研究分享：投稿與寫作技巧

座長　黃奕琿 技術長（台大醫院）、王秀珊 技術長（三軍總醫院）

摘要

學術研究成果的發表是研究工作的重要環節，也是專業知識交流與累積的重要途徑。本課程將從實務角度介紹論文投稿形式、投稿流程及論文寫作技巧。首先說明常見的投稿形式，包括研討會論文與期刊論文；研討會分為壁報展示與口頭報告，期刊依出版模式區分為傳統訂閱制與開放取用期刊，並說明其特色與選擇考量。其次介紹期刊投稿流程，包括資料準備、行政審查、正式審查、審查意見回覆及結果通知。論文寫作部分將以核醫技術領域之原著論文之論文架構，逐一說明各部分的撰寫重點與常見問題，並結合實際研究及投稿經驗，分享論文撰寫、期刊選擇與審查意見回覆之實務技巧，協助臨床工作者建立研究成果發表的基本概念。

講者



龔瑞英

醫事放射師

台中榮民總醫院

現職	臺中榮民總醫院核子醫學科　醫事放射師
學歷	中臺科技大學　醫學影像暨放射科學系
經歷	彰濱秀傳紀念醫院　醫事放射師
專長	核子醫學、影像處理、輻射防護、醫學教育
特殊成就	第 13 屆原子能安全績優獎（醫療應用類個人獎）

講者介紹

16:40–17:00　第三會議室

論文寫作及研究分享：研究計畫準備工作

座長　黃奕琿 技術長（台大醫院）、王秀珊 技術長（三軍總醫院）

摘要

臨床上醫事放射師擔負影像後處理的任務，醫院升等、放射師進階申請、為了評鑑需求，都會有寫論文或進行研究計畫的需求，今年核醫學會年會的醫技人員課程，針對這些需求我們設計了一堂課，由不同的教師來跟大家分享：如何找題目、投稿與寫作技巧、研究計畫準備工作，希望用輕鬆的方式經驗分享，讓放射師了解如果進入論文寫作及研究的世界。

我的部分是分享要送研究計畫前，有哪些準備工作，需要具備那些條件，無論是自己想單獨完成或是與同事、同儕一起完成，如何跨出第一步，跨出去後真的會發現一點也不難，希望大家都可以得到一些收穫。

講者



陳惠萍

副主任

台東基督教醫院

現職	東基醫療財團法人台東基督教醫院　核醫科技術組長/教學部副主任
學歷	中台科技大學　放射科學研究所放射化學暨輻射生物組
經歷	聯新國際醫院　核醫科技術組長 林新醫院　核醫科技術組長
專長	核子醫學造影、正子造影、輻射防護、醫事放射師教學系統性規劃及建置
特殊成就	建置核子醫學組醫事放射師 CBME 教學系統

講者介紹

15:10–15:30 第四會議室

PSMA and SSTR-Targeted Theranostics: A Practical Perspective and Experience

座長 黃文盛 教授（彰濱秀傳紀念醫院）、莊佩儒 醫師（台大醫院）

摘要

Theranostics transforms personalized oncology by integrating molecular diagnostic imaging with targeted systemic radionuclide therapy. The National Cyclotron and PET Centre, Chulabhorn Hospital, has established a comprehensive, fully integrated theranostic service system. Our center operates under internationally recognized standards, achieving QUANUM, DSC prostate (where Lu-177 PSMA therapy is a pivotal component), and EARL theranostic accreditations. We provide advanced diagnostic imaging using PET/CT and 3-Tesla PET/MRI, supported by GMP/GDP PICs-certified in-house cyclotron production of radiopharmaceuticals. This includes Ga-68 and F-18 PSMA for prostate cancer, Ga-68 DOTATATE for neuroendocrine tumors, and investigational ^{18}F-AlF-NOTA-Octreotide.

Our practical clinical experience underscores the value of multidisciplinary integration in optimizing patient outcomes. In treating metastatic castration-resistant prostate cancer with Lu-177 PSMA, our analysis highlighted the critical role of pretherapeutic PSMAPET/CT imaging. Specifically, PET-derived semiquantitative parameters—total tumor volume (PSMA-TV), total lesion uptake (PSMA-TLU), and total lesion quotient (PSMA-TLQ)—served as significant negative predictors of biochemical response in patients without liver metastasis.

Despite robust clinical capabilities, expanding access to theranostics faces notable barriers. Affordability and reimbursement of these agents are pivotal in ensuring equitable access. It is imperative for stakeholders, including governments, insurers, and healthcare providers, to develop sustainable pricing models and reimbursement strategies. Furthermore, fortifying nuclear medicine facilities requires comprehensive healthcare professional training, infrastructure development, and international collaborations to facilitate vital knowledge sharing and technology transfer.

講者

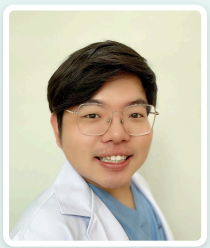

Dr. Dheeratama Siripongsatian

Physician

Chulabhorn Hospital, Thailand

現職	Nuclear Medicine Physician, National Cyclotron and PET Centre, Chulabhorn Hospital, Chulabhorn Royal Academy
學歷	2023 Clinical and Research Fellowship in Nuclear Medicine, Erasmus University Medical Center, Netherlands 2020 Higher graduate diploma program in clinical medical sciences (radiology), Khon Kaen University 2015 Doctor of medicine, Khon Kaen University
經歷	6 years Nuclear Medicine Physician, National Cyclotron and PET Centre, Chulabhorn Hospital 3 years Nuclear Medicine Resident, Division of Nuclear Medicine, Department of Radiology, Faculty of Medicine, Khon Kaen University

講者介紹

15:30–15:50 第四會議室

Building Sustainable PSMA Theranostic Radiopharmaceuticals in Thailand: Eight Years from Tc-99m SPECT to Ac-225 Alpha Therapy

座長 黃文盛 教授（彰濱秀傳紀念醫院）、莊佩儒 醫師（台大醫院）

摘要

Thailand has progressively established a sustainable theranostic radiopharmaceutical program over the past eight years, integrating clinical implementation, local radiopharmaceutical development, and international collaboration. The journey began in February 2018 with the first clinical theranostic application in Thailand using ^{68}Ga-PSMA-I&T, followed by ^{68}Ga-DOTATATE. Successful molecular imaging of prostate cancer and neuroendocrine tumors provided the foundation for therapeutic applications, leading to ^{177}Lu-PSMA-I&T and subsequently ^{177}Lu-DOTATATE. For peptide receptor radionuclide therapy, pharmaceutical-grade amino acid solutions for renal protection were implemented in accordance with international PRRT guidelines.

Following the COVID-19 pandemic, increasing clinical demand for prostate cancer imaging motivated the introduction of ^{18}F-PSMA-1007 through collaboration with Osaka University, Japan. Its batch production capability, allowing imaging of more than 10 patients per production run, substantially increased our capacity to serve growing patient numbers. Building on our experience with ^{177}Lu-PSMA-I&T, we subsequently advanced to ^{225}Ac-PSMA-I&T, marking an important step toward targeted alpha therapy in Thailand. This development was supported by the Joint Research Center (JRC) in Karlsruhe, Germany, where hands-on training in ^{225}Ac radiolabeling provided essential expertise for establishing the methodology locally.

Recognizing that sustainable theranostics requires not only advanced radionuclides but also accessibility and affordability, we developed a ^{99m}Tc-based PSMA imaging methodology as a more affordable SPECT alternative for prostate cancer imaging, particularly where PET resources remain limited. This eight-year experience demonstrates a stepwise strategy for building sustainable theranostics while strengthening local expertise, technology transfer, and international partnerships.

講者



Shuichi Shiratori

Associate Professor

Faculty of Medicine Siriraj Hospital, Mahidol University

現職	Associate Professor, Radiology, Faculty of Medicine Siriraj Hospital, Mahidol University
學歷	PhD, Graduate School of Pharmaceutical Sciences Chiba University, Japan 2002-2005 MSc, Graduate School of Pharmaceutical Sciences Chiba University, Japan 2000-2002 BSc, Faculty of Pharmaceutical Sciences, Chulalongkorn University, Thailand 1991-1996
經歷	Assoc. Prof., Faculty of Medicine Siriraj Hospital, Mahidol University, Thailand 2020-present Assoc. Prof., Faculty of Medicine, Chulalongkorn University, Thailand 2015-2020 Assoc. Prof., Faculty of Medicine, Fukushima medical University, Japan 2012-2014 Assoc. Prof., Faculty of Medicine, Yokohama City University, Japan 2005-2012

ORAL PRESENTATION

口頭論文摘要

第四會議室（門診大樓 1 樓） 共 18 篇

10:50–11:30	口頭論文-臨床組	OC1、OC2、OC3、OC4
11:30–12:10	口頭論文-基礎組	OB1、OB2、OB3、OB4、OB5
13:30–14:10	口頭論文-臨床組	OC5、OC6、OC7、OC8、OC9
14:10–14:50	口頭論文-基礎組	OB6、OB7、OB8、OB9

口頭論文索引

編號	題目	發表者	頁
OB1	利用[18F]FEPPA正子造影評估α-突觸核蛋白PFFs誘導之帕金森氏症小鼠模型早期神經發…	馮意庭	55
OB2	Biodistribution and Therapeutic Efficacy of Umbilical Cord Mesenchymal Stem Cell-…	王美惠	56
OB3	Automated Production and Quality Evaluation of Ga-68-3BP-3940 Injection Using a …	羅盛男	57
OB4	Preclinical Evaluation of [18F]MFBG PET for Cardiac Sympathetic Imaging in an Isopr…	邱晉宏	59
OB5	Preclinical Feasibility Evaluation of PARP-1-Specific Radiolabeled Tracers for NSCLC …	法里亞・罕	60
OB6	品質風險管理策略應用於檢測F-18 FDG未知不純物	許耘萱	61
OB7	Ga-68-3BP-3940注射液分析方法開發與確效暨臨床製造品質驗證	楊詩涵	62
OB8	Preclinical Evaluation of 68Ga/177Lu-DO3A-FAPI for FAP-Targeted PET Imaging and I…	黎昱璇	63
OB9	64Cu-Labeled Fibrin for Imaging Cerebral Fibrin Pathology in Alzheimer's Disease	翁茂琦	64
OC1	Hopkins versus Deauville Scoring on FDG PET for Esophageal Cancer Response after …	鄭雯欣	65
OC2	Clinical Profile and Biochemical Discordance in Initially Non–Radioiodine-Avid Meta…	楊因因	66
OC3	Occipital Perfusion is Relatively Preserved as Cognition Declines on Cerebral Perfusi…	郭之凡	67
OC4	Longitudinal Brain FDG PET Demonstrates Treatment-Associated Prefrontal Metabol…	王建程	68
OC5	Technical Validation of a Thyroid Uptake Probe as an Alternative to a Well-Type r-Co…	劉家寧	69
OC6	探討淋巴造影肢體影像在乳癌轉移之應用	張春梅	70
OC7	Dynamic 18F-Flutemetamol PET for Differentiating Cardiac Amyloidosis Subtypes an…	李婷嫣	71
OC8	放射性藥物調劑錯誤事件之根本原因分析與矯正措施	許耘萱	72
OC9	Radiation Risk Perception and Acceptance of Advanced Liquid Processing System (A…	王妤珊	73

口頭論文 基礎組 11:30–12:10 第四會議室 OB1

原著論文

利用[18F]FEPPA正子造影評估α-突觸核蛋白PFFs誘導之帕金森氏症小鼠模型早期神經發炎狀態

[1]馮意庭, [1]翁啓昌

[1]長庚大學

發表者 馮意庭

Keywords 分子影像

Background

帕金森氏症是一種常見的神經退化性疾病，其主要病理特徵包括多巴胺神經元退化，以及α-Syn異常聚集形成路易氏小體。近年研究顯示，神經發炎與小膠質細胞活化於帕金森氏症早期病程中扮演重要角色，其中TSPO可作為小膠質細胞活化相關的生物標誌，因此可透過TSPO PET進行活體神經發炎評估。本研究採用人類α-Syn PFFs誘導之帕金森氏症小鼠模型，並評估TSPO放射性示蹤劑 [^{18}F]FEPPA應用於帕金森氏症早期神經發炎偵測之可行性。

Method

本研究首先建立 [^{18}F]FEPPA之實驗室手動放射合成流程，並進行放射化學純度、莫耳活性及放射性產率等品質分析。隨後將人類α-Syn PFFs單側注射至C57BL/6小鼠紋狀體，於注射後 1、3 及 5 個月進行PET影像分析，以評估各腦區TSPO表現之變化。為進一步驗證PET影像結果，於活體影像分析後進行自動輻射顯影及病理組織分析，並透過Iba-1、TSPO及pS129免疫螢光染色，評估小膠質細胞密度、活化型態及α-Syn病理分布，進一步探討其與PET影像訊號之相關性。

Results

本研究建立 [^{18}F]FEPPA手動放射合成流程（n=10），放射化學純度皆 >99%，莫耳活性為 15.1±11.6 GBq/μmol。PET活體影像分析以全腦為ROI顯示，PFFs注射組於注射後 3個月之 [^{18}F]FEPPA攝取量較未注射組約增加 20%，而 1 及 5 個月則未呈現相同程度之差異，顯示TSPO訊號於不同時間點具有非線性變化。進一步以自動放射自顯影分析發現，[^{18}F]FEPPA訊號主要分布於脈絡叢及血管等生理性TSPO高表達區域；相較之下，腦實質區域之訊號較低，活體PET所觀察之全腦訊號可能受到背景TSPO表現及partial volume effect影響。免疫螢光分析顯示，多數腦區之小膠質細胞密度未達顯著差異，惟變形蟲型小膠質細胞比例於注射後 3 個月顯著增加，顯示此時期小膠質細胞活化較為明顯，與全腦PET訊號變化一致。此外，雙重免疫螢光染色顯示，小膠質細胞活化與pS129病理變化具有時序性關聯；神經發炎相關變化於較早期出現，而pS129病理則隨時間於不同腦區逐漸累積，顯示兩者具有不同之時序及空間分布特徵。

Conclusion

綜合本研究結果，人類α-Syn PFFs小鼠模型可產生α-Syn病理堆積，且病程進展伴隨神經發炎反應；此變化可透過 [^{18}F]FEPPA PET進行活體觀察，顯示 [^{18}F]FEPPA具有評估帕金森氏症早期神經發炎之潛力。然而，部分腦區如脈絡叢及血管具有較高的生理性TSPO表現，加上PET空間解析度限制，可能使早期神經發炎訊號不易與背景訊號區分。因此，[^{18}F]FEPPA PET仍應搭配組織學分析及其他生物標誌進行綜合評估，以更完整地反映帕金森氏症病程中的神經發炎變化。

口頭論文 基礎組 11:30–12:10 第四會議室 OB2

原著論文

Biodistribution and Therapeutic Efficacy of Umbilical Cord Mesenchymal Stem Cell-Derived Exosomes in an Alzheimer's Disease Mouse Model

[1]王美惠, [1]何宗澧, [1]詹振勳, [1]鄭凱鴻, [2]謝秀梅, [3]林奏延

[1]國家原子能科技研究院
[2]國立師範大學
[3]艾萬霖生技股份有限公司

發表者 王美惠

Keywords 藥物開發 | 臨床前藥物研究 | 分子影像

Background

Alzheimer's disease (AD) is the leading cause of dementia, characterized by progressive memory loss and cognitive decline. This study evaluates the therapeutic potential and biodistribution of exosomes isolated from Wharton's jelly mesenchymal stem cells (WJMSC exosomes) in a 5xFAD transgenic mouse model, specifically examining their effects on beta-amyloid aggregation and spatial cognitive function.

Method

5xFAD mice received weekly intravenous tail vein injections of WJMSC exosomes (2 x 10^9 exosomes/dose) for four consecutive weeks. Exosomes were tagged with Ga-67/Ga-68 to synthesize a dual-modality SPECT/PET tracer. Brain beta-amyloid burden was quantified via PET-CT imaging using F-18 Florbetaben. Spatial learning and memory were evaluated using the Barnes maze test. Tracer tracking was conducted to map exosome localization in both healthy and 5xFAD mice.

Results

The Ga-67/Ga-68 exosome labeling achieved a 97% efficiency rate, significantly outperforming conventional international rates of 20–30%. WJMSC exosome treatment produced statistically significant improvements in spatial memory ($p < 0.05$, $n = 6$) and marked reductions in brain beta-amyloid accumulation ($p < 0.05$, $n = 6$). Exosomes accumulated primarily in the liver and spleen. However, 5xFAD mice demonstrated higher uptake in both the brain and bones compared to healthy controls. 5xFAD mice exhibited lower overall bone density alongside increased skeletal exosome absorption.

Conclusion

The therapeutic efficacy of WJMSC exosomes in reversing AD-like pathology appears closely linked to their ability to target brain tissue. Beyond cognitive improvements, the observed higher bone uptake and reduced bone density in 5xFAD mice point to osteoporosis as a potential comorbidity of Alzheimer's disease. Ultimately, these results demonstrate that WJMSC exosomes represent a promising, cell-free biotherapeutic approach for treating AD.

口頭論文 基礎組 11:30–12:10 第四會議室 OB3

原著論文

Automated Production and Quality Evaluation of Ga-68-3BP-3940 Injection Using a Modular-Lab PharmTracer System in a GMP-Grade PET Radiopharmaceutical Facility

[1,2]Sheng-Nan Lo, [1]Hsin-Chun Lin, [1]Shih-Han Yang, [1]Ling-Man Hung, [1]Ting-Chum Lin, [1]Yu-Yi Huang, [1,3]Ming-Hsin Li

[1]和信醫院
[2]Advancharis Co., Ltd.
[3]Alliance Innovation Theranostics Pharma Ltd.

發表者 羅盛男

Keywords Fibroblast Activation Protein (FAP) | Automated Radiosynthesis | GMP Compliance / Quality Control | Modular-Lab PharmTracer | Ga-68-3BP-3940

Background

Fibroblast activation protein (FAP) is an important radiotheranostic target widely expressed in cancer-associated fibroblasts of many solid tumors. 3BP-3940, a DOTA-conjugated cyclic peptide designed to enhance tumor uptake and retention, represents a promising next-generation FAP radiotracer. Here, Koo Foundation Sun Yat-Sen Cancer Center, in collaboration with Alliance Innovation Theranostics Pharma Ltd. and 3BP, established an automated, GMP-compliant production and quality evaluation process for Ga-68-3BP-3940 injection to support its clinical translation in Taiwan.

Method

The 3BP-3940 precursor (100 µg, 3BP) was dissolved in a reaction mixture containing buffer, sodium acetate, ascorbic acid, and ethanol, and loaded into a pre-installed synthesis cassette for automated radiosynthesis using the Modular-Lab PharmTracer (Eckert & Ziegler). Approximately 1.2 GBq of Ga-68 chloride (GalliaPharm®) was reacted at 85°C for 10 min. The crude product was purified using a C18 cartridge, formulated with 0.9% NaCl, transferred to an automated dispensing system (µDDSA) within a Grade A hot cell, sterile-filtered, and sampled for quality control testing.

Results

Three consecutive batches of Ga-68-3BP-3940 injection were successfully and reproducibly manufactured using the MLPT automated system. Quality control (QC) results for all final products consistently complied with the predefined center release specifications. The final formulations were clear, colorless, and free of visible particulate matter, with a pH ranging from 5.0 to 7.0. Radionuclidic identity was confirmed by a half-life of 61–75 minutes, and the radionuclidic purity was ≧ 99.9%. The radiochemical purity was ≧ 95% as determined by radio-TLC and ≧ 90.0% by radio-HPLC. Additionally, the ethanol content was < 10%, and bacterial endotoxins were < 35 EU/mL (derived from a 5 mL maximum injection volume). Both sterility and filter membrane integrity testing successfully passed the criteria.

（續下頁）

口頭論文 基礎組（續）

11:30–12:10 第四會議室 OB3

Automated Production and Quality Evaluation of Ga-68-3BP-3940 Injection Using a Modular-Lab PharmTracer System in a GMP-Grade PET Radiopharmaceutical Facility

Conclusion

Clinical production of Ga-68-3BP-3940 injection using the GAIA V2 synthesis module and All-In-One mini synthesis module has been reported previously (Ammour et al., J Vis Exp, 2025; Greifenstein et al., iScience, 2023). In the present study, we demonstrated that our center can reproducibly produce Ga-68-3BP-3940 injection using the MLPT automated synthesis system in a high-standard GMP-grade PET radiopharmaceutical production facility, with three consecutive batches meeting the predefined quality specifications. The establishment of this production process provides an important foundation for a future investigator-initiated trial (IIT) and may enable the introduction of a novel molecular imaging tool for patients with FAP-expressing tumors, thereby facilitating the clinical translation of international advances in FAP radiotheranostics in Taiwan.

口頭論文 基礎組 11:30–12:10 第四會議室 OB4

原著論文

Preclinical Evaluation of [18F]MFBG PET for Cardiac Sympathetic Imaging in an Isoproterenol-Induced Heart Failure Model

[1,2]邱晉宏, [1]李婷嫣, [1,3]柯冠吟, [2]翁啓昌, [1]鄭媚方

[1]臺大醫院
[2]長庚大學
[3]臺大癌醫中心分院

發表者 邱晉宏

Keywords 分子影像 | 臨床前藥物研究

Background

Heart failure is accompanied by progressive cardiac sympathetic dysfunction, which is closely associated with disease progression and adverse outcomes. Although [123I]MIBG SPECT is clinically used for cardiac sympathetic imaging, its utility remains limited by the inherent constraints of SPECT imaging. As a PET analogue of MIBG, [18F]MFBG has the potential to provide improved quantitative assessment of cardiac sympathetic function; however, its biological performance in experimental heart failure has not been fully characterized. This study aimed to evaluate cardiac sympathetic dysfunction using [18F]MFBG PET in an isoproterenol induced heart failure mice model.

Method

C57BL/6 mice were used to establish an isoproterenol (ISO) induced cardiac injury model by subcutaneous administration of ISO at 10 mg/kg/day for 7 consecutive days, while untreated mice served as controls. Dynamic PET/CT imaging was performed following intravenous injection of [18F]MFBG (18.5 MBq), and CT guided whole heart and forelimb skeletal muscle VOIs were defined for quantitative analysis. Myocardial tracer uptake was quantified as the heart to muscle standardized uptake value ratio (SUVR), and differences between groups were analyzed using Mann-Whitney U Test.

Results

Four ISO treated mice showed significantly reduced left ventricular ejection fraction LVEF) compared with five controls (41± 9.8% vs. 66± 6.0%, P = 0.007), confirming successful establishment of the heart failure model. Whole heart [18F]MFBG PET demonstrated significantly reduced myocardial tracer uptake in the ISO group, with SUVR decreasing from 3.8±0.7 in controls to 2.2±0.2 in ISO treated mice (P = 0.036). These findings indicate impaired cardiac sympathetic function following ISO induced myocardial injury and support the feasibility of [18F]MFBG PET for differentiating diseased from normal myocardium in this experimental heart failure model.

Conclusion

[18F]MFBG PET detected altered cardiac sympathetic function in ISO treated mice, supporting its feasibility as a molecular imaging approach for evaluating cardiac sympathetic dysfunction.

口頭論文 基礎組 11:30–12:10 第四會議室 OB5

原著論文

Preclinical Feasibility Evaluation of PARP-1-Specific Radiolabeled Tracers for NSCLC Molecular Imaging

[1]法里亞 • 罕, [2]朱哲興, [4]Robert H, [2]許靖涵, [3]鍾宜秀, [1,3]翁啟昌

[1]長庚大學
[2]清華大學
[3]林口長庚醫院
[4]University of Pennsylvania, Philadelphia

發表者 法里亞 • 罕

Keywords [^{125}I]KX1 | [^{18}F]FTT | Non-small-cell lung cancer (NSCLC) | PARP-1 | 分子影像

Background

Poly(ADP-ribose) polymerase (PARP) inhibitors have demonstrated clinical benefit in several BRCA-mutated and homologous recombination-deficient cancers. However, responses in non-small-cell lung cancer (NSCLC) remain heterogeneous, and not all patients benefit equally. Differences in tumor PARP-1 expression may partly contribute to this variability. This study evaluated whether two complementary rucaparib-derived radiotracers, [^{125}I]KX1 and [^{18}F]fluorthanatrace ([^{18}F]FTT), could distinguish H460 and A549 NSCLC models with different PARP-1 expression profiles at the cellular, tissue, and in vivo levels.

Method

PARP-1 expression in H460 and A549 cells was assessed by immunofluorescence staining. [^{125}I]KX1 was synthesized,characterized by radio-HPLC, and evaluated using saturation binding assays, with 20 μM olaparib used to define nonspecific binding. [^{18}F]FTT was synthesized by nucleophilic radiofluorination and evaluated for radiochemical yield, purity, molar activity, and in vitro stability. Intramuscular H460 and A549 xenografts underwent [^{18}F]FTT PET/CT imaging. Tumor tissues were subsequently examined by PARP-1 immunofluorescence and in vitro [^{125}I]KX1 autoradiography with and without olaparib competition.

Results

H460 cells exhibited higher PARP-1 expression and greater [^{125}I]KX1 binding capacity than A549 cells. [^{125}I]KX1 was obtained with a radiochemical yield of 57.4 ± 3.9% and radiochemical purity >99%. [^{18}F]FTT was produced with a decay-corrected radiochemical yield of 24.7 ± 4.6%, radiochemical purity >99%, and molar activity of 117.5 ± 15.7 GBq/μmol. The tracer remained >99% intact in saline at 37°C for up to 3 h. PET/CT demonstrated higher relative [^{18}F]FTT uptake in H460 tumors than in A549 tumors. Tumor PARP-1 immunofluorescence and [^{125}I]KX1 autoradiography showed the same overall pattern, while olaparib competition reduced the autoradiographic signal, supporting PARP-mediated binding.

Conclusion

[^{125}I]KX1 and [^{18}F]FTT distinguished H460 and A549 NSCLC models with different PARP-1 expression profiles across cellular, tissue, and in vivo analyses. These findings provide proof-of-concept support for PARP-targeted molecular imaging as a noninvasive strategy for characterizing PARP-1 expression in NSCLC. Further validation in larger cohorts and more clinically relevant models is warranted.

口頭論文 基礎組 14:10–14:50 第四會議室 OB6

其他

品質風險管理策略應用於檢測F-18 FDG未知不純物

[1]許耘萱, [1]蘇博仁, [1]何志豪, [2]羅欽瑾, [1]陳輝墉, [1]殷國維

[1]義大醫院
[2]新光醫院

發表者 許耘萱

Keywords 品質風險管理 | 殘餘溶劑

Background

本研究旨在建立套用品質風險管理（Quality Risk Management, QRM）之標準處置流程，於FASTlab2合成器生產F-18 FDG製程中，GC設備檢測殘餘溶劑圖譜上，出現一未知波峰，導入前瞻性屏障分析，進行品質風險辨識、風險評量、風險應對、進行風險管制作為。最終產出減災作為或可接受風險結果的評價，作為品質風險監測管制流程。

Method

1. 參考中華藥典通則 (2467) 對於策略選項作出指示，而美國藥典一般資訊 <1086>/ ICH Q3A/Q3B同時也提供製劑有機不純物管制決策樹，作為管制指引。

2. 啟動第三公正單位 (委託SGS台灣檢驗科技股份有限公司超微量工業安全實驗室)，針對產品樣本依中華藥典通則對於策略選項進行分析。

3. 參照法規，進行分析方法確認。參照供應商官宣文件:COA、White Paper等，作為佐證。

Results

1. 由SGS微量工業安全實驗室完成不純物鑑別試驗 (定性)、定量試驗、確效分析試驗。

2. 定性實驗結果對照GE公司 2015 White Paper，確認為內生性不純物Acetic Acid/ Acetate。

3. 定量實驗結果，樣品Acetic Acid含量為 0.443 mg/ml。而Likelihood in GE white paper規範濃度範圍為 0.9-1.4 mg/ml；本樣品濃度顯低於其規範。

Conclusion

1. 溶劑毒性等級與安全暴露量評估

本研究樣品鑑別出Acetic Acid含量為 0.443 mg/ml，依據中華藥典第九版通則〈2467〉「殘留溶劑」規定屬第三類殘留溶劑：對人體毒性潛勢極低者，每日允許暴露量（PDE）為 50 mg/day以上（或濃度限制在 5,000 ppm/ 0.5% 以下）。本樣品符合藥典對藥品安全之要求。

2. 以USP <1086>與ICH Q3A/Q3B評析

製劑製程中，藥品不純物須劃分為「製程相關不純物」與「降解產物」。若藥典個論尚未包含特定異常波峰之合格標準，產製單位有責任依科學實證建立分析方法與驗收標準（Acceptance Criteria）。本研究主動進行方法確效與定量，補足了法規未涵蓋之監測範圍。

3. 主動式品質風險管理（QRM）與製程持續改善

GC檢測時發現問題，即時回饋原廠，原廠初步研判該波峰可能為「雜訊（Noise）並建議忽略」。然而，基於正子藥品製程高品質要求，評估該波峰具高度再現性，應認定為「重大製程未知變化」，決策啟動 QRM 流程，風險辨識與評量：透過第三方檢測證實其毒性風險在可接受範圍（ALARP原則）。

風險控制與回饋：藥物終產品除符合藥典各項品管項目標準外，對於本次研究結果，仍如實地將數據回饋原廠，建議針對FASTlab2合成組套（Cassette）純化管柱與前處理流程進行設計改善，達到主動維護產品安全與品質目的。

口頭論文 基礎組 14:10–14:50 第四會議室 OB7

原著論文

Ga-68-3BP-3940注射液分析方法開發與確效暨臨床製造品質驗證

[3]楊詩涵, [3,1]李銘忻, [3,2]羅盛男, [3]黃玉儀, [3]林欣純

[1]群創生物科技有限公司
[2]恩典科研股份有限公司
[3]和信醫院

發表者 楊詩涵

Keywords 臨床前藥物研究 | 品管 | Ga-68-3BP-3940 | Fibroblast Activation Protein | FAP | 分析方法確效 | GMP compliance

Background

Ga-68-3BP-3940為一種以鎵 -68 標記之纖維母細胞活化蛋白（Fibroblast Activation Protein, FAP）靶向正子放射性藥物，可藉由與腫瘤微環境中高表現之FAP結合，作為正子斷層掃描（PET imaging）之分子影像探針，具有腫瘤診斷及臨床應用潛力。由於鎵 -68放射性藥品半衰期短，品質管制方法須兼具快速性、準確性及可靠性，以確保產品於臨床使用前符合品質要求。本研究旨在建立符合GMP規範之Ga-68-3BP-3940注射液品質管制方法，依ICH分析方法確效原則完成品質分析方法之建立與驗證，並透過連續三批GMP製造及安定性試驗，評估分析方法之適用性、製程一致性及產品品質穩定性，建立可應用於臨床製造與產品放行之 GMP 品質管制平台。

Method

本研究以GMP等級Ga-68-3BP-3940注射液為研究對象，建立完整品質管制流程，檢驗項目包括成品放射活度濃度、比活度、外觀、放射核種特性、放射性核種純度、pH值、放射性核種純度、放射化學純度、放射化學不純物、殘餘溶劑、細菌內毒素、無菌試驗及濾膜完整性等，而其中放射化學純度分別利用Radio-HPLC及Radio-TLC進行分析。並針對Radio-HPLC 與 Radio-TLC 分析方法進行系統適用性、可重複性、線性範圍、量測方法靈敏度、專一性、精密度、準確度、同一性及放射化學純度等項目評估，繼而確認分析方法確效程序方法規範之標準。此外，以連續三批GMP製造批次進行品質一致性及 2 小時安定性試驗，以確認分析方法之適用性與產品品質穩定性。

Results

Radio-HPLC分析方法之主峰保留時間及峰面積變異係數 (%RSD)分別是 <1% 及 <5%；線性迴歸係數 (R^2) >0.95，精密度標準差 <10%，放射化學純度 ≥ 90 %。而Radio-TLC分析方法主峰面積百分比的標準偏差 <0.2 %；線性迴歸係數 (R^2)>0.99，精密度標準差 <10%，放射化學純度 >97 %，RCR ≥ 91%，均符合預設標準。連續三批GMP製造批次均完成品質管制，各項檢驗結果皆符合產品放行規格；2 小時安定性試驗顯示成品放射活度濃度、比活度、外觀、放射核種特性、放射性核種純度、pH值、放射化學純度、放射化學不純物及細菌內毒素等關鍵品質屬性均維持於可接受範圍。

Conclusion

本研究成功建立符合GMP要求之Ga-68-3BP-3940注射液品質管制方法，並完成分析方法確效。所建立之分析方法具良好之可靠性及再現性，可應用於產品放行檢驗及後續臨床製造品質監測。連續三批GMP生產結果證實製程具有良好一致性及穩定性，提供本院 (和信醫院) 進行IIT(Investigator-Initiated Trial)臨床試驗產品放行及法規申請之品質保證依據，並支持FAP分子影像藥物之臨床轉譯與後續應用。

口頭論文 基礎組 14:10–14:50 第四會議室 OB8

原著論文

Preclinical Evaluation of 68Ga/177Lu-DO3A-FAPI for FAP-Targeted PET Imaging and Its Therapeutic Potential

[1]黎昱璇, [1]蘇毓禎, [1]陳傳霖

[1]陽明交通大學

發表者 黎昱璇

Keywords 藥物開發 | 試劑 | 製藥 | 解剖學 /CT/MR | 分子影像 | 造影儀器

Background

Fibroblast activation protein (FAP) is highly expressed on cancer-associated fibroblasts (CAFs) and represents a promising target for cancer imaging and radioligand therapy. This study designed DO3A-FAPI based on the UAMC1110 scaffold and compared it as a [68Ga]-labeled PET imaging agent with [68Ga]Ga-FAPI-04 (the DOTA-modified FAPI). Finally, Lu-177 was further labeled to obtain [177Lu]Lu-DO3A-FAPI, and its potential as a therapeutic agent was evaluated.

Method

The DO3A-FAPI precursor and non-radioactive reference compounds were synthesized, followed by radiolabeling with 68Ga and 177Lu. Radiochemical yield and purity were evaluated using radio-TLC and HPLC. Biological evaluation was performed using HT1080-FAP-GFP++ cells and a U-87 MG xenograft mouse model, with FAPI-04 as a reference compound.

Results

DO3A-FAPI was successfully synthesized and radiolabeled with both 68Ga and 177Lu. [68Ga]Ga-DO3A-FAPI showed specific binding to FAP-expressing cells, with an IC50 of 1.96 nM, indicating high binding affinity. PET/MR imaging demonstrated clear and sustained tumor accumulation, with a T/M ratio of 19.405 ± 6.397 at 120 min, higher than 10.87 ± 4.37 for [68Ga]Ga-FAPI-04, indicating improved tumor-to-background contrast. Biodistribution studies of DO3A-FAPI confirmed tumor accumulation and predominant renal clearance. [177Lu]Lu-DO3A-FAPI showed T/M ratios of 12.47 ± 0.76, 13.01 ± 0.91, 10.46 ± 0.32, and 10.57 ± 0.14 at 1, 4, 24, and 48 h, respectively, indicating prolonged tumor retention and supporting its potential as a therapeutic agent.

Conclusion

68Ga/177Lu-DO3A-FAPI were successfully developed and biologically evaluated. [68Ga]Ga-DO3A-FAPI exhibited high FAP binding affinity, a higher tumor-to-muscle ratio, and improved tumor-to-background contrast compared with [68Ga]Ga-FAPI-04. [177Lu]Lu-DO3A-FAPI demonstrated prolonged tumor retention, supporting its potential as a therapeutic agent. These findings support DO3A-FAPI as a promising platform for FAP-targeted theranostic applications.

口頭論文 基礎組 14:10–14:50 第四會議室 OB9

原著論文

64Cu-Labeled Fibrin for Imaging Cerebral Fibrin Pathology in Alzheimer's Disease

[1]翁茂琦, [1]羅佳茜, [1]陳振宗, [1]夏建忠, [2]張剛瑋

[1]國家原子能科技研究院
[2]臺北醫學大學

發表者 翁茂琦

Keywords 分子影像 | 臨床前藥物研究 | 造影儀器 | 定量分析

Background

Cerebrovascular dysfunction and blood-brain barrier (BBB) disruption contribute to Alzheimer's disease (AD) progression by promoting cerebral fibrin deposition and neuroinflammation. However, no clinically established PET tracer is available for imaging cerebral fibrin. This study evaluated a novel 64Cu-labeled fibrin-targeted PET tracer for detecting fibrin-associated vascular pathology in AD.

Method

A DOTA-conjugated fibrin-targeting ligand was radiolabeled with 64Cu and characterized by radio-HPLC and radio-TLC. Radiochemical stability and pharmacokinetics were evaluated. PET imaging was performed in transgenic AD mice and wild-type controls. Ex vivo autoradiography was conducted using postmortem human brain tissues from AD patients and non-demented controls, with quantitative analysis of the frontal cortex and hippocampus.

Results

64Cu-fibrin was synthesized with radiochemical purity exceeding 95% and remained stable for 24 h. Pharmacokinetic analysis demonstrated prolonged biphasic blood clearance. PET imaging showed significantly higher brain uptake in AD mice, particularly in the frontal cortex and hippocampus. Autoradiography confirmed increased tracer binding in human AD tissues, with signal intensities approximately 1.83-fold higher in the frontal cortex and 2.04-fold higher in the hippocampus than in control brains.

Conclusion

64Cu-fibrin enables visualization of fibrin-associated cerebrovascular pathology in both AD mice and human brain tissues, supporting its potential as a complementary PET biomarker for assessing vascular dysfunction in Alzheimer's disease.

口頭論文 臨床組 10:50–11:30 第四會議室 OC1

原著論文 臨床診斷

Hopkins versus Deauville Scoring on FDG PET for Esophageal Cancer Response after CCRT

[1]鄭雯欣, [1]張雁翔
[1]高雄長庚醫院
發表者 鄭雯欣

Keywords 分子影像

Background

To compare Hopkins criteria and Deauville 5-point scale (DS) in post-CCRT FDG PET for predicting pathologic complete response (pCR) in esophageal cancer.

Method

Thirty-two consecutive esophageal cancer patients who received CCRT and post-therapy FDG PET in 2025 were retrospectively reviewed. PET images were scored using Hopkins criteria and DS. Pathologic findings or clinical and imaging follow-up served as the reference standard.

Results

Eleven patients had residual tumor; 21 achieved pCR. DS showed higher sensitivity (90.9% vs. 72.7%) but lower specificity (66.7% vs. 90.5%). Accuracy favored Hopkins (84.4% vs. 75.0%). Both criteria significantly predicted outcomes ($p=0.002$ and $p < 0.001$, respectively). McNemar test revealed systematic disagreement ($p=0.016$): DS classified 7 extra cases as positive. PPV favored Hopkins (80.0% vs. 58.8%); NPV favored DS (93.3% vs. 86.4%).

Conclusion

Hopkins criteria is more reliable for predicting pCR, whereas DS is more sensitive for detecting residual tumor after CCRT.

口頭論文 臨床組 10:50–11:30 第四會議室 OC2

原著論文 臨床治療或診療合一

Clinical Profile and Biochemical Discordance in Initially Non–Radioiodine-Avid Metastatic Differentiated Thyroid Cancer

[1]楊因因, [1]王佩文, [1]張雁翔

[1]高雄長庚醫院

發表者 楊因因

Keywords 分子影像

Background

Radioiodine (RAI) therapy is a standard treatment for metastatic differentiated thyroid cancer (DTC). However, a subset of patients presents with distant metastases that are non–RAI-avid at initial evaluation, challenging disease assessment and management. This study aimed to characterize the clinicopathological features of this population, with particular emphasis on the relationship between tumor burden and biochemical markers.

Method

We retrospectively reviewed 38 consecutive DTC patients with distant metastases treated between 2012 and 2025. Patients were classified as non–RAI-avid (n = 20) or RAI-avid (n = 18) based on initial post-therapeutic whole-body scans. Demographic characteristics, tumor features, metastatic patterns, and stimulated serum thyroglobulin (Tg) levels were compared between groups.

Results

Several aggressive clinicopathological features were significantly more common in the non–RAI-avid group, including male sex (50% vs. 16.7%, p = 0.04), classic papillary thyroid carcinoma histology (55% vs. 5.6%, p = 0.001), gross extrathyroidal extension (T3b–T4: 60% vs. 16.7%, p = 0.001), and lymph node metastases (85% vs. 27.8%, p = 0.001). With respect to tumor burden, patients in the non–RAI-avid group had larger primary tumors (median diameter 3.4 cm vs. 1.8 cm, p = 0.20) and had a tendency to multi-organ distant metastases (60% vs. 38.9%, p = 0.19). Notably, despite the higher prevalence of aggressive local disease, stimulated serum Tg levels tended to be lower in the non–RAI-avid group compared with the RAI-avid group (median 69 ng/mL vs. 469 ng/mL, p = 0.136).

Conclusion

Patients with initially non–RAI-avid metastatic DTC frequently present with aggressive pathological features, including gross extrathyroidal extension and extensive nodal involvement. The observed discordance between substantial structural disease and relatively lower serum Tg levels, although not statistically significant, may reflect impaired tumor differentiation and reduced Tg-secreting capacity. This potential biochemical–structural mismatch limits the utility of Tg as a surrogate marker of disease burden in non–RAI-avid DTC and supports closer clinical monitoring and earlier consideration of alternative therapeutic approaches.

口頭論文 臨床組 10:50–11:30 第四會議室 OC3

原著論文 臨床診斷

Occipital Perfusion is Relatively Preserved as Cognition Declines on Cerebral Perfusion SPECT: A Compensatory Hypothesis in Lewy Body Disease

[1]郭之凡, [1]洪光威, [1]黃文盛, [2]曾聖彬, [2]楊惠絜, [2]倪于晴, [3]邱百誼

[1]彰濱秀傳紀念醫院
[2]國家原子能科技研究院
[3]秀傳紀念醫院

發表者 郭之凡

Keywords 分子影像 | 影像處理 / 軟體 | 定量分析 | 失智症 | 枕葉低灌流

Background

Occipital hypoperfusion is a characteristic SPECT finding in Lewy body disease. Although cognitive decline generally accompanies progressive whole-brain hypoperfusion, we observed on visual reading that occipital hypoperfusion appeared paradoxically less prominent in more impaired patients. We hypothesized that this reflects perfusion compensation for failing visuospatial networks, which is still not well recognized.

Method

Cerebral perfusion SPECT from 464 patients with Lewy body disease was processed using ECDaim to generate Z-score maps referenced to a normal database. Hypoperfusion extent (proportion of voxels with Z-score > 2) was calculated. Cognitive Abilities Screening Instrument (CASI) scores were related to global extent by Spearman correlation, and to occipital extent by linear regression adjusted for global extent.

Results

Global extent correlated negatively with CASI ($\rho = -0.206$, $p < 0.001$). After adjustment for global extent, however, higher CASI was associated with greater occipital extent (standardized $\beta = 0.118$, $p < 0.001$).

Conclusion

Contrary to the expected global decline, occipital perfusion was relatively preserved in patients with worse cognition, consistent with a compensatory perfusion mechanism.

口頭論文 臨床組 10:50–11:30 第四會議室 OC4

原著論文 臨床診斷

Longitudinal Brain FDG PET Demonstrates Treatment-Associated Prefrontal Metabolic Decline in Patients with Esophageal Cancer: Impact of Normalization Strategy

[1]王建程

[1]中山醫大附設醫院

Keywords 定量分析 | 影像處理/軟體 | 病人安全 | 危險因子

Background

Cancer-related cognitive impairment has been associated with altered cerebral glucose metabolism after systemic anticancer therapy. However, longitudinal brain FDG PET data in patients with esophageal cancer remain limited, and the influence of image normalization on the detection of treatment-associated metabolic changes is uncertain. This study investigated longitudinal cortical metabolic changes in patients with esophageal cancer and evaluated the impact of different normalization strategies.

Method

This retrospective study included 78 patients with esophageal cancer who underwent two FDG PET examinations encompassing their documented chemotherapy period. Patients with structural or neurodegenerative brain disease, intracranial malignancy, brain radiotherapy, or exposure to chemotherapy for other malignancies were excluded. Cortical uptake was quantified using automated ROI-based analysis and expressed as database-referenced Z scores normalized to global brain, pons, or cerebellar uptake. Exploratory whole-brain ROI analysis was followed by construction of an anatomically defined bilateral prefrontal composite comprising the bilateral lateral and medial prefrontal cortices. Pre- and post-treatment composites were compared using paired tests. Agreement in patient-level changes across normalization strategies was assessed using Spearman correlation. A two-factor repeated-measures ANOVA evaluated the effects of time, normalization, and their interaction, followed by Holm-adjusted pairwise comparisons.

Results

Global normalization demonstrated significant post-treatment reductions in all four prefrontal ROIs and the left anterior cingulate cortex. The global-normalized bilateral prefrontal composite decreased from −1.38 to −1.88, with a mean change of −0.505 (95% CI, −0.752 to −0.258; t=4.07, p<0.001; Cohen’ s d=0.461). The pons-normalized composite showed a smaller, nonsignificant decline (mean change, −0.225; p=0.063), whereas cerebellar normalization showed minimal change (mean change, −0.088; Wilcoxon p=0.615). Composite changes remained moderately to strongly correlated across normalization methods (ρ=0.577–0.793, all p<0.001). A significant time-by-normalization interaction was observed (Greenhouse–Geisser-corrected F=10.72, p<0.001, partial η^2=0.122). Global normalization yielded a greater decline than pons normalization (Holm-adjusted p=0.027) and cerebellar normalization (p<0.001). Chemotherapy duration showed weak inverse correlations with composite changes across all normalization strategies, but none reached statistical significance.

Conclusion

Longitudinal FDG PET demonstrated treatment-associated prefrontal metabolic decline in patients with esophageal cancer. Although patient-level changes were correlated across normalization methods, their measured magnitude and statistical detectability differed significantly. Global normalization produced the most pronounced and spatially coherent prefrontal changes in this cohort, whereas calendar-based chemotherapy duration did not adequately explain individual metabolic decline.

口頭論文 臨床組 13:30–14:10 第四會議室 OC5

原著論文 臨床診斷

Technical Validation of a Thyroid Uptake Probe as an Alternative to a Well-Type r-Counter for MAG3 clearance in Tc99m-MAG3 Renal Scintigraphy: A Preliminary Study

[1]侯景維, [1]王心怡, [1]蔡世傳, [1]劉家寧, [1]林宜瀞

[1]臺中榮民總醫院

發表者 劉家寧

Keywords 造影儀器

Background

Single-sample plasma clearance of Tc-99m MAG3 conventionally requires a well-type γ-counter, which entails dedicated quality-control procedures and considerable maintenance costs. We investigated whether a widely available thyroid uptake (TU) probe could serve as an alternative counting device, and additionally compared plasma-based clearance with a camera-based method.

Method

In Phase 1, twelve Tc-99m standards (0.025–1 μCi, in duplicate) were counted on both a well-type γ-counter and a TU probe (Biodex Atomlab 950) at a fixed 18-cm geometry to derive a cross-calibration factor by linear regression. In Phase 2, we retrospectively analyzed 16 patients undergoing Tc-99m MAG3 renography with a single 44-minute plasma sample. Each plasma sample was counted on both systems, and clearance was calculated using the Tauxe single-sample formula. Agreement was assessed by Bland–Altman analysis and Lin's concordance correlation coefficient (CCC). Camera-based clearance was compared with the plasma-sampling method, with subgroup analysis by CKD stage.

Results

Cross-calibration showed excellent linearity (R^2 = 0.9991) with proportional-type error of approximately ±3%. Converted counts from the two systems agreed closely (mean difference +0.54%; 95% limits of agreement, −8.8% to +9.9%; CCC = 0.987). At the clearance level, agreement remained high (CCC = 0.984) with a small systematic difference of −3.62%. In contrast, camera-based clearance correlated moderately with the plasma method (r = 0.801) but systematically underestimated clearance by a mean of 30.1%; the underestimation was larger in CKD stage III–V patients (44.3%) than in stage I–II patients (19.1%).

Conclusion

With simple cross-calibration, a TU probe can replace a well-type γ-counter for single-sample MAG3 clearance measurement, reducing equipment maintenance costs. Camera-based clearance correlates well with the plasma method but systematically underestimates clearance, particularly in patients with impaired renal function, warranting caution in clinical interpretation.

口頭論文 臨床組 | 13:30–14:10 | 第四會議室 | OC6

統合分析 | 臨床診斷

探討淋巴造影肢體影像在乳癌轉移之應用

[1]張春梅, [2]陳佳惠

[1]高雄榮民總醫院
[2]義守大學醫學影像暨放射科學系

Keywords 乳癌 | 淋巴掃描 | 鎝 -99m phytat

Background

手部表皮淺層 (皮下或組織間隙) 注**射微量**放射性同位素（(Tc-99m phytate)，藉由淋巴系統吸收並引流，再用伽瑪攝影儀拍攝影像，主要用來評估肢體淋巴水腫及診斷淋巴管阻塞。本研究分析核醫肢體淋巴造影偵測結果，提供術後併發症較佳的治療方針。

Method

回溯性收集高雄榮總 2024 年 08 月至 2026 年 07 月，實施Lymphoscintigraphy共有 452 例，其中手部淋巴攝影有 54 例。使用excel分析。女性占 94.4%（51 人），男性占 5.6%。年齡跨度為 27 至 83 歲，平均年齡為 57.5 歲，主要集中於 45–65 歲中壯年族群。

Results

統計 2024 年 08 月至 2026 年 07 月，實施Lymphoscintigraphy共 54 例。依據台灣淋巴攝影分期（Taiwan Lymphoscintigraphy Staging, TLS）分級彙整。正常：主淋巴管與近端淋巴結清晰顯影，無皮下逆流 (6 例)；輕度局部阻塞：淋巴結數量減少，無皮下逆流 (15例)；中度局部阻塞：淋巴管擴張或顯影減少，伴隨局部 / 遠端皮下逆流 (25 例)；重度局部阻塞：主淋巴管顯影極差或缺失，伴廣泛 / 整條肢體皮下逆流 (6 例)；完全阻塞：近端淋巴結完全未顯影，嚴重皮下逆流或放射性同位素滯留注射處 (5 例)。乳癌術後（上肢水腫）：占整體案例 88% 以上，多為乳癌切除術（MRM/BCS）伴隨腋下淋巴結清掃後引發。婦科與非乳癌腫瘤：包含子宮頸癌、子宮內膜癌術後引發之雙/ 單下肢水腫；以及四期肺癌接受放化療後引發之左上肢水腫。原發 / 長期水腫：73歲男性，具 40 年以上右下肢長期水腫史。術後追蹤案例：部分患者報告中載明已接受淋巴靜脈吻合術（LVA）。雙側評估案例：包含雙側肢體之個別 TLS 分期紀錄（LLE: P-2 / RLE: P-1；LLE: L-0 / RLE: T-6）。

Conclusion

以乳癌切除腋下淋巴結後引發的上肢淋巴水腫（RUE/LUE）為大宗，少數包含婦科癌症（子宮頸癌、子宮內膜癌）、肺癌放化療後以及原發性 / 長期下肢水腫。淋巴水腫的復健之路，對乳癌存活者而言，是一生持續關注與管理的重要課題。期待核醫臨床影像及新科技的研發，能為乳癌存活者帶來更即時、個人化與專業照護選擇，更進一步改善其生活品質。

口頭論文 臨床組

13:30–14:10 第四會議室 OC7

原著論文 臨床診斷

Dynamic 18F-Flutemetamol PET for Differentiating Cardiac Amyloidosis Subtypes and Pre-Clinical TTR Carriers

[1]李婷嫣, [1]陳怡潔, [1]黃奕琿, [1]洪益欣, [1]趙啟超, [1]林彥宏, [1]鄭媚方

[1]臺大醫院

發表者 李婷嫣

Keywords 分子影像 | 定量分析

Background

Cardiac amyloidosis (CA) primarily comprises transthyretin (ATTR) and light-chain (AL) subtypes. Although bone-seeking SPECT agents and amyloid-specific PET tracers hold significant promise for subtype differentiation, non-invasive identification profiling for asymptomatic TTR mutation carriers has not yet been established. Here, we investigated whether kinetic model-based dynamic 18F-flutemetamol (FMM) PET can serve as a robust imaging biomarker to distinguish CA subtypes and identify pre-symptomatic TTR carriers.

Method

Between July 2025 and May 2026, 16 predominantly biopsy-proven subjects (mean age, 64.6; 10 males, 6 females) were prospectively enrolled, comprising patients with ATTR-CM (hereditary, n = 7; wild-type, n = 2), AL amyloidosis (n = 2), TTR mutation carriers (n = 4), and one healthy control. All participants underwent standardized 99mTc-pyrophosphate (PYP) scintigraphy and dynamic 18F-FMM imaging. A 30-minute dynamic 18F-FMM PET acquisition was performed following the injection of 5 mCi of the radiotracer. The heart-to-contralateral lung (H/CL) ratio and visual score was derived from 3-hour PYP images. Myocardial standardized uptake values (SUV), myocardial-to-background ratios (MBR), and retention fractions (RF) were measured at 10, 20, and 30 minutes. The retention index (RI) was calculated from time-activity curves. Statistical significance was assessed via the Kruskal-Wallis test with post-hoc pairwise comparisons.

Results

On PYP imaging, the H/CL ratio was significantly higher in the ATTR-CM group compared to TTR carriers (1.48 [1.30–2.04] vs. 1.18 [1.08–1.30], p = 0.020), and trended higher than the AL group, though lacking statistical significance (1.48 [1.30–2.04] vs. 1.27 [1.17-1.37], p = 0.553), and visual scoring exhibited an identical trend. For FMM imaging, inter-group differences were significant across all time points for both SUVs and RFs. Compared to TTR carriers, the AL group exhibited significantly higher SUVs (5.55 [5.32–5.77] vs. 0.94 [0.84–1.67], 4.22 [3.05–5.39] vs. 0.34 [0.30–0.82], 3.78 [2.28–5.28] vs. 0.24 [0.19–0.71] at 10, 20, 30 minute respectively, allp < 0.05) and RFs (79.2 [61-97] vs. 18.15 [15-31], 65.6 [32-99] vs. 6.9 [5-15], 60.95 [24-98] vs. 5.3 [3-13]). The retention index effectively distinguished TTR carriers from both AL patients (0.02 [0.02–0.03] vs. 0.10 [0.05–0.15], p = 0.047) and the ATTR-CM group (0.02 [0.02–0.03] vs. 0.04 [0.03–0.10], p = 0.047). Conversely, the MBR showed no significant difference among the cohorts (ATTRCM, TTR carrier, and AL: 1.50 [1.24-3.00], 1.51 [1.22-1.65], 2.86 [2.11-3.60], p = 0.231).

Conclusion

Dynamic 18F-FMM PET may provide pharmacokinetic quantification (SUV, RF, and RI) to help differentiate AL amyloidosis from pre-symptomatic carriers, while the retention index may help marginally distinguish the ATTR-CM from carriers.

口頭論文 臨床組 13:30–14:10 第四會議室 OC8

經驗分享

放射性藥物調劑錯誤事件之根本原因分析與矯正措施

[1]許耘萱, [1]邱育琪, [1]何志豪, [1]蘇博仁, [1]林明佳, [1]陳輝墉

[1]義大醫院

發表者 許耘萱

Keywords 放射性藥物 | 根本原因分析 | 瑞士乳酪模型

Background

以一起核醫放射性藥物誤用事件為案例，透過根本原因分析（Root Cause Analysis, RCA）、事件時間軸重建、標準作業程序（Standard Operating Procedure, SOP）差異分析及瑞士乳酪模型（Swiss Cheese Model）辨識事件過程中之防護屏障失效，建立「根本原因 — 矯正措施 — 成效指標」架構，作為核醫藥物調劑持續風險控制機制。

Method

本研究採單一事件回溯性案例分析。以一名接受心肌灌注掃描之病人所發生的放射性藥物誤用事件。首先重建事件時間軸，並將實際作業流程與既定 SOP 逐項比對進行差異分析；其次利用RCA 分析人員、設備／環境、藥品／物料、流程／制度等因素，再以瑞士乳酪模型檢視各層級防護屏障之失效情形。最後依根因提出對應改善措施，並以教育訓練完成率、雙人核對率、條碼辨識執行率、異常事件發生率及追蹤期間之作業件數等指標評估改善結果。

標準作業程序與事件差異分析

1. 放射性藥物 / 放射性核種供應商交付: 廠商同時交付兩種外包裝類似藥物 (標示不明確)。

2. 核醫藥師與藥商人員應當面對點藥物劑量、數量、簽收 (時間、人員): 僅口頭複誦確認，未確實進行簽收單簽認。

3. 藥師於同時間應只調劑單一藥物: 同時混用兩種外包裝類似藥物作調劑。

4. 完成調劑作業、交付使用: 依SOP執行。

5. 掃描檢查作業: 經放射師作影像掃描時，發現影像異常。

經魚骨圖分析，從人、機、料、法 4 構面探討異常原因發現:(1) 廠商藥品包裝與標示缺乏明顯辨識性、(2) 放射性藥物未落實雙人即時核對機制、(3)SOP執行與稽核制度不足 (4) 人員教育訓練與能力評核機制不完整 (5) 生物安全操作櫃（Biological Safety Cabinet, BSC）照明不足

擬定改善對策

對策 1 檢討廠商交貨與對接 / 簽認流程。

對策 2 盤點、檢視核醫藥師相關作業SOP:制定「核醫藥師訓練及評核標準作業程序書」。

對策 3 增加BSC內部照明燈具。

對策 4 造成病人意外曝露，評估增加罹患癌症風險度程序。

對策改善成效

成效 1. 經建立雙重簽認制度、要求廠商實施「專罐專用」管理機制、增加條碼辨識機制；實施後未再發生異常。

成效 2. 制定並實施核醫藥師訓練計畫；並強調新進藥師訓練計畫書中要項及評核 / 定期再評核機制。依據SOP完成訓練，且經評核通過；經半年後執行再度通過評核。成效 3. 增加BSC照明燈具提升視野明亮度，降低眼睛疲勞。

成效 4. 以 xrayrisk.com進行病人罹患增加癌症風險度評估，經輸入相關參數評估結果，風險增加機率為 0 %。

Conclusion

核醫放射性藥物調劑錯誤多屬複合型系統安全事件，其形成原因往往來自多重防護層失效，而非單一個人疏失。RCA 方法有助於辨識潛在組織管理與流程設計缺陷。建立高可靠度核醫製藥安全系統，包括標準化驗證程序、資訊化管理及病人安全文化，對降低放射性藥物事件發生率具有重要意義。

口頭論文 臨床組 13:30–14:10 第四會議室 OC9

原著論文 非診療之臨床相關主題

Radiation Risk Perception and Acceptance of Advanced Liquid Processing System (ALPS)-Treated Water among Medical Students in Taiwan and Japan

[1]王妤珊, [2]松永妃都美, [2]高村昇, [1]林立凡

[1]三軍總醫院核子醫學部

[2]日本長崎大學原爆後障害研究所

發表者 王妤珊

Keywords Radiation Safety | Risk Perception | Treated Water

Background

The discharge of Advanced Liquid Processing System (ALPS)-treated water from the Fukushima Daiichi Nuclear Power Station poses an important challenge in radiation risk communication. Although international assessments have indicated negligible radiological impacts, public perceptions and concerns vary across regions. Understanding how medical students, as future healthcare professionals, perceive radiation-related risks is essential for effective science communication and informed decision-making.

Method

A questionnaire-based survey was conducted among 1,120 medical students from Taiwan (n = 323) and Japan (n = 797) to explore perspectives on ALPS-treated water. Responses regarding radiation-related perceptions and attitudes were collected for comparative analysis.

Results

Acceptance of ALPS-treated water was substantially higher among Japanese medical students than among Taiwanese medical students (89.2% vs. 51.1%). The pattern of factors associated with acceptance also differed between the two countries. In Taiwan, acceptance was more closely related to knowledge engagement and information-seeking behavior, whereas in Japan, governmental and regulatory trust played a more prominent role. These findings suggest a knowledge–attitude gap among Taiwanese medical students, in whom greater engagement with technical information did not necessarily correspond to a level of acceptance comparable with that observed in Japan.

Conclusion

Medical students in Taiwan and Japan showed marked differences in acceptance of ALPS-treated water and in the factors associated with their perceptions. The findings underscore the importance of understanding regional differences in radiation risk perception to improve communication strategies for environmental health concerns.

INDEX

壁報論文索引

PB 基礎組、PC 臨床組，依編號排列；點選編號或題目可跳至該篇摘要

編號	題目	發表者	頁
PB-001	Production Strategies for FAPI-Based PET Tracers: A Radiochemical Comparison of […	邱晉宏	79
PB-002	高齡化與 80歲以上核醫資源佔比之趨勢研究	李怡旻	80
PB-003	財政管制壓力下的常規影像門診化移轉：台灣 TW-DRG 制度對全身骨骼掃描利用率衝擊…	李怡旻	81
PB-004	輕柔影像運動對兒童核醫利用的影響	李怡旻	82
PB-005	能力試驗的檢體在保存條件穩定下是否有臨床可應用價值	顏慧婷	83
PB-006	巨量資料分析中統計顯著與臨床實質差異之探討：以 21 年核子醫學檢查基線特徵為例	李怡旻	84
PB-007	Implementation of [18F]FET Production in a Taiwanese Radiopharmaceutical Plant: …	孟凡傑	85
PB-008	RIA 實驗室I-125 放射性廢水儲放管理與排放策略評估研究 -以南部某醫院核醫科為例	卓世傑	86
PB-009	Quality Risk Management in Process Changes and Validation of Ga-68-CXCR4-Like an…	林欣純	87
PB-010	Identification of Consistent Neuroimaging Biomarkers for Predicting Mild Cognitive I…	曾聖彬	88
PB-011	PEGylation of Boronotryptophan Improves Injectable Formulation and Boron Accu…	陳祥平	89
PB-012	Multitask 3D Residual Attention U-Net for Brain Parcellation Using T1W MRI and CT	林珺媛	90
PB-013	Deep Learning-Based Volumetric Synthesis of 99mTc-MAA Liver SPECT from Two Ort…	王佳柔	91
PB-014	放射免疫分析實驗室品質指標之建立與成效分析	郭珮怡	92
PB-015	新進輻射工作人員劑量計遺失改善矯正計畫	陳輝墉	93
PB-016	[^{68}Ga]NOTA-Tri-mannose作為腫瘤相關巨噬細胞正子影像探針之研究	詹振勳	94
PB-017	放射免疫分析實驗室 Counter污染事件之原因分析與雙重背景值監測改善成效	王安美	95
PB-018	Comparison of two FAPI –based PET tracers: Preclinical Evaluation of [18F]AlF- and […	黎昱璇	96
PB-019	Longitudinal [18F]Florbetaben PET/MR Imaging Reveals Reduced Amyloid Burden a…	陳穎柔	97
PB-020	TBDD於Alpha核素治療之動態體內劑量評估：整合Parent–Daughter Kinetics與再分布…	楊詩涵	98
PB-021	MIM多參數定量分析於 ^18F-Flutemetamol 類澱粉正子斷層造影之臨床附加價值：全域…	羅浚哲	99
PB-022	Taguchi Optimization of TLD-100H Readout Parameters for Radiation Dose Assessm…	黃琪雯	100
PB-023	Full Factorial Optimization of TLD Readout for Environmental Radiation Monitoring i…	黃琪雯	101
PB-024	極簡化骨質疏鬆風險評估：BMI 與核心骨折史的預測力	李怡旻	102
PB-025	Applications of Radiomics: From Basic Research to Clinical Practice—Practical Tips a…	陳至豪	103
PB-026	Machine learning using dynamic frames for reduced acquisition time in Tc-99m bone…	李昕迪	104
PB-027	Radiomics-based quality assurance of gamma camera uniformity	李昕迪	105
PB-028	Serial SPECT/CT-Based Patient-Specific Organ and Lesion Dosimetry Following ^177…	方怡珺	106
PB-029	在18F-FDG PET/CT上使用OncoFreeze AI技術在肺部病灶的統計攝取參數與無使用OncoF…	曾柏銘	107
PB-030	使用EQ PET讓不同正子儀器間的SUV具有共同一致性標準	曾柏銘	108
PB-031	實施Tw-DRG制度對心肌灌注掃描門住診轉移之衝擊	李怡旻	109
PB-032	FT4 RIA試劑中 Ligand 與 Tracer 添加順序對分析結果之差異	王怡文	110

壁報論文索引（續）

編號	題目	發表者	頁
PC-001	固態胃排空掃描之技術陷阱：食道清除延遲導致之異常數據分析與病例討論	陳怡如	111
PC-002	PET/CT中光電倍增管故障假影之延伸研究:單一與雙模組異常之比較	吳麗君	112
PC-003	第二次延長掃描排除直腸FDG假陽性攝取：PET/CT病例報告	李將瑄	113
PC-004	生化復發且骨掃描穩定之攝護腺癌病人：rhPSMA PET發現隱匿性骨轉移病例報告	王嘉鴻	114
PC-005	Rare Streak Artifact on CT Images in an Obese Patient During PET/CT Imaging: A Cas…	蘇于婷	115
PC-006	Tubular Adenoma在18F-FDG PETCT 之影像表現	李佩璇	116
PC-007	Combining the prognostic values of 18F-FDG PET features with clinical variables usi…	陳昱宏	117
PC-008	探討巨大肝囊腫於MDCT與Tl-201心肌灌注掃描之影像特徵一致性	游慧貞	118
PC-009	Multimodality Nuclear Medicine Imaging of Active Heterotopic Ossification Followin…	莊紫翎	119
PC-010	Five-Toe Socks Sign on FDG PET/CT	莊紫翎	120
PC-011	Prefrontal Hypoperfusion and Limbic Hyperactivity in Treatment-Resistant Schizoaff…	莊紫翎	121
PC-012	Clinical Utility of Hepatic Arterial Perfusion Imaging in Patients with Advanced Hepat…	游冬齡	122
PC-013	The Role of FDG PET/CT in the Diagnosis of Intramedullary Spinal Cord Metastases fr…	游冬齡	123
PC-014	放射免疫室 I-125 操作人員輻射安全資格評估與管理優化	方雅潔	124
PC-015	Thoracic Rotation Causes Misclassification of the Heart-to-Contralateral Lung Ratio …	陳至豪	125
PC-016	18F-FDG PET radiomic features are associated with “spread through air space” in …	陳昱宏	126
PC-017	三相式骨骼造影意外發現主動脈瘤	朱秀蘭	127
PC-018	Lu-177 PSMA 治療相關醫療人員之職業輻射曝露：實證導向文獻回顧	黃兆駿	128
PC-019	Evaluating Post-Treatment Brain Neoplasms with Thallium Scan	游舜宇	129
PC-020	暫時性瀰漫性肝臟放射性攝取於乳癌患者 Tc-99m RBC MUGA 追蹤檢查 -病例報告	王榛婷	130
PC-021	鐳-177 治療給藥方式對核醫工作人員各職類輻射劑量之影響：重力法與幫浦輸注系統之…	林亭君	131
PC-022	核子醫學臨床排程登記系統之建置與行政作業效益評估	羅浚哲	132
PC-023	Parotid gland metastasis from carcinoma of the breast: detection with F-18 FDG PET/…	黃柏濤	133
PC-024	常規 2 mCi 鉈-201 心肌灌注影像與配對 3 mCi 檢查的盲讀技術品質比較	黃俊穎	134
PC-025	核子醫學科排定檢查取消之五年分析：病患因素與低成本流程改善方向	郭彥伶	135
PC-026	Oncocytic adenoma of thyroid initially presented as incidentally tumor with extrem…	李昕迪	136
PC-027	不同數位教學模式對醫事放射實習學生輻射污染處置能力之教育成效評估	龔瑞英	137
PC-028	原發性醛固酮症之實驗室診斷流程—右側腎上腺腺瘤個案	張素雲	138
PC-029	Dual-time-point FDG PET/CT for differentiating vaccination induced axillary inflamm…	楊舒雅	139
PC-030	近兩年放射免疫分析異常值簡訊處置率之比較	廖建國	140
PC-031	嚴重正子藥物滲漏對標準攝取值之影響-重新造影個案分析	林友琮	141
PC-032	下肢淋巴閃爍造影中左側鎖骨上及腋下區異常顯影	陳薇璇	142
PC-033	Polyostotic Fibrous Dysplasia With Pathological Femoral Fracture (McCune Albright …	盧淑玫	143
PC-034	2025年精神科患者甲狀腺功能、葉酸及維生素B12檢驗異常之盛行率分析： 北部某醫學…	蕭如妏	144
PC-035	BECKMAN試劑 FT4與FT4 Plus比較	韓璞	145

壁報論文索引（續）

編號	題目	發表者	頁
PC-036	細胞保存液之檢體檢測BECKMAN PTH試劑	韓璞	146
PC-037	放射免疫分析TSH試劑使用效率分析及庫存管理	黃筱崴	147
PC-038	Lu-177 PSMA治療後尿布廢棄物之輻射劑量率衰減與儲存時間評估	董韋銓	148
PC-039	流程再設計縮短一日法心肌灌注造影檢查時間之成效	張焯婷	149
PC-040	Intense 18F-FDG Uptake in Gouty Tophi: A Potential Diagnostic Pitfall in Therapeutic …	陳怡勳	150
PC-041	A retrospective study on radiation dose assessment for Patients and Medical Staff in …	俞長青	151
PC-042	降低糖尿病患者腸道 FDG攝取對影像之影響	江泰林	152
PC-043	Diagnostic Efficacy and Clinical Utility of Nuclear Medicine Perfusion Scanning for Su…	吳俊昌	153
PC-044	藥師於核醫放射配體治療臨床試驗之實務角色與跨專業團隊合作	洪綾蔓	154
PC-045	Discordance Between Serum PSA and PSMA PET/CT–Defined Disease Burden Across …	詹宏彬	155
PC-046	Ga-67在良性黃體囊腫病變異常攝取之病例報告	林昱璁	156
PC-047	乳癌患者頸椎C1破壞性病灶之影像診斷誤差：細胞型神經鞘瘤於骨骼掃描及18F-FDG PE…	林昱璁	157
PC-048	Differential association between salivary gland scintigraphy functional parameters a…	王昱豐	158
PC-049	從護理實務探討 Tc-99m MDP 骨骼掃描於手腕注射之放射性藥物滲漏風險	王苡安	159
PC-050	Hot Hand 現象於Tc-99m MDP全身骨骼掃描之案例分析－護理注射品質討論與改進	王苡安	160
PC-051	FDG PET/CT Detects Occult Cholangiocarcinoma Presenting as Diffuse Peritoneal Ca…	陳朝榮	161
PC-052	PSMA PET/CT於攝護腺癌生化復發之骨盆淋巴結轉移：病理驗證與術後影像評估病例報告	蔡沛君	162
PC-053	以不同平臺軟體分析腎絲球過濾率	魏文祺	163
PC-054	Not Very Common Occurrence of Enchondroma in 99mTc MDP Bone Scintigraphy an…	蕭聿謙	164
PC-055	Rare Occurrence of Bone Metastasis of Distal Tibia without Cancer History in 99mTc …	蕭聿謙	165
PC-056	後腹膜膿瘍模擬惡性腫瘤之氟化去氧葡萄糖正子斷層造影表現	陳羿吟	166
PC-057	Diagnostic Value of Gallium-67 Scintigraphy and Bone Scan for Occult Infection Loca…	吳俊昌	167
PC-058	Primary Renal Lymphoma: Report of A Case	程紹智	168
PC-059	Early Post-Treatment Lu-177-PSMA Imaging: A Potential Biomarker of Treatment Res…	李佩瑛	169
PC-060	Diagnostic Yield of 18F-FDG PET/CT versus Contrast-Enhanced CT in Critically Ill Pati…	吳俊昌	170
PC-061	利用核醫分流/腹膜腔/胸膜腔掃描檢查腹膜透析滲漏之案例分享	童惠珊	171
PC-062	18F-rhPSMA-7.3 正子造影偵測攝護腺癌局部復發並導引放射治療：一病例報告	張佳琪	172
PC-063	Neurological sign in a breast cancer patient with multiple bony metastasis on 18F-F…	蔡季蓉	173
PC-064	不同排程系統對於心肌血流灌注造影檢查未完成率之影響	楊郁茹	174
PC-065	Pituitary Stalk Metastasis from Breast Cancer Presenting as Panhypopituitarism: The…	李哲皓	175
PC-066	Diagnostic Accuracy of 18F-FET PET in Brain Gliomas: A Meta-Analysis Stratified by T…	何宗穎	176
PC-067	同位素治療中心輻射廢棄物管理經驗分享	吳忠順	177
PC-068	Diagnostic Accuracy of Tc-99m-MAG3 Renal Scintigraphy for Detecting Acute Rejecti…	吳俊昌	178
PC-069	Diagnostic Accuracy, Advantages, and Limitations of Brain Death Scintigraphy Comp…	吳俊昌	179
PC-070	18F-FDG PET/CT Findings of Heterotopic Ossification Mimicking Malignancy	沈淑禎	180

壁報論文索引（續）

編號	題目	發表者	頁
PC-071	Incidental Detection of Early-Stage Ovarian Cancer on 18F-FDG PET/CT During a Heal…	沈淑禎	181
PC-072	Head-to-head Comparative Meta-analysis of 18F-FET PET vs. MRI and Other Imaging …	鄭如伶	182
PC-073	Sternal Bone Metastasis from Prostate Cancer Mimicking Ectopic Parathyroid Tissue …	丁意玲	183
PC-074	Feasibility and Personalized Dosimetry of [177Lu]Lu-DOTATATE Therapy in a Child wi…	徐丞	184
PC-075	Optimizing Tc-99m PYP Myocardial Imaging for ATTR-CM Diagnosis Through SPECT/…	黃琪雯	185
PC-076	18F-FDG PET/CT for Differentiating Hypopharyngeal and Cervical Esophageal Cancer…	黃琪雯	186
PC-077	台灣放射製藥專業人才核心能力與可信賴專業活動之建構:放射製藥人才之能力導向教育…	李庚穎	187
PC-078	Pulmonary Infarction Secondary to Lung Cancer Presenting with Concordant PET Ri…	郭建瑋	188
PC-079	治療後復發性神經母細胞瘤之 ^{18}F-FDOPA 與 ^{18}F-FDG PET/CT 影像表現不一致	羅浚哲	189
PC-080	Acute Cholecystitis During Lu-177 PSMA-617 Radioligand Therapy: A Case Report	柳侑昇	190
PC-081	Multimodality Nuclear Imaging for Intermittent Gastrointestinal Bleeding: A Case Re…	黃琪雯	191
PC-082	比較使用不同微量吸管TSH檢驗結果之差異	沈宜瑾	192
PC-083	全身骨骼掃描中膀胱 Donut Sign：兩病例報告	張秀瑛	193
PC-084	全身骨骼掃描中 Arterial Hand Sign 之影像表現：病例報告	張秀瑛	194
PC-085	三相骨掃描對於周邊軟組織發炎之特異性侷限與氟18葡萄糖正子電腦斷層掃描之輔助診…	籃瑋承	195
PC-086	The Osteoporosis Paradox in Men with Benign Prostatic Hyperplasia: Metabolic Synd…	陳保良	196
PC-087	18F-rhPSMAPET/CT於攝護腺癌術後生化復發之診斷與術後追蹤：病例報告	王雅萍	197
PC-088	放射師Gallium-67發炎掃描判讀教學：以感染性關節炎偵測定位為例	許幼青	198
PC-089	胰島素內分泌腫瘤病人接受同位素治療之照護經驗從單一個案到病房照護常規之建立	潘怡蓁	199
PC-090	乳癌術前插針定位對核醫前哨淋巴結定位檢查耗時之影響	黃美瑩	200
PC-091	Gallium-67狼瘡性腎炎造影於平面與SPECT/CT半定量分析之一致性比較	陳彥榕	201
PC-092	Visualization of the Liver on Nuclear Bone Scan in a Case of Clopidogrel-Induced He…	莊雅雯	202
PC-093	Normal-Organ [^{18}F]FDG Uptake in Metformin-Treated Patients with Type 2 Diabetes: …	黃文盛	203
PC-094	腦部多巴胺轉運體影像：人工 ROI 與自動量化分析之判讀一致性比較	呂麗如	204
PC-095	CT-Based Generation of Synthetic Bone Scintigraphy Images: A Proof-of-Concept Stu…	許祐寬	205
PC-096	核醫科品質指標分析工具P管制圖即時監控平台之開發與應用	張添信	206
PC-097	應用擬真情境演練提升核醫科急救應變技能之經驗分享	陳薇璇	207
PC-098	結合教學影片與情境模擬之核醫臺灣台語教學課程：實習生學習反應之初探	王苡安	208
PC-099	從擬真模擬競賽到臨床實踐：團隊資源管理與病人安全之經驗分享	陳薇璇	209
PC-100	轉移性去勢抗性攝護腺癌病人接受Radium-223治療之完成施打率探討	張添信	210
PC-101	運用目視化管理優化核醫檢查交班流程之經驗分享	陳薇璇	211
PC-102	結合AI衛教短影片於放射碘-131治療：提升病人輻射防護安全認知與放射師衛教給藥流程…	段玟卉	212
PC-103	運用HFMEA改善造影作業流程之成效分析	廖建國	213
PC-104	運用根本原因分析(RCA)改善核醫肺灌注檢查之靜脈外滲與藥物殘留	林至群	214
PC-105	醫事放射職類核子醫學領域可信賴專業活動(EPAs)於放射實習生之應用	張嘉容	215

壁報論文索引（續）

編號	題目	發表者	頁
PC-106	攝護腺癌患者在骨頭掃描及 18F-PSMA掃描中的轉移性超級掃描分享	許文齡	216
PC-107	Predictive Value of PSMA PET Radiomics for PSA Progression-Free Survival After Met…	黃玉儀	217
PC-108	Discovery of Diffuse Large B-Cell Lymphoma via Lymphoscintigraphy SPECT/CT in a …	曾昶深	218
PC-109	Clinical Utility of 18F-FDG PET/CT in Head and Neck Squamous Cell Carcinoma: Case…	許雅晴	219
PC-110	Code-less, LLM-Assisted Development of a Cross-Platform, HIS-Interoperable Struct…	李碧芳	220
PC-111	Comparative Safety and Real-World Survival Outcomes of 177Lu-PSMA-617 versus 1…	諶鴻遠	221
PC-112	臺灣五十年核子醫學研究發展：以 Web of Science Core Collection 收錄文獻為基礎之書…	郭之凡	222

壁報論文 基礎組

PB-001

原著論文

Production Strategies for FAPI-Based PET Tracers: A Radiochemical Comparison of [68Ga]FAPI-46 and [18F]FAPI-74

[2,1]邱晉宏, [2]簡御庭, [2]黃潔宜, [2]鄭媚方

[1]長庚大學
[2]臺大醫院

發表者 邱晉宏

Keywords 藥物開發 | 製藥

Background

The increasing clinical adoption of fibroblast activation protein inhibitor (FAPI) based PET imaging has created a growing need for production strategies that can accommodate different clinical service models. Generator produced [68Ga]FAPI tracers provide rapid on-site preparation for low-volume imaging, whereas cyclotron produced [18F]FAPI tracers enable larger batch production and regional distribution. However, practical radiochemical comparisons supporting these complementary implementation strategies remain limited.

Method

[68Ga]FAPI-46 and [18F]FAPI-74 were prepared as representative generator and cyclotron produced FAPI PET tracers, respectively, using automated synthesis modules (Modular-Lab eazy and Tracerlab FX-FDG). Three independent production runs were performed for each tracer. Production performance was evaluated by total synthesis time, end of synthesis activity, decay corrected radiochemical yield, and radiochemical purity. Radiochemical identity and purity were determined by radio HPLC and/or radio iTLC, with additional quality control including pH, residual solvents, radionuclide identity, and stability testing for 2 h and 4 h after synthesis for [68Ga]FAPI-46 and [18F]FAPI-74, respectively. Comparative analysis included synthesis time, usable activity after quality control, estimated patient doses per batch, and production characteristics relevant to on-site and centralized production models.

Results

Both [68Ga]FAPI-46 and [18F]FAPI-74 were successfully prepared in three independent production batches with reproducible radiochemical performance. The radiochemical yield was 61±4 % for [68Ga]FAPI-46 and 15±3 % for [18F]FAPI-74, respectively, while radiochemical purity exceeded 95 % for both tracers. Both products maintained acceptable radiochemical stability for up to 2 h ([68Ga]FAPI-46) and 4 h ([18F]FAPI-74). Despite comparable product quality, the two radionuclide platforms demonstrated distinct production characteristics. Generator-produced [68Ga]FAPI-46, with a maximum starting activity of approximately 35 mCi under the current production conditions, enabled rapid on-site preparation within approximately 20 min, achieving an end of synthesis activity of 740 MBq and supporting 1–3 patient doses per batch. In contrast, cyclotron-produced [18F]FAPI-74, with an initial activity of approximately 1 Ci under the current production conditions, required a longer production time (50 min) but achieved an end of synthesis activity of 3.7 GBq, supporting greater than 10 doses per batch. These complementary production characteristics support different operational requirements, with [68Ga]FAPI-46 favoring decentralized, low-volume production and [18F]FAPI-74 facilitating centralized manufacturing and regional distribution.

Conclusion

Our findings suggest that tracer selection should be determined not only by molecular design but also by production logistics and clinical service requirements. The complementary characteristics of generator and cyclotron produced FAPI tracers provide flexible solutions for molecular imaging centers with different production capacities and patient volumes.

壁報論文 基礎組

PB-002

原著論文

高齡化與 80歲以上核醫資源佔比之趨勢研究

[1]李怡旻, [1,2]莊紫翎

[1]大林慈濟醫院
[2]慈濟大學

發表者 李怡旻

Keywords 行政管理

Background

過往研究顯示人口結構的改變乃為驅使核子醫學科（以下簡稱核醫科）檢查需求上升的主要因素，然而隨著醫學的進步，平均餘命不斷上升，臨床上常見 80歲以上老年。這些高齡老人常有行動不便需攙扶、皮膚較薄增加輻射藥物注射難度等進而增加人員的工作負擔。本研究目的旨在探究80歲以上老年病人患者在過去 20年間的檢查量比例變化，並進一步預測未來五年比例，藉此展現人口老化對核醫檢查需求的實質衝擊。

Method

本研究為回溯性研究，資料來源為南部某準醫學中心核子醫學科檢查資料庫，資料期間為 2004 至2023 年。根據檢查日期及病人出生日期計算病人年齡，篩選出 80歲以上病人，並以每人每年一筆計算，因考量核醫 20 年總檢查量有增加的趨勢，因此本研究以標準化方式計算80歲以上病人核醫利用率（標準化利用率 = 80歲以上病人 / 全部核醫病人*100）。採用SAS® OnDemand f- or Academics進行資料處理與統計分析，以描述性統計顯示標準化核醫利用率，並以Jonckheere-Terpstra檢定（以下簡稱J-T檢定）時間和標準化核醫利用率間是否存在非線性趨勢，進一步建構 3年移動平均平滑模型以排除年度隨機雜訊並分離核心軌跡。預測效能透過歷史回測進行驗證，因 COVID-19 期間並非常規醫療利用波動，模型之平均絕對百分比誤差 (MAPE)為 16.62%，最終推估至2030年的前瞻需求。

Results

本研究以每人每年一筆計算共計 158,828筆，其中 80歲以上共有 12,876筆標準化核醫利用率，分別介於 2.69%~13.67%之間，20年間成長率高達408.18%。而J-T檢定結果顯示時間與標準化核醫利用率間存在非線性趨勢，且達統計顯著水準 (Z = 4.28, P < .001)，模型推估至 2030 年，該族群的資源配置率將由早期 2.69%增長至 12.15%。儘管受疫情干擾醫療利用（回測 MAPE = 16.62%，仍屬統計可接受良好預測範疇），但結果仍揭示高齡需求的持續攀升。

Conclusion

80歲以上病患在過去20年間標準化核醫利用率呈現爆炸性成長，未來幾年仍將持續上升。若以每日50位核醫檢查患者（含骨質密度檢查）推估每日病人中將有6位為80歲以上患者，無形中加重醫護同仁的工作負擔。本研究雖僅針對單一機構進行分析，然而台灣早已邁入高齡化社會，80歲以上患者大幅成長絕非單一機構經驗，故建議全台醫療機構應盡早規畫並訂定相關因應對策。

壁報論文 基礎組

PB-003

原著論文

財政管制壓力下的常規影像門診化移轉：台灣 TW-DRG 制度對全身骨骼掃描利用率衝擊之長期資料微觀實證研究

[2]李怡旻, [1,2]莊紫翎

[1]慈濟大學

[2]大林慈濟醫院

發表者 李怡旻

Keywords 行政管理

Background

全身骨骼掃描（以下簡稱骨骼掃描）是乳癌與攝護腺癌追蹤骨轉移的重要工具。雖然健保法規規範癌症病人住院免受限於 DRG 制度規範，然 2016 年全面引進ICD-10-PCS（外科處置碼）後，癌症病人一旦入院接受切除手術，該次住院仍會被歸類為外科 DRG案件而受到住院天數約束。臨床醫師為避免術前等待檢查而拉長住院天數，傾向將計畫性的骨骼掃描策略性地提前在門診完成。據此，本研究利用單一機構 14 年的長期數據，旨在分析 2016 年實施ICD-10-PCS後，住院期間骨骼掃描及正子造影之利用率的實際變動趨勢，並探討臨床端在健保財政壓力下的因應策略。

Method

本研究為縱貫性研究設計，資料來源為南部某準醫學中心 2009至 2023年核子醫學科檢查資料庫。此外，以同時期不受 DRG制度影響之正子造影檢查作為陰性對照 (Negative control)，有鑑於 ICD-10-PCS實施的期間為 2016年年初起，故依年度區分為實施前（2009–2015年）和實施後（2016–2023年）。以SAS® OnDemand for Academics進行資料處理與統計分析，以多元邏輯斯迴歸探究在控制年齡變項後實施 ICD-10-PCS對是否於住院期間進行檢查的影響，最終比較兩項檢查勝算比差異。

Results

本研究收錄骨骼掃描、PET檢查分別為 28,746筆、2,964筆。骨骼掃描檢查在實施前門、住院檢查的筆數分別為 9,865 (75.94%)、3,125 (24.06%)筆，實施後則分別為12,412 (78.78%)、3,344 (21.22%)筆，並達統計顯著差異(P < 0.001)。PET檢查在實施前門、住院檢查的筆數分別為 634 (84.65%)、115 (15.35%)筆，實施後則分別為 1,826 (82.81%)、379 (17.2%)筆，未達統計顯著差異。多元邏輯斯迴歸結果顯示實施後住院時進行骨骼掃描檢查的勝算比為 0.81 (P <0.001)，而年齡每增加一歲其住院進行骨骼掃描檢查的勝算比為 1.016 (P < 0.001)。而在 PET部分，顯示實施後住院時進行PET檢查的勝算比為 1.121未達統計顯著水準，年齡亦未達統計顯著水準。

Conclusion

2016年 ICD-10-PCS 制度實施後，住院骨骼掃描利用率顯著下降 19%，而陰性對照組 PET 則反向增長。此對比證實包裹支付政策能精準引導常規檢查門診化，同時揭示了前線醫療在財政壓力下仍堅守癌症照護的臨床剛性。本研究受限於 COVID-19 疫情對整體核醫量能的潛在干擾，且缺乏細部診斷碼以區分癌症分期與發炎病因。未來研究應納入特定疾病診斷架構，以更完整評估前線醫療在長期財政制約下的策略性行為調適。

壁報論文 基礎組

PB-004

原著論文

輕柔影像運動對兒童核醫利用的影響

[2]李怡旻, [1,2]莊紫翎

[1]慈濟大學

[2]大林慈濟醫院

發表者 李怡旻

Keywords 行政管理

Background

自 2008 年全球推廣「輕柔影像 (Image Gently)」運動以來，優化兒科輻射劑量與降低發育中組織的游離輻射風險已成為臨床共識。然而，此倡議對實際醫療處方行為的長期影響仍缺乏實證。本研究旨在探討兒科病患（≤ 18歲）核醫影像利用率之長期演變與差異。

Method

本研究為一項回溯性世代研究，擷取南部某準醫學中心核子醫學科自 2004 年至 2024 年核醫資訊管理系統資料，研究對象為檢查時未滿 18 歲之兒科病患。採用 SAS® OnDemand for Academics進行資料處理與統計分析。有鑑於本資料庫屬科室層級，無全院兒科就醫母群體資料，因此，研究結果為核醫檢查的每年數量。統計分析分為兩部分：(1) 以描述性統計 (Descriptive statistics)呈現研究對象之人口學特徵與年齡分佈；(2) 以年為時間單位，運用負二項式迴歸模型 (Negative Binomial Regression) 評估過去 20 年小兒核醫檢查總量之長期時間序列趨勢與 COVID-19 疫情造成的衝擊。

Results

共有 490 筆資料共計 330 位病人。平均年齡為 9.79 (6.56) 歲，男性為 168位 (50.91%)，平均每年23.33 (15.31) 件，2004–2024 年每年檢查總量如圖一。經負二項式迴歸分析顯示，小兒核醫檢查總量呈現顯著的逐年遞減趨勢，平均而言，每增加一年檢查總量顯著下降約 9.16% (Incidence Rate Ratio [IRR] = 0.9084，95% CI: 0.8695 – 0.949，P < 0.001)。而敏感性分析（2004–2019年）結果顯示，檢查量展現趨近顯著的緩步遞減趨勢 (P = 0.066)。

Conclusion

本研究證實，過去 20 年小兒核醫總量呈現顯著萎縮，暗示「輕柔影像(Image Gently)」等輻射防護倡議與無輻射替代檢查（如超音波、MRI）的普及，確實已成功帶動臨床決策的典範轉移。然而，受限於小兒核醫之基礎使用量原本即偏低（地板效應），此一政策發酵過程並非斷崖式驟跌，而以溫和的長期遞減呈現，直到 COVID-19疫情爆發，其醫療利用造成結構性斷層，且疫情後至今未見回升跡象。

壁報論文 基礎組 **PB-005**

經驗分享

能力試驗的檢體在保存條件穩定下是否有臨床可應用價值

[1]顏慧婷

[1]嘉義基督教醫院

Keywords 放射免疫分析

Background

能力試驗為臨床常使用的測試方式去了解各種儀器及方法且提供可比較的數據，外部品質比對也可為精確度調查。通常能力試驗樣本只拿來當作一次性使用，此次我們以RANDOX為主軸去比較冷凍保存樣本進行解凍後的測試，樣本穩定度為何?

Method

1. 所有RANDOX能力試驗樣本皆由當日泡製完成操作後，分裝於尖頭離心管中放置於-80°C冷凍保存。

2.RANDOX的樣本收集2024年1-12月、2025年1-12月及2026隨機抽兩個月進行測試。

3.AFP、CEA兩項由RIA方法操作得到數值，四項CA125、CA153、CA199、T4由自動化儀器測得數值，共收集到26組共156筆的資料。

4.將操作結果與RANDOX每月的結果報告，算Deviation的方式做比較。

5.將樣本放兩週後，將2024隨機抽一組及2025隨機抽兩組出來操作共18筆報告的看是否差異性。

Results

1.2024年、2025年及2026年的樣本26組共156筆的資料，我們發現到計算出的Deviation%，2025年RIA操作AFP CEA的數值皆可以落入10%以內但自動分析儀做出數值CA125、CA153、CA199、T4四個項目裡CA199有5組數值超出10%。

2.2024年的樣本數值有多組超過10%大多為數值較高的樣本。

3.將檢體放兩週後隨機抽樣共3組12筆資料計算Deviation%皆可以落入10%內。

Conclusion

從臨床檢驗科轉任到放射免疫分析室以來，發現到RIA的操作方式並不容易受到溶血或是脂血的干擾反而測出的數據很穩定，以前在檢驗科做能力試驗的時候學長姊都教導能力試驗是一次性檢體不能再使用誤差會很大，這次挑選RANDOX樣本作測試後發現比想像中穩定且計算數值差異性並不大，以觀察來看建議使用一年內的樣本較穩定如保存方式夠穩定是可以用於如臨床樣本不夠可供允收比對，但如果數值破百的樣本變異性較大所以不建議使用。

壁報論文 基礎組 **PB-006**

原著論文

巨量資料分析中統計顯著與臨床實質差異之探討：以 21 年核子醫學檢查基線特徵為例

[2]李怡旻, [1,2]莊紫翎

[1]慈濟大學

[2]大林慈濟醫院

發表者 李怡旻

Keywords 行政管理

Background

本研究旨在建立台灣南部某醫院長達 21 年之核子醫學檢查利用之流行病學基線特徵，並探討在巨量資料分析中，導入效應量 (Effect Size) 以校正過度顯著 p 值之必要性與臨床應用價值。

Method

採回溯性觀察研究設計，蒐集研究醫院自2004年1月1日~2024年12月31日止之核子醫學科檢查相關資料。採用 SAS® OnDemand for Academics進行資料處理與分析，並以平均數、標準差等統計方法描述人口學變項概況。並進一步以 T檢定探討本科前五大檢查（骨質密度檢查、全身骨骼掃描、心肌灌注檢查、正子造影、多頻道心室功能攝影），性別是否造成首次受檢年齡之差異。考量巨量資料易導致過度顯著之情形，故藉由效果量 (Effect Size) 評估實質臨床差異，依 Cohen's d 判定準則，若 $d < 0.2$ 則視為極微效應。

Results

本研究共收錄 21 年間計 207,668人次之檢查紀錄。在針對前五大高頻檢查（骨質密度、全身骨骼、心肌灌注、正子造影及多頻道心室功能攝影）進行病患首次受檢紀錄之歸戶分析中，微觀結果顯示各組受檢者性別與年齡皆達常態統計顯著差異 ($p <$

0.05)。然經進一步導入效應量檢定，骨質密度檢查、全身骨骼掃描、心臟灌注檢查、正子造影、多頻道心室功能攝影之Cohen's d分為別0.23、0.05、0.20、0.09、0.11。其實質臨床絕對年齡差異極微，實證了臨床排檢決策高度依循標準化適應症，無因性別產生受檢年齡之偏誤。

Conclusion

在巨量資料的常態性統計檢定中，極易因樣本數龐大而產生無臨床意義的統計顯著 ($p < 0.05$)。本研究透過效果量分析證實，性別與受檢年齡之實質差異極微，此結果客觀驗證了本院 21 年來排檢決策的高度中立性與標準化。此一長期資料庫基線特徵的確立，將可作為未來進一步分析外部衝擊（如傳染病疫情、健保政策調整）對各項檢查利用趨勢影響之穩固基礎。

壁報論文 基礎組

PB-007

原著論文

Implementation of [18F]FET Production in a Taiwanese Radiopharmaceutical Plant: From Automated Synthesis to Eu. Ph. Quality Control

[1]孟凡傑, [1]鍾安琪, [1]林双喆, [1]蔡炘恩, [1]王詩晴, [1]黃雅婷, [1]黃雅瑤, [3]林可翰, [2]何宗穎, [1]張智- 偉

[1]普瑞默生物科技
[2]基隆長庚紀念醫院
[3]臺北榮民總醫院

發表者 孟凡傑

Keywords 製藥 | 藥物開發

Background

Introduction: O-(2-[18F]fluoroethyl)-L-tyrosine ([18F]FET) is an amino acid PET radiotracer used in neuro-oncologic imaging, particularly for gliomas. For clinical supply, the final product should be reproducibly manufactured under PIC/S GMP conditions, comply with pharmacopoeial specifications, and remain stable during the intended handling and distribution period. This study evaluated the automated production, quality control, stability, and representative clinical use of [18F]FET manufactured at a PIC/S GMP facility in Taiwan.

Method

Methods: [18F]FET was produced on a GE FASTlab 2 synthesizer using a commercial ABX disposable cassette (FT-02-H), reagent kit (FT-102), and the ABX cassette sequence. Three consecutive batches were synthesized by nucleophilic radiofluorination, acidic deprotection, solid-phase extraction purification, formulation, and sterile filtration. Quality control was performed according to the European Pharmacopoeia monograph for Fluoroethyl-L-tyrosine (18F) injection (Monograph 02466). Stability was evaluated for up to 12 h at 30 ± 2 °C/65 ± 5% RH and 40 ± 2 °C/75 ± 5% RH. Representative [18F]FET PET images from two clinical cases were also reviewed descriptively.

Results

Results: All three batches were completed within 48 min. Starting [18F]fluoride activities ranged from 132.4 to 185.7 GBq, and final activities at the end of synthesis were 56.0–64.1 GBq. The non-decay-corrected radiochemical yield was 34.1%–42.4% (mean, 37.1 ± 4.6%; n = 3). The final product volume was 23 mL, with activity concentrations of 2.43–2.79 GBq/mL. All batches met the pharmacopoeial release specifications. Radiochemical purity was 97%–98%, radionuclidic purity was 100%, and bacterial endotoxin levels were below 0.6 IU/mL; all sterility tests showed no growth. The product remained within specification for 12 h under both tested storage conditions. Representative clinical PET images showed [18F]FET uptake in brain lesions after administration of the product prepared in this study.

Conclusion

Conclusions: Automated production of [18F]FET using a commercial ABX cassette on the GE FASTlab 2 platform consistently yielded a product that met European Pharmacopoeia specifications and remained stable for up to 12 h. These findings support its use for project-based clinical manufacturing, routine clinical supply, and short-term distribution in a PIC/S GMP setting.

壁報論文 基礎組

PB-008

原著論文

RIA 實驗室I-125 放射性廢水儲放管理與排放策略評估研究 -以南部某醫院核醫科為例

[1]卓世傑, [1]顏玉安

[1]奇美醫院

發表者 卓世傑

Keywords 實驗室安全 | 輻射防護 | 實驗室流程改善 | 流程優化 | 行政管理

Background

放射性廢水之儲存管理與排放作業為RIA（Radioimmunoassay）實驗室依法必須執行的重要工作。為符合輻射防護及法規要求，各RIA實驗室需設置適當數量與容量之放射性廢水儲存桶，以利廢水之衰變貯存、管理及後續排放。然而，在有限空間條件下，如何提升廢水桶之使用效率、優化儲放管理流程及建立有效之排放策略，以降低廢水累積量並兼顧法規遵循與作業效能，為實務運作上重要課題。因此，本研究以RIA實驗室產生之碘 -125 放射性廢水為研究對象，評估其儲放管理模式與減量排放策略，以探討兼具安全性、合規性與管理效益之最佳化方案。

Method

收集南部某醫院核醫科RIA實驗室產出之 6 桶（每桶 300 公升，總計 1,800 公升）I-125 廢水，追蹤其自民國 109 年至 111 年間之初始及量測活度。利用放射性衰變公式（I-125半衰期採 60 天標準值），評估並對比「分 6 桶 300 公升獨立儲放」與「1 桶 1,800 公升集中儲放」兩種管理模式對等待時間之影響。此外，亦模擬加入 600 m^3已處理完成不含放射性物質之院內廢水，稀釋後符合放流法規（60.9 Bq/L）所需天數。

Results

第 1 桶廢水於 109.08.13 儲滿時之反推活度濃度約為 170,417 Bq/L。至第 6 桶檢測日（111.03.02）時，分桶管理之早期廢水已大幅衰變（如第 1 桶降至 219.6 Bq/L），6 桶混合之總活度為 (1.19*10^7 Bq)（約 322.57mCi），混合活度濃度為 6,630.6 Bq/L。不稀釋狀態下，混合廢水需再冷卻 406.0 天始可達排放標準；在模擬與 600 m^3非放射性廢水混合之情境下，濃度可降至 19.83 Bq/L，達到放流濃度限制。

Conclusion

研究證實「分桶儲存、分批衰變、先進先出」的管理模式在縮短早期廢水儲存週期、分散洩漏風險及防範交叉污染上，顯示分桶儲存及先進先出管理模式於放射性廢水衰變管理上具有較佳之實務應用價值。

壁報論文 基礎組 **PB-009**

原著論文

Quality Risk Management in Process Changes and Validation of Ga-68-CXCR4-Like and Ga-68-FAPI-Like Radiopharmaceuticals

[1]林欣純, [1]羅盛男, [1]楊詩涵, [1]林亭君, [1]洪綾蔓, [1,2]李銘忻, [1]黃玉儀

[1]和信醫院

[2]群創生物科技公司

發表者 林欣純

Keywords 製藥 | 品保 | 流程優化

Background

為配合Theranostics藥物調劑方法多樣性，將Ge-68/Ga-68發生器由Grade C合成盒熱室，移至同室Grade C背景之ISO 5核醫標靶調劑工作站，使可同時支援自動化合成與cold kit調劑兩模式。上述變更可能影響發生器淘洗與合成反應銜接；另合成卡匣變更亦可能造成與加熱模組介面相容性差異，影響Ga-68藥物標誌產率。本研究依循ICH Q9品質風險管理精神，以Ga-68-CXCR4-like藥物為首要驗證標的，對發生器移址後製程進行測試與驗證，並延伸至Ga-68-FAPI-like藥物，以確認矯正預防措施(CAPA)於跨藥物間之適用性與製程變更之有效性。

Method

Ga-68-CXCR4-like藥物首次製程測試，發生器淘洗率符合規格，終產品符合放行規格，惟衰變校正產率僅29.7%，較歷史趨勢偏低。透過根本原因分析，逐項檢視影響關鍵品質屬性(CQA)之關鍵製程參數(CPP)，確認兩項根本原因：(1)發生器移址後，自淘洗至反應起始時間間隔由原4-5分鐘延長至16分，Ga-68衰變損失活度，並與decay產生之Zn-68於標幟過程可能形成競爭反應；(2)合成卡匣新批次reaction vial與加熱模組adaptor介面相容性欠佳，影響反應溫度致反應不完全。據此訂定CAPA，調整關鍵設計要素以強化關鍵構面：(1)縮短淘洗至反應起始時間至6分鐘內；(2)訂製adaptor以密合反應瓶介面。措施實施後執行三批次Ga-68-CXCR4-like藥物製程驗證，比對其產率、放射化學純度與歷史趨勢。為驗證CAPA是否同步適用於Ga-68-FAPI-like藥物製程，彙整其歷史批次資料，於CAPA後同時執行三批次驗證，與歷史產率趨勢比對。

Results

調整後Ga-68-CXCR4-like藥物三批次產率為65.86 ± 0.18% (Mean±SD)，CV 0.27%，歷史產率為67.87±7.52% (n=11)，回復至正常範圍，RCP 97.10-98.14%均符合放行規格(>97%)。Ga-68-FAPI-like藥物歷史產率為64.07% ±5.96% (n=7)，CAPA後三批次產率為64.57 ± 1.91%，CV 2.96%，RCP 99.90-99.99%均符合放行規格(>97%)。顯示CAPA效果不僅限於CXCR4-like藥物，於FAPI-like藥物製程亦可驗證重現，且批間一致性優於歷史批次。

Conclusion

本研究之場域與作業模式變更，未偏離原廠技術移轉之CPP，各批次CQA及放行規格亦符合要求。依ICH Q9品質風險管理架構辨識與評估製程變更之風險，經RCA確認產率下降之根本原因，再以CAPA訂定矯正預防措施，經兩類藥物各三批次驗證，產率恢復歷史水準且批間一致。證實風險已受控，且措施具跨藥物之重現性與適用性，支持發生器同時支援自動合成與調劑雙重作業模式之可行性，可作為導入多模式Ga-68製備場域之實務參考。

壁報論文 基礎組

PB-010

原著論文

Identification of Consistent Neuroimaging Biomarkers for Predicting Mild Cognitive Impairment Progression Using Tc-99m ECD SPECT: A Comparison of Three Feature Selection Methods

[1]曾聖彬, [1]楊惠絜, [1]倪于晴, [1]林家榆, [1]林志崑, [2]張瓊之

[1]國家原子能科技研究院
[2]高雄長庚醫院

發表者 曾聖彬

Keywords 分子影像 | 智慧醫療 (ML/DL/LLM) | 影像處理 / 軟體

Background

Early prediction of mild cognitive impairment (MCI) progression to Alzheimer's disease (AD) is important for timely intervention. In this study, 30-month clinical follow-up was used to define conversion status, and baseline Tc-99m ECD SPECT images of MCI patients were classified as progressive MCI (pMCI) or stable MCI (sMCI). We aimed to identify robust brain regions associated with MCI progression by comparing statistical and machine learning-based feature selection methods.

Method

This retrospective study, conducted in collaboration with Kaohsiung Chang Gung Memorial Hospital, included 120 MCI subjects, comprising 62 pMCI patients who progressed to AD within 30 months and 58 sMCI patients who remained stable for at least 30 months. Baseline Tc-99m ECD SPECT images underwent spatial normalization using SPM5 and intensity normalization using the whole cerebellum as the reference region. Regional cerebral blood flow features were extracted from 91 brain regions using a modified Automated Anatomical Labeling (AAL) atlas. Three feature selection approaches were compared: age-adjusted voxel-wise Statistical Parametric Mapping (SPM), F-score feature selection, and Random Forest-Recursive Feature Elimination (RF-RFE).

Results

Baseline Tc-99m ECD SPECT demonstrated the potential to differentiate pMCI from sMCI. Using RF-RFE, the classification model achieved an accuracy of 75.00%, sensitivity of 66.67%, specificity of 83.33%, and area under the receiver operating characteristic curve (AUC) of 0.80. Importantly, substantial overlap in predictive brain regions was observed across the SPM, F-score, and RF-RFE approaches. Regions consistently identified as important for differentiating pMCI included the orbital part of the superior frontal gyrus, orbital part of the inferior frontal gyrus, parahippocampal gyrus, fusiform gyrus, and inferior temporal gyrus. Hypoperfusion in these regions is consistent with the neurodegenerative patterns associated with AD progression.

Conclusion

Tc-99m ECD SPECT combined with multi-method feature selection demonstrated promise for predicting MCI progression to AD. The consistent identification of key brain regions across statistical and machine learning approaches highlights their potential as imaging biomarkers for future predictive modeling of MCI conversion to AD.

壁報論文 基礎組

PB-011

原著論文

PEGylation of Boronotryptophan Improves Injectable Formulation and Boron Accumulation in LAT-1–Expressing Glioma Cells, with a Single-Animal [18F]-PET Feasibility Pilot

[1]陳祥平, [1]俞鐘山, [1]許富淳, [1]黃奎元, [1]謝登山, [2]樊修秀, [1]許榮鈞

[1]清華大學

[2]國家原子能科技研究院

發表者 陳祥平

Keywords 藥物開發 | 分子影像 | 臨床前藥物研究

Background

Tri-Boc–protected boronotryptophan is a candidate LAT-1–targeting carrier for boron neutron capture therapy (BNCT), but its poor aqueous solubility precludes formulation for tail-vein injection. We evaluated polyethylene glycol (PEG) conjugation as a prodrug strategy to improve solubility without compromising cellular boron accumulation, and explored whether a terminally [18F]-labeled congener could be visualized by PET.

Method

5- and 6-boronopinacol tryptophan cores were conjugated with PEG200, PEG600 and PEG1000. Cell viability (up to 1 mM with 0.8 % DMSO) and 10B accumulation (ICP-MS; three concentrations; 1, 2 and 4 h) were assessed in LAT-1–expressing U87 and LN229 glioma cells, with BPA-fructose as comparator. TB-6-BT-PEG200 was tosylated and radiofluorinated (K[18F]F, Kryptofix 2.2.2, K2CO3, DMF) to give [18F]F-8. As a single-animal feasibility pilot (n = 1 per cell line), dynamic PET was acquired from 0 to 60 min in subcutaneous U87 and LN229 xenograft mice. Particle size was determined by dynamic light scattering.

Results

PEGylation permitted testing at 1 mM without cytotoxicity, compared with 482 µM for BPA-fructose. 10B accumulation reached 15–50 ppm. In U87, all PEGylated analogs exceeded BPA-fructose (< 3 ppm), with TB-6-BT-PEG1000 highest at approximately 30 ppm; LN229 uptake was variable and declined over time. [18F]F-8 was obtained in 1.7 % non-optimized radiochemical yield (EOB, decay-corrected) with logP 0.65 ± 0.04. In the pilot scan, tumor was visualized in both models, with higher relative uptake in U87 (18 %) than in LN229 (3 %). Tumor-to-muscle ratios were high but fluctuated between time frames, and no variance estimate is possible from a single animal. Brain uptake was below 1 %. Mean diameter was 173.1 ± 25.0 nm for TB-6-BT-PEG200 versus 505.4 nm for the PEG600 congener, indicating aggregation with longer chains.

Conclusion

PEG conjugation renders boronotryptophan formulable at BNCT-relevant concentrations while preserving in-vitro boron accumulation, and short-chain PEG200 is compatible with nucleophilic radiofluorination. The imaging component establishes workflow feasibility only. Because the 18F label resides on the PEG terminus distal to the hydrolyzable ester, [18F]F-8 reports the distribution of the PEG fragment rather than 10B directly; quantitative tumor selectivity requires a powered cohort with metabolite analysis.

壁報論文 基礎組

PB-012

原著論文

Multitask 3D Residual Attention U-Net for Brain Parcellation Using T1W MRI and CT

[1]林珺媛, [3]施政廷, [1]吳東信, [2]楊邦宏

[1]陽明交通大學
[2]臺北榮民總醫院
[3]中國醫藥大學

發表者 林珺媛

Keywords 智慧醫療 (ML/DL/LLM)

Background

Brain parcellation establishes reproducible anatomical units for quantitative and visual neuroimaging assessment. Most parcellation pipelines rely on high-resolution T1-weighted MRI, whereas many routine clinical and nuclear medicine examinations include CT but not MRI. The lower soft-tissue contrast of CT complicates fine-grained anatomical delineation and limits automated regional analysis across imaging workflows. This study developed a modality-flexible deep learning framework to segment the same brain regions from either T1-weighted MRI or CT, thereby extending parcellation to a broader range of neuroimaging examinations.

Method

The publicly available CERMEP-iDB-MRXFDG dataset, comprising paired T1-weighted MRI and CT from 37 healthy adults, was used. Preprocessing included bias-field correction, multimodal registration, brain-centered cropping, and intensity normalization. FreeSurfer-derived labels from T1-weighted MRI were harmonized into a 35-class reference segmentation. A coarser auxiliary segmentation mask was used to reinforce learning of major tissue and anatomical groups. A subject-level split assigned 30 subjects (960 patches) to training and 7 subjects (224 patches) to validation. A 3D multitask residual attention U-Net learned from both modalities within a unified framework. Online augmentation included rotation, translation, scaling, elastic deformation, contrast and gamma adjustment, Gaussian noise and blurring, and low-resolution simulation. Performance was evaluated using the mean Dice similarity coefficient (DSC) and 95th-percentile Hausdorff distance (HD95) for overall, brain, cortical, white matter, and basal regions.

Results

Across overall, brain, cortical, white matter, and basal regions, respectively, T1-weighted MRI achieved DSC values of 0.903 / 0.899 / 0.891 / 0.968 / 0.918 and HD95 values of 1.16 / 1.13 /

1.17 / 1.00 / 1.01 mm. CT achieved corresponding DSC values of 0.719 / 0.695 / 0.654 / 0.818 / 0.817 and HD95 values of 2.06 / 2.18 / 2.30 / 2.13 / 1.74 mm. White matter and basal regions retained relatively strong CT performance, whereas cortical delineation showed the greatest modality-related decline.

Conclusion

The 3D multitask residual attention U-Net enabled 35-class brain parcellation from T1-weighted MRI and CT within a unified framework. The high MRI accuracy and retained CT performance, particularly in white matter and basal regions, support the feasibility of modality-flexible anatomical segmentation. Further improvement in cortical delineation may broaden its application in CT-based neuroimaging workflows.

壁報論文 基礎組

PB-013

原著論文

Deep Learning-Based Volumetric Synthesis of 99mTc-MAA Liver SPECT from Two Orthogonal Planar Projections

[1]王佳柔, [2]施政廷, [1]吳東信, [3]楊邦宏

[1]陽明交通大學
[2]中國醫藥大學
[3]臺北榮民總醫院

發表者 王佳柔

Keywords 分子影像 | 劑量學 (Dosimetry)

Background

Three-dimensional SPECT enables regional assessment of radiotracer distribution but requires substantially greater acquisition effort than planar imaging, which may limit its use in repeated or extended-field imaging. This proof-of-concept study investigated whether a projection-fusion U-Net could synthesize volumetric technetium-99m macroaggregated albumin (99mTc-MAA) liver SPECT from two orthogonal planar projections.

Method

Retrospective 99mTc-MAA liver SPECT studies from 65 patients were included. Fifty-nine patients were used for model training, and six held-out patients were used for validation. For each patient, anterior-posterior and lateral planar projections were computationally derived from the corresponding SPECT volume and used as paired two-dimensional inputs, while the original SPECT volume served as the reference. A 2D-to-3D projection-fusion U-Net was developed to extract and integrate features from both projections and generate a volumetric SPECT image. Rotation-based augmentation was repeated 200 times during training. Performance was evaluated within high-activity liver regions, defined as voxels with a normalized reference SPECT intensity greater than 0.30, using the structural similarity index measure (SSIM) and normalized mean absolute error (NMAE).

Results

In the six held-out patients, the generated volumes preserved the dominant intrahepatic activity distribution observed on reference SPECT. Within the predefined high-activity liver regions, the model achieved an SSIM of 0.9901 ± 0.0044 and an NMAE of 5.05 ± 1.60%. Representative comparisons demonstrated close spatial correspondence between the generated and reference SPECT volumes.

Conclusion

A projection-fusion U-Net synthesized 3D 99mTc-MAA liver SPECT from two orthogonal projections with high regional structural similarity and low normalized intensity error. These findings support the technical feasibility of planar projection-based volumetric SPECT synthesis. Further validation using independently acquired planar images, larger patient cohorts, and absolute activity measurements is required before application to quantitative dosimetry or reduced-acquisition clinical workflows.

壁報論文 基礎組 **PB-014**

經驗分享

放射免疫分析實驗室品質指標之建立與成效分析

[1]郭珮怡

[1]成大醫院

Keywords 品管 | 實驗室安全

Background

品質指標（Quality Indicators）為量化醫療品質與臨床成效之核心工具。本科依循台灣醫事檢驗學會推動之『台灣臨床實驗室品質指標系列』（TLIS），建立符合 ISO 15189 及醫院評鑑要求之監控系統，涵蓋檢驗前、中、後三大階段，以確保檢驗品質與病人安全。

Method

1. 資料來源：彙整 2015 至 2026 年度管理審查會議之品質監控數據。

2. 主要監控指標：

・檢驗中指標：

報告更改件數、實驗室能力試驗不合格件數。

3. 檢驗後指標：報告逾時件數、委外報告逾時件數。

4. 分析與改善機制：依據實驗室歷史表現設定閾值，透過每月品管會議進行查核；並於每年管理審查時評估指標資料收集方法與目標值之合宜性，據以修訂數值及調整指標提報策略。

Results

1.報告逾時量：逾時件數由 <10 件顯著下降至 <3 件，呈現持續且穩定的品質優化。

2.報告更改量：更改件數由 <10 件大幅下降至 <1 件，透過導入不符合事件處理程序，有效強化報告正確性。

3.能力試驗表現：合格率由 >80% 提升至 >97.2%。為強化風險管理，於 2025 年度將指標計算與收集方法修訂為「不合格件數 <2 件」，持續監控以滿足實驗室精準需求。

4.委外報告時效：於 2017 年度修正指標計算與收集方式，改以「委外報告逾時件數」進行監控，逾時件數自 <10 件成功管控至 <4 件。

Conclusion

本研究證實，雖然 TLIS 系統建議多數指標採用『百分比』作為單位，但針對放射免疫分析 (RIA) 此類實驗室，將單位轉換為『件數』進行操作型定義，能更直接地反映檢驗流程異常，進而提升改善效率，此模式可作為臨床實驗室指標在地化調整之參考。

壁報論文 基礎組

PB-015

經驗分享

新進輻射工作人員劑量計遺失改善矯正計畫

[1]邱育琪, [1]黃薪蓉, [1]許耘萱, [1]陳輝墉

[1]義大醫院

發表者 陳輝墉

Keywords 輻射防護 | 曝露劑量 (Exposure)

Background

新進輻射工作人員劑量計遺失，因不熟悉通報流程，致延遲通報。藉由PDCA品管手法，經決策樹進行原因分析，擬訂改善策略，進行流程改善；最終分析成效並落地實施。

Method

1. 本研究係依據核能安全委員會「輻射工作人員劑量異常案件處理作業導則」及本院「L3-612-A輻射工作人員劑量異常案件處理作業準則」研擬矯正 / 改善措施

1. 依據決策樹進行原因分析，輻射工作人員劑量計遺失改善矯正計畫，啟動PDCA矯正措施:P- 確認問題 (1) 環境中防錯機制不足：更換刷手服處缺乏明顯提醒。(2) 新進人員訓練缺口：職前教育訓練未涵蓋佩章遺失通報時效與流程，致同仁發現遺失至通報延遲 2 天。D- (1)張貼提醒文宣於更衣室刷手服回收桶上方及佩章架旁顯眼處，收資訊透明化效果。(2) 強化新進人員訓練機制，將劑量佩章遺失通報流程增列入新進人員訓練計畫中，規定新進人員須於到職第 1 週內完成。C-(1)佩章遺失事件：改善前、後，透過防錯機制與宣導進行成效評價及效果持續追蹤。(2) 新進人員訓練及評核：訓練課程完成後，進行評核，紀錄留存備查。(3) 警示標語圖卡及簡易通報流程圖等資訊透明化張貼；並宣導同仁完成閱覽。A-(1)將「L3-612-A輻射工作人員劑量異常案件處理作業準則」佩章管理及異常事件通報流程納入單位標準作業程序，持續落實執行。(2) 於全院輻射防護教育訓練中，加強劑量佩章遺失通報流程宣導。(3) 將劑量佩章遺失通報流程納入新進人員訓練計畫中，並於到職後一週內完成通報流程訓練及測驗。

Results

1. 當月工作日誌顯示該人員工作量安排無異於其他月份，且根據當月份劑量報告顯示，與其搭配工作的同仁之劑量與過去一年所接受劑量並無差異；可合理推定該人員應無劑量超過調查等基準之疑慮。

2. 依據PDCA擬定輻射工作人員劑量計遺失改善矯正計畫改善完畢，將持續追蹤成效。

Conclusion

1. 本院共計設置 7 名專責輻防人員，本件由核醫科輻防師負責啟動訪談、調查、資訊收集及調查報告之撰寫；心導管主管協助矯正措施之執行，例如補正訓練程序、資訊透明化海報製作等，充分體現跨單位橫向協作架構，在實務實施流程中，可順暢運行。

2. 新進人員 (尤其是剛畢業同仁)，從學程邁入職涯開始，應視為「零」基礎；相關基本法規應從入職第一天便開始給予訓練及宣導；本次延遲通報便是一次極佳的學習經驗。

3. 班表紀錄應妥善保存，如遇異常狀況，將成為人員曝露劑量評估重要之依據，因此，無論是工作內容與工作量適當匹配，可同時符合勞動條件及人員曝露劑量評估之佐證。

資訊透明化實施於輻射作業區宣導，提醒同仁落實各項作業 (例如佩章管理、鉛護具置放等常規作業)，避免因過於熟稔而忽略「工作落實」之重要性。

壁報論文 基礎組

PB-016

原著論文

[^{68}Ga]NOTA-Tri-mannose作為腫瘤相關巨噬細胞正子影像探針之研究

[1]詹振勳, [1]李婉綺, [1]何宗澧, [1]徐敏軒, [1]于鴻文, [1]王美惠

[1]國家原子能科技研究院

發表者 詹振勳

Keywords 分子影像

Background

腫瘤微環境中常伴隨腫瘤相關巨噬細胞（tumor-associated macrophages, TAMs）浸潤現象產生，其中M2型巨噬細胞高度表現甘露醣受體，並與腫瘤發展有密切相關。本研究合成 [Ga-68]NOTA-Tri-mannose放射性示蹤劑，利用甘露醣對甘露醣受體之靶向特性，探討其作為腫瘤相關巨噬細胞正子影像探針之可行性。

Method

我們合成 [Ga-68]NOTA-Tri-mannose藥物，並以放射性薄層色譜分析（radio-TLC）確認其放射化學純度及藥物穩定性。[Ga-68]NOTA-Tri-mannose經由尾靜脈注射至MDA-MB-231腫瘤小鼠，利用正子放射電腦斷層攝影搭配PMOD 4.0影像軟體進行正子造影與影像分析定量作業，評估其藥物在小鼠體內分布與腫瘤組織標的能力。

Results

[Ga-68]NOTA-Tri-mannose藥物室溫震盪 15 分鐘即標誌完成，不需純化步驟，放化純度可達 100%，其藥物穩定度於室溫存放 4 小時放化純度仍可保持 9 成以上。PET/CT影像部分，[Ga-68]NOTA-Tri-mannose藥物在腫瘤組織在有積聚訊號，T/N ratio最高可達到10.12。

Conclusion

[Ga-68]NOTA-Tri-mannose藥物具有製備快速且操作簡便之優勢。小鼠PET/CT影像顯示，腫瘤區域具有明顯藥物積聚訊號，藥物代謝器官腎臟及膀胱亦可觀察到訊號，但在其他正常器官未見明顯攝取。綜合以上實驗結果顯示[Ga-68]NOTA-Tri-mannose對於腫瘤組織具有良好標靶性。

壁報論文 基礎組 **PB-017**

經驗分享

放射免疫分析實驗室 Counter污染事件之原因分析與雙重背景值監測改善成效

[1]王安美

[1]台北馬偕醫院

Keywords 放射免疫分析 | 品管 | 實驗室安全 | 實驗室流程改善

Background

放射免疫分析 (Radioimmunoassay,RIA) 檢測過程涉及I-125等放射性核種，若操作過程發生試劑濺出或污染，可能造成Counter偵測系統及工作環境污染，影響檢驗作業與實驗室輻射安全。本篇內容主要針對RIA實驗室Counter污染事件進行原因分析，並導入「雙重背景值監測」及標準化操作流程，以降低污染事件發生率並提升實驗室安全管理。

Method

針對污染事件進行事件回溯與原因分析，評估污染發生之操作環節及人員經驗等相關因素，經分析發現，污染主要與I-125操作中液體溢出冰污染試管外部有關。改善措施包括：每項實驗開始counting 前先進行Counter背景值檢測，確認儀器背景值正常後始可執行實驗之counting ; 實驗完成後再次進行背景值之監測，形成「實驗前背景值確認 + 測後背景值確認」之雙重監測機制，並配合操作流程標準化及人員教育訓練。同時建立污染事件監測指標，作為持續品質改善之依據。

Results

改善前曾發生非常嚴重 Counter 污染事件共 3 次，經導入雙重背景值監測及相關預防措施後，改善期間嚴重污染事件降至 0 次。此流程改善核心由原先「污染發生後再處理」，改善為「實驗前確認 → 實驗中預防 → 實驗後確認 → 異常立即處理」，藉由測前背景值確認，可於counting前即可掌握Counter狀況；測後再次確認Counter狀況則可及早發現潛在污染，降低污染持續擴大的風險。改善措施亦提升人員對I-125操作風險及污染預防之警覺性。

Conclusion

RIA實驗室Counter污染主要與放射性試劑操作過程中的試管外污染有關。導入「雙重背景值監測」結合標準化操作及人員教育訓練，可有效提升污染事件之早期發現與預防能力。實驗室經分析檢討改善後，嚴重污染事件由 3 次降至 0 次，顯示雙重背景值監測具實務上的預防成效，可作為RIA實驗室放射性污染風險管理及品質持續改善之參考。

壁報論文 基礎組 **PB-018**

原著論文

Comparison of two FAPI –based PET tracers: Preclinical Evaluation of [18F]AlF- and [68Ga]-NODA-FAPI for Fibroblast Activation Protein Targeted PET Imaging

[1]黎昱璇, [1]蘇毓禎, [1]陳傳霖

[1]陽明交通大學

發表者 黎昱璇

Keywords 藥物開發 | 分子影像 | 造影儀器 | 解剖學 /CT/MR | 試劑

Background

Fibroblast activation protein (FAP) is highly expressed on cancer-associated fibroblasts (CAFs) and has emerged as an attractive target for tumor imaging and radioligand therapy. FAPI-based radiopharmaceuticals have demonstrated good tumor uptake and low background activity in both preclinical and clinical studies. This study compares the potential of NODA-FAPI conjugates labeled with [18F]AlF and [68Ga] as PET imaging agents for fibroblast activation proteins.

Method

The NODA-FAPI precursor and non-radioactive reference compounds were synthesized, followed by radiolabeling with 18F AlF and 68Ga. Radiochemical yield and purity were evaluated using radio-TLC and HPLC. Biological evaluation was performed using HT1080 and HT1080-FAP-GFP++ cell lines and a U-87 MG xenograft mouse model.

Results

NODA-FAPI was successfully synthesized and labeled with both 18F and 68Ga, with radiochemical purity greater than 95%. Both tracers showed specific binding to FAP-expressing cells, with IC50 values of 5.92 nM for [18F]AlF-NODA-FAPI and 70.6 nM for [68Ga]Ga-NODA-FAPI. PET/MR and biodistribution studies showed similar pharmacokinetic profiles, with predominant urinary and fecal excretion. PET/MR imaging showed that [18F]AlF-NODA-FAPI had a T/M ratio of 19.64 ± 4.24 at 120 min, higher than 6.60 ± 2.76 for [68Ga]Ga-NODA-FAPI, indicating higher tumor uptake and better tumor-to-background contrast.

Conclusion

[18F]AlF-NODA-FAPI and [68Ga]Ga-NODA-FAPI were successfully developed and biologically evaluated. [18F]AlF-NODA-FAPI exhibited higher in vitro binding affinity and a higher tumor-to-muscle ratio in PET/MR imaging and biodistribution studies. These findings support the potential of NODA-FAPI as a tracer for FAP-targeted PET imaging.

壁報論文 基礎組

PB-019

原著論文

Longitudinal [18F]Florbetaben PET/MR Imaging Reveals Reduced Amyloid Burden and Improved Cognitive Performance Following ND108E Treatment in APP/PS1 Mice

[2]陳穎柔, [2]邱創新, [2]游宗勳, [1]王寶嵒, [2]葉信顯

[1]陽明交通大學
[2]三軍總醫院

發表者　陳穎柔

Keywords　臨床前藥物研究 | 分子影像

Background

ND108E is a novel hyaluronic acid–hormone conjugate with blood–brain barrier permeability and potential neuroprotective effects. This study evaluated whether ND108E could reduce cerebral amyloid-β (Aβ) accumulation and improve cognitive function in APP/PS1 transgenic mice.

Method

Female APP/PS1 mice underwent ovariohysterectomy at approximately 3 months of age and received vehicle, low-dose ND108E, or high-dose ND108E by monthly subcutaneous injection. Longitudinal Aβ deposition was evaluated using [^{18}F]florbetaben ([^{18}F]FBB) PET/MR imaging, with cortical and hippocampal binding quantified using reference-tissue Logan analysis. Spatial learning and recognition memory were assessed using the Morris water maze (MWM) and novel object recognition (NOR) tests.

Results

Vehicle-treated mice showed progressive cortical Aβ accumulation and marked hippocampal Aβ elevation with age. ND108E attenuated Aβ accumulation, with the most consistent effect observed in the high-dose group. At the late imaging time point, hippocampal Aβ binding was significantly reduced in ND108E-treated mice, with a greater reduction in the high-dose group ($p<0.01$). High-dose ND108E also reduced cortical Aβ binding, although the effect was less pronounced. In the MWM, ND108E-treated mice showed progressive improvement in learning performance, and both treatment groups performed significantly better than vehicle controls by the final training day ($p<0.05$). In the NOR test, high-dose ND108E significantly increased the discrimination index and novel-object exploration ($p<0.05$). Long-term spatial memory showed a favorable but nonsignificant trend.

Conclusion

ND108E treatment was associated with reduced cerebral Aβ burden, particularly in the hippocampus, together with improved spatial learning and recognition memory. These findings support further investigation of ND108E as a potential therapeutic strategy for Alzheimer’ s disease.

壁報論文 基礎組　　**PB-020**

原著論文

TBDD於Alpha核素治療之動態體內劑量評估：整合Parent–Daughter Kinetics與再分布效應

[1]楊詩涵, [1,3]李銘忻, [1,2]羅盛男, [1]黃玉儀

[1]和信醫院
[2]恩典科研股份有限公司
[3]群創生物科技有限公司

發表者　楊詩涵

Keywords　劑量學 (Dosimetry) | Ac-225 | Alpha radionuclide therapy

Background

Alpha核素標靶治療具有高線性能量傳遞及短射程等特性，但α粒子無法直接由臨床影像定量。以Ac-225為例，其衰變產生之daughter nuclides可能因反衝效應脫離標靶載體並重新分布，使parent與daughter具有不同生物動力學。若假設兩者具有相同分布或維持平衡，可能造成腫瘤及正常器官劑量偏差。本研究提出Total Body Dynamic Dosimetry（TBDD）架構，整合全身動態生物分布、parent–daughter kinetics及時間積分活度（TIA），建立Alpha核素動態體內劑量評估模式。

Method

以Ac-225衰變鏈建立TBDD之parent–daughter區室模型。依據已發表人體定量SPECT/CT研究，利用Fr-221約 218 keV及Bi-213約 440 keV之γ射線作為daughter分布與動力學指標，並納入 78 keV能窗及衰減、散射與解析度校正。將daughter依衰變後行為區分為原位滯留與重新分布區室，由多時間點影像建立器官及病灶之時間－活度曲線，經時間積分取得TIA，再結合MIRD或體素劑量學估算吸收劑量。以已發表之Ac-225人體影像及daughter migration研究進行外部驗證。

Results

文獻資料支持TBDD之核心假說。Ac-225-PSMA-I&T人體定量SPECT/CT研究顯示，腎臟Bi-213與Fr-221之有效半衰期分別約為 27 ± 6 及 24 ± 6 小時，且Bi-213/Fr-221腎臟SUV比值於 24 至 48 小時增加約 9%，顯示daughter-specific kinetics具有時間依賴性。另有Ac-225-DOTATATE daughter migration模型研究顯示，忽略daughter migration時，腎臟吸收劑量平均低估約 10.2%，腫瘤吸收劑量平均高估約 22.9%。上述結果支持parent–daughter kinetics及重新分布可改變組織TIA，進而影響吸收劑量估算。

Conclusion

既有人體定量影像及daughter migration研究支持TBDD之理論可行性。Alpha核素治療劑量評估若僅依賴單一時間點影像或parent–daughter平衡假設，可能無法充分反映daughter重新分布造成之劑量差異。TBDD整合多時間點定量影像、daughter-specific kinetics及TIA，可作為個人化Alpha核素治療動態劑量學之概念架構，後續將透過phantom、Monte Carlo simulation及臨床定量影像進一步驗證。

壁報論文 基礎組

PB-021

原著論文

MIM多參數定量分析於 ^18F-Flutemetamol 類澱粉正子斷層造影之臨床附加價值：全域Centiloid、標準攝取值比與區域Z分數之應用

[1]羅浚哲

[1]中山醫大附設醫院

Keywords 類澱粉正子斷層造影 | ^18F-flutemetamol | MIM Software

Background

類澱粉正子斷層造影主要以視覺判讀區分類澱粉陽性（amyloid positive, A+）與陰性（amyloid negative, A−）。MIM Software可提供Centiloid（CL）、標準攝取值比（standardized uptake value ratio, SUVr）及區域Z分數，作為視覺判讀之量化輔助。本研究旨在探討MIM多參數定量結果與核醫專科醫師視覺判讀之關係，並評估其對類澱粉負荷與區域分布之補充資訊。

Method

回溯分析 10 位接受 18F-flutemetamol amyloid PET之個案，依專科醫師視覺判讀分為A+及A−各 5 例。使用MIM Software取得Global CL、Global SUVr及 6 個皮質區域之SUVr與Z-score。兩組以Mann–Whitney U test比較，並以Global SUVr >1.15評估與視覺判讀之一致率。

Results

A+組之全域CL顯著高於A−組（50.92±33.85 vs. 0.14±13.73，p=0.008）；全域SUVr亦顯著較高（1.372±0.281 vs. 0.950±0.117，p=0.008）。A+組之平均區域Z分數為 4.53±3.02，顯著高於A−組之 −0.01±1.19（p=0.008）；每位病人Z分數 ≥2 之異常區域數量，A+組為5.0±1.4 區，A−組為 0.6±0.9 區（p=0.010）。

以全域SUVr >1.15作為量化參考時，與專科醫師A+/A−視覺判讀共有 9/10 例結果一致，一致率為 90%。唯一視覺判讀與此全域SUVr參考值不一致之病例，其視覺判讀為A+、BAPL為 2，但全域SUVr為 1.13；進一步區域分析顯示後扣帶回、楔前葉、下內側額回及前扣帶回Z分數分別為 3.48、2.76、2.46 及 2.18。

另有一例接受抗類澱粉治療後之病例，其視覺判讀為A−且全域SUVr為 1.06，與全域量化結果一致；然而區域分析仍顯示楔前葉及外側顳葉Z分數分別為 3.28 及 2.24，呈現局部攝取升高。

Conclusion

MIM Software所得全域CL、全域SUVr及區域Z分數可有效區分專科醫師視覺判讀之A+與A−病例，且以全域SUVr >1.15作為本研究量化參考值時，與視覺判讀具有 90%一致率。除全域類澱粉負荷外，區域SUVr及Z分數可進一步提供類澱粉沉積空間分布之量化資訊。本研究中，區域分析於一例全域量化與視覺判讀不一致病例及一例抗類澱粉治療後病例中呈現額外的局部攝取資訊；惟目前樣本數有限，其在邊界病例(Borderline)及治療後追蹤之臨床價值仍需更大樣本進一步驗證。

壁報論文 基礎組 **PB-022**

原著論文

Taguchi Optimization of TLD-100H Readout Parameters for Radiation Dose Assessment in an Isotope Therapy Center

[1,2]黃琪雯, [2]陳柏文, [1]翁瑞鴻, [2]陳健懿

[1]中山醫大附設醫院
[2]中山醫學大學

發表者 黃琪雯

Keywords 劑量學 (Dosimetry) | 輻射防護

Background

Accurate radiation dose assessment is important for radiation protection in isotope therapy centers (ITCs), particularly when medical staff may need to respond to unexpected events during I-131 therapy. Thermoluminescent dosimeter (TLD)-100H is a potential tool for assessing radiation exposure; however, its measurement performance depends on the readout conditions of the TLD reader. This study aimed to use the Taguchi method to optimize the readout parameters of a Harshaw 3500 reader for TLD-100H, providing a standardized measurement protocol as a basis for future clinical radiation dose assessment in ITCs.

Method

A total of 162 TLD-100H dosimeters were irradiated to a dose of 2.28 mGy in three batches for Taguchi optimization. Five control factors were evaluated using an orthogonal array design: preheating time (10–15 s), heating rate (6–10 °C/s), initial temperature (110–150 °C), maximum temperature (220–240 °C), and post-irradiation readout time (12–24 h). The optimal combination of readout conditions was determined based on the signal-to-noise (S/N) ratio.

Results

Among the experimental groups, G12 achieved the highest S/N ratio of 40.66, compared with 21.59 under the original readout conditions. The S/N ratio increased by 1.88-fold under the optimized conditions. The optimal TLD-100H readout parameters were a preheating time of 15 s, a heating rate of 6 °C/s, an initial temperature of 150 °C, a maximum temperature of 240 °C, and a post-irradiation readout time of 24 h.

Conclusion

The Taguchi method successfully identified an optimized combination of TLD-100H readout conditions for the Harshaw 3500 reader, resulting in a higher S/N ratio than the original setup. The optimized protocol provides a standardized basis for subsequent TLD-based radiation dose assessment. Further validation using personal dosimeters and measurements under actual or simulated I-131 emergency exposure scenarios is warranted to evaluate its applicability to occupational radiation dose assessment in isotope therapy centers.

壁報論文 基礎組 **PB-023**

原著論文

Full Factorial Optimization of TLD Readout for Environmental Radiation Monitoring in a PET/CT Facility

[1,2]黃琪雯, [2]蘇冠豪, [1]翁瑞鴻, [2]陳健懿

[1]中山醫大附設醫院
[2]中山醫學大學

發表者 黃琪雯

Keywords 劑量學 (Dosimetry)

Background

Positron emission tomography/computed tomography (PET/CT) is widely used for cancer diagnosis and staging and involves both positron annihilation photons and X-ray radiation. Thermoluminescent dosimeters (TLDs) are useful for long-term environmental radiation monitoring; however, their measurement performance depends on the readout conditions of the TLD reader. Although full factorial design (FFD) has been applied to optimize TLD readout parameters, its application to environmental radiation monitoring in PET/CT facilities remains clinically relevant. This study aimed to optimize the readout conditions of a Harshaw 3500 reader for TLD-100H and subsequently apply the optimized protocol to environmental radiation monitoring in a PET/CT facility.

Method

A TLD-100H system with a Harshaw 3500 reader was optimized using a 2^3 full factorial design. Three reader parameters—preheating temperature, heating rate, and maximum temperature—were evaluated using eight experimental combinations. The optimal readout condition was determined based on the signal-to-noise (S/N) ratio.

The optimized protocol was subsequently applied to environmental radiation monitoring in the PET/CT facility of the Department of Nuclear Medicine, Chung Shan Medical University Hospital. A total of 107 monitoring points were selected throughout the facility. TLDs were placed at designated locations and replaced monthly over a six-month period to evaluate the spatial distribution and temporal variation of environmental radiation levels.

Results

The S/N ratio increased from 12.15 under the original readout conditions to 20.87 under the optimized conditions. The optimal Harshaw 3500 parameters were a preheating temperature of 120°C, a heating rate of 11°C/s, and a maximum temperature of 230°C.

During the six-month monitoring period, environmental radiation levels varied among different locations within the PET/CT facility. The measured monthly radiation levels ranged from **0.13 ± 0.08 to 5.18 ± 1.14 mSv/month**, with the highest levels observed in the treatment room. Spatial differences in environmental radiation were observed across the monitored areas.

Conclusion

Full factorial design successfully identified an optimized TLD-100H readout condition for the Harshaw 3500 reader and improved the S/N ratio compared with the original setup. Application of the optimized protocol to 107 monitoring points over six months demonstrated spatial and temporal variations in environmental radiation within the PET/CT facility. These findings support the practical use of optimized TLD monitoring for environmental radiation assessment and radiation protection management. Further assessment of occupational exposure should incorporate individual personal dosimetry rather than directly comparing environmental monitoring results with occupational dose limits.

壁報論文 基礎組

PB-024

原著論文

極簡化骨質疏鬆風險評估：BMI 與核心骨折史的預測力

[2]李怡旻, [1,2]莊紫翎

[1]慈濟大學

[2]大林慈濟醫院

發表者 李怡旻

Keywords 危險因子 | Dual-Energy X-Ray Absorptiometry (DXA) | Body Mass Index (BMI) | Fracture History | Risk Assessment | Conditional Logistic Regression

Background

年齡與性別為骨質疏鬆症常見危險因子。然觀察性研究中，若兩組受試者之人口學特徵分佈懸殊，單以傳統多變量迴歸校正仍可能受殘差干擾影響。本研究採用 1:1 年齡與性別個案對照配對，旨在平衡基線共變數分佈，進而探討控制年齡與性別後，個人過往骨折史、父母髖部骨折史及身體質量指數（BMI）對雙能量X光吸收測量法（DXA）判定骨質疏鬆症之獨立關聯，並進一步評估結合上述指標之風險模型鑑別能力。

Method

採回溯性研究，資料來源為南部某準醫學中心機構進行之門診及住院骨質密度檢查數據，資料蒐集期間為 2019 年 1 月 1 日至 2023 年 12 月 31 日。本研究採性別、年齡進行 1:1 有無骨質疏鬆配對方式篩選樣本，且若受試者有多筆檢查紀錄，則僅將最早一筆資料納入分析。骨質密度檢查設備乃採用雙能量X線吸收測量法，骨質疏鬆定義乃是依據世界衛生組織 (WHO) 的骨密度測量標準（T值 ≤ −2.5）作為判定標準，過去有無骨折與父母有無髖部骨折病史為受試者自行填答，BMI為檢查當天量測。使用 SAS® OnDemand for Academics，統計方法使用個數、百分比、條件式羅吉斯迴歸評估各變項之勝算比，並以受試者工作特徵曲線下面積（AUC）評估預測模型之鑑別效能。

Results

本研究共計 11,114 人，配對後每組為 5,557 位，女性患者為 9,800 位 (88.2%)，平均年齡為 72.1 ± 10.8 歲 (P = 1.000)。以條件式邏輯斯迴歸結果顯示在控制其他條件下有骨折病史者，其發生骨質疏鬆的勝算比為沒有骨折病史者的 1.39 倍 (95%CI: 1.28–1.51)、有父母髖部骨折病史者，其發生骨質疏鬆的勝算比為沒有父母髖部骨折病史者的 1.52倍 (95%CI: 1.18–1.96)，兩者均為顯著危險因子；然而 BMI 具顯著保護效應，每增加一單位可降低約 13.7% (95%CI: 0.853–0.873) 骨鬆勝算比，且達統計顯著差異。為評估常規門診之篩檢效益，本研究進一步構建預測模型。結果證實，傳統僅依賴「骨折病史」及「父母髖部骨折病史」的模型鑑別力極為侷限 (AUC = 0.546)；然而，將 BMI 納入模型後，整體預測鑑別度顯著上升至 AUC = 0.666。

Conclusion

在年齡與性別配對後，較低BMI、個人骨折史及父母髖部骨折史均與DXA定義之骨質疏鬆顯著相關。單獨使用骨折史的鑑別能力有限，而加入BMI後AUC由 0.546 提升至 0.666，顯示BMI可提供額外的風險區分資訊。然而，模型整體鑑別力仍屬有限，且研究對象來自接受DXA檢查的臨床轉介族群，可能存在選擇及回憶偏差。未來仍需進行內部及外部驗證，並確認適當切點、敏感度與臨床淨效益，才能評估其作為第一線骨質疏鬆篩檢工具的可行性。

壁報論文 基礎組 PB-025

文獻綜述

Applications of Radiomics: From Basic Research to Clinical Practice—Practical Tips and Future Perspectives

[1]陳至豪, [1,3]陳孟穎, [1]趙芸瑄, [2]陳志成

[1]臺北榮民總醫院
[2]陽明交通大學
[3]國立臺北護理健康大學

發表者 陳至豪

Keywords 影像組學 (Radiomics) | 影像處理 / 軟體 | 智慧醫療 (ML/DL/LLM) | 分子影像

Background

Since the concept of radiomics was formally introduced by Philippe Lambin and colleagues in 2012, radiomics has rapidly emerged as a prominent field in medical imaging, radiation therapy, and biomedical research. In the era of artificial intelligence (AI), radiomics has also become an important approach for extracting quantitative and interpretable imaging biomarkers, providing valuable insights into the otherwise “black-box” nature of AI models.

Literature Review

This review summarizes the current applications of radiomics, ranging from basic research to clinical practice, through a comprehensive review of the literature. In basic research, radiomics can effectively reflect intratumoral heterogeneity and decode global gene expression programs in diseases such as liver cancer through noninvasive imaging (radiogenomics).[1][2] In clinical diagnostic practice, radiomics has demonstrated significant potential; for instance, it has been used to differentiate pseudoprogression from early tumor progression in glioma patients post-chemoradiation using FET PET,[3] and to accurately predict the grade of hepatocellular carcinoma based on non-contrast-enhanced MRI.[6] Furthermore, it has been widely applied in the diagnosis and treatment evaluation of lung cancer [4] and melanoma.[7] Recent studies also highlight that fusion models combining deep learning and radiomics can further enhance the accuracy of clinical tasks, such as predicting the invasiveness of lung adenocarcinoma. [5]

Key considerations and practical tips for radiomics workflow implementation—including image acquisition, segmentation, feature extraction, feature selection, and model development—are discussed. To ensure the scientific rigor and reproducibility of imaging biomarkers, we strongly emphasize that feature extraction and computation must strictly adhere to the Image Biomarker Standardisation Initiative (IBSI) guidelines. Ultimately, embracing IBSI-standardized workflows and deepening the integration of radiomics with AI technologies will be pivotal for its successful translation into routine clinical practice.[8][9] The paper concludes by outlining emerging applications and future perspectives for radiomics in the medical field.

References

1. E. Segal. et al., "Decoding..." Nature Biotechnology. 2007; 25:675-680
2. E.Henriksson . et al., "2-Deoxy-2-[F18]fluoro-D-glucose..." Anticancer Research. 2007; 27:2155-2159.
3. Lohmann, Philipp, et al. "FET PET radiomics..." Cancers 12.12 (2020): 3835.
4. Sun, Qian, et al. "Deep learning..." Scientific Reports 15.1 (2025): 29285.
5. Pan, Feng, et al. "Application..." Frontiers in Pharmacology 14 (2023): 1295511.
6. Wu, Minghui, et al. "Predicting..." European radiology 29.6 (2019): 2802-2811.
7. Rosa Falcone, et al. ""Application..." Cancers (2025) 17.19: 3130.
8. Zwanenburg, Alex, et al. "Image..." arXiv preprint arXiv:1612.07003 (2016).
9. Zwanenburg, Alex, et al. "The image..." Radiology 295.2 (2020): 328-338.

壁報論文 基礎組

PB-026

原著論文

Machine learning using dynamic frames for reduced acquisition time in Tc-99m bone scintigraphy

[1,2]李昕迪, [2]魏澤人, [1]郭建瑋

[1]屏東榮民總醫院
[2]陽明交通大學

發表者 李昕迪

Keywords 智慧醫療 (ML/DL/LLM) | Bone scintigraphy

Background

To achieve optimal image quality of bone scintigraphy, guidelines recommend adequate acquisition counts, often resulting in prolonged imaging times. Machine learning (ML)-based denoising offers the potential to improve image quality in low-count scans, yet its clinical applicability remains uncertain.

Method

We retrospectively collected delayed bone scans acquired in dynamic mode (3 s/frame, 100 frames, 256×256 matrix) from 198 patients (466 images) acquired on a Siemens Intevo Excel system 2-4 hours after intravenous administration of Tc-99m MDP. The dataset was split at image level into training (70%), validation (15%), and testing (15%) sets. Summed frames were used to simulate acquisition durations ranging from 3 to 300 s. During training, eight frames were sampled as input, 0–5 randomly selected frames zeroed out, resulting in effective inputs of 3-8 frames. Target images were generated by summing 10-100 frames. The 2D U-Net model was trained with L1 loss for 500 epochs. For testing, 6-frame inputs (18-second) were used to generate images corresponding to 20-frame acquisitions (60-second). Image similarity was quantitatively assessed using structural similarity index measure (SSIM) and peak signal-to-noise ratio (PSNR). In addition, an investigator reader and an independent blinded nuclear medicine physician evaluated randomized, unlabeled pairs of generated and reference images by identifying the real acquisition and rating diagnostic confidence and image quality using 5-point Likert scales.

Results

In the testing set, the generated images achieved a mean SSIM of 0.899 and a mean PSNR of 34.52 dB compared with the corresponding acquired 20-frame (60-s) reference images. The investigat- or reader and the independent blinded reader correctly identified the reference images in 92.9% and 55.7% of image pairs, respectively. For the investigator and independent readers, diagnostic confidence scores for the generated images were 4.50 ± 0.58 and 4.59 ± 0.55, respectively, compared with 4.16 ± 0.77 and 4.49 ± 0.61 for the reference images. Image quality scores for the generated images were 4.14 ± 0.52 and 4.86 ± 0.39, respectively, compared with 3.29 ± 0.54 and 3.97 ± 0.34 for the reference images.

Conclusion

Based on the current evidence, machine learning using short dynamic-frame inputs demonstrated the technical feasibility of generating longer-acquisition images, with performance comparable to that of acquired reference images.

壁報論文 基礎組

PB-027

原著論文

Radiomics-based quality assurance of gamma camera uniformity

[1,2]李昕迪, [2]魏澤人, [2]貝瑞發

[1]屏東榮民總醫院
[2]陽明交通大學

發表者 李昕迪

Keywords 品保 | 造影儀器 | 影像組學 (Radiomics)

Background

Conventional gamma camera uniformity QC relies on integral and differential uniformity (IU/DU) measurements and visual assessment of flood images. However, visually apparent spatial abnormalities may occur despite acceptable IU/DU values. Radiomics provides quantitative characterization of image texture, but its application in QC remains limited. This study explored its feasibility for detecting abnormalities in gamma camera uniformity images.

Method

Data were retrospectively collected from routine QC of a Siemens Intevo Excel gamma camera. Intrinsic flood images were acquired using a point source with 30,000K counts per detector and processed using the manufacturer-provided curvature correction. All images met routine IU/DU acceptance criteria, with no additional post-processing.

Images were classified as normal or abnormal by an experienced nuclear medicine technologist.

Radiomic features were extracted from the UFOV using PyRadiomics, including first-order, GLCM, GLSZM, GLRLM, NGTDM, and GLDM features.

Discriminative performance was evaluated using ROC analysis. Features with AUC >0.90 were retained. Redundancy was reduced using an absolute Spearman correlation threshold of 0.75; for highly correlated feature pairs, the feature with the higher AUC was retained.

Results

A total of 117 QC datasets comprising 234 intrinsic flood images (222 normal and 12 abnormal) were included in this study. A total of 25 radiomic features achieved an AUC > 0.90. After redundancy reduction using the predefined Spearman correlation threshold, four radiomic features remained after feature selection: GLCM Correlation (AUC = 0.997), NGTDM Coarseness (AUC = 0.988), GLSZM Gray Level Non-Uniformity (AUC = 0.983), and GLRLM Run Entropy (AUC = 0.983).

Conclusion

Radiomic analysis showed strong potential as a quantitative adjunct for distinguishing abnormal from normal gamma camera intrinsic flood images. Larger independent datasets are needed to confirm the reproducibility and generalizability of these findings.

壁報論文 基礎組 **PB-028**

原著論文

Serial SPECT/CT-Based Patient-Specific Organ and Lesion Dosimetry Following ^177Lu-PSMA-617 Therapy

[1]方怡珺, [2]蔡富任, [2]詹宏彬, [2]邱宇莉, [1]張似璞, [1]蔡惠予, [2]諶鴻遠

[1]清華大學

[2]高雄榮民總醫院

發表者 方怡珺

Keywords 劑量學 (Dosimetry) | 分子影像

Background

^177Lu-PSMA-617 radioligand therapy is an important treatment option for patients with metastatic castration-resistant prostate cancer (mCRPC). However, inter-patient differences in biodistribution and clearance may result in different organ absorbed doses despite a fixed prescribed activity. Therefore, patient-specific dosimetry may provide useful information for characterizing individual dose distributions.

This study aimed to perform preliminary patient-specific dosimetry of normal organs and tumor lesions using serial SPECT/CT in patients with mCRPC treated with ^177Lu-PSMA-617.

Method

Five patients receiving ^{177}Lu-PSMA-617 therapy were included, contributing 10 treatment cycles with administered activities of 6.65–7.05 GBq per cycle. Post-treatment SPECT/CT images were acquired at 4–6, approximately 24, and 168–192 h after administration.

Patient-specific dosimetry was performed using the absorbed dose rate (ADR) workflow in OpenDose3D, with all visually identifiable tumor lesions delineated by a nuclear medicine physician. Tumor analysis included 25 distinct VOIs, yielding 54 measurements across four cycles in two patients. Absorbed doses were normalized to the actual administered activity and reported as absorbed dose coefficients in Gy/GBq.

Results

Normal-organ absorbed dose coefficients across five patients at cycle 1 averaged 0.67 ± 0.26 Gy/GBq for kidneys and 0.21 ± 0.11 Gy/GBq for liver (mean ± SD). Median tumor absorbed dose coefficients at cycle 1 were 0.15 and 1.92 Gy/GBq in the two patients. In the latter patient, median (Q1–Q3) coefficients for 14 matched lesions were 1.97 (1.38–3.57), 1.21 (0.51–1.67), and 0.32 (0.16–1.91) Gy/GBq at cycles 1–3, respectively.

Conclusion

In this preliminary clinical series, serial SPECT/CT-based dosimetry showed inter-patient differences in organ and tumor absorbed dose coefficients and inter-cycle changes in tumor dose distributions within one patient. Future work will refine the dosimetry workflow and investigate factors associated with dose differences and their relationships with clinical outcomes in an expanded cohort.

壁報論文 基礎組 **PB-029**

統合分析

在18F-FDG PET/CT上使用OncoFreeze AI技術在肺部病灶的統計攝取參數與無使用OncoFreeze的相關差異

[1]曾柏銘, [1]姚維仁, [1]沈淑禎

[1]聖馬爾定醫院

發表者 曾柏銘

Keywords 造影儀器

Background

肺部病灶於FDG PET/CT檢查時易受呼吸運動影響，造成影像模糊與SUV低估。本研究評估Siemens Horizon平台之OncoFreeze AI呼吸調控技術，探討其對肺部病灶半定量參數之影響。

Method

回顧性收集 2025 年 4 月至 7 月接受 18F-FDG PET/CT檢查之肺癌患者。納入具有可測量肺部病灶者共 31 例。每位患者選取一處具代表性且可測量之肺部病灶進行分析，共納入 31 個肺部病灶，比較OncoFreeze與非OncoFreeze重建影像之SUVmax、SUVpeak及MTV (以 40% Local Max為閾值）差異; 另記錄分析病灶位於上、中、下肺野之分布情形。統計分析採用配對樣本 t 檢定（Paired-samples t-test）評估兩種重建方式之各項參數差異，以 P<0.05 代表具統計顯著性。

Results

68Ge假體分析顯示兩種重建方式之SUVmax、SUVpeak及MTV差異均小於 5%，未見明顯定量偏差。31 個分析病灶中，上、中及下肺野分別為 9、12 及 10 個。臨床病灶分析顯示，OncoFreeze AI可使SUVmax增加 12.6%（8.55±6.86 vs. 7.59±5.92；p<0.001）、SUVpeak增加 5.9%（6.00±4.83 vs. 5.66±4.70；p=0.00095），而MTV降低 20.5%（16.85±18.89 vs. 21.21±24.48 cm^3；p=0.0068）。

Conclusion

OncoFreeze AI 可降低呼吸運動對肺部病灶 PET/CT 影像之影響，使 SUVmax 與 SUVpeak 增加，並降低 MTV。68Ge 假體結果顯示其未造成明顯定量偏差，顯示 OncoFreeze 可減少呼吸運動對肺部病灶定量參數之影響。惟其對肺部病灶定量評估準確性及臨床決策與病患預後之實際效益，仍有待結合病理及臨床結果進一步驗證。

壁報論文 基礎組

PB-030

經驗分享

使用EQ PET讓不同正子儀器間的SUV具有共同一致性標準

[1]曾柏銘, [1]姚維仁, [1]沈淑禎

[1]聖馬爾定醫院

發表者 曾柏銘

Keywords 造影儀器

Background

正子造影 (Positron Emission Tomography/Computed Tomography, PET/CT) 檢查中的標準攝取值 (Standardized Uptake Value,SUV）為重要定量指標，但不同設備、重建演算法及參數設定可能造成SUV差異，影響跨設備與長期追蹤比較。Siemens 的EQ・PET技術透過後處理演算法，使影像定量結果符合歐洲核醫學會研究有限公司 (EANM Research Ltd., EARL)標準，以提升SUV的一致性與可比性。本研究旨在評估不同的EQ・PET校正參數對新舊兩台機器的校正效益。

Method

使用PTW Phantom假體及 18F-FDG模擬臨床掃描環境，分別於西門子 (Siemens)舊機Biograph TruePoint與新機Biograph Horizon進行掃描。利用西門子後處理軟體syngo.via之VOI Isocontour量測各球體（直徑 10 mm 至 37 mm）之SUV值，並於syngo.via內，使用不同的EQ・PET 校正參數下進行分析，比較與歐洲核醫學會研究有限公司（EARL）所提供的回收係數標準目標值 (EARL RC target)之差異。

Results

隨著 EQ・PET 校正參數增加，各尺寸球體與EARL RC target之活度濃度逐漸趨近。在 5 mm 條件下，10 mm 與 13 mm 小球體偏差分別達 45.9% 與 35.5%；當參數調整至 7–9 mm時，各尺寸球體誤差顯著收斂。綜合比較新舊系統，經分析發現在 EQ・PET 採用 8.1 mm 之半高全寬（Full Width at Half Maximum, FWHM）最佳參數設定下，各尺寸球體（10 mm、13 mm、17 mm、22 mm、28 mm、37 mm）與目標值之差異分別為 -0.1%、-4.4%、4.8%、-1.6%、7.4% 及 5.9%，使新舊機器間的整體平均絕對百分比差異成功降至最低的 4.0%。

Conclusion

EQ・PET 技術可有效降低不同 PET/CT 設備與重建條件所造成之 SUV 差異，使定量結果更符合 EARL 標準。本研究顯示 8.1 mm 為最適的 EQ・PET校正參數，可作為本院新舊PET/CT 儀器間 SUV 一致化之最佳設定；該項技術亦可用於不同廠商、不同機型，有助於臨床追蹤、療效評估及多中心研究之定量標準化。

壁報論文 基礎組

PB-031

原著論文

實施Tw-DRG制度對心肌灌注掃描門住診轉移之衝擊

[2]李怡旻, [1,2]莊紫翎

[1]慈濟大學

[2]大林慈濟醫院

發表者 李怡旻

Keywords 行政管理

Background

2014年 7 月 1 日起健保署擴大實施第二階段 Tw-DRGs（臺灣版全民健保住院診斷關聯群，以下簡稱 DRG）政策，將循環系統主要疾病之住院案件納入定額包裹支付，迫使檢查轉移至門診進行，以減緩院方的財政壓力。然而心肌灌注掃描（以下簡稱 MPI）為評估缺血性心臟病與術前心血管風險之關鍵診斷，於臨床實務中具備不可替代時間急迫性與特定需求。據此，本研究利用 20 年縱貫性資料，並以 DRG 排除項目正子造影檢查（以下簡稱PET）作為對照，旨在評估臨床決策在面對財政管制壓力時的行為調適與剛性需求，期望透過長期微觀視角，揭示DRG政策對前線醫療資源配置的實質影響。

Method

本研究為縱貫性研究設計，資料來源為南部某準醫學中心 2004 至 2023 年核子醫學科檢查資料庫。有鑑於 DRG實施的期間為 2014 年中旬，因此本研究依年度區分為實施DRG前（2004–2013 年）和實施 DRG後（2015–2023 年）。又因心血管疾病好發於中高齡老年，因此進一步將病人區分為是否 80 歲以上的高齡者。採用 SAS® OnDemand for Academics進行資料處理與統計分析，以多元邏輯斯迴歸探究在控制年齡變項後實施DRG對是否於住院期間進行檢查的影響，最終比較兩項檢查勝算比差異。

Results

本研究收錄 MPI、PET檢查分別為 26,669 筆、2,964 筆。MPI檢查在實施 DRG前門、住院檢查的筆數分別為 13,330 (91.73%)、1,201 (8.27%) 筆，實施後則分別為 9,934 (93.72%)、666 (6.28%) 筆，並達統計顯著差異 (P < 0.001)。PET檢查在實施 DRG前門、住院檢查的筆數分別為 255 (93.41%)、18 (6.59%) 筆，實施後則分別為 2027(82.60%)、427(17.4%)筆，達統計顯著差異 (P < 0.001)。多元邏輯斯迴歸結果顯示實施 DRG後住院時進行 MPI檢查的勝算比為 0.700 (P <0.001)，而在高齡者其住院時進行 MPI查的勝算比為 2.32 (P <0.001)達統計顯著水準。而在 PET部分，結果顯示顯示實施 DRG後住院時進行 PET檢查的勝算比為 2.94 (P <0.01)達統計顯著水準，而高齡者部分則未達統計顯著水準。

Conclusion

在實施 DRG制度後住院時進行 MPI檢查量減少 30%，但在對於 80 歲以上高齡者其檢查量則增加 1.32 倍，然而不受 DRG制度影響的 PET檢查則是較實施前增加 1.94 倍。本研究結果揭示健保署政策對於醫療機構具有一定影響力，然而在財務壓力下臨床醫師在面臨高齡者仍傾向於住院期間進行 MPI檢查，以維護病人生命安全。

壁報論文 基礎組

PB-032

經驗分享

FT4 RIA試劑中 Ligand 與 Tracer 添加順序對分析結果之差異

[1]王怡文, [1]蕭如妏, [1]楊淳淳, [1]程紹智

[1]台北慈濟醫院

發表者　王怡文

Keywords　放射免疫分析 | 試劑

Background

FT4 RIA 試劑採用的是 competitive radioimmunoassay。病人的檢體加入 ^{12}uI Tracer與Ligand於coated tube進行競爭型的反應。實驗中 ^{12}uI Tracer的量是 400µl、Ligand的量為 100µl，FT4檢體所需的量僅為 25µl，容易因加入的先後順序而不便判斷是否有漏加情況。在檢體已加入coated tube的情況下，針對先加Ligand再加 ^{12}uI Tracer或先加 ^{12}uI Tracer再加Ligand做個別觀察比較。

Method

收集檢體 60 支。以先加Ligand再加 ^{12}uI Tracer及先加 ^{12}uI Tracer再加Ligand同時檢測。

1. 描述性統計

60 組配對檢體中，先加 Ligand 組（A）平均值為 1.5467，先加 Tracer 組（B）為 1.4822，平均差為 0.0645，A 組約高 **4.35%**。

2. 配對差值分析

平均配對差為 +0.0645，SD = 0.0797，95% CI：0.0439–0.0851。共 47 組（78.3%）A 組較高，顯示差異方向一致。

3. 配對 t 檢定

(t(59)=6.271)，(p<0.001)，兩種添加順序的測定結果有顯著差異。

4. 極端值分析

最低值為 A 組 0.62、B 組 0.44（第 5 組）；最高值分別為 2.14（A 組，第 10 組）及 2.12（B 組，第 22 組）。移除第 5 組後，差異仍具統計顯著性，顯示結果並非僅由單一低值造成。極端值仍須依品質規則進一步判定。

5. QC 品質控制

A 組 QC 平均值為 1.145，B 組為 1.050，差值為 0.095，A 組約高 **9.05%**，與病人檢體結果呈現相同方向。惟每組僅測定 2 次，仍須對照 QC 目標值及允收範圍進一步確認。

Conclusion

結果顯示，「先加 Ligand、後加 Tracer」的平均測定值為 1.5467 ± 0.2955，而「先加Tracer、後加 Ligand」為 1.4822 ± 0.2998，前者平均高出 0.0645，約 4.35%。

配對結果中，47/60 組（78.3%）呈現先加 Ligand 組測定值較高；配對 t 檢定顯示兩種添加順序存在統計上顯著差異（t(59) = 6.271，p < 0.001）。

低值敏感度分析顯示，移除第 5 組低值配對後，整體差異仍維持相同方向且具有統計顯著性，顯示結果並非僅由單一低值造成。批次 QC 平均值亦呈現先加 Ligand 組較高的方向。整體而言，試劑添加順序可能影響 FT4 RIA 測定結果，建立一致的標準操作流程對維持檢驗結果的一致性與可靠性具有重要性。本研究初步支持將「先加Tracer、後加 Ligand」列為後續標準化操作流程的評估方向。

壁報論文 臨床組

PC-001

個案報告 臨床診斷

固態胃排空掃描之技術陷阱：食道清除延遲導致之異常數據分析與病例討論

[1]陳怡如, [1]王秀珊

[1]三軍總醫院

發表者 陳怡如

Keywords 定量分析

Background

胃排空掃描(GES)目前仍是定量評估胃動力及診斷胃輕癱的金標準。Tseng等人(2014)已建立華人燕麥餐正常值基準，半排空時間(T1/2) ≤ 85分鐘；1、2、3小時之胃殘留率低於65%、28%與8%。然而，GES判讀高度依賴定量數據，在食道功能障礙患者中，非胃部因素常導致計算結果產生顯著偏差。本案旨在分析「食道清除延遲」引發之影像異常，探討其對參數的干擾與臨床對策。

Case report

本案例針對一位臨床主訴疑似胃動力功能異常的87歲女性進行檢查。研究採用標準化試餐，由43克即食燕麥混合200 mL熱水並加入1mCi 99mTc-DTPA組成。檢查流程要求患者於坐姿下10分鐘內完食，隨後立即採仰臥位(Supine)進行影像擷取，內容涵蓋90分鐘動態掃描（30秒/幀），以及在2小時與3小時分別擷取的30°左前斜位(LAO)靜態影像。數據分析則透過Power-exponential fit模型進行擬合，藉此計算患者的半排空時間(T1/2)與各時段的胃部殘留百分比。

本個案的定量數據呈現極端且非生理性的異常，對比Tseng (2014)基準胃排空顯著延遲。患者的半排空時間(T1/2)高達829.6分鐘，遠超85分鐘的正常上限，此外1、2、3小時胃部殘留百分比分別為101%、74% 及58%，均顯著高於Tseng定義的正常基準（分別為< 65%、< 28% 與 < 8%）。透過連續影像序列觀察證實101%的非生理殘留率是因食道清除延遲所致，放射性藥物在攝食初期滯留於食道下段，隨後才陸續進入胃部感興趣區域(ROI)。放射性藥物延後進入胃部造成初始活性計算偏差，進而嚴重高估排空參數。

Conclusion

本個案1小時殘留率達101%屬非生理性異常，證實「食道清除延遲」會導致初始活性計算基準產生偏差，進而極端高估半排空時間(T1/2)。此類技術陷阱可見於各年齡層之食道動力異常者，因此臨床判讀必須結合影像序列觀察，確認藥物是否順利入胃。若數據異常，建議應進一步釐清障礙來源（如動力功能或結構病變），以確保診斷精確並避免誤診。

壁報論文 臨床組 **PC-002**

原著論文 非診療之臨床相關主題

PET/CT中光電倍增管故障假影之延伸研究:單一與雙模組異常之比較

[1]吳麗君, [1]顏玉安, [1]李將瑄

[1]奇美醫院

發表者 吳麗君

Keywords 造影儀器 | 有趣影像

Background

一般認為正子造影設備通過每日正子品保（daily quality assurance, DQA）後，當日所得PET影像即具可信度。

Method

本院於一週內發生3次PET DQA異常。第一次異常發現第17號模組第9號及第0號模組第3號光電倍增管（photomultiplier tube, PMT）異常。依原廠工程師建議執行正子校正(PET calibration)並重新建立基準值（establishing a baseline）後，再次執行DQA且結果符合允收標準，因此進行當日病人檢查。然而，第一位病人之PET冠狀面影像於背部出現明顯條紋假影。其後再次執行正子校正並重新建立基準值後，假影即未再出現。隔2日及隔1日後又分別發生相似情況。比對9年前的報告，當時單一PMT損壞且位置位於左下側或右下側時，可於肝臟PET 橫斷面觀察到明顯放射狀條紋假影。

Results

雖然DQA結果均通過允收標準，但當損壞PMT位於病人上方時，病人背部PET冠狀面仍可見明顯條紋假影，證實PMT損壞位置與假影產生具有相關性。

比對前次報告，當時單一PMT損壞且位置位於左下側或右下側時，可於肝臟 PET 橫斷面觀察到明顯放射狀條紋假影。本次事件則為雙模組 PMT同時損壞，分別位於第 0 模組與第 17 模組，兩處異常皆可能在肝臟橫斷面形成放射狀條紋假影，但因兩組假影同時存在，且方向與角度不同，彼此交錯重疊，反而在橫斷面的單一明顯條狀假影較不明顯。

另一方面，前次報告中 PMT損壞位置位於左下側或右下側，於背部 PET冠狀面則未見明顯條紋假影。相較之下，本次於背部 PET冠狀面可見明顯直條狀假影，推測與雙模組PMT損壞皆位於病人正上方有關。其產生之放射狀假影向背部方向重複投射，且因距離異常來源較遠，假影間距逐漸變寬。此外，背部組織背景相對均勻，因此條紋假影更明顯。

Conclusion

兩處損壞PMT皆位於病人上方，而病人背部因貼近平坦檢查床且分布均勻，位於距離損壞PMT較遠的位置，因此於冠狀面易形成明顯條紋假影；相對地，腹部表面因解剖結構非平面，故未出現顯著假影。與過去單一PMT損壞案例相比，本研究因損壞位置不同而導致假影方向差異；此外，雙模組PMT損壞所造成之假影可能彼此重疊，使橫斷面假影較不明顯，此現象亦與單一PMT損壞案例不同。

壁報論文 臨床組 **PC-003**

病例系列 臨床診斷

第二次延長掃描排除直腸FDG假陽性攝取：PET/CT病例報告

[1]李將瑄, [1]吳麗君, [1]顏玉安

[1]奇美醫院

發表者 李將瑄

Keywords 影像組學 (Radiomics) | 有趣影像

Background

18F-FDG PET/CT廣泛應用於腫瘤診斷、分期及治療後追蹤。然而骨盆腔影像常受到腸道生理性攝取、尿路放射活性及腸道蠕動等因素影響，造成影像判讀困難。本研究報告一例直腸FDG異常攝取假影，藉由短時間重複延遲掃描成功排除病灶，以提供臨床判讀參考。

Method

69歲男性肺癌病史，曾接受胸腔鏡手術、放射治療及化學治療，因懷疑肺癌復發接受18F-FDG PET/CT檢查。病人禁食6小時後接受10 mCi 18F-FDG注射，注射後60分鐘進行初期掃描，90分鐘進行延遲掃描。影像顯示肺部結節無明顯FDG攝取，但延遲影像於直腸區域出現團塊狀高FDG攝取，影像表現類似腫瘤病灶。約15分鐘後於相同條件下再次進行延遲掃描，未給予灌腸、排便、步行或其他促進腸蠕動措施，結果原先直腸高攝取團塊完全消失。

Results

由於肺癌轉移至大腸相當罕見，且病灶於短時間內完全消失，不符合惡性病灶表現。推測此現象與直腸蠕動造成PET與CT配準差異或局部腸壁暫時性收縮有關，導致FDG攝取呈現假陽性影像。重複延遲掃描成功排除偽病灶，避免誤判。

Conclusion

當PET/CT檢查於直腸或骨盆腔出現局部FDG異常攝取，而影像表現與臨床狀況不一致時，可考慮於短時間後進行重複延遲掃描。此方法無須額外侵入性處置，即有機會藉由腸道蠕動變化排除假影，提高PET/CT判讀準確性並降低偽陽性診斷風險。

壁報論文 臨床組 **PC-004**

個案報告 臨床診斷

生化復發且骨掃描穩定之攝護腺癌病人：rhPSMA PET發現隱匿性骨轉移病例報告

[1]王嘉鴻, [1]曾能泉

[1]童綜合醫院

發表者 王嘉鴻

Keywords 有趣影像

Background

Tc-99m MDP Bone Scan骨掃描為攝護腺癌骨轉移追蹤之常用影像工具，但其主要反映骨質重塑反應，對於早期或尚未產生明顯成骨反應之轉移病灶可能偵測受限。rhPSMA PET/CT則可直接評估腫瘤細胞PSMA表現，於生化復發病人之病灶定位具有重要價值。

Case report

一名高風險轉移性攝護腺癌患者，接受雄性素剝奪治療後PSA由199.286 ng/mL下降至0.772 ng/mL，後續逐漸上升至2.078 ng/mL（2025年7月）及3.618 ng/mL（2025年9月），符合生化復發。2025年8月Tc-99m MDP骨掃描未見明確疾病進展，病灶評估為穩定狀態。為評估PSA上升原因，病人於同年10月接受F-18 rhPSMA PET檢查，結果顯示攝護腺局部復發、左側上直腸淋巴結轉移以及左肩胛骨（SUVmax 6.53）骨轉移。後續再次於11月進行BONE SCAN，同樣評估為穩定狀態。值得注意的是：左肩胛骨病灶於2025年8月及11月前後兩次Bone Scan均未呈現明顯惡性攝取表現，顯示Bone Scan並未反映rhPSMA PET所揭露之左肩胛骨轉移病灶。

Conclusion

本案例顯示，即使Bone Scan追蹤結果呈現穩定且未見明顯進展，rhPSMA PET仍可於生化復發階段發現Bone Scan未能明確顯示之活動性骨轉移及局部復發病灶。Bone Scan與PSMA PET反映不同生物學特性，兩者於攝護腺癌生化復發及骨轉移評估上具有重要互補價值。

壁報論文 臨床組 **PC-005**

個案報告 非診療之臨床相關主題

Rare Streak Artifact on CT Images in an Obese Patient During PET/CT Imaging: A Case Report

[1]蘇于婷, [1]李將瑄, [1]吳麗君

[1]奇美醫院

發表者 蘇于婷

Keywords 有趣影像

Background

There are several artifacts caused by a variety of factors such as patient or scanner conditions in PET/CT imaging . The common artifacts include respiratory artifacts,metal artifacts and so forth. In this case, an unusual streak artifact was noticed during PET/CT imaging. Since its appearance differed from common artifacts, this case is presented for discussion.

Case report

A 46-year-old male patient with lymphoma underwent a PET/CT scan in 2026. The patient was 174.3 cm tall and weight was 118.4 kg. CT parameters were 120 kVp and 15 mA for the early-phase acquisition. The CT images demonstrated a streak artifact located anterior to the vertebral column, extending from the lung to the pelvis.For the delayed-phase acquisition, CT current was 30 mA. The artifact remained visible but appeared less conspicuous.Following the delayed-phase scan, an additional acquisition was performed using 50 mA for CT current. The artifact remained visible but appeared much less conspicuous.A review of the patient's PET/CT examination in 2023 with a height of 173 cm and weight of 102 kg demonstrated the same artifact but was less conspicuous than that observed in 2026.

Conclusion

This case demonstrates that the artifact was less conspicuous as tube current increased. In addition, the artifact appeared to be more conspicuous with greater patient weight. The phenomenon is presumed to be associated with photon starvation caused by obesity and reconstruction effects in low-dose CT imaging. Although the artifact did not affect clinical diagnosis, technologists and physicians should be aware of its potential occurrence during low-dose PET/CT in obese patients.

壁報論文 臨床組 **PC-006**

個案報告 臨床診斷

Tubular Adenoma在18F-FDG PETCT 之影像表現

[1]李佩璇, [1]楊朝瑋

[1]澄清醫院

發表者 李佩璇

Keywords 有趣影像

Background

18F-FDG PET/CT已廣泛應用於癌症的分期、治療反應評估及復發追蹤。除原發腫瘤外，PET/CT偶爾可發現與癌症無關的意外病灶（incidental findings）。其中，大腸局灶性FDG攝取具有重要的臨床意義，可能代表良性腺瘤、癌前病變或惡性腫瘤，需進一步檢查以確認診斷。

Case report

一名 52 歲女性患者因右側乳癌，於 2023 年 4 月接受PET/CT檢查。在注射 18F-FDG (10 mCi) 約 60 分鐘後進行掃描。掃描結果顯示右側乳房、右側腋下淋巴、右側內乳淋巴及骨盆腔左側 (疑似乙狀結腸) 有FDG攝取增強。PET/CT 除顯示乳癌相關病灶外，另於乙狀結腸處發現局灶性異常FDG攝取，病理切片顯示為Tubular adenoma(管狀腺瘤)。Tubular adenoma為常見的大腸腺瘤性息肉，屬於癌前病變。由於腺瘤細胞葡萄糖代謝增加，可於 18F-FDG PET/CT 呈現局灶性FDG攝取。

Conclusion

Tubular adenoma在 18F-FDG PET/CT上可呈現不同程度的FDG攝取，其表現受病灶大小、病理型態及異生程度影響。由於與大腸癌之代謝表現具有重疊，PET/CT無法單獨作為鑑別診斷工具。對於偶發性局灶性大腸FDG攝取，建議進一步接受大腸鏡檢查，以排除進展性腺瘤或惡性病灶。

壁報論文 臨床組 **PC-007**

原著論文 臨床診斷

Combining the prognostic values of 18F-FDG PET features with clinical variables using random survival forest in patients with lung adenocarcinoma treated with EGFR-targeted therapy

[1,2]陳昱宏, [1]呂昆翰, [2]王咏璇, [1,2]朱崧肇, [2]林智斌, [2]劉淑馨

[1]慈濟大學
[2]花蓮慈濟醫院

發表者 陳昱宏

Keywords 影像組學 (Radiomics) | 分子影像

Background

Many clinical and 18F-FDG PET-derived features are valuable prognostic biomarkers for patients with lung adenocarcinoma treated with EGFR-targeted therapy. However, traditional Cox regression model is able to include only limited variables. We aim to use random survival forest to integrate clinical and PET-based prognostic factors.

Method

We retrospectively analyzed pre-treatment 18F-FDG PET from 132 patients with lung adenocarcinoma treated with EGFR-targeted therapy. We extract primary tumor and whole body SUVmax, MTV, TLG, and respiratory-stable features (first-order entropy, joint entropy, sum entropy, run entropy, sphericity, IDN, and IDMN) from 18F-FDG PET using Pyradiomics. We used random survival forest to integrate the prognostic values of PET-derived image features and clinical variables for predicting progression survival (PFS). We used a step-wise approach to eliminate redundant variables that exhibited negative relative importance. The number of trees and minimal nodal size were 1000 and 12, respectively. We estimated the c-index of the model for our cohort using bootstrap method (1000 bootstrap samples). This study was funded by NSTC (113-2314-B-303-018-MY2).

Results

There were 103 patients experienced progression or death. The final model out-of-bag error rate and standardized continuous ranked probability score were 0.393 and 0.153, respectively. The final model included total sphericity, total TLG, total MTV, IDMN, IDN, ever smoker, brain metastasis, pleural effusion, total SUVmax, and age. The estimated c-index of the model for the cohort in predicting PFS was 0.760 (95% CI of 0.705-0.811).

Conclusion

Our preliminary results showed that random survival forest is feasible for integrating 18F-FDG PET-derived features and clinical variables in predicting PFS in patients with lung adenocarcinoma treated with EGFR-targeted therapy. This model may be valuable for risk stratification and may be used to guide tailored therapeutic strategies.

壁報論文 臨床組

PC-008

個案報告 臨床診斷

探討巨大肝囊腫於MDCT與Tl-201心肌灌注掃描之影像特徵一致性

[1]游慧貞, [1]黃貞文, [1]李佩珊, [1]朱筱萍, [1]朱秀蘭

[1]高雄醫學大學

發表者 游慧貞

Keywords 造影儀器 | 影像組學 (Radiomics)

Background

本病例為一名68歲女性患者，因腹部不適及脊椎退化性症狀接受多偵測器電腦斷層（MDCT）評估。當次影像除顯示心臟肥大（Cardiomegaly）、少量心包膜積水及主動脈粥狀硬化等心血管系統改變外，亦意外發現顯著肝臟病灶。本文旨在探討該巨大肝囊腫在解剖構造影像（MDCT）與功能性顯像（Tl-201 NM Scan）中的影像特徵與臨床診斷價值。

Case report

患者於2025年8月接受腹部與脊椎之MDCT檢查。採用多平面重建（MPR）技術，評估冠狀面（Coronal）與矢狀面（Sagittal）之影像，以釐清腹內器官之解剖關係與血管分布。後於同年11月，患者因心血管風險評估接受Thallium-201心肌灌注掃描（MPI）。針對兩項檢查之影像進行對照分析，特別觀察病灶之質量效應（Mass effect）及其對追蹤劑攝取之影響。MDCT影像證實於左肝葉存在一巨大囊性病灶，最大徑約12.8公分。後續之Tl-201心肌灌注掃描顯示，在肝臟相對應位置呈現明顯之放射性攝取缺損（Photopenic defect），即典型之「冷區」（Cold spot），證實該病灶內部缺乏血流灌注與具代謝活性之組織。

Conclusion

本病例呈現巨大肝囊腫在不同顯像原理下的特徵一致性。MDCT檢查提供精確的解剖定位與病灶對周邊組織（如膽管）的壓迫資訊；而Tl-201則進一步確認其非腫瘤性（非實質性）的生物學特性。此種意外發現在心肌灌注掃描中具有重要的臨床警示意義。儘管目前患者臨床診斷傾向為良性單純性肝囊腫，但鑑於其體積龐大並已造成膽管壓迫，建議轉診肝膽腸胃內科或外科，評估是否需進行介入性抽吸或手術治療，以緩解壓迫症狀並預防併發症。

壁報論文 臨床組

PC-009

個案報告 臨床診斷

Multimodality Nuclear Medicine Imaging of Active Heterotopic Ossification Following Severe Traumatic Brain Injury

[1,2]莊紫翎

[1]慈濟大學

[2]大林慈濟醫院

Keywords 有趣影像

Background

Heterotopic ossification (HO) is abnormal bone formation in soft tissues, affecting 11–76% of patients after traumatic brain injury (TBI). Early diagnosis is challenging because its clinical manifestations often mimic infection. Three-phase Tc-99m MDP bone scintigraphy detects HO weeks before radiographic ossification, while Ga-67 citrate and Tl-201 scintigraphy provide complementary information on inflammatory and metabolic activity.

Case report

A 28-year-old man sustained severe TBI following a motorcycle accident and underwent multiple neurosurgical procedures. His hospital course was complicated by recurrent brain abscess and Pseudomonas aeruginosa bacteremia requiring prolonged antibiotic therapy. He was readmitted with persistent fever one day after discharge. Ga-67 inflammation scan demonstrated increased uptake in the bilateral hips, left shoulder, and left posterior back, with SPECT/CT localizing the bilateral hip lesions to periarticular soft tissue calcifications. One week later, three-phase Tc-99m MDP bone scintigraphy demonstrated increased perfusion, blood-pool activity, and intense delayed extraskeletal uptake at hips, left shoulder and upper back, consistent with active HO. Serial radiographs of hips showed no periarticular calcification two months after injury but extensive ossification four months after injury. Tl-201 scintigraphy demonstrated patchy uptake in the bilateral hips and left axillary region, indicating metabolically active HO. The patient died six months after injury because of progressive clinical deterioration.

Conclusion

This case illustrates the complementary roles of multimodality nuclear imaging in characterizing active HO. Three-phase Tc-99m MDP bone scintigraphy remains the most sensitive modality for early detection, whereas Ga-67 citrate and Tl-201 provide additional information on inflammatory and metabolic activity. Differential diagnosis includes myositis ossificans (MO), soft tissue sarcomas, and infection. Unlike the localized MO following direct muscle trauma, neurogenic HO after TBI is typically multifocal and periarticular. Severe TBI, prolonged immobilization, and recurrent infections likely contributed to the extensive HO. Multimodality nuclear imaging enables comprehensive assessment of disease activity and extent, facilitating evaluation of lesion maturity before surgical intervention.

壁報論文 臨床組 **PC-010**

個案報告 臨床診斷

Five-Toe Socks Sign on FDG PET/CT

[1,2]莊紫翎

[1]慈濟大學
[2]大林慈濟醫院

Keywords 有趣影像

Background

F-18 fluorodeoxyglucose (FDG) PET/CT is widely used for oncologic staging but can demonstrate uptake in benign inflammatory and infectious conditions. Inflammatory cells express high levels of glucose transporters, resulting in FDG accumulation at sites of inflammation. Recognition of characteristic patterns of benign FDG uptake is essential to avoid false-positive interpretations. We present a case demonstrating a novel imaging sign—the "five-toe socks sign"—caused by tinea pedis.

Case report

A 73-year-old man with synchronous primary lung cancers (right upper lobe squamous cell carcinoma and left lower lobe adenocarcinoma, both stage IIA) underwent FDG PET/CT for staging. Intense uptake was observed in the right upper lobe lesion (SUVmax 18.0). Incidentally, mild symmetric FDG uptake was noted between the toes bilaterally, creating an appearance resembling five-toe socks on maximum-intensity-projection and transaxial images. Fused PET/CT localized this uptake to the interdigital spaces (SUVmax 1.3 right, 2.4 left). Physical examination revealed chronic pruritic interdigital dermatitis with scaling, maceration, and fissuring. Dermatologic evaluation confirmed tinea pedis. Follow-up PET/CT after topical antifungal treatment demonstrated complete resolution of interdigital uptake.

Conclusion

Dermatophyte infections induce inflammatory glucose metabolism, resulting in focal FDG uptake detectable on PET/CT. While FDG uptake in cutaneous inflammatory conditions is well-documented, the characteristic bilateral interdigital pattern of tinea pedis has not been previously described as a distinct imaging sign. The symmetric distribution and anatomic localization to interdigital spaces create the distinctive "five-toe socks" appearance. This case demonstrates that benign inflammatory processes can mimic pathologic uptake. The relatively low SUVmax values (1.3-2.4), symmetric distribution, and clinical correlation helped distinguish this benign finding from metastatic disease. Resolution after antifungal therapy confirmed the inflammatory etiology. Recognition of this sign prevents misinterpretation and unnecessary investigations, emphasizing the value of integrating PET findings with physical examination in comprehensive patient assessment.

壁報論文 臨床組 **PC-011**

個案報告 臨床診斷

Prefrontal Hypoperfusion and Limbic Hyperactivity in Treatment-Resistant Schizoaffective Disorder

[1,2]莊紫翎
[1]慈濟大學
[2]大林慈濟醫院

Keywords 有趣影像

Background

Treatment-resistant schizoaffective disorder remains a major therapeutic challenge. Brain perfusion SPECT with Tc-99m ECD allows visualization of regional cerebral perfusion abnormalities associated with psychosis and mood disorders.

Case report

A 52-year-old woman with a family history of schizophrenia and bipolar disorder developed her first depressive episode at the age of 41, followed by auditory hallucinations and delusions at 46 years of age. Despite multiple antipsychotics (olanzapine, lurasidone, amisulpride, and haloperidol), antidepressants (vortioxetine and mirtazapine), repeated psychiatric admissions, and electroconvulsive therapy since 2019, her psychotic and depressive symptoms persisted with poor functional recovery. She was diagnosed with treatment-resistant schizoaffective disorder in 2025. Brain perfusion scintigraphy with Tc-99m ECD demonstrated marked hypoperfusion in the orbitofrontal, ventromedial prefrontal, anterior cingulate, and dorsolateral prefrontal cortices, accompanied by relative hyperperfusion in the hippocampus and amygdala on two-tailed eZIS analysis.

Conclusion

The observed perfusion pattern highlights disruption of the prefrontal-limbic network, a key neurobiological substrate implicated in treatment-resistant psychosis. Marked hypoperfusion in the prefrontal cortices may underlie impaired executive function, emotional dysregulation, cognitive deficits, and persistent negative symptoms. In contrast, relative hyperperfusion of the hippocampus and amygdala suggests limbic hyperactivity, which has been linked to aberrant salience attribution and excessive subcortical dopaminergic signaling, contributing to persistent hallucinations and delusions. This dissociation between prefrontal hypofunction and limbic hyperactivity provides an imaging correlate of treatment resistance in schizoaffective disorder. Recognition of this dual perfusion signature may facilitate earlier identification of refractory patients and support the development of individualized therapeutic approaches, including targeted neuromodulation strategies.

壁報論文 臨床組 PC-012

原著論文 臨床診斷

Clinical Utility of Hepatic Arterial Perfusion Imaging in Patients with Advanced Hepatocellular Carcinoma Undergoing Hepatic Arterial Infusion Chemotherapy.

[1]游冬齡, [1]卓俊宏, [1]陳淑芬, [1]藍昇輝

[1]門諾醫院

發表者 游冬齡

Keywords Hepatocellular carcinoma | Hepatic arterial infusion chemotherapy | hepatic arterial perfusion imaging

Background

Hepatic arterial infusion chemotherapy (HAIC) is an established treatment for advanced hepatocellular carcinoma (HCC). The purpose of this study is to evaluate the clinical utility of hepatic arterial perfusion imaging (HAPI) in detecting extrahepatic perfusion prior to HAIC.

Method

There were 156 patients with advanced HCC were collected retrospectively for analyzing. All patients underwent HAPI prior to HAIC. Imaging was performed immediately following transcatheter hepatic arterial injection of 4 mCi Tc-99m MAA diluted in 20 mL of normal saline. Extrahepatic perfusion to the GI tract, spleen, and lungs was assessed. In cases where GI perfusion was identified, catheter repositioning was performed before initiation of chemotherapy. In cases where lung perfusion was identified, Lung perfusion ratio was calculated as: (lung counts / injected dose counts) × 100%.

Results

Extrahepatic GI perfusion was identified in 32 patients (20.1%), involving the stomach in 10 patients, the small intestine in 16, and both regions in 6. Catheter repositioning was performed in all affected patients, resulting in complete resolution of GI perfusion in every case. Splenic perfusion was observed in 13 patients (8.3%). Pulmonary tracer shunting was detected in 121 patients (77.6%), with lung perfusion ratios ranging from 4.1% to 52.1%.

Conclusion

HAPI is a highly valuable imaging modality for patients undergoing HAIC. It enables detection of extrahepatic perfusion, facilitates timely catheter adjustment, and significantly reduces the risk of serious GI complication. Routine integration of HAPI into the HAIC workflow may enhance treatment safety and optimize therapeutic delivery in patients with advanced HCC.

壁報論文 臨床組 **PC-013**

個案報告 臨床診斷

The Role of FDG PET/CT in the Diagnosis of Intramedullary Spinal Cord Metastases from Breast Cancer: A Case Report

[1]游冬齡, [1]林孝府, [1]陳翌真, [1]陳淑芬

[1]門諾醫院

發表者 游冬齡

Keywords Breast cancer | FDG PET/CT | Intramedullary spinal cord metastasis

Background

Intramedullary spinal cord metastasis (ISCM) is a rare but devastating complication of breast cancer and is frequently associated with rapid neurological deterioration and poor prognosis. We report a case in which FDG PET/CT provided important complementary information for the diagnosis of ISCM.

Case report

A 49-year-old woman with a history of left breast cancer (pT1cN0M0, Stage I) underwent modified radical mastectomy in 2011 followed by adjuvant chemotherapy and endocrine therapy. In October 2023, she developed progressive neurological symptoms, including chest wall numbness, perianal sensory disturbance, and right thigh numbness. FDG PET/CT demonstrated multiple hypermetabolic foci involving the thoracic spinal cord, lumbar spinal cord, and cauda equina, raising strong suspicion for metastatic involvement of the central nervous system. Subsequent spinal MRI revealed multiple contrast-enhancing T2-hyperintense intramedullary lesions at the T3–T5 and T10 levels, consistent with the FDG PET/CT findings.

Conclusion

This case highlights the value of FDG PET/CT in the evaluation of suspected intramedullary spinal cord metastases from breast cancer. FDG PET/CT can identify metabolically active lesions, correlate with neurological manifestations, and provide clinically meaningful evidence.

壁報論文 臨床組 **PC-014**

經驗分享 非診療之臨床相關主題

放射免疫室 I-125 操作人員輻射安全資格評估與管理優化

[1]方雅潔

[1]國泰醫院

Keywords 放射免疫分析 | 碘-125

Background

本院放射免疫室人員原須完成36小時輻安訓練並考取國家「操作人員輻射安全證書」，且每年需回訓6小時。繁重的考證壓力與高流動率導致培訓成本沉重，亦降低人員入職與留任意願。為解決人力痛點，本單位與輻防室合作，重新評估放射免疫分析操作人員之法定資格需求，期以優化管理機制。

Method

依據《放射性物質與可發生游離輻射設備及其輻射作業管理辦法》，統計本室每月I-125進貨總活度。因每月平均進貨2至3次，故以月進貨總活度除以2作為「單次最大使用活度」之評估基準。將此活度與法定豁免管制量比對，判定輻射作業類別（登記備查或許可類），進而確認人員法定資格。

Results

經評估，本室 I-125 最大活度為 58.9 MBq。依《游離輻射防護安全標準》，I-125 豁免管制活度為 1 MBq，本室使用量為豁免量之 58.9 倍。依管理辦法第 14 條規定，非密封放射性物質活度於豁免量100 倍以下者屬「登記備查類」。本室活度未達 100 倍之許可門檻，依法確認屬登記備查類。

Conclusion

本院 I-125 作業屬「登記備查類」，操作人員依法免領輻安證書，免除 36 小時訓練與國家考試，僅需完成 18 小時一般輻防訓練即可操作。此法規釐清與管理修正，不僅確保合規，更大幅減輕人員考證壓力與院方培訓成本，有效提升招募與留任率。

壁報論文 臨床組 **PC-015**

病例系列 臨床診斷

Thoracic Rotation Causes Misclassification of the Heart-to-Contralateral Lung Ratio on 99mTc-PYP Scintigraphy: A Four-Case Series

[1]陳至豪, [1]徐景龍, [1]徐尉淳, [1]王昱豐

[1]臺北榮民總醫院

發表者 陳至豪

Keywords 影像處理/軟體 | 分子影像 | 造影技術 | PYP Scan

Background

The heart-to-contralateral lung (H/CL) ratio is a widely used semiquantitative parameter on 99mTc-pyrophosphate (99mTc-PYP) scintigraphy for the evaluation of transthyretin cardiac amyloidosis (ATTR-CM). The H/CL ratio is derived from two-dimensional planar region-of-interest (ROI) analysis. However, thoracic rotation resulting in an anterior oblique projection may alter the measured counts within the ROI by changing the relative projection of the heart and adjacent thoracic structures, consequently affecting H/CL ratio measurements. This technical pitfall is easily overlooked and may lead to inaccurate semiquantitative assessment of ATTR-CM.

Method

Patients with suspected ATTR-CM underwent planar scintigraphy 3 hours after intravenous administration of 740 MBq of 99mTc-PYP. H/CL ratios were calculated using standard two-dimensional planar ROI analysis. SPECT/CT was subsequently performed to confirm myocardial tracer localization and assess thoracic orientation. In patients with thoracic rotation, repeat planar imaging was acquired using an optimized anteroposterior (AP) projection based on the SPECT/CT findings, followed by recalculation of the H/CL ratio.

Results

Four patients with thoracic rotation demonstrated substantial changes in H/CL ratios after optimization of the AP projection. H/CL ratios changed from 1.54 to 1.30, 1.47 to 1.23, 1.69 to 1.29, and 1.10 to 1.33, indicating that thoracic rotation may either overestimate or underestimate semiquantitative measurements depending on the direction of rotation. Two patients were reclassified across the commonly used diagnostic threshold (H/CL = 1.5) after correction of thoracic rotation, resulting in a change in clinical interpretation. SPECT/CT clearly identified thoracic rotation and facilitated optimization of the planar acquisition angle before repeat H/CL ratio measurement.

Conclusion

Thoracic rotation can significantly influence H/CL ratio measurements by altering the relative projection of the heart and adjacent thoracic structures on planar 99mTc-PYP scintigraphy. This easily overlooked technical pitfall may result in erroneous semiquantitative assessment of ATTR-CM. Routine review of SPECT/CT images before H/CL ROI analysis may help identify thoracic rotation and avoid an underrecognized source of H/CL ratio error, thereby improving the reliability of semiquantitative assessment in 99mTc-PYP scintigraphy.

壁報論文 臨床組 **PC-016**

原著論文 臨床診斷

18F-FDG PET radiomic features are associated with “spread through air space” in patients with lung adenocarcinoma undergoing curative surgery

[1,2]陳昱宏, [2]呂昆翰, [2,1]陳彥璋, [1,2]朱崧肇, [1]林智斌, [1]張比嵩, [1]劉淑馨

[1]花蓮慈濟醫院
[2]慈濟大學

發表者 陳昱宏

Keywords 分子影像 | 影像組學 (Radiomics)

Background

18F-FDG PET-based radiomic features have increasingly been used in research for lung adenocarcinoma. Recently, spread through air space (STAS) on surgical pathology has been recognized as an important prognostic factor. We evaluate whether18F-FDG PET features are associated with STAS.

Method

We retrospectively analyzed pre-treatment 18F-FDG PET/CT from 76 patients with lung adenocarcinoma underwent curative surgery. STAS was determined by pathologists from H&E stains of surgical specimens. We extract primary tumor SUVmax, MTV, and respiratory-stable features (first-order entropy, joint entropy, sum entropy, run entropy, sphericity, IDN, and IDMN) from 18F-FDG PET/CT using Pyradiomics. The volume-of-interests of transmission CT were manually adjusted to prevent mis-registration. We used Mann-Whitney U test to compare the distribution of 18F-FDG PET/CT derived features between patients with and without STAS. This study was funded by NSTC (113-2314-B-303-018-MY2).

Results

There were 16 patients who had STAS on examination of their surgical pathological specimens. Among all18F-FDG PET-derived features, patients with STAS exhibited significantly higher primary tumor SUVmax ($p = 0.040$), first-order entropy ($p = 0.030$), joint entropy ($p = 0.037$), sum entropy ($p = 0.028$), and run entropy ($p = 0.034$) than patients without STAS. Transmission CT-derived image features did not show significant difference between patients with and without STAS.

Conclusion

Lung adenocarcinoma with STAS appears to exhibit higher glycolytic activity and heterogeneity. The image-based glycolytic features are associated with unfavorable histopathological findings and may be valuable pre-surgical biomarkers for prognostic evaluation and therapeutic guidance.

壁報論文 臨床組 **PC-017**

個案報告 臨床診斷

三相式骨骼造影意外發現主動脈瘤

[1]朱秀蘭, [1]莊雅雯, [1]游慧貞

[1]高雄醫學大學

發表者 朱秀蘭

Keywords 造影儀器 | 解剖學/CT/MR

Background

三相式骨骼掃描（Tc-99m MDP）檢查結合血流、血池與骨骼影像，經由靜脈注射放射性磷酸鹽藥物，利用成骨作用附著於骨骼系統，具高靈敏度與特異性以評估骨骼關節病變。此檢查適用於鑑別診斷骨髓炎、蜂窩性組織炎、壓力性骨折、骨骼缺血壞死、異位性骨化、風濕免疫疾病等病症。

Case report

本次報告探討兩例男性患者（分別為64歲與88歲），主訴皆為下肢蜂窩性組織炎，至核醫科進行三相式骨骼例行性常規檢查。核醫影像顯示，兩位患者在第二相（血池相）的全身造影中，均意外發現腹部主動脈處有顯著的放射性藥物異常蓄積（熱區，hot spot）；然而，在隨後的第三相（遲發骨骼相）掃描時，該腹部熱區皆已廓清消失。此影像特徵提示腹部區塊有異常的血池滯留。隨後回溯查看兩位患者先前的電腦斷層（CT）影像紀錄，證實該血池相熱區之解剖位置，正對應於患者原先即確診的腹主動脈瘤（AAA）。

Conclusion

本病例提示臨床，三相式骨骼掃描之血池相異常放射性訊號，與既有血管病變高度相關，具備回溯判讀之影像印證價值。當臨床於第一相（血流相）或第二相（血池相）發現異常放射性活性增高時，必須全面審慎評估，鑑別並排除血管動脈瘤等非感染性動態血流病變，以避免將其誤判為局部組織感染或骨髓炎之影像表現。

壁報論文 臨床組 **PC-018**

文獻綜述 臨床治療或診療合一

Lu-177 PSMA 治療相關醫療人員之職業輻射曝露：實證導向文獻回顧

[1]黃兆駿, [1]陳雅凰, [1]賴佳玟, [1]李柏葦, [1]張哲瑋

[1]亞東醫院

發表者 黃兆駿

Keywords 曝露劑量 (Exposure) | 輻射防護

Background

Lu-177 PSMA放射配體治療為轉移性去勢抗性攝護腺癌的重要治療選項。治療流程涉及放射藥物處理、靜脈給藥及治療後照護，相關醫療人員可能接受職業性游離輻射曝露。本研究以實證導向文獻回顧，回答參與 Lu-177 PSMA 治療流程之醫療人員於常規作業下可能接受之職業輻射曝露劑量。

Literature review

方法：本研究以 PEO 架構設定臨床問題，於 2026 年 7 月 31 日使用 PubMed 進行文獻搜尋，結合 MeSH terms 與 title/abstract keywords，以 Lu-177 PSMA、radiation exposure、radiation protection、external exposure、external dose 及 dose rate 為核心概念。納入與醫療人員曝露、個人劑量、照護者劑量、病人周圍劑量率及輻射安全實務相關之人類研究；依與臨床問題之直接性進行證據定位。

結果：PubMed 初始搜尋獲得 71 篇文獻，限制 human studies 後為 56 篇；經標題與摘要篩選後，納入 13 篇相關文獻，其中 4 篇可直接提供醫療人員個人劑量資料。於各研究常規流程與量測條件下，單次治療相關人員曝露多為 μSv 等級，不同職類量測值多約為 2–10 μSv。部分研究顯示，2 mm鉛屏蔽可降低給藥相關人員曝露。病人周圍 1 m 劑量率於治療早期約為 25–40 μSv/h，於治療後 4–6小時約為 12–27 μSv/h，並隨時間下降；照護者累積劑量約為 20–1170 μSv。病人周圍劑量率與照護者劑量屬補充性作業情境資料，不能取代醫療人員個人職業劑量。

結論：現有直接證據顯示，Lu-177 PSMA 常規治療相關醫療人員之單次職業曝露多為 μSv等級。然而，各研究之治療活度、工作流程、防護條件、職類、量測位置與時間點不同，且缺乏長期分職類累積個人劑量及健康效應資料，因此不宜將單次量測結果視為固定劑量或直接外推至所有機構。院內仍應以個人劑量監測紀錄評估實際職業曝露，並依 ALARA原則持續優化給藥、照護及污染處理流程。

壁報論文 臨床組 PC-019

個案報告 臨床診斷

Evaluating Post-Treatment Brain Neoplasms with Thallium Scan

[1]游舜宇

[1]大林慈濟醫院

Keywords 造影儀器

Background

Post-treatment evaluation of brain neoplasms is essential for assessing therapeutic response and determining the need for additional treatment. However, treatment-related changes, particularly radiation necrosis, often mimic tumor recurrence on conventional MRI, making accurate interpretation challenging. Functional imaging can provide valuable complementary information by distinguishing viable tumor tissue from post-treatment effects. Although amino acid PET imaging, such as fluciclovine PET, offers excellent diagnostic performance for this purpose, its high cost and limited availability may restrict its routine clinical use. In such situations, thallium-201 brain scintigraphy represents a more accessible and cost-effective alternative.

Beyond its role in the initial evaluation of brain tumors, thallium brain scintigraphy is also useful for post-treatment response assessment. Thallium uptake reflects viable tumor tissue and is typically not increased in treatment-related inflammation or radiation necrosis. Consequently, it can aid in differentiating recurrent tumor from post-treatment necrosis. On follow-up imaging, focal thallium uptake exceeding background cerebral activity suggests the presence of residual or recurrent viable neoplasm, whereas absent or markedly reduced uptake favors treatment-related necrosis or a favorable therapeutic response.

Case report

A 51-year-old man with a history of left frontoparietal glioblastoma, status-post tumor resection and chemoradiotherapy showed persistent soft tissue lesions on MRI scans. Fluciclovine PET scan was considered to determine if MRI findings were post-treatment necrosis or contained residual viable tumor; however, due to patient’ s poor financial situation, a cheaper alternative was preferred. Thallium-201 brain scan was chosen and showed no tracer activity, likely suggesting no viable neoplasm in the brain. Patient was followed up in the outpatient clinic with periodic MRI and thallium brain scans. On the third scan there were focal areas of increased tracer uptake in the left temporal region, suggesting tumor recurrence. Corresponding MRI findings confirmed disease recurrence, and the patient subsequently underwent further treatment.

Conclusion

This case demonstrates that thallium-201 brain scintigraphy is a practical and cost-effective imaging modality for the post-treatment evaluation of brain neoplasms. By differentiating viable tumor from treatment-related necrosis, it may serve as a valuable alternative when advanced PET imaging is unavailable or financially inaccessible.

壁報論文 臨床組 **PC-020**

個案報告 臨床診斷

暫時性瀰漫性肝臟放射性攝取於乳癌患者 Tc-99m RBC MUGA 追蹤檢查 -病例報告

[1]王榛婷, [1]張淑敏, [1]張晉銓

[1]高醫中和紀念醫院

發表者 王榛婷

Keywords 分子影像

Background

多門控心室造影（MUGA）利用 Tc-99m 標記紅血球（Tc-99m RBC）進行心血池造影，可提供準確且再現性高的左心室射出分率（LVEF）測量，因此廣泛應用於接受具心臟毒性化學治療之乳癌患者心功能監測。正常情況下，Tc-99m RBC應主要分布於循環血池，非心臟器官僅呈現低背景活性。然而，受紅血球標記效率、病人生理狀態或技術因素影響，可能出現非典型放射性分布，影響影像判讀及 LVEF評估。本病例報告一名乳癌患者於連續 MUGA 追蹤期間出現一次性瀰漫性肝臟放射性攝取增加，並於後續檢查恢復正常之特殊影像表現。

Case report

一名63歲乳癌女性患者於化療期間接受Tc-99m RBC MUGA檢查以監測左心室功能，共完成三次檢查。第一次檢查顯示心血池放射性分布正常，心臟影像清晰，肝臟僅呈現正常背景活性。第二次追蹤檢查時，發現肝臟出現瀰漫性放射性攝取增加，與前次相比明顯增亮，但未觀察到胃部放射性聚積增加或其他典型游離 Tc-99m pertechnetate 分布。第三次追蹤檢查則顯示肝臟放射性分布恢復正常，心血池影像亦恢復良好，未再出現異常肝臟攝取。

Conclusion

文獻指出，Tc-99m RBC MUGA的影像品質可能受到紅血球標記效率、病人生理狀態及標記或影像採集等技術因素影響。當標記效率降低時，可增加背景放射性活性並降低心血池與背景組織的對比，進而影響影像判讀及左心室功能評估。然而，本病例第二次檢查雖出現瀰漫性肝臟放射性攝取增加，卻未伴隨胃部放射性聚積增加，因此與典型游離 Tc-99m pertechnetate所造成之生物分布並不完全一致。由於目前文獻對於此類「僅肝臟瀰漫性攝取增加」的機轉報告有限，因此單純以 Tc-99m RBC標記失敗解釋仍有所不足。除標記效率變化外，標記程序、影像採集條件或其他暫時性的生理因素亦可能影響 Tc-99m RBC的體內分布，但本病例缺乏足夠證據以確認其真正機轉。另一方面，患者於第三次追蹤檢查時肝臟攝取已恢復正常，且臨床並無持續性肝臟疾病或局部肝臟病灶之相關證據，因此固定性肝臟病變的可能性相對較低。

本病例提醒臨床醫師及核醫放射師，在判讀 MUGA影像時，除應評估左心室功能外，亦應注意非心臟器官之放射性分布。當出現肝臟瀰漫性攝取增加且未伴隨典型胃部攝取時，建議結合病人臨床病史、前後追蹤影像及檢查品質進行綜合判讀，避免直接歸因於 Tc-99m RBC 標記失敗或肝臟病變，以提升 MUGA 檢查之判讀準確性。

壁報論文 臨床組 **PC-021**

經驗分享 臨床治療或診療合一

鐳-177 治療給藥方式對核醫工作人員各職類輻射劑量之影響：重力法與幫浦輸注系統之經驗分享

[1]林亭君

[1]和信醫院

發表者 林亭君

Keywords 輻射防護

Background

鐳-177（^{177}Lu）放射性核素治療已廣泛應用於^{177}Lu-Lutathera（神經內分泌腫瘤）及^{177}Lu-PSMA（攝護腺癌）之治療。由於^{177}Lu同時釋放β粒子及γ射線，職業輻射防護為重要議題。傳統重力靜脈滴注法（Gravity infusion）工作人員需長時間接觸放射源；自動幫浦輸注系統（Pump infusion）理論上可縮短接觸時間、降低暴露。本文比較兩種給藥方式對核醫工作人員輻射劑量之影響。

Method

回顧性分析本科室2022年8月至2026年5月^{177}Lu治療之電子個人劑量計（EPD）紀錄。^{177}Lu-PSMA共90次（重力法79次、幫浦法11次），^{177}Lu-Lutathera共22次（重力法20次、幫浦法2次）。比較各次治療期間醫師、放射師、藥師及核醫護理師之每次平均全身劑量（μSv）。治療劑量約 86–208 mCi，視病情調整。

Results

^{177}Lu-PSMA重力法（n=79）各職類每次平均全身劑量：醫師3.2、放射師9.6、藥師3.3、核醫護理師4.1 μSv。幫浦法（n=11）醫師、放射師及藥師之平均劑量分別為3.0、6.0及2.2 μSv，較重力法分別降低6%、38%及33%，以放射師降幅最顯著。^{177}Lu-Lutathera重力法（n=20）各職類平均劑量：醫師4.3、放射師14.2、藥師3.4、核醫護理師5.9 μSv；幫浦法（n=2）放射師及藥師分別為7.5及2.5 μSv，較重力法降低47%及26%，趨勢與PSMA相符。兩種藥物之核醫護理師幫浦法劑量均較重力法升高（PSMA +68%；Lutathera +36%），原因詳見結論。Lutathera幫浦法樣本數尚少（n=2），持續記錄中。

Conclusion

幫浦輸注系統可有效降低^{177}Lu治療期間醫師、放射師及藥師之職業輻射暴露，符合ALARA原則。惟兩種藥物之護理師幫浦法劑量均不降反升，分析為護理師設定幫浦時站立於屏蔽推車旁側，缺乏等效屏蔽所致；調整流程後劑量已改善。此經驗提醒，引入新設備時應對所有職類建立完整劑量監測機制，方能確保全面的職業輻射防護。

壁報論文 臨床組 **PC-022**

原著論文

核子醫學臨床排程登記系統之建置與行政作業效益評估

[1]羅浚哲, [1]張砡慈

[1]中山醫大附設醫院

發表者 羅浚哲

Keywords 智慧醫療 (ML/DL/LLM) | 行政管理 | 數位化系統

Background

核子醫學每日排程包含病人基本資料、檢查項目、放射性藥品、劑量及給藥時間。過去工作人員須由醫院資訊系統逐筆查閱並輸入Excel，再人工完成檢查名稱轉換、特殊檢查拆分、重複資料排除及排序，耗費時間且增加重複性行政負擔。本研究建置規則式核子醫學每日排程自動轉換系統，評估其對排程製作時間及使用者感受之影響。

Method

本研究以Python開發本機端圖形化系統。使用者將醫院資訊系統排程資料批次貼入後，系統可自動擷取病人資料、辨識檢查項目、帶入放射性藥品與劑量、計算給藥時間，並執行特殊流程拆分、去重、排序、預覽修改、Excel輸出及自動備份。

本研究採導入前後比較設計。導入前期間為2026年1月至6月，共處理約9,679筆排程；導入後期間為2026年7月至2026年8月4日，共處理約1,587筆。另由3名實際使用者以五點量表評估作業效率、調閱資料便利性、時間與人力節省感受、操作便利性與學習門檻及整體滿意度，結果以平均值±標準差表示。

Results

每日排程製作時間由導入前24.5分鐘降至導入後7.2分鐘，平均減少17.3分鐘，縮短70.6%。

作業效率由1.67±0.58分提升至5.00±0.00分；調閱資料便利性由1.67±0.58分提升至4.67±0.58分；時間與人力節省感受由1.67±0.58分提升至4.67±0.58分；操作便利性與學習門檻由2.00±0.00分提升至5.00±0.00分；整體滿意度由1.33±0.58分提升至5.00±0.00分。導入期間未發生程式異常中止、檔案損毀、資料遺失或其他重大異常事件。

Conclusion

規則式核子醫學每日排程自動轉換系統可將逐筆人工輸入流程轉換為批次解析、自動處理及人工覆核模式。導入後排程製作時間降低70.6%，並提升作業效率、資料調閱便利性、操作便利性及整體滿意度。本系統具備規則可調整、本機端執行、人工覆核及自動備份等特性，可作為核子醫學部門推動流程數位化與品質改善之實務應用。

壁報論文 臨床組 **PC-023**

個案報告 臨床診斷

Parotid gland metastasis from carcinoma of the breast: detection with F-18 FDG PET/CT

[1]黃柏濤, [1]李佩瑛, [1]黃玉儀

[1]和信醫院

發表者 黃柏濤

Keywords 分子影像

Background

Parotid gland metastasis from breast cancer is rare and often mimics salivary gland tumors, posing diagnostic challenges and delaying appropriate management. We herein present such a rare case detected with F-18 FDG PET/CT.

Case report

A 58-year-old woman was admitted to the hospital with left upper arm swelling and a palpable left breast mass for about 2 months. After core needle biopsy, the patient was diagnosed with invasive ductal carcinoma of left breast. Staging F-18 FDG PET/CT was performed for systemic survey and demonstrated a hypermetabolic mass in left breast, a hypermetabolic nodular lesion in left parotid space, multiple hypermetabolic left axillary and left supraclavicular lymph nodes, and diffuse skin uptake over left breast. Histopathological and immunohistochemical examinations of left parotid nodule, left axillary and left supraclavicular lymph nodes confirmed the diagnosis of parotid gland metastasis from locally advanced breast cancer (T4N3M1).

Conclusion

Breast cancer rarely metastasizes to the parotid gland. However, early recognition is critical for timely diagnosis and treatment. Based on this case, we underline the importance of unusual metastasis in a patient with breast cancer. In addition to conventional images, F-18 FDG PET/CT should also be considered in the preoperative evaluation of patients with locally advanced breast cancer.

壁報論文 臨床組 **PC-024**

原著論文 | 非診療之臨床相關主題

常規 2 mCi 鉈-201 心肌灌注影像與配對 3 mCi 檢查的盲讀技術品質比較

[1]黃俊穎

[1]義大醫院

Keywords 曝露劑量 (Exposure) | 輻射防護 | 病人安全

Background

Tl-201 心肌灌注造影的輻射劑量高於 Tc-99m 製劑，而指引對注射活度只給範圍，3 mCi 習慣上被當成固定標準。2022 年起 Tl-201 供應短缺，本院在供應受限期間將 85 公斤以下成人改為 2 mCi 流程，並回頭檢視影像品質是否撐得住。

Method

回顧 2020 年 1 月至 2026 年 4 月之 Tl-201 MPI 排程，納入 ≥18 歲且 ≤85 公斤者，剔除重複與無劑量紀錄後共 7,530 例；劑量明確為 2 或 3 mCi 者 7,418 例（2 mCi 1,600 例、3 mCi 5,818 例），2.5 mCi 之 112 例不納入主要比較。以性別完全相同、體重差距小於 0.2個標準差、年齡差異最小化，配對 50 對 2 mCi 與歷史 3 mCi 影像（男 28 對、女 22 對；72.2±8.4 歲；62.7±9.7 公斤），皆在同機（Symbia Evo Excel）、同準直器（LEAP）、同 FBP 重建下取得。3 位盲讀者（1 位醫師、2 位放射師）以 4 分序位評清晰度與雜訊 / 偽影，採配對 Wilcoxon 檢定與 bootstrap 95% 信賴區間。

Results

清晰度兩組無差異（P=0.439）。雜訊 / 偽影方面 2 mCi 不差且略受偏好（P=0.003），達滿分 4.0 者 2 mCi 41/50、3 mCi 22/50。總分 2 mCi 7.60±0.47、3 mCi 7.40±0.53，配對差異0.20（95% CI 0.00–0.39），P=0.023。70–85 公斤次族群無差異（P=0.700）。2 mCi 組並非只做低風險病人：≥70 歲 918 例、≥80 歲 312 例、70–85 公斤 542 例。累計省下 1,600 mCi（59.2 GBq）Tl-201，依 ICRP 128 係數約減少 9.6–10.4 Sv 集體有效劑量，逾 1,200 次低劑量胸部 CT 之等效。

Conclusion

在現有攝影平台下，85 公斤以下成人使用 2 mCi 可維持影像之技術可判讀性，同時累積實質輻射與同位素減量。此為供應短缺下之劑量優化，兼具 ALARA 與綠色核子心臟學之意義。

壁報論文 臨床組　　PC-025

原著論文　非診療之臨床相關主題

核子醫學科排定檢查取消之五年分析：病患因素與低成本流程改善方向

[1]郭彥伶, [1]黃俊穎, [1]徐華鎂

[1]義大醫院

發表者　郭彥伶

Keywords　流程優化 | 衛教 | 行政管理

Background

核子醫學檢查牽涉放射性藥物準備與檢查時段安排，病患沒來不只是時段空掉，前線還要聯繫候補、重排流程。先摸清楚取消集中在哪裡、原因是什麼，才知道改善該從何處下手。

Method

單中心回顧性觀察研究，納入 2021 至 2025 年排程異動紀錄共 2,095 筆。以取消事件為主要終點，依預設規則將取消原因歸為 13 類；對具完整完成量資料之 Bone scan 與Tl-201，計算排定檢查取消率（取消件數／完成檢查數＋取消件數）與病患因素取消率。比例以 Wilson method 估計 95% 信賴區間，年度間比較以卡方檢定。

Results

五年共 1,044 人次取消（各年 199、205、240、210、190 人次）。Bone scan 470 人次、Tl-201 338 人次，合計占 77.4%。前三大原因類別為醫療決策改變 226 人次（21.6%）、病患意願或檢查準備不足 190 人次（18.2%）、聯絡失敗 173 人次（16.6%）。合併聯絡失敗、忘記或記錯時間、意願或準備不足、時間衝突、交通與身體狀況等病患因素共 666 人次（63.8%），各年度介於 58.8%–67.9%（p=0.160）；再加計醫療決策改變則占 85.4%。Bone scan 之排定檢查取消率 3.36%（470/13,975；95% CI 3.08–3.68）、病患因素取消率 2.28%（318/13,975；95% CI 2.04–2.54）；Tl-201 分別為 3.26%（338/10,356；95% CI 2.94–3.62）與 1.99%（206/10,356；95% CI 1.74–2.28）

Conclusion

取消集中於高量體檢查，且多與病患確認不足及排檢前臨床決策改變有關。可優先推動標準化電訪腳本、檢查前準備檢核、重點檢查雙次人工提醒與結構化取消原因記錄等低成本改善措施。

壁報論文 臨床組 **PC-026**

個案報告 臨床診斷

Oncocytic adenoma of thyroid initially presented as incidentally tumor with extremely high FDG uptake

[1]李昕迪, [1]郭建瑋

[1]屏東榮民總醫院

發表者 李昕迪

Keywords 有趣影像 | FDG | 甲狀腺

Background

Incidental focal FDG uptake in the thyroid on PET/CT often suggests malignancy. However, certain benign lesions may also show intense metabolic activity, potentially mimicking cancer. We report a case of oncocytic adenoma of the thyroid initially presenting as an incidental tumor with extremely high FDG uptake.

Case report

A 69-year-old woman with poorly differentiated cervical carcinoma, stage IVB, underwent F-18 FDG PET/CT after chemoradiotherapy for treatment response evaluation. The scan demonstrated near-complete metabolic remission of the primary tumor, mild uptake in a left adnexal cystic lesion (SUVmax 1.3–1.6, later confirmed as mucinous cystadenoma), and no significant FDG-avid pelvic lymphadenopathy. Incidentally, a 2 cm hypodense left thyroid nodule exhibited extremely high FDG uptake (SUVmax 81.0, increasing to 102.7 on delayed imaging).

Ultrasound revealed a 1.92 × 1.47 × 1.75 cm oval, solid, markedly hypoechoic nodule with regular margins, no calcification, and TI-RADS 4B classification. Fine-needle aspiration cytology reported “oncocytic follicular neoplasm cannot be excluded.” Left thyroid lobectomy pathology confirmed an oncocytic adenoma (follicular adenoma, oncocytic variant) composed of proliferative oncocytic follicular cells in microfollicular, normofollicular, and solid patterns, without capsular or vascular invasion, thereby excluding oncocytic carcinoma. According to current NCCN and ATA guidelines, confirmed benign oncocytic adenomas do not require completion thyroidectomy, radioactive iodine ablation, or TSH suppression therapy; routine follow-up with neck ultrasound is recommended.

The patient continued treatment for her cervical carcinoma. During one year of follow-up, there was no evidence of recurrent thyroid lesion or other findings suggestive of oncocytic carcinoma.

Conclusion

Oncocytic adenomas and carcinomas differ by their invasion into surrounding tissues; because both have abundant mitochondria, FDG uptake cannot distinguish them, and diagnosis relies on histopathologic proof of capsular or vascular invasion.

壁報論文 臨床組 **PC-027**

原著論文 非診療之臨床相關主題

不同數位教學模式對醫事放射實習學生輻射污染處置能力之教育成效評估

[1,2]龔瑞英, [1]張志維, [1]陳耀文, [1,2]蔡世傳, [2]張振榮, [1,2]林宜瀞

[1]臺中榮民總醫院
[2]中臺科技大學

發表者 龔瑞英

Keywords 輻射防護 | 教學

Background

輻射污染處置屬於低頻率、高風險（Low-Frequency, High-Risk）之臨床應變能力，實習學生於臨床環境中缺乏實際操作機會。為建構臨床核心勝任能力，本研究近年逐步導入線上數位教材與沉浸式虛擬實境（Virtual Reality, VR）等多元學習平台，並運用客觀結構化臨床考試（OSCE）評估不同數位教學模式對學生輻射污染處置能力之教育成效。

Method

本研究採縱貫性成效評估，收集 2022 年至 2025 年接受輻射污染處置訓練並完成 OSCE 測驗之實習學生資料 (n=70)。各年度教學介入如下：2022 年實施傳統大堂課結合線上教材；2023 年採用多元平台線上數位學習；2024 年導入 VR 沉浸式情境模擬；2025 年持續深化數位模組教學。以各年度學生之 OSCE 通過率及平均分數為主要評估指標，並進行跨年度教學成效之差異分析。

Results

2022 年未接受教學前，學生 OSCE 通過率為 0.0%，平均分數僅 8.11±9.92分；於接受實體大堂課與線上教材後，通過率大幅提升至 62.5%，平均分數達 48.40±10.45分。2023 年至 2025 年持續導入不同數位教學模式後，整體通過率穩定維持於 51.4% 至 63.6%，平均分數介於 46.09±20.45至54.30±10.75分。其中，結合 VR 沉浸式情境教學之年度（2024 年），學生通過率達歷年最高（63.6%），顯示沉浸式體驗能有效強化學生於複雜情境下之臨床操作穩定度。

Conclusion

數位教學平台可有效突破罕見臨床事件之練習限制，顯著建立實習學生之輻射污染處置能力。結合情境式線上學習與 VR 沉浸式模擬訓練，能維持穩定且優異之 OSCE臨床展能，符合勝任導向醫學教育（CBME）精神，為未來醫學教育推動高風險模擬教學與數位轉型提供具體之實證參考。

壁報論文 臨床組 **PC-028**

個案報告 臨床診斷

原發性醛固酮症之實驗室診斷流程—右側腎上腺腺瘤個案

[1]張素雲, [1]黃筱崴, [1]沈宜瑾, [1]廖建國, [1,2]莊紫翎

[1]大林慈濟醫院
[2]慈濟大學

發表者 張素雲

Keywords 放射免疫分析

Background

原發性醛固酮增多症（Primary Aldosteronism, PA）是最常見的續發性高血壓之一，約占高血壓患者5–10%，主要因腎上腺分泌過量醛固酮所致。患者常出現頑固性高血壓、低血鉀及腎素活性抑制等臨床表現。實驗室檢驗在PA診斷中扮演關鍵角色，由初步的血清電解質、醛固酮/腎素比值（ARR）篩檢，到確診試驗及腎上腺靜脈採血（Adrenal Venous Sampling, AVS），皆需仰賴醫事檢驗師提供準確可靠的檢驗結果，以協助臨床判斷病灶位置及治療策略。

Case report

本病例為53歲男性，高血壓合併持續性低血鉀，使用四種降血壓藥，雙下肢無力，因懷疑原發性醛固酮症住院接受檢查。實驗室檢驗流程包括：1.血液生化檢驗: 血鉀（K^+）腎功能，2.內分泌檢驗: Plasma Aldosterone Concentration（PAC），Plasma Renin Activity（PRA），Aldosterone-to-Renin Ratio（ARR），3.影像學檢查: 腹部電腦斷層（CT），

4.腎上腺靜脈採血（AVS）同步採集右側、左側腎上腺靜脈及周邊靜脈血液，測定Aldosterone及Cortisol濃度，以Cortisol確認採血位置正確性，再計算Aldosterone/Cortisol比值進行判讀。各項血中荷爾蒙濃度於不同時間點之檢驗結果，顯示ARR明顯大於特定臨界值，通常大於 20 至30時，即高度懷疑有此原發性醛固酮症。而腎上腺靜脈採血(AVS)檢驗結果顯示，右側腎上腺靜脈Aldosterone濃度顯著高於左側及周邊血液，高度懷疑為右側功能性腺瘤。另外，腹部電腦斷層檢查結果也顯示右側腎上腺約21.23 mm低密度腫瘤，因此診斷為腎上腺腺瘤(Adrenal adenoma)。

Conclusion

本案例呈現原發性醛固酮症完整之實驗室診斷流程。ARR為國際公認之PA篩檢工具，本案例因PRA受到明顯抑制，使ARR持續升高，提供重要診斷依據。AVS為目前定位診斷黃金標準，藉由同步測定Aldosterone與Cortisol，可確認導管位置及避免採血誤差，提高判讀之可靠性。醫事檢驗師於本案例中負責荷爾蒙分析品質控制，PRA與Aldosterone精確檢測，ARR計算與報告，AVS檢體採集流程管理，檢驗數據整合分析，充分展現醫事檢驗師在PA診斷中的專業價值。

壁報論文 臨床組 PC-029

原著論文 臨床診斷

Dual-time-point FDG PET/CT for differentiating vaccination induced axillary inflammatory lymphadenopathy from metastasis in patient with breast cancer

[1]楊舒雅, [1]古瑋凱, [1]沈志傑, [1]劉仁賢

[1]振興醫院

發表者 楊舒雅

Keywords 定量分析 | 造影儀器

Background

FDG-avid axillary lymph nodes (LN) are common to be detected in breast cancer patients following vaccination of COVID-19 or influenza on the deltoid muscle of the arm and is difficult to be differentiated from axillary metastatic lymphadenopathy (mLN). Dual-time-point FDG PET/CT has been applied in various cancers for differentiating inflammation from cancer. This study aims to differentiate inflammatory lymphadenopathy (iLN) from mLN by dual-time-point PET/CT.

Method

25 breast cancer patients received COVID-19 vaccination and 13 patients received influenza vaccination within 3 months were included. PET/CT was performed at 60 min and 120 min after FDG injection. FDG-avid LNs were defined by visual interpretation (>blood pool) and SUVmax >2.5. Difference of SUVmax between 60 min and 120 min PET/CT (SUVmax) was calculated for LNs with SUVmax60 > 2.5. All affected LNs were proved by pathological examination or MRI.

Results

There were 46 mLNs in 15 patients with SUVmax60 ranging from 2.5-11.2 (mean±SD = 6.8±2.1) and 73 iLNs in 23 patients with SUVmax60 form 2.6-13.0 (7.9±2.6). No difference between SUVmax60 of mLNs and iLNs (6.8±2.1 vs 7.9±2.6, p=NS) nor difference between of SUVmax mLNs and iLNs (1.5±2.3 vs 1.2±2.8, p=NS) were noted. No difference of SUVmax of mLNs and iLNs is between COVID-19 vaccination and influenza vaccination (7.6±3.0 vs 7.3±2.6).

Conclusion

In patients with breast cancer who received COVID-19 vaccination or influenza vaccination within 3 months prior to FDG PET/CT examination, SUVmax60 of FDG avidity and the difference between SUVmax60 and SUVmax120 (SUVmax) obtained from dual-time-point PET/CT were unable to differentiate FDG-avid iLN from mLN.

壁報論文 臨床組 **PC-030**

原著論文 非診療之臨床相關主題

近兩年放射免疫分析異常值簡訊處置率之比較

[1]廖建國, [1]張素雲, [1]游舜宇

[1]大林慈濟醫院

發表者 廖建國

Keywords 放射免疫分析

Background

透過簡訊將重要異常值(警告值)通報給臨床醫師，為實驗室同仁的重要工作，而臨床醫師接獲簡訊通報後是否進行適當的處置，更是攸關病人安全的重要議題。本研究目的即為比較近兩年臨床醫師簡訊回覆處置的比率，以探討近兩年本院雙向簡訊通報之成效。

Method

以本院雙向簡訊訊息查詢管理系統，收集2025年1月至2026年6月之臨床醫師回覆明細，分別計算異常值簡訊之每月處置率以及24小時處置率，其中24小時處置率再依不同科別進行分析，以比較各科醫師處置情形。異常值通報項目及通報上限，分述如下: AFP (> 100 ng/mL)、CEA (> 10 ng/mL)、CA125 (> 200 U/mL)、CA15-3 (> 50 U/mL)、CA19-9 (> 150 U/mL)、PSA (> 10 ng/mL)、SCC (> 3.5 ng/mL)、TPA (> 130 U/L)及Thyroglobulin (> 100 ng/mL)。

Results

總計收集2815件簡訊通報個案，其中2025年為1949件，而2026年1-6月為866件。分析結果顯示，2026年1-6月的平均總處置率為99.83%，而24小時處置率則為87.17%，此結果與2025年分別的兩項數值(99.21%、86.50%)相近，無顯著差異(P >

0.05)。顯示臨床醫師每月接獲放射免疫分析的簡訊通知後，絕大部份均能回覆處置情形，而在24小時內回覆的比率，則有80%以上，此結果與國內某些醫學中心的同儕值相近。另外，分析各科醫師之24小時內處置率的資料，發現心臟內科、風濕免疫科、家醫科、神經內科之處置率(100%)最高，而耳鼻喉頭頸外科、大腸直腸外科的處置率則相較偏低(平均值未達80%)，顯示耳鼻喉頭頸外科、大腸直腸外科可以優先考慮進行監控及改善。

Conclusion

分析結果顯示，近兩年臨床醫師之總處置率皆在98%以上，而24小時處置率則皆在80%以上，若要求在24小時內回覆，則仍有改進的空間。未來可配合院方政策，並針對通報配合度不高的科別，進行提醒與溝通，以持續提升簡訊處置率。

壁報論文 臨床組

PC-031

原著論文 臨床診斷

嚴重正子藥物滲漏對標準攝取值之影響-重新造影個案分析

[1]林友琮, [1,2]龔瑞英, [1,2]黃莆蓉, [1,2]蔡世傳, [1,2]林宜瀞

[1]臺中榮民總醫院核子醫學科
[2]中臺科技大學醫學影像暨放射科學系

發表者 林友琮

Keywords 藥物滲漏 | 正子造影 | SUV

Background

正子造影（Positron Emission Tomography, PET）廣泛應用於腫瘤診斷、分期、治療反應評估及追蹤，標準攝取值（Standardized Uptake Value, SUV）為正子造影常用之半定量分析指標。SUV 數值除受病患生理狀態、影像擷取時間及重建條件影響外，實際進入體內之放射性藥物活度亦為重要因素。若注射過程發生藥物滲漏，可能降低全身組織及病灶之放射性藥物攝取，造成 SUV 低估，進而影響影像判讀。本研究回溯分析嚴重正子藥物滲漏後重新造影之個案，比較前後影像 SUV 變化，以探討嚴重藥物滲漏其對SUV之影響。

Method

本研究回溯2024-2025年8497名案例，收集嚴重漏針重新執行第二次造影之正子檢查案例，一共收集 6位病患(嚴重滲漏率0.07%)。分別於兩次造影影像測量注射藥物滲漏處、肝臟、大腿正常軟組織及病灶之 SUVmax。每位病患選取 2 處前後影像可對應之病灶，共分析 12個病灶，比較兩次造影各部位 SUVmax 變化。

Results

6 位病患於第一次造影可見明顯注射部位藥物嚴重滲漏，重新注射後，注射部位 SUVmax 均明顯下降，由 1476.48 ± 2615.69下降至 16.12±12.38。正常組織與病灶SUVmax攝取上升，肝臟由 1.97 ± 0.52上升至 2.72 ± 0.86(增加 1.38 倍)。大腿由 0.61 ± 0.33上升至 0.92 ± 0.15(增加 1.51 倍)。病灶1由4.74 ± 2.55增加至10.40 ± 6.55，病灶2由3.11 ± 2.15增加至7.04 ± 5.44。12個病灶由3.93 ± 1.50增加至 8.72 ± 3.98(增加 2.31 倍)。

Conclusion

嚴重正子藥物滲漏可能降低實際進入全身循環之放射性藥物量，不僅影響正常生理性攝取，對病灶SUV的影響更為明顯，可能造成病灶代謝活性低估。建議執行正子藥物注射前應確實確認靜脈留置針位置及管路通暢度，注射過程及注射完成後亦應注意注射部位是否有疼痛、腫脹或異常放射性藥物滲漏，以降低藥物滲漏對 SUV 定量分析及臨床判讀造成之影響。

壁報論文 臨床組 **PC-032**

個案報告 臨床診斷

下肢淋巴閃爍造影中左側鎖骨上及腋下區異常顯影

[1]陳薇璇, [1,2]莊紫翎

[1]大林慈濟醫院
[2]慈濟大學

發表者 陳薇璇

Keywords 有趣影像

Background

下肢淋巴閃爍造影（lymphoscintigraphy）是評估淋巴水腫常用的核醫檢查，經雙足趾蹼皮下注射Tc-99m phytate後，示蹤劑循足部淋巴管上行，依序經膝窩淋巴結、腹股溝淋巴結、髂淋巴結，匯入腰淋巴幹與乳糜池，再經胸導管於左鎖骨下靜脈與左頸內靜脈交界處注入靜脈系統。由於示蹤劑進入血液後迅速被稀釋，正常情況下左側腋下淋巴結與兩側頸部淋巴結幾乎不會顯影；若於此區域出現異常放射性積聚，臨床上需考慮胸導管逆流、部分淋巴流出阻塞、側支淋巴通路異常，或注射技術誤入靜脈等可能原因。

Case report

一名88歲女性，因雙下肢水腫，臨床懷疑淋巴水腫，安排下肢淋巴閃爍造影檢查。經雙足趾蹼皮下注射Tc-99m phytate後，影像顯示雙下肢淋巴系統顯影清晰，依序引流至雙側腹股溝區，再匯入腹腔淋巴系統。延遲2小時影像中，右側腹股溝淋巴結數量少於左側，符合右下肢淋巴水腫之表現。此外，左側鎖骨上/頸根區及腋窩區可見中度放射性追蹤劑聚集，此為下肢淋巴閃爍造影中較不典型之顯影部位。左側鎖骨上/頸根區局部積聚可能反映胸導管末端之生理性引流，但輕度胸導管逆流或部分淋巴流出阻塞亦可能導致左側腋窩區之示蹤劑攝取。左頸根部區是胸導管與靜脈的交匯處，有時可見小區域亮點，屬正常終末顯影。病人的胸部X光顯示Port-A catheter置入於左鎖骨下區，懷疑是引起淋巴逆流或阻塞而於左側腋窩顯影的原因。

Conclusion

本案例於下肢淋巴閃爍造影中，除右下肢淋巴水腫之典型表現外，另呈現左側鎖骨上/頸根及腋窩區之異常顯影，此類表現在臨床上並不常見。由於下肢淋巴引流正常路徑不經過腋下區，判讀時應避免將此異常顯影誤認為病理性腋下淋巴結病灶或轉移，而應優先考慮胸導管末端生理性顯影、輕度胸導管逆流或部分淋巴流出阻塞等可能性。本病例胸部 X 光顯示左鎖骨下區 Port-A catheter置入後狀態，考量導管位置可能影響局部靜脈回流或造成淋巴引流受阻，推測左側鎖骨上/頸根及腋窩區之顯影，可能與胸導管壓力增加及逆流現象相關。。本案例提醒核醫判讀時，應熟悉淋巴引流解剖及胸導管逆流之相關表現，以提高診斷準確性並避免誤判。

壁報論文 臨床組 PC-033

個案報告 臨床診斷

Polyostotic Fibrous Dysplasia With Pathological Femoral Fracture (McCune Albright Syndrome) : The Role of 99mTc-MDP Bone Scintigraphy Case Report

[1]盧淑玫, [1]許友齡

[1]嘉義基督教醫院

發表者 盧淑玫

Keywords 有趣影像

Background

Fibrous dysplasia (FD) is a benign fibro-osseous disorder in which normal bone is replaced by abnormal fibrous tissue and immature bone. It may involve a single bone or multiple skeletal sites. Polyostotic fibrous dysplasia (PFD) can cause bone pain, deformity, and pathological fractures. Whole-body 99mTc-methylene diphosphonate (99mTc-MDP) bone scintigraphy is useful for detecting multifocal skeletal involvement and assessing overall disease burden.

Case report

A 12-year-old boy presented with a pathological fracture of the left femoral shaft. Two years earlier, he experienced sudden left thigh pain with a popping sound while running, followed by a fall. Plain radiography demonstrated a pathological fracture of the left femoral shaft, and surgical treatment was performed (Fig. A/B).During postoperative follow-up, whole-body 99mTc-MDP bone scintigraphy revealed increased radiotracer uptake in the left ilium, left femoral shaft, and left tibia, suggesting multifocal skeletal involvement (Fig. C). Histopathological examination of the femoral lesion demonstrated a fibro-osseous lesion favoring fibrous dysplasia. The combined clinical, radiographic, scintigraphic, and pathological findings supported the diagnosis of polyostotic fibrous dysplasia involving the left ilium, left femur, and left tibia. Final clinical diagnosis McCune Albright syndrome with left femur shaft, left proximal tibial FD. Thus emphasizing the crucial role of 99m Tc-MDP bone scan in the diagnosis of extensive FD and guides in understanding of the polyostotic involvement.

Conclusion

Polyostotic fibrous dysplasia may involve multiple skeletal sites and present with complications such as pathological fracture and bone deformity. McCune-Albright syndrome (MAS) is typically described by the association of cutaneous (coffee-at-milk spots), endocrine (endocrine hyperfunction most often precocious puberty), and fibrous dysplasia (FD). In general, FD seems to be the most common component of MAS but very rarely precocious puberty can be found in association with café-au-lait skin pigmentation in the absence of FD (about 1% of the cases). Whole-body 99mTc-MDP bone scintigraphy provides a useful method for identifying additional skeletal lesions and assessing overall disease burden. In this case, bone scintigraphy demonstrated multifocal involvement beyond the site of the presenting femoral fracture, highlighting its value in the evaluation and follow-up of polyostotic fibrous dysplasia.

壁報論文 臨床組 **PC-034**

原著論文 非診療之臨床相關主題

2025年精神科患者甲狀腺功能、葉酸及維生素B12檢驗異常之盛行率分析： 北部某醫學中心RIA實驗室回溯性研究

[1]蕭如妏, [1]楊淳淳, [1]王怡文, [1]程紹智

[1]台北慈濟醫院

發表者 蕭如妏

Keywords 放射免疫分析

Background

甲狀腺功能與維生素B12、葉酸代謝與神經系統功能密切相關，其異常可能伴隨認知、情緒及精神症狀。甲狀腺疾病及營養缺乏屬於可辨識與處置的潛在生理因素，因此相關檢驗常納入精神症狀及認知功能異常患者之鑑別診斷。過去研究顯示，精神科患者可能存在甲狀腺功能異常及葉酸、維生素B12不足，但不同研究之盛行率差異較大。本研究利用本院RIA實驗室資料，同時分析精神科患者甲狀腺功能及營養相關指標之異常情形。

Method

採回溯性研究，收集 2025 年 1 月 1 日至 12 月 31 日接受精神科臨床評估，且同時檢測Free T4、TSH、Vitamin B12及Folic acid之患者，共 1,851 例。所有檢測均由本院RIA實驗室依標準作業流程執行，異常值依本院檢驗方法及參考區間判定。以描述性統計計算各檢驗項目及多項指標同時異常之比例。

Results

共納入 1,851 例。Folic acid缺乏率為**5.51%（102/1,851）**，Vitamin B12缺乏率為**0.81%（15/1,851）**；TSH異常率為**5.29%（98/1,851）**，Free T4異常率為**0.32%（6/1,851）**。TSH與Free T4同時異常者為**0.16%（3/1,851）**；Folic acid、Vitamin B12、TSH及Free T4四項同時異常者為**0.11%（2/1,851）**。

Conclusion

本研究顯示，葉酸缺乏較Vitamin B12缺乏常見，此趨勢與 2024 年Rajen等人精神科族群研究結果相近。甲狀腺相關異常則以TSH異常為主，明顯高於Free T4異常。TSH異常可能反映subclinical thyroid dysfunction、早期甲狀腺功能變化，亦可能受疾病狀態、藥物及其他生理因素影響，因此**TSH異常率不宜直接視為甲狀腺疾病盛行率**。此外，四項指標同時異常僅占 0.11%，顯示多重異常相對少見，但此類患者仍值得進一步評估營養狀態、藥物使用及內分泌因素。本研究發現精神科患者中，**葉酸缺乏及TSH檢驗異常較為常見，而四項指標同時異常相對少見**。甲狀腺及營養相關檢驗可提供精神科患者潛在生理異常的重要資訊，作為臨床鑑別評估之參考。然而，檢驗異常並不等同於確診疾病，仍應結合臨床症狀、病史、藥物使用及後續檢查進行整體判讀。

壁報論文 臨床組 **PC-035**

經驗分享 非診療之臨床相關主題

BECKMAN試劑 FT4與FT4 Plus比較

[1]韓璞

[1]國泰醫院

Keywords 試劑 | 放射免疫分析 | 定量分析 | 實驗室流程改善

Background

本實驗室使用之FT4試劑廠牌由CIS轉換為BECKMAN，在隔年BECKMAN原廠公告已研發出新一代FT4試劑(FT4 Plus)，兩試劑差異為FT4 Plus的實驗流程較簡易，檢體加入tube後可直接加入tracer，而原FT4試劑實驗流程檢體加入tube後再分別加入tracer和ligand，另外In kit control由1個濃度增加為2個濃度，同時亦排除biotin對實驗上的影響。本實驗室FT4項目檢測量較大，若可更換成FT4 Plus，可加速實驗流程，亦可減輕實驗室同仁負擔。

Method

實驗室對FT4 Plus進行檢驗試劑評估，包含精密度、精確度、參考值驗證以及相關性。本實驗室使用第三方品管液進行精密度與精確度測試，結果需在原廠範圍內。參考值驗證則從健康正常人中，挑選出男性10名，女性10名，檢測結果至少18人落入原廠所提供參考值之範圍。另外使用兩試劑測試20位病人FT4數值，允收標準為相關係數R2≧0.95。除此之外，需衡量試劑成本、收費標準、檢體量、人力成本，亦參考其他醫院之使用情況。

Results

FT4 Plus試劑之精密度與精確度測試結果皆在原廠範圍內。同時參考值驗證檢測結果20人皆落入原廠所提供參考值之範圍。而試劑之相關性結果R2=0.997≧0.95。然而FT4 Plus試劑價格高於原FT4試劑，且使用FT4 Plus試劑的醫院家數與使用量皆偏少。

Conclusion

FT4 Plus試劑完成試劑評估，結果皆符合實驗室之允收，雖然如此，仍因FT4 Plus試劑價格過高，對於本實驗室的財務評估上，不符效益。同時FT4 Plus試劑的醫院家數與使用量皆偏少，當實驗室病人報告或品管有偏差時，需與其他醫院進行室間比對，亦有困難。經實驗室針對FT4 Plus試劑完整評估後，本實驗室仍維持使用原FT4試劑。

壁報論文 臨床組 **PC-036**

經驗分享 非診療之臨床相關主題

細胞保存液之檢體檢測BECKMAN PTH試劑

[1]韓璞

[1]國泰醫院

Keywords 試劑 | 放射免疫分析 | 定量分析

Background

本實驗室之PTH試劑除了操作血液檢體外，亦有副甲狀腺組織清洗液檢體，當內分泌醫師操作甲狀腺超音波時，醫師進行副甲狀腺細胞穿刺後，會打入細胞保存液送至細胞室，同時將組織清洗液送至本實驗室檢測PTH。近期內分泌醫師詢問是否可直接使用已經打入副甲狀腺細胞之細胞保存液檢體做PTH檢測，因副甲狀腺細胞穿刺取得檢體量較少，此一檢體需分注至細胞保存液與清洗液中，可能因採集檢體不足而影響檢驗結果。因此若可以使用已經打入副甲狀腺細胞之細胞保存液檢體做PTH檢測，不只可增加報告正確率，也可減少清洗組織液的準備。

Method

因副甲狀腺細胞穿刺的檢體少，不易收集，且檢體需打入10C.C.細胞保存液，故先以血漿加入細胞保存液，並採用稀釋方式進行測試。取正常與不正常之血漿檢體，分別加入試劑提供之稀釋液、清洗液與細胞保存液，檢測原倍、2倍、5倍與10倍，確認病人之數值是否會受影響。

Results

當試管中只加入清洗液與細胞保存液時，皆測出為低值，將正常與不正常之血漿檢體加入清洗液與細胞保存液，並做稀釋2倍、5倍與10倍，加入清洗液之稀釋結果與原倍數值並無太大差異，但加入細胞保存液之稀釋後數值皆為低值，與原倍數值差異大。

Conclusion

以血漿檢體做為測試，細胞保存液無法做出與清洗液之相同結果，可能細胞保存液之成分仍會影響PTH，導致檢測數值偏低，影響檢驗結果，因此推測無法使用打入副甲狀腺細胞之細胞保存液檢體做PTH檢測，故細胞保存液無法取代清洗液。

壁報論文 臨床組 **PC-037**

統合分析 非診療之臨床相關主題

放射免疫分析TSH試劑使用效率分析及庫存管理

[1]黃筱崴, [1]張素雲, [1]沈宜瑾, [1]廖建國, [1]游舜宇

[1]大林慈濟醫院

發表者 黃筱崴

Keywords 試劑 | 放射免疫分析

Background

TSH為本科放射免疫分析實驗室高檢驗量的項目，試劑成本占日常營運相當比例。除病人檢體的檢驗件數外，試劑亦消耗於品質管制（QC）、校正（Calibration）及重新檢測（Recheck），若未妥善規劃訂貨 (每月 1 次) 及庫存管理，易造成試劑浪費及增加營運成本。本研究目的為分析近 18 個月TSH試劑使用情形，評估試劑使用率以及庫存管理之適當性，以作為實驗室精實管理之參考。

Method

收集 2025 年 1 月至 2026 年 6 月間，共 18 個月的TSH試劑進出及庫存紀錄，紀錄內容包括進貨量、檢體量、品管 (含校正) 量、複驗（Recheck）量及結存量等項目，各項目皆以檢測量 (test)登錄。分別分析每月初驗使用率、複驗使用率、品管使用率等數值，進行比較。計算方式如下: 初驗使用率 =(病人檢體量 / 總消耗量) x100%，品管使用率 =(QC+CAL量)/ 總出庫量x100%，複驗使用率 =(RECHECK量 / 總出庫量) x100%。

Results

近 18 個月總計收集 25987 件TSH的檢驗個案 (病人檢體量)，平均每月 1443.7 件 (1190~1656件)。初驗使用率每月平均為 81.7%(78.6%～85.1%)，其中 2025 年 5 月最低 (78.6%)，2026 年 4 月最高 (85.1%)，顯示 2025 年使用伽瑪計數器新機後初驗使用率逐漸提升。品管使用率月平均為 6.6%(5.3%～7.4%)。各月份變化幅度小，表示品質管制需求穩定，未因檢驗量增加而明顯增加QC消耗，符合放射免疫分析品質管理需求 (< 10%)。複驗使用率月平均為 11.7%(8.0%～14.3%)，其中 2025 年前半年 11%～14.3%，2026 年逐漸下降至 8.0%～11.2%，顯示重新檢測需求降低，推測與儀器穩定度提升有關，也顯示實驗室使用新機後品質已有改善。在庫存管理方面，TSH試劑的 18 個月進貨量介於 1,200～3,500 tests，除 2025 年 6 月及 2026 年 5 月因預期作業量增加，調高檢驗需求而導致進貨量較高外，其他各月份之試劑進貨量皆與消耗量相當，進貨量控制適當，且未發生試劑短缺情形。

Conclusion

TSH試劑之初驗使用率平均為 81.7%，QC及Calibration約占 6～7%，試劑使用情形符合放射免疫分析的品質管理需求，而Recheck率由最高 14.3% 下降至最低 8%，顯示使用新機後重新檢測需求降低。18 個月的試劑庫存，皆未發生試劑短缺，且庫存管理具有良好彈性，可機動調整進貨，以符合臨床需求。實驗室定期分析試劑使用情形，評估試劑使用率以及庫存管理之適當性，可作為實驗室精實管理之重要依據。

壁報論文 臨床組　　**PC-038**

經驗分享　非診療之臨床相關主題

Lu-177 PSMA治療後尿布廢棄物之輻射劑量率衰減與儲存時間評估

[1]董韋銓, [1]龔瑞英, [1]陳耀文, [1]吳玫萱, [1]林宜瀞

[1]臺中榮民總醫院

發表者　董韋銓

Keywords Lu-177 | 廢棄物 | 劑量率

Background

Lu-177 PSMA 治療後主要經腎臟代謝並由尿液排泄，可自行如廁患者之放射性排泄物可經醫院及民間污水系統處理；然而，部分患者可能因疾病因素長期使用尿布，而尿布及相關廢棄物可能殘留較高且集中的放射性物質，本研究探討尿布廢棄物存放至環境背景值所需時間，作為後續廢棄物管理及處置之參考依據。

Method

本研究回溯 2025-2026 年Lu-177 PSMA治療個案，收集患者使用之尿布廢棄物，(一位為失禁病人尿布，一位為少量排尿病人尿布)。於存放期間每週使用輻射偵檢器(LUDLUM、MODEL3000)進行量測，偵測廢棄物表面及 1 公尺處之輻射劑量率。持續偵測至表面劑量率降至背景值為止，以評估放射性衰減降至接近背景值所需之存放時間。

Results

失禁病人尿布之初始表面劑量率**為 958.7～1353μSv/h(1130.0±201.2μSv/h)**。隨儲存時間增加，表面劑量率持續下降，第 11 週降至**0.303～0.420μSv/h(0.348 ± 0.062μSv/h)**，第12 週降至背景值。**1 公尺處**初始劑量率**為 36.72～63.10μSv/h(49.97 ±13.21μSv/h)**，第 7週降至 0.25～0.45μSv/h(**0.34 ± 0.10 μSv/h)**，第 9 週全數降至背景值。

少量排尿病人尿布之初始表面劑量率**為 311.3～387.6μSv/h(349.45 ± 54.37μSv/h)**。第10 週**降至 0.23～0.24 μSv/h(0.235 ± 0.007μSv/h)**，第 11 週全數降至背景值。**1 公尺**處初始劑量率**為 10.06～11.37μSv/h(10.72 ± 0.93μSv/h)**，第 5 週**降至 0.24～0.26μSv/h(0.25 ± 0.01μSv/h)**。

Conclusion

本研究顯示，Lu-177 尿布廢棄物之劑量率會隨時間持續下降，且其衰減趨勢與 Lu-177物理半衰期一致。初始劑量率較高及尿布廢棄量較大者，達到背景值所需之儲存時間相對較長。建議**至少儲存 12 週後，再進行劑量率量測；確認劑量率已降至背景值後，再進行後續清運處置**。

壁報論文 臨床組　　**PC-039**

原著論文　臨床診斷

流程再設計縮短一日法心肌灌注造影檢查時間之成效

[1]張焯婷, [1]龔瑞英, [1]葉珊汝, [1]林宜瀞

[1]臺中榮民總醫院

發表者　張焯婷

Keywords　心肌血流灌注造影 | 流程再設計 | 檢查時間

Background

一日法 Tc-99m MIBI 心肌血流灌注造影需於同日完成休息相與壓力相造影，流程包含放射性藥物注射、藥物負荷、用餐、等待及影像造影等多項作業，整體檢查時間較長，增加病人於院內等候及停留時間。本研究透過重新設計檢查流程及導入數位化流程管理系統，評估流程優化對縮短總檢查時間及提升作業效率之成效。

Method

本單位原一日法心肌血流灌注造影採「壓力相先、休息相後」之執行流程。為提升檢查效率，重新設計為「休息相先、壓力相後」，並同步優化放射性藥物注射、藥物負荷、用餐及造影之時間安排，同時導入檢查流程管理系統進行流程數位化管理。以病人完成全部檢查時間減去報到時間定義為總檢查時間，比較流程再設計前後之差異。流程再設計前納入 25 名病人（2017 年 9 月至 10 月），流程再設計後納入 46名病人（2026 年 7 月），比較兩組病人之總檢查時間。

Results

流程再設計前，病人平均總檢查時間為 328 ± 26 分鐘；流程再設計並導入檢查流程管理系統後，平均總檢查時間降至 206 ± 56 分鐘，平均縮短 122 分鐘，改善率達 37.2%，顯示流程再設計可有效縮短病人整體檢查時間，提升檢查流程效率。

Conclusion

透過重新調整休息相與壓力相之執行順序，優化放射性藥物注射、藥物負荷、用餐及造影之時間安排，並結合檢查流程管理系統進行數位化流程管理，可有效縮短一日法心肌血流灌注造影之總檢查時間，減少病人於院內停留時間並提升作業效率。本研究結果可作為核子醫學多階段、複雜檢查流程再設計與效率改善之參考。

壁報論文 臨床組 **PC-040**

個案報告 臨床診斷

Intense 18F-FDG Uptake in Gouty Tophi: A Potential Diagnostic Pitfall in Therapeutic Response Assessment of DLBCL

[1]陳怡勳, [1]杜東峻

[1]嘉義基督教醫院

發表者 陳怡勳

Keywords 有趣影像

Background

Gout is a common inflammatory arthropathy caused by the deposition of monosodium urate (MSU) crystals in joints and soft tissues. These crystals trigger an inflammatory cascade by activating the NLRP3 inflammasome, leading to the massive release of pro-inflammatory cytokines such as IL-1β. Although 18F-FDG PET/CT is the gold standard for staging and evaluating Diffuse Large B-cell Lymphoma (DLBCL), FDG is a non-specific marker of glucose metabolism that also accumulates in active inflammatory cells like macrophages and neutrophils.

Case report

A 63-year-old male with DLBCL and a history of tophaceous gout underwent a PET/CT scan for response assessment after completing four cycles of R-CHOP. The images revealed intense, focal FDG accumulation in the juxta-articular soft tissue of the elbow joints (SUVmax 9.22). The corresponding CT images showed these areas to be hyperdense, partially calcified nodular structures consistent with gouty tophi. Given the patient's clinical history and the characteristic periarticular localization on CT, these findings were identified as metabolically active gouty tophi rather than extra-nodal lymphomatous involvement.

Conclusion

Severe or acute gout can manifest with intense hypermetabolic activity on PET/CT, often mimicking malignancy or systemic infection. Previous reports have shown that the SUVmax of gouty tophi can be significantly high, with values ranging from 5.1 to as high as 11.8. This metabolic intensity reflects the "cytokine storm" and recruitment of synovial lining cells during crystal-induced inflammation. In oncological patients, particularly those with DLBCL, the presence of FDG-avid tophi can lead to diagnostic errors and overstaging. A critical diagnostic feature is the "mismatch" between the anatomical CT findings—such as juxta-articular erosive lesions with sclerotic, overhanging borders—and the metabolic pattern. Recognizing these patterns is decisive in shifting the clinical focus from suspected tumor progression to appropriate anti-inflammatory management.

壁報論文 臨床組 **PC-041**

原著論文 臨床治療或診療合一

A retrospective study on radiation dose assessment for Patients and Medical Staff in Lutetium-177 targeted radionuclide therapy

[1]俞長青, [2]丁健益
[1]高雄榮民總醫院
[2]中山醫大附設醫院

發表者 俞長青

Keywords 曝露劑量 (Exposure)

Background

Lutetium-177 (177Lu) is a theranostic radionuclide increasingly used in the treatment of neuroendocrine tumors (NETs) and metastatic castration-resistant prostate cancer (mCRPC). Its β-particles offer effective tumor cell killing, while its accompanying γ-emissions enable imaging for treatment monitoring. Precise radiation dosimetry is essential to optimize therapeutic results and minimize toxicity to healthy organs. This retrospective study aims to evaluate the radiation dose distribution in patients undergoing 177Lu-targeted therapy and to assess the potential exposure to external radiation to medical staff during treatment procedures, while also reviewing related dosimetry methodologies and radiation safety measures.

Method

This study primarily referenced data from 26 patients who underwent ^{177}Lu-targeted radionuclide therapy, including patients with NETs and prostate cancer. The evaluation involved analyzing radiation dose distribution from various data sources using the MIRD method. The study also reviewed the current development of dosimetry methods and radiation protection protocols applied in clinical settings to ensure the safety of patients and healthcare workers.

Results

The kidneys and bone marrow were identified as the main organs of risk in 177Lu-DOTATATE therapy, while the parotid glands, lacrimal glands, and bone marrow were the main potential risk organs in 177Lu-PSMA therapy. The conventional MIRD (Medical Internal Radiation Dosimetry) method demonstrated an overall error of approximately 25% in the estimation of renal doses, highlighting its limitations in personalized dosimetry. A single injection of 7400 MBq of 177Lu-labeled agents could result in an estimated whole-body effective dose ranging from 0.02 to 1.09 Sv for patients.

Conclusion

Our findings indicate that precise dose assessment is crucial for enabling individualized treatment planning. Furthermore, with the implementation of appropriate radiation protection and measures. The occupational radiation exposure levels for medical personnel are considered safe and manageable.

壁報論文 臨床組 **PC-042**

原著論文 臨床診斷

降低糖尿病患者腸道 FDG攝取對影像之影響

[1]江泰林, [1]柴發順, [1]歐玲君, [1]林聖哲, [1]陳遠光, [1]葉加祿

[1]新光醫院

發表者 江泰林

Keywords 糖尿病 FDG PET/CT 腸道 FDG 攝取

Background

F-18 FDG PET/CT對於大腸癌有極高的敏感度，整條均勻廣泛性的FDG攝取，多半非惡性病變，對於單一且邊界明顯的FDG攝取，則需考慮腫瘤可能性，FDG被腸壁攝取可能與腸道平滑肌收縮及腸道黏膜細胞的葡萄糖代謝有關，腸道內出現FDG聚積因而增加影像判讀困難，並可能造成病灶誤判。糖尿病患者，尤其接受口服降血糖藥物治療者，較容易出現腸道 FDG 廣泛性攝取。本研究藉由正子造影前口服緩瀉劑、對比劑及水，來降低糖尿病受檢者腸道FDG的聚積，提高影像品質，改善腸道FDG聚積對影像的干擾。

Method

本研究收集正子受檢者、無大腸直腸癌病史，正在接受糖尿病藥物治療者 74 人，檢查前一天停止服用糖尿病藥物，依值班醫師執行方式分為兩組，將糖尿病用藥治療的受檢者分成施打 FDG 前口服緩瀉劑Magvac 200 mL，加入對比劑Conray 5 mL，並飲用水 500 mL的實驗組 31 人和未口服緩瀉劑加對比劑的對照組 43 人。影像分析將大腸分為升結腸、橫結腸、降結腸及乙狀結腸－直腸，四個腸段區。另由兩位正子中心醫師及一位放射師，在不知受檢者分組及臨床資料的情況下，依腸道 FDG 攝取範圍進行影像品質評分，本研究依腸道FDG聚積範圍及程度評分1–10 分，分數越高代表影像品質越佳。影像品質優者 10 分（全腸道無聚積）、8-9 分（一腸道少量或局部輕微聚積）、6-7 分（兩腸段有輕至中度聚積）、4-5 分（其中三腸段有輕至中度聚積）、2-3 分（其中三腸段以上中度重度聚積）、1 分為（全腸道廣泛性聚積）。比較兩組腸道FDG聚積干擾發生率、受影響腸段分布及影像品質評分，並以Student’s t 檢定分析兩組差異。

Results

服用緩瀉劑及對比劑組 31 名受檢者，有 15 人出現腸道FDG聚積，發生率為 48.3%，共發現 29 個腸段受干擾。未服用緩瀉劑加對比劑的 43 人受檢者中，有 30 人出現腸道FDG聚積，發生率為 69.7%，共發現 56 個腸段受干擾。兩組腸道聚積干擾發生率具有統計學意義（p=0.032）。腸段分布分析顯示，實驗組共 29 個受干擾腸段，升結腸6段、橫結腸 8 段、降結腸 4 段及乙狀結腸－直腸區 11 段；對照組共 56 個受干擾腸段，升結腸 6 段、橫結腸 7 段、降結腸 17 段及乙狀結腸－直腸 26 段，兩組皆以乙狀結腸－直腸區最常出現FDG聚積。影像品質評分，實驗組平均分數為 7.6 ± 2.1 分，對照組平均分數為 5.9 ± 2.3 分，兩組差異具有統計學意義（P = 0.0012）。

Conclusion

糖尿病患者接受正子造影檢查時，口服降糖尿病藥物可促進腸道黏膜細胞攝取及利用葡萄糖，FDG 會隨葡萄糖代謝增加而在腸道聚積。腸道生理性FDG聚積可能造成影像判讀干擾。提高PET影像品質以協助醫師臨床診斷，是我們應盡的責任。對於糖尿病藥物治療的正子造影受檢者，施打FDG前喝下緩瀉劑加對比劑及水是預防性的作法，使腸道提早受到緩瀉劑作用，可有效降低腸道FDG聚積干擾的發生率，並改善整體影像品質。

壁報論文 臨床組 PC-043

文獻綜述 臨床診斷

Diagnostic Efficacy and Clinical Utility of Nuclear Medicine Perfusion Scanning for Suspected Pulmonary Embolism in ICU Patients: A Systematic Review

[1]吳俊昌, [1]鄭伃嫊, [1]邵泓臻, [1]何佩恩

[1]台北馬偕醫院

發表者 吳俊昌

Keywords 分子影像 | 造影儀器 | 解剖學 /CT/MR

Background

Diagnosing suspected acute pulmonary embolism (PE) in intensive care unit (ICU) patients remains challenging. Although computed tomography pulmonary angiography (CTPA) is the gold standard, iodinated contrast poses risks of contrast-induced nephropathy and hypersensitivity reactions, limiting its utility in patients with renal impairment or contrast allergies. Nuclear medicine lung perfusion scanning has emerged as a valuable alternative, offering a high negative predictive value to exclude PE while avoiding complications. However, a systematic synthesis of its clinical utility in the ICU setting remains lacking.

Literature review

Guided by PRISMA principles, a systematic search of PubMed, Embase, and the Cochrane Library was performed using terms combining "intensive care unit," "pulmonary embolism," "perfusion scan," and "V/Q/SPECT." The synthesis highlights several advantages of nuclear perfusion imaging. In ICU patients with renal impairment, avoiding iodinated contrast is a major strength; perfusion scanning requires only microcurie tracer doses (e.g., 99mTc-MAA) without compromising renal safety. It also serves as a reliable alternative for patients with severe contrast hypersensitivity or body mass exceeding CT limits. Most importantly, a normal perfusion scan offers an excellent negative predictive value, enabling clinicians to confidently discontinue anticoagulants in bleeding-prone patients. Conversely, technical and diagnostic challenges persist. Parenchymal diseases, such as pneumonia, atelectasis, or ARDS, are common in ICU patients and frequently generate non-embolic perfusion defects, compromising diagnostic specificity. Mechanical ventilation further prevents standard inhaled ventilation protocols, leaving many patients with perfusion-only studies that yield high indeterminate scan rates. Furthermore, perfusion imaging lacks the broad diagnostic coverage of CTPA for alternative acute conditions, such as pneumothorax or aortic dissection, and is limited by longer scanning times. Nevertheless, hybrid SPECT/CT imaging addresses many limitations by refining anatomical localization and markedly reducing inconclusive results, highlighting the utility of perfusion imaging in tailored ICU diagnostic pathways.

壁報論文 臨床組 **PC-044**

原著論文 | 臨床治療或診療合一

藥師於核醫放射配體治療臨床試驗之實務角色與跨專業團隊合作

[1]洪綾蔓

[1]和信醫院

Keywords 放射配體治療 | 臨床試驗 | 試驗藥品管理

Background

近年來，精準醫療與核子醫學的結合使放射配體治療（Radioligand Therapy, RLT），如以鐳 -177（Lu-177）為基礎的標靶放射性藥物，成為治療晚期神經內分泌腫瘤與前列腺癌等重大疾病的突破性療法，以放射配體治療藥物為主的臨床試驗也陸續展開。

由於放射配體治療藥物兼具「藥品」與「放射性物質」雙重特性，其臨床試驗執行除須遵循試驗計畫書及藥品優良臨床試驗規範外，亦涉及放射性試驗藥品管理、輻射防護、無菌操作等多重要求。核醫藥師的專業參與，與試驗主持人、研究護理師、醫事放射師、輻射防護人員及試驗委託者跨專業合作，確保試驗診斷和治療流程順利與用藥品質保證。

Method

本院依藥品優良臨床試驗規範、臨床試驗計畫書、試驗藥品手冊、各試驗之標準作業程序及其他相關法規，建立放射配體治療試驗藥品管理流程。核醫藥師參與試驗啟動前評估作業與團隊訓練，放射藥品無菌調劑環境維護和監控，試驗進行期間執行放射配體治療相關試驗藥品接收、儲存、溫度監測、庫存及管理；協助臨床試驗團隊調整安排病人篩選診斷與放射配體治療及後續影像追蹤排程，進行處方資料核對、放射活度確認、無菌調劑及給藥流程協作；給藥後完成殘餘活度確認、實際給予劑量計算、藥品回收與放射性廢棄物管理，並協助收集和完成診斷及治療相關各項文件製作、紀錄、保存和管理；遇有藥品相關流程偏差或異常事件時，啟動評估、通報並追蹤改善。

Results

在實務運作中，核醫藥師於放射配體治療臨床試驗團隊中之核心角色：

1. **試驗藥品與輻安雙重合規管理**：藥師結合臨床試驗與輻射安全相關規範，建立放射性試驗藥品的接收、儲存、調劑、品質管制及廢棄物處理之標準作業，確保藥品帳務零誤差及調劑過程零輻射污染事件。

1. **跨專業溝通與受試者用藥安全**：透過標準化藥事作業與跨專業溝通，建立涵蓋試驗啟動、藥品管理、治療執行至後續追蹤的完整流程。藥師可於給藥前進行多重核對，協助確認受試者身分、處方、試驗時程、藥品資訊及放射活度；治療過程中則協調藥品調劑、運送與給藥銜接，並確保藥品可追溯性及文件完整性。藉由跨專業分工合作及即時溝通機制，有助於降低流程疏漏與試驗偏差風險，並提升試驗藥品管理品質、執行一致性及受試者用藥安全。

Conclusion

藥師在核醫放射配體治療臨床試驗中，不僅負責試驗藥品管理與調劑，更是串聯臨床治療、品質管理、輻射安全及試驗規範的重要角色。建立標準化流程與跨專業協作模式，可強化試驗執行品質及受試者安全，並彰顯核醫藥師在新興精準治療臨床研究中的專業價值。未來應持續推動藥師在核醫領域的專業培訓，深化跨團隊協作模式，以應對日益增長且複雜的放射標靶治療臨床試驗挑戰。

壁報論文 臨床組 **PC-045**

原著論文 臨床診斷

Discordance Between Serum PSA and PSMA PET/CT–Defined Disease Burden Across Clinical States in Prostate Cancer

[1]諶鴻遠, [1]陳盈伸, [2]李明展, [1,2]詹宏彬

[1]高雄榮民總醫院
[2]國立中山大學

發表者 詹宏彬

Keywords 分子影像

Background

To evaluate the association between serum PSA levels and PSMA PET/CT–defined disease burden, and to identify clinically relevant discordance across different clinical states of prostate cancer.

Method

We retrospectively reviewed 133 18F PSMA PET/CT examinations (18F PSMA-1007, n=76; 18F rhPSMA-7.3, n=57) in 129 patients. Patient-level analyses retained one eligible examination per patient. Disease burden was classified as B0 (no definite disease), B1 (locoregional M0 disease), B2 (1–3 distant lesions), or B3 (≥4 distant lesions and/or visceral metastasis). Clinical state was categorized as initial/hormone-sensitive disease, biochemical recurrence/PSA persistence, or advanced/castration-resistant disease/pre-radioligand therapy. PSA analysis used the latest pre-PET value within 90 days. Discordance was defined as PSA <1 ng/mL with M1 disease or PSA ≥10 ng/mL with M0 disease.

Results

Disease burden was classifiable in 128 patients, of whom 103 had an eligible PSA–PET pair (B0/B1/B2/B3: 11/38/19/35). PSA correlated moderately with ordinal PET burden (Spearman ρ=0.530, p<0.001). Among patients with a defined clinical state, B3 prevalence was 76.7% (33/43) in advanced/castration-resistant disease, 20.6% (7/34) at initial/hormone-sensitive assessment, and 6.7% (3/45) in biochemical recurrence/PSA persistence (p<0.001). Nevertheless, 12/35 patients (34.3%) with PSA <1 ng/mL had M1 disease, including 4 (11.4%) with B3 disease, whereas 7/34 (20.6%) with PSA ≥10 ng/mL remained M0. Overall discordance was 18.4% (19/103; 95% CI, 12.1–27.0%).

Conclusion

PSA showed only a moderate relationship with PSMA PET/CT–defined disease burden, which varied substantially across clinical states. Nearly one-fifth of patients demonstrated clinically important discordance, supporting PSMA PET/CT as a complementary whole-body assessment when PSA alone may be misleading.

壁報論文 臨床組　　**PC-046**

個案報告　臨床診斷

Ga-67在良性黃體囊腫病變異常攝取之病例報告

[1]林昱璁, [1]陳薇璇, [1]廖建國, [1]莊紫翎

[1]大林慈濟醫院

發表者　林昱璁

Keywords　有趣影像 | 影像組學 (Radiomics) | 分子影像

Background

背景介紹：Gallium-67 (Ga-67)常被用於協助診斷慢性發炎、膿瘍、特定感染以及追蹤惡性腫瘤 (何杰金氏淋巴瘤) 之偵測，但其攝取的原因並非都為感染，良性發炎、組織修復及部分腫瘤性病變亦可能呈現異常攝取。女性骨盆腔附件區病灶的影像鑑別尤其複雜，Ga-67影像結果需與臨床症狀、實驗室檢查及解剖影像綜合判讀。本病例描述一名甲狀腺癌術後長期追蹤患者，因持續性白血球增多及右側骨盆腔病灶接受Ga-67掃描，最終經手術及病理證實為良性卵巢病變。

Case report

病例報告：一名 35 歲女性，之前有甲狀腺癌病史，曾接受甲狀腺切除術及I-131治療，後續接受左旋甲狀腺素 (Levothyroxine)抑制治療。長期追蹤期間甲狀腺球蛋白(thyroglobulin, Tg)維持低值，rhTSH刺激檢查未見明顯殘餘病灶，整體疾病狀況穩定。九年後因持續性白血球增多及輕微右下腹疼痛進行腹部電腦斷層檢查。影像顯示右側骨盆腔約 12 × 14 mm囊性病灶，當時鑑別診斷可能為正常卵泡、卵巢膿瘍或腫瘤。之後接受Ga-67發炎掃描，影像上除生理性攝取外，於 6 小時影像可見升結腸攝取，雙側乳房攝取，為生理性變化，SPECT/CT顯示右下側骨盆腔子宮附件區呈現輕度Ga-67放射性攝取。由於病人持續白血球增多、右側腹部壓痛及右側骨盆腔病灶持續存在，臨床無法排除慢性骨盆腔感染或卵巢膿瘍，因此接受腹腔鏡手術。術中發現右側卵巢囊腫、混濁腹水、骨盆腔沾黏及左側副輸卵管囊腫，並於直腸漿膜表面發現兩處疑似子宮內膜異位症病灶。手術完成右側部分卵巢切除及囊腫剝除、骨盆腔沾黏分離與疑似子宮內膜異位症病灶電燒。病理檢查顯示右側卵巢為出血性黃體囊腫（hemorrhagic corpus luteal cyst），左側為輸卵管旁囊腫（paratubal cyst），均屬良性病變。

Conclusion

結論：本病例顯示，良性婦科病變亦可能呈現Ga-67輕度異常攝取，尤其在慢性發炎、組織反應或骨盆腔沾黏的情況下，可能造成類似感染病灶的影像表現。雖然本病例Ga-67於右側骨盆腔僅呈輕度攝取，並未呈現典型高度活動性膿瘍的表現，但結合持續性白血球增多、右下腹疼痛及CT所見，仍需考慮感染性病灶並進一步處置。最終手術及病理證實為良性卵巢及輸卵管旁囊腫。因此，Ga-67影像對骨盆腔病灶的判讀應結合CT解剖資訊、臨床表現、實驗室數據及病理結果，避免單憑放射性攝取判定為感染或惡性病變。

壁報論文 臨床組 **PC-047**

個案報告 臨床診斷

乳癌患者頸椎C1破壞性病灶之影像診斷誤差：細胞型神經鞘瘤於骨骼掃描及18F-FDG PET/CT的表現

[1]林昱璁, [1]陳薇璇, [1]廖建國, [1]莊紫翎

[1]大林慈濟醫院

發表者 林昱璁

Keywords 有趣影像 | 分子影像 | 影像組學 (Radiomics)

Background

背景介紹：乳癌患者於治療後發現新的骨質破壞性病灶時，臨床上通常首先考慮骨轉移。然而，部分良性腫瘤亦可能造成局部骨質破壞及異常放射性同位素攝取，導致影像表現出類似惡性腫瘤的現象。細胞型神經鞘瘤 (Cellular schwannoma)為少見的周邊神經鞘腫瘤，雖屬良性腫瘤，但如果發生於脊椎附近時仍可能造成鄰近骨骼侵蝕，且呈現較高的 18F-FDG攝取。本病例旨在探討細胞型神經鞘瘤在核醫全身骨骼掃描及FDG PET/CT的影像上對於乳癌骨轉移的影像特徵及診斷的誤差。

Case report

病例報告：一名 45 歲女性，過去具有右側乳癌病史，診斷為浸潤性乳管癌，pT1cN3aM0、Stage IIIC，ER (+)、PR(+)及HER2 (+)，曾接受右側乳房全切除術、腹直肌皮瓣乳房重建 (TRAM flap reconstruction)、輔助性化學治療及trastuzumab標靶治療。2020 年因持續性頸部疼痛接受影像檢查，在CT影像發現左側C1頸部椎體有逐漸增大的腫塊及明顯骨質破壞，首先考慮乳癌骨轉移。後續 99mTc-MDP全身骨骼掃描顯示頸部左側C1椎體有明顯局部放射性攝取增加，左側乳突區亦可見放射性攝取。之後再安排正子攝影，18F-FDG PET/CT顯示左側頸椎旁C1腫塊合併骨質破壞，呈現明顯FDG攝取，SUVmax約7.3，因此影像上高度懷疑轉移性病灶。後續MRI檢查顯示腫瘤沿左側頸椎C1神經分布，伴隨神經孔擴大及左側椎體旁延伸，考慮周邊神經鞘腫瘤。患者接受腫瘤切除手術，病理檢查最終證實為細胞型神經鞘瘤，並接受 5 次總劑量為 3000cGy的SBRT治療。追蹤骨骼掃描仍顯示左側C1椎體攝取增加，SPECT/CT定位C1左側類似蝕骨性病灶（應為術後錐體切除）與前側活性攝取。後續MRI長期追蹤顯示殘存病灶維持穩定，未見支持乳癌骨轉移之證據。

Conclusion

結論：本病例顯示，細胞型神經鞘瘤即使為良性腫瘤，仍可能造成明顯頸椎C1骨質破壞，並在骨骼掃描及 18F-FDG PET/CT上呈現高度攝取，而造成類似乳癌骨轉移的現象。SPECT/CT雖然可提供病灶更精確的解剖定位，但仍無法單獨區分良惡性病變或是術後變化。因此，對於具有癌症病史且出現單一脊椎破壞性病灶的患者，應整合骨骼掃描、SPECT/CT、FDG PET/CT及MRI等多種類型影像，並將神經鞘腫瘤納入鑑別診斷，必要時仍應透過組織病理確認，及參考系列影像，以避免誤診為骨轉移及後續不必要的治療。

壁報論文 臨床組

PC-048

原著論文 臨床診斷

Differential association between salivary gland scintigraphy functional parameters and autoantibody levels in patients with suspected Sjögren's syndrome: a comparative analysis of parotid and submandibular glands with longitudinal follow-up

[1]王昱豐, [2]莊美華, [3]莊紫翎

[1]臺北榮民總醫院
[2]馬偕醫護管理專科學校
[3]大林慈濟醫院

發表者 王昱豐

Keywords Salivary gland scintigraphy • Sjögren's syndrome • Anti-Ro/SSA antibody • Submandibular gland • Maximum secretion score • Steiger's test • Longitudinal analysis

Background

Salivary gland scintigraphy (SGS) is an established functional imaging modality for evaluating glandular involvement in Sjögren's syndrome. Although quantitative parameters such as time to maximum counts (Tmax) and time from citric acid stimulation to minimum counts (Tmin) have been associated with rheumatoid factor (RF) seropositivity, the differential relationships between parotid and submandibular gland functional scores and autoantibody profiles remain unclear. This study also evaluated longitudinal changes in serological markers over a median follow-up of 3.6 years.

Method

This retrospective study included 109 patients who underwent SGS for sicca symptoms or suspected Sjögren's syndrome between April 2020 and May 2022. Ten quantitative scintigraphic parameters were derived from bilateral parotid and submandibular gland time–activity curves. Spearman correlations were calculated between scintigraphic parameters and anti-Ro/SSA, anti-La/SSB, and RF. Steiger's test was used to compare correlations between submandibular and parotid maximum secretion (MS) scores with anti-SSA. Group differences were assessed using Kruskal–Wallis and post-hoc Mann–Whitney U tests. Partial correlation, logistic regression, and Wilcoxon signed-rank tests were also performed.

Results

The submandibular MS score was the only scintigraphic parameter significantly correlated with all three autoantibodies: anti-SSA ($r=-0.425$, $p<0.001$), anti-SSB ($r=-0.228$, $p=0.018$), and RF ($r=-0.258$, $p=0.010$). Its correlation with anti-SSA was significantly stronger than that of the parotid MS score, as confirmed by Steiger's test ($p=0.042$), whereas no significant differences were observed for anti-SSB or RF. After adjustment for age and sex, the partial correlation with anti-SSA strengthened to $r=-0.519$ ($p<0.001$). Logistic regression identified submandibular MS score as the only variable independently associated with anti-SSA seropositivity (OR=0.959, $p=0.037$). Longitudinal analysis showed significant decreases in anti-SSA ($p=0.014$) and ESR ($p=0.001$), with correlated changes between the two markers ($r=0.413$, $p=0.021$). Anti-SSA seroconversion was uncommon (2/53 patients).

Conclusion

The submandibular gland MS score showed a stronger and relatively independent association with anti-SSA than the parotid MS score, supporting its potential role as a gland-specific functional correlate of anti-SSA–related salivary gland involvement. Anti-SSA and ESR showed correlated longitudinal decreases in the follow-up subset, suggesting that these markers may reflect partially shared temporal changes; however, their role in disease monitoring requires validation with paired clinical and imaging follow-up.

壁報論文 臨床組 **PC-049**

經驗分享 非診療之臨床相關主題

從護理實務探討 Tc-99m MDP 骨骼掃描於手腕注射之放射性藥物滲漏風險

[1]王苡安, [1]廖建國, [1]莊紫翎

[1]大林慈濟醫院

發表者 王苡安

Keywords 病人安全 | 衛教

Background

背景介紹：放射性藥物滲漏（radiopharmaceutical extravasation）可能影響影像品質及診斷準確性。Fernandes 等人（2023）指出，以手腕（wrist）作為注射部位，其藥物滲漏風險約為手部（hand）的 3.12 倍，因此不建議作為常規注射位置。然而，目前國內針對骨骼掃描病人不同注射部位與藥物滲漏之相關研究仍相當有限。本研究旨在分析本院核醫科骨骼掃描病人以手腕注射放射性藥物之滲漏發生情形，並與國外文獻進行比較。

Method

材料方法：本研究採回溯性研究設計，收集 2026 年 1 月 2 日至 2026 年 6 月 30 日期間接受Tc-99m MDP骨骼掃描之 360 位病人資料，分析其放射性藥物注射手腕及是否發生藥物滲漏。統計接受手腕注射病人的滲漏發生率，並與Fernandes等人（2023）研究結果進行比較。本院核醫科主治醫師依照骨骼掃描影像及臨床紀錄判定，主要是從影像中疑似注射部位有一顆亮點，再看檢查紀錄單確認打針的位置，另外也會從正面及背面的影像來研判，如果正反面影像一面有亮，另一面沒有亮，即可判讀藥物滲漏。

Results

結果：360 位受試者中，共有 51 位（14.2%）接受手腕（wrist）靜脈注射，其餘病人接受手背、前臂、手肘及腳部等部位注射。51 位手腕注射病人皆未發生放射性藥物滲漏，手腕注射之滲漏率為 0%。此結果與Fernandes等人（2023）報告手腕注射滲漏率 52.4%，且相較於手部具有 3.12 倍滲漏風險之結果並不一致。本研究中，手腕注射並未觀察到藥物滲漏事件，未能重現Fernandes等人（2023）提出手腕為高風險注射部位之結果。造成差異可能與研究族群、注射流程、護理人員靜脈注射技術、手腕注射適應症選擇及藥物滲漏判定方式不同有關。

Conclusion

結論：本研究顯示，在完善的注射評估、標準化操作流程及熟練護理技術下，手腕作為骨骼掃描放射性藥物注射部位未必增加藥物滲漏風險。未來仍需多中心及大樣本研究進一步驗證，以建立更適合國內臨床實務之注射部位選擇依據。

壁報論文 臨床組 **PC-050**

個案報告 非診療之臨床相關主題

Hot Hand 現象於Tc-99m MDP全身骨骼掃描之案例分析－護理注射品質討論與改進

[1]王苡安, [1]廖建國, [1]莊紫翎

[1]大林慈濟醫院

發表者 王苡安

Keywords 有趣影像 | 病人安全

Background

背景：全身骨骼掃描（Whole-body Bone Scintigraphy）是核子醫學常用檢查之一，利用Tc-99m MDP評估骨骼代謝及骨轉移情形。然而，注射過程中誤入動脈，因局部動脈灌流增加，可能造成單側上肢骨骼及軟組織異常放射性聚積，形成罕見的 Hot Hand現象。此種注射偽影不僅降低影像判讀品質，更可能造成骨病灶偽陽性判讀，影響臨床診療決策。本案例藉由分析 Hot Hand 形成原因及影像特徵，探討核醫護理人員於靜脈注射流程中的改善策略，以提升影像品質及病人安全。

Case report

病例報告：57 歲男性，具有吸菸史及僵直性脊椎炎病史，診斷為右肺下葉鱗狀細胞癌（Clinical stage IIIA），接受同步放射治療、化學治療及 Durvalumab 維持治療。後續追蹤胸部電腦斷層發現右肺下葉腫瘤有增大趨勢，懷疑疾病進展，因此安排 Tc-99m MDP 全身骨骼掃描，評估是否有骨轉移。影像結果顯示：左前臂及左手骨骼與軟組織呈現均勻且明顯放射性聚積。雙側腎臟及膀胱顯影正常。未見其他骨骼異常攝取。經本院核醫科醫師臨床及影像判讀，排除局部感染、骨病灶及淋巴回流異常後，診斷為 Hot Hand 現象，推測係因注射時誤入動脈所致。針對此次事件進行護理注射流程檢討，以下為判斷注射動脈及靜脈的分析，正常靜脈觸摸無明顯搏動、注射時回血平穩、影像顯示全身均勻分布；如打到動脈時觸摸有明顯搏動、注射時回血快速、影像單側手聚積顯影。注射核醫藥物前以生理食鹽水確認回血及管路通暢。發現疑似動脈時，請勿繼續施打，以利影像判讀及後續追蹤。

Conclusion

結論：Hot Hand雖屬核醫骨骼掃描少見之注射偽影，但對影像品質及診斷正確性具有重要影響。本案例顯示，完善的靜脈注射技術、正確血管辨識能力及標準化注射流程，可有效降低示蹤劑誤入動脈的風險。護理人員持續技巧精進、注射流程標準化，不僅可提升核醫影像品質，更能降低偽陽性判讀及避免不必要檢查，進一步提升病人安全與醫療照護品質。

壁報論文 臨床組 **PC-051**

個案報告 臨床診斷

FDG PET/CT Detects Occult Cholangiocarcinoma Presenting as Diffuse Peritoneal Carcinomatosis Misdiagnosed on Contrast-Enhanced CT

[1]陳朝榮

[1]阮綜合醫院

Keywords 有趣影像

Background

The peritoneum is a preferred site of metastasis for several primary malignancies, principally colorectal carcinoma in men and ovarian cancer in women, as well as primary gastric, pancreatic, and adrenocortical carcinomas. In contrast, peritoneal carcinomatosis originating from cholangiocarcinoma is not common. Here, we present a case of cholangiocarcinoma that initially manifested as massive peritoneal carcinomatosis. The primary hepatic lesion was occult on contrast-enhanced abdominal CT but was ultimately identified using F-18 FDG PET/CT.

Case report

A 70-year-old female patient presented with epigastric pain persisting for approximately one month. Contrast-enhanced abdominal CT revealed diffuse peritoneal thickening and nodules without an obvious primary malignancy; therefore, the differential diagnoses included peritoneal carcinomatosis and tuberculous peritonitis. A diagnostic laparoscopic biopsy of the peritoneal lesions revealed metastatic adenocarcinoma, though the primary origin remained unclear. Given the unknown primary malignancy, the patient was referred for F-18 FDG PET/CT evaluation. The scans revealed a hypermetabolic tumor in the left lobe of the liver, along with suspected diffuse peritoneal carcinomatosis within the abdominopelvic cavity. No other potential primary lesions, including in the ovaries, were detected; thus, primary cholangiocarcinoma was highly suspected. A subsequent biopsy of the left hepatic tumor confirmed the diagnosis of cholangiocarcinoma. A retrospective review of the initial contrast-enhanced abdominal CT identified an obscure, ill-defined hepatic lesion that had been easily overlooked.

Conclusion

In conclusion, this case highlights an unusual presentation of cholangiocarcinoma, which initially manifested solely as diffuse peritoneal carcinomatosis without regional lymph node or bone metastases. F-18 FDG PET/CT served as a valuable diagnostic tool in confirming the intrahepatic cholangiocarcinoma as the primary malignant origin, which had been overlooked on the initial contrast-enhanced abdominal CT.

壁報論文 臨床組 **PC-052**

個案報告 臨床診斷

PSMA PET/CT於攝護腺癌生化復發之骨盆淋巴結轉移：病理驗證與術後影像評估病例報告

[1]蔡沛君

[1]童綜合醫院

Keywords 攝護腺癌 | PSMA PET/CT | 骨盆淋巴結轉移 | 18F-flotufolastat

Background

攝護腺癌接受根除性攝護腺切除術後若出現生化復發（biochemical recurrence, BCR），精準定位低腫瘤負荷或微小復發病灶，對後續局部治療決策至關重要。傳統解剖影像對小體積淋巴結轉移的偵測敏感度有限。18F-flotufolastat（18F-rhPSMA 7.3；Posluma）可藉由攝護腺特異性膜抗原（PSMA）的表現進行分子影像定位。本病例呈現一名術後 PSA 再度上升患者，經系列PSMA PET/CT追蹤發現左側骨盆淋巴結轉移，並以手術病理確認，術後再以 PSMA PET/CT 評估局部治療結果，呈現影像、病理與治療反應之完整關聯。

Case report

患者為 63 歲男性，攝護腺癌pGS 3+4，接受根除性攝護腺切除術。術後約 1 年因PSA上升（轉入本院時 0.591 ng/mL）接受影像追蹤；患者另有先前骨病灶影像及放射治療病史。初次PSMA PET/CT（PSA 0.538 ng/mL）未見明顯異常骨盆淋巴結；約半年後第二次檢查（PSA 0.857 ng/mL）仍未見骨盆淋巴結病灶。其後PSA逐步上升，於術後約 2年 3 個月升至 1.69–2.13 ng/mL，第三次PSMA PET/CT顯示左側內髂區新出現一顆直徑約0.65 cm之淋巴結，雖體積微小，卻呈明顯PSMA高攝取（SUVmax 4.92），疑似淋巴結轉移。依據影像定位，患者後續接受骨盆淋巴結廓清術；病理證實為轉移性攝護腺癌，免疫組織化學染色顯示腫瘤細胞PSMA陽性（98%，+++）及NKX3.1陽性，與PET影像之高 PSMA攝取表現一致。術後約 3 個月，PSA降至 0.543–0.699 ng/mL；第四次 PSMA PET/CT顯示已無左側內髂淋巴結病灶，且未見其他明顯PSMA高攝取之殘存或新發轉移病灶。

Conclusion

本病例顯示，PSMA PET/CT在攝護腺癌術後生化復發情境下，可偵測小體積之骨盆淋巴結轉移，並提供明確的病灶定位以協助後續手術處置。該病灶之PSMA高攝取經手術病理及免疫組織化學證實為轉移性攝護腺腺癌，與PET/CT影像發現相互印證；術後PSMA PET/CT則顯示原病灶分子影像訊號消失，且未見明顯可辨識之殘存或新發轉移病灶，可提供局部治療後影像追蹤之客觀依據。本病例強調PSMA PET/CT在攝護腺癌術後生化復發之系列追蹤中，對淋巴結轉移病灶的偵測與定位價值，以及其與手術病理結果及術後影像變化之相關性。

壁報論文 臨床組 **PC-053**

原著論文 臨床診斷

以不同平臺軟體分析腎絲球過濾率

[1]魏文祺, [1]陳至豪, [1]胡蓮欣, [1,2,3]王昱豐

[1]臺北榮民總醫院
[2]陽明交通大學
[3]元培醫事科技大學

發表者 魏文祺

Keywords GFR | Tc99m-DTPA | GATES

Background

核子醫學腎絲球過濾率 (Glomerular Filtration Rate, GFR)檢查是用於監測腎臟功能的重要方法之一，比起血液監測方法，其優點是可以得到整體與個別腎臟的腎絲球過濾率。在核醫部門常會同時擁有不同廠牌的造影設備及面臨造影儀器的汰舊換新或分析軟體的更新。因此，在不同廠牌的造影設備間及影像處理工作站更新後是否能得到相同、穩定、正確的檢查數據，對病患後續的病情追蹤至關重要。本研究的目的是比較在不同的廠牌造影設備平臺上，使用蓋氏法 (GATES)分析腎絲球過濾率，在統計上是否會有顯著不同。

Method

本研究為回溯性研究，做影像數據重分析。61 筆接受核子醫學腎絲球過濾率檢查病例，原始影像採集及分析方法採用蓋氏法 (GATES)，造影儀器使用Siemens E-cam，病患所注射的放射性藥品為 3 mCi的Tc99m-DTPA，採動態造影模式，每 15 秒一幀影像，總共採集 6 分鐘。影像分析使用GE Xeleris與Siemens E-soft影像處理工作站內腎臟分析軟體。統計方法採用線性回歸分析與Bland-Altman Plot。統計軟體軟使用MedCalc® Statistical Software version 23.6.1 (MedCalc Software Ltd, Ostend, Belgium; 2026)。

Results

GE Xeleris 與Siemens E-soft左腎腎絲球過濾率數值分別為 33.31±15.25；34.21±15.88。右腎為 34.08±13.96；35.16±14.28。總腎絲球過濾率數值分別為 67.40±23.43 與69.37±24.53。R2=0.97，P=0.12。結果顯示在GE Xeleris與Siemens E-soft的腎絲球過濾率數值並無顯著性差異。

Conclusion

使用蓋氏法 (GATES)分析腎絲球過濾率，即使在不同的造影平臺上也能得到相同與穩定的結果。

壁報論文 臨床組 **PC-054**

個案報告 臨床診斷

Not Very Common Occurrence of Enchondroma in 99mTc MDP Bone Scintigraphy and SPECT: a Case Report

[1]蕭聿謙, [1]張哲瑋, [1]汪姍瑩, [1]吳彥雯

[1]亞東醫院

發表者 蕭聿謙

Keywords 有趣影像 | 分子影像 | 影像組學 (Radiomics)

Background

Although enchondroma is not very rare, but not so common in routine practice of nuclear medicine. According to the literatures, diagnosis and differential diagnoses of enchondroma, osteochondroma, and chondrosarcoma are important for clinical treatment. Because there were not so many reports concerning enchondroma, we present a case of enchondroma elucidated by 99mTc MDP bone scan and SPECT.

Case report

The 41 year-old man had history of hepatocellular carcinoma in S6, pT1bN0MB, stage IB, BCLC stage A, s/p laparoscopic S6 wedge hepatectomy. He had progressive rising of tumor markers with CA-199 48.80 U/mL and AFP 300.00 ng/mL in OPD follow-up. He was admitted for further study and treatment. During hospitalization, CT showed four recurrent HCCs in the right liver. MRI of the right leg revealed a 4.0 × 2.0 × 1.7 cm proximal tibial marrow lesion without cortical destruction or soft tissue extension, with differential diagnosis including enchondroma, low-grade chondrosarcoma, and metastasis. Bone scan was arranged and showed a hot area with osteosclerotic change, suspecting bone tumor, bone metastasis, osteomyelitis, or other etiology in right tibia. He underwent curettage biopsy and bone grafting of the right proximal tibial lesion. Pathology showed enchondroma. His right leg wound remained clean and healing well. He was followed-up in OPD.

Conclusion

Diagnosis of enchondroma relies on X-ray, CT, MRI, and pathological examination, which is relatively challenging. Some authors tried to utilize molecular genetics and radiomics for the differential diagnosis between enchondroma, osteochondroma, and chondrosarcoma. In this case report, we suggest 99m-Tc MDP bone scintigraphy and SPECT could be important for the diagnosis and differential diagnoses of enchondroma, which could be also important for the treatment planning for the patient. And the utilization of molecular genetics and radiomics and AI could be the future developmental direction for more accurate diagnosis and treatment.

壁報論文 臨床組 **PC-055**

個案報告 臨床診斷

Rare Occurrence of Bone Metastasis of Distal Tibia without Cancer History in 99mTc MDP Bone Scintigraphy: a Case Report

[1]蕭聿謙, [1]賴佳玟, [1]汪姍瑩, [1]吳彥雯

[1]亞東醫院

發表者 蕭聿謙

Keywords 分子影像 | 有趣影像 | 影像組學 (Radiomics)

Background

Although bone metastases of cancer noted in bone scintigraphy are quite common in routine practice, peripheral bone metastasis without previous cancer history is relatively uncommon in routine practice of nuclear medicine. According to the literatures, peripheral bone metastases are relatively rare reported, nor studied. Because there were few reports concerning peripheral bone metastases, we present a case of peripheral bone metastases without cancer history elucidated by 99mTc MDP bone scintigraphy and SPECT.

Case report

The 63 year-old man suffered from DOE progressed noted in recent months. In our OPD, chest X-ray was arranged and showed ground glass hazziness / consolidation and volume reduction at left lung, and pleural effusion(s) on the left. In OPD follow-up, left lung mass with brain metastasis were suspected, and bone scan, chest CT, and brain MRI were arranged. The initial bone scintigraphy was performed and reported without a pathological diagnosis, and which reported suspicious fracture, bone tumor, bone metastasis, arthritis, or other etiology in left lower femur, near left knee, and suspicious avascular necrosis, femoral fracture, bone metastasis, arthritis, or other etiology in right hip. Subsequent CT was done and showed suspicious advanced lung cancer at LUL, and indeterminate hepatic nodules. Brain MRI revealed no MR evidence of brain metastasis. CT-guide biopsy showed ATS wedge biopsy, mixed inflammation and focal hemorrhagic necrosis, and no evidence of malignancy. The patient developed left knee sprain injury while going to restroom and knee pain. X-ray showed displaced fracture at the left distal femur and suspicious right proximal femoral neck fracture. MRI was arranged and showed suspicious metastasis with pathologic fracture at left distal femur. ORIF and tumor excision of left distal tibia was done and pathology showed squamous cell carcinoma, metastatic, and fracture.

Conclusion

Peripheral bone metastasis without previous cancer history is relatively uncommon in routine practice of nuclear medicine. In this case report, we present a rare case of peripheral bone metastases without cancer history elucidated by 99mTc MDP bone scintigraphy and SPECT. Further study and statistical correlation could be the future development direction.

壁報論文 臨床組 **PC-056**

個案報告 臨床診斷

後腹膜膿瘍模擬惡性腫瘤之氟化去氧葡萄糖正子斷層造影表現

[1]陳羿吟, [2]李岱芸, [1]林家揚

[1]高雄市立小港醫院 (委託財團法人私立高雄醫學大學經營)
[2]輔英科技大學附設醫院

發表者 陳羿吟

Keywords 18F-FDG PET/CT | 感染發炎 | 不明熱

Background

患者長期因背部疼痛所擾，於術後發炎相關指數，如CRP(C-reactive protein)與ESR(erythrocyte sedimentation rate)等仍遠高於正常值範圍，臨床為進一步確認是否為骨髓炎復發、找出感染發炎原因與位置並訂定後續治療方針故尋求 18F-FDG PET/CT掃描檢查幫助。

Case report

本案例為一 45 歲女性，過去曾有脊椎感染病史，年初因持續性的背部不適多次就醫，於七月MRI檢查顯示腰椎壓迫性骨折、退化性關節炎，遂於九月接受手術治療。由於患者術後持續發燒，CRP、ESR持續偏高，且blood culture驗出MRSA(methicillin-resistant Staphylococcus aureus)，臨床上懷疑患者可能有骨髓炎、或其他感染的可能性，遂安排 18F-FDG PET/CT掃描檢查尋找感染發炎位置。

經 18F-FDG PET/CT掃描檢查結果，發現感染位置在右後腹腔，可能為術後傷口發炎感染所致，而非原先臨床上懷疑的骨髓炎。根據此次檢查結果，於隔日進行感染清創，取下的組織病理送驗證實為膿瘍感染。而患者於術後疼痛狀況明顯改善，且持續追蹤發炎指數，CRP與ESR皆顯著下降。

Conclusion

雖然 18F-FDG PET/CT掃描目前主要應用於腫瘤癌症相關的檢查，在國內全民健康保險之給付適應症也以癌症為主，但其在感染發炎與不明原因發燒的偵測上已逐漸受到重視，可幫助臨床診斷與治療策略制定。

壁報論文 臨床組 **PC-057**

文獻綜述 臨床診斷

Diagnostic Value of Gallium-67 Scintigraphy and Bone Scan for Occult Infection Localization in Critically Ill ICU Patients: A Systematic Review

[1]吳俊昌, [1]張佩琦, [1]王靜

[1]台北馬偕醫院

發表者 吳俊昌

Keywords 造影儀器 | 分子影像

Background

Sepsis and septic shock are major causes of death in the ICU, and finding the infection source early improves survival. However, the source is often hard to find with standard tests. 18F-FDG PET/CT(18F-fluorodeoxyglucose positron emission tomography/computed tomography) can help locate hidden infections, but it is costly and not always covered by insurance. Gallium-67 scan and bone scan are conventional nuclear medicine tests that may offer similar value. Ga-67 collects at sites of infection or inflammation, while bone scan detects abnormal bone activity, useful for bone infections. Whether these conventional tests still have real diagnostic value in ICU patients has not been systematically reviewed.

Literature review

Following PRISMA guidelines, we searched PubMed/MEDLINE, Embase, and the Cochrane Library using search terms for the population ("ICU" OR "critically ill" OR "sepsis"), intervention ("gallium-67" OR "bone scan" OR "scintigraphy"), and outcome ("diagnostic yield" OR "occult infection"). A prospective study of 32 mechanically ventilated febrile ICU patients utilized Ga-67 scintigraphy to localize pulmonary and non-pulmonary infection sites (Meduri et al., 1996). Similarly, a Taiwanese cohort study of 117 patients found that Ga-67 scintigraphy provided a new diagnosis in 16% of ICU patients with occult sepsis (Intern Emerg Med, 2011). In contrast, an earlier 37-patient case series demonstrated that Ga-67 was useful early in the course of illness but offered limited value later on (Rozet et al., 2000). No study has evaluated bone scans alone for detecting general occult infection in ICU patients. Instead, clinicians primarily use bone scans in combination with Ga-67 when suspecting bone or spinal infections. Furthermore, the only previous ICU imaging review (Huang et al., 2020) identified a single gallium study but excluded it due to a lack of accuracy data. To date, no review has synthesized this historical evidence within the context of modern ICU practice.

壁報論文 臨床組 **PC-058**

個案報告 臨床診斷

Primary Renal Lymphoma: Report of A Case

[1,2]程紹智, [1]楊宗翰, [1]周育祥

[1]台北慈濟醫院
[2]慈濟大學

發表者 程紹智

Keywords 分子影像

Background

Primary renal lymphoma, accounting for less than 1% of extranodal lymphomas, is an exceptio nally rare clinical entity because the renal parenchyma typically lacks intrinsic lymphatic tissue. Most instances of renal involvement occur secondary to systemic hematological malignanci es, with diffuse large B-cell lymphoma. (DLBCL) being the most common histological subtype encountered in clinical practice. The pathogenesis is hypothesized to involve the migration of malignant lymphoid cells from the renal capsule or the recruitment of lymphoid tissue during chronic inflammatory states.

Case report

A 72-year-old female who presented with a five-day history of right flank pain and progressive systemic edema affecting the face, eyelids, and lower extremities. Clinical examination was notable for persistent nausea and vomiting, while laboratory findings revealed severe renal impairment, characterized by hyponatremia (129 mEq/L), hyperkalemia (6.0 mEq/L), a BUN of 71 mg/dL, and a serum creatinine of 6.6 mg/dL. Initial abdominal CT imaging demonstrated bilateral renal enlargement with associated perinephric fat stranding. Although anatomical imaging suggested malignancy, F-FDG PET/CT was crucial in revealing the full extent of the disease, identifying intense tracer uptake in the right kidney and para-aortic lymph nodes, alongside multiple focal skeletal lesions. A subsequent percutaneous biopsy of the right renal cortex confirmed dense lymphocytic infiltration, establishing a definitive pathological diagnosis of DLBCL. Despite intensive clinical intervention, the patient succumbed to respiratory failure within one month of presentation.

Conclusion

Renal lymphoma should be the first consideration in patients presenting with bilateral renal enlargement and acute kidney injury. F-FDG PET/CT transcends the limitations of anatomical imaging by providing quantitative metabolic data that distinguishes lymphoma from other renal masses and identifies occult systemic involvement. As demonstrated in this case, the ability of PET/CT to detect skeletal lesions was essential for accurate staging and informing the terminal prognosis. Early recognition through metabolic imaging remains the most critical factor in guiding biopsy and initiating life-saving systemic therapy.

壁報論文 臨床組

PC-059

原著論文 臨床治療或診療合一

Early Post-Treatment Lu-177-PSMA Imaging: A Potential Biomarker of Treatment Response and Survival in Metastatic Prostate Cancer Department of Nuclear Medicine, Koo Foundation Sun Yat-Sen Cancer Center, Taipei, Taiwan

[1]李佩瑛, [1]黃玉儀, [1]黃柏濤

[1]和信醫院

發表者 李佩瑛

Keywords 分子影像

Background

Post-treatment Lu-177-PSMA imaging performed early in the treatment course may provide an early indicator of treatment effectiveness. But its relationship with biochemical response and clinical outcomes remains incompletely characterized. This study evaluated whether early changes in post-treatment Lu-177-PSMA imaging response are associated with PSA change, PSA-PFS, and OS.

Method

Twenty-three patients with metastatic prostate cancer treated with at least two cycles of 177Lu-PSMA were retrospectively evaluated. Imaging response between cycles 1 and cycle 2 was categorized as partial response (PR) and non-PR. Percentage PSA change was calculated between PSA before treatment to PSA at 12 weeks after the first treatment or before cycle 3. PSA50 response was defined as a ≥50% reduction in PSA. PSA-PFS was defined as the interval from first Lu-177-PSMA treatment to confirmed PSA progression according to PCWG3 criteria or death, whichever occurred first. Associations between imaging response and PSA response were assessed using Fisher’s exact and Mann–Whitney tests. Kaplan–Meier and log-rank analyses were performed for PSA-PFS and OS.

Results

Ten of 23 patients (43.5%) demonstrated PR on early post-treatment imaging. PSA50 response occurred in 8/10 (80.0%) patients with imaging PR compared with 1/13 (7.7%) patients with non-PR imaging (p = 0.0007). Patients with imaging PR also demonstrated greater PSA reduction, with a median PSA decrease of 78.3%. Median PSA reduction was 0.8% in the non-PR group (p = 0.00014). Patients with imaging PR had longer median PSA-PFS than those with non-PR imaging (349 vs 136 days; log-rank p = 0.170). Median OS was not reached in the imaging PR group, compared with 508 days in the non-PR group (p = 0.094). Nine patients achieved PSA50 response. Median PSA-PFS was 355 days in PSA50 responders versus 136 days in non-responders (log-rank p = 0.106; HR 0.47, 95% CI 0.19–1.19). Median OS was not reached in PSA50 responders versus 508 days in non-responders (log-rank p = 0.073; HR 0.31, 95% CI 0.08–1.19).

Conclusion

Early changes in post-treatment Lu-177-PSMA imaging were associated with PSA decline and PSA50 response. Imaging PR and PSA50 response both demonstrated trends toward longer PSA-PFS and OS, although they did not reach statistical significance. Early post-treatment Lu-177-PSMA imaging and PSA kinetics may provide complementary early indicators of treatment outcome, and merit validation in larger cohorts.

壁報論文 臨床組 **PC-060**

文獻綜述 臨床診斷

Diagnostic Yield of 18F-FDG PET/CT versus Contrast-Enhanced CT in Critically Ill Patients with Occult Sepsis: A Systematic Review

[1]吳俊昌, [1]林詠喻, [1]陳慕凡

[1]台北馬偕醫院

發表者 吳俊昌

Keywords 分子影像 | 造影儀器

Background

Sepsis and septic shock remain leading causes of ICU mortality. Delayed source control worsens outcomes. However, the primary focus often stays occult despite extensive work-up. Contrast-enhanced CT (CECT) is the current standard of care. Yet it covers only targeted anatomical regions, frequently overlooks non-cavitary infections, and risks contrast-induced kidney injury. Whole-body 18F-FDG PET/CT(18F-fluorodeoxyglucose positron emission tomography/computed tomography) offers a metabolic alternative. By detecting inflammatory activity before structural changes appear, it may outperform CECT, though direct comparisons remain scarce.

Literature review

Following PRISMA guidelines, we searched PubMed/MEDLINE, Embase, the Cochrane Library, and Web of Science. Search terms will combine population ("ICU" OR "critically ill" OR "sepsis"), intervention ("FDG-PET/CT"), and comparator ("contrast-enhanced CT" OR "CECT"). The diagnostic performance of 18F-FDG PET/CT is well established. A 2026 meta-analysis of 8 studies (228 patients) reported 91% sensitivity and 78% specificity for infectious foci (Treglia et al., 2026). In the largest study to date, FDG-PET/CT identified an infection focus in 91% of patients and altered clinical management in over half (van Leer et al., 2025). However, no study has directly compared FDG-PET/CT against CECT within the same patient cohort. Without head-to-head evidence, clinicians lack clear guidance on whether FDG-PET/CT should replace or complement CECT in routine ICU practice. This review is the first to systematically synthesize the comparative evidence between both modalities.

壁報論文 臨床組 **PC-061**

經驗分享 臨床診斷

利用核醫分流/腹膜腔/胸膜腔掃描檢查腹膜透析滲漏之案例分享

[1]童惠珊

[1]童綜合醫院

Keywords 腹膜透析 | 核醫分流 / 腹膜腔 / 胸膜腔掃描

Background

腹膜透析是可以不用到醫療院所且讓洗腎患者更便於居家作業的方式，替代腎臟進行毒素與水分交換，透過導管注入透析液，將體內廢物及水分在腹腔透析，相較血液透析大幅降低感染風險，不過仍有腹膜炎或橫膈膜破洞之風險存在。本篇案例是一位腹膜透析患者在家進行透析時發現洗出的透析液變少且下腹部腫脹，懷疑可能是腹腔的透析液滲漏到腹股溝而導致。

Method

本案例為一名 70 歲男性慢性腎臟疾病患者，因在家腹膜透析時發現洗出的透析液變少且下腹部腫脹前來就醫，醫生懷疑鼠蹊部或陰囊處有滲漏情形，便來安排核醫分流 / 腹膜腔 / 胸膜腔掃描，使用藥物為Tc-99m DTPA 5mCi，儀器型號為GE Discovery NM/CT 670ES、LEHRS準直儀。檢查流程先請患者平躺檢查檯，將透析管接上並將體內舊的透析液流出，再把DTPA藥物注射進全新的透析液，搖晃透析液使藥物均勻分布後掛上點滴架讓透析液注入患者體內，等全部透析液都注入體內後開始收集影像，收集影像時間點為第 10、20、30 和第 60 分鐘，影像位置為CHEST、ABD和PELVIS，count收 500kcts，最後針對病灶區加照SPECT/CT影像。影像由經驗豐富的兩位核子醫學專科醫師進行判讀分析，根據影像學特徵來找出滲漏的位置。

Results

在檢查第 10 分鐘時發現腹部有放射性聚集，第 20 分鐘時左側腹股溝管處有大量的藥物攝取，收集完第 60 分鐘影像後，利用SPECT/CT影像確認左側腹股溝管 / 腹壁下緣靠近恥骨聯合左上方的位置確實有滲漏的情形。

Conclusion

本案例顯示，Tc-99m DTPA 分流 / 腹膜腔 / 胸膜腔掃描對於檢查腹膜透析病人滲漏情形非常有臨床價值，其應用在評估人工分流管通暢度（Shunt Patency）也可以診斷橫膈膜缺損與異常滲漏和導引治療與外科手術規劃。與其他檢查影像相比，像是超音波、電腦斷層和磁振造影，核醫檢查對於微小簍管有極高的敏感度，也可以提供液體確實的流向與通暢度，且低劑量和無對比劑過敏風險。

壁報論文 臨床組 **PC-062**

個案報告 臨床診斷

18F-rhPSMA-7.3 正子造影偵測攝護腺癌局部復發並導引放射治療：一病例報告

[1]張佳琪, [1]曾能泉

[1]童綜合醫院

發表者 張佳琪

Keywords 分子影像

Background

攝護腺癌治療後若出現攝護腺特異性抗原（prostate-specific antigen, PSA）再次上升，如何準確定位復發病灶，對後續治療策略至關重要。傳統 99mTc-MDP 全身骨骼造影主要用於骨轉移評估，對攝護腺床或膀胱頸等局部軟組織復發的偵測能力有限。18F-rhPSMA-7.3 可藉由前列腺特異性膜抗原（prostate-specific membrane antigen, PSMA）表現提供高對比之分子影像資訊，有助於生化復發患者之病灶定位。本病例著重呈現 18F-rhPSMA-7.3 正子造影在傳統骨骼造影未能提供局部復發線索時，發現疑似攝護腺床／膀胱頸復發病灶，並進一步導引局部放射治療之臨床價值。

Case report

本病例為 65 歲男性，於 2020 年因 PSA 升高 (10.270 ng/dL)接受攝護腺全切除手術治療，治療後 PSA 下降至背景值 (<0.008 ng/dL)並持續追蹤。2025 年追蹤期間 PSA上升 (0.186 ng/dL)，考慮生化復發可能。病患同時接受傳統 99mTc-MDP 全身骨骼造影，未發現明顯骨骼轉移病灶，故後續接受 18F-rhPSMA-7.3 PET/CT 檢查，於攝護腺床／膀胱頸鄰近區域發現局部異常 PSMA 攝取 (SUVmax 7.0)，高度懷疑局部復發。臨床團隊依據此分子影像結果，轉介放射腫瘤部門針對攝護腺床進行放射線治療；治療後追蹤顯示 PSA明顯下降至接近背景值 (<0.008 ng/dL)，支持該局部 PSMA 陽性病灶具有重要臨床相關性，亦顯示 rhPSMA PET/CT 對治療靶區選擇與療效評估具有實際影響。

Conclusion

本病例顯示，對於攝護腺癌治療後 PSA 再次上升之患者，18F-rhPSMA-7.3 PET/CT 可補足傳統骨骼造影僅著重骨轉移評估的限制，進一步定位攝護腺床／膀胱頸等局部復發病灶。更重要的是，本病例中 rhPSMA 所發現之疑似局部復發病灶直接影響後續放射治療決策，且治療後 PSA 明顯下降至接近背景值，形成「影像定位 — 治療導引 —生化反應」之臨床證據鏈。18F-rhPSMA-7.3 正子造影因此不僅具有生化復發病灶偵測價值，亦可在個別化治療規劃與療效追蹤中提供關鍵資訊。

壁報論文 臨床組 PC-063

個案報告 臨床診斷

Neurological sign in a breast cancer patient with multiple bony metastasis on 18F-FDG PET/CT: A Case Report

[1]蔡季蓉, [1]江孟庭, [1]蔡雅茹, [1]洪進昇

[1]北醫附設醫院

發表者 蔡季蓉

Keywords 有趣影像 | 分子影像

Background

The role of 18F-FDG PET/CT in breast cancer patient with neurological sign might be limited due to high normal brain tissue uptake. However, if we can distinguish the neurological disorder is originated from which organ by FDG PET, unnecessary anxiety or urgent examination could be omitted. We report a case of breast cancer history with new multiple bony metastasis on FDG PET/CT who presented with unilateral tongue deviation.

Case report

A female patient had history of invasive ductal carcinoma in right breast and underwent partial mastectomy 7+ years ago. The final stage was pT2N1M0. During regular follow up, the patient developed hip pain, the MR showed metastatic lesions involving the vertebral bodies and the spinous processes of the thoracolumbosacral spine. The following FDG-PET depicted multiple bones/bone marrow, left supraclavicular, left mediastinum LNs and LUL metastases. At the same time, the patient developed the symptom of right-sided tongue deviation when sticking out. Initially, the clinical physician worried about stroke sign, and thus arranged brain CT, but brain CT is negative, then arranged brain MRI. The radiologist noticed that patient had tongue deviation history, so he especially mentioned metastatic lesions in right clivus with involvement of right hypoglossal canal in the report. Multidisciplinary discussion is very important, when we radiologist/nuclear medicine physician realized the clinical request, we could focus on if the tumor involved area cause possible nerve injury, such as hypoglossal canal/nerve in multiple bone metastases cases. The patient’ s symptom relieved after taking cdk4/6 inhibitor (Kisqali) as treatment of advanced breast cancer.

Conclusion

We describe a case of breast cancer with multiple bone metastases on FDG PET/CT who presented with tongue deviation associated with skull base metastasis. It is easily ignored the linkage between neurological sign and bone metastases in cancer patients. The FDG-PET whole body imaging provides initial information to recognize tumor location and possibly related symptoms.

壁報論文 臨床組 **PC-064**

原著論文 臨床診斷

不同排程系統對於心肌血流灌注造影檢查未完成率之影響

[1]楊郁茹, [1]林莉芳, [1]龔瑞英, [1]蔡世傳, [1]林宜瀞

[1]臺中榮民總醫院

發表者 楊郁茹

Keywords 心肌血流灌注造影 | 排程系統 | 檢查未完成率

Background

核醫心肌血流灌注造影檢查使用之放射性藥物具有物理衰減及使用時效性，檢查排程除須考量病人預約需求，亦須配合藥物訂購及每日檢查量。過去本單位採人工排程，由人員進行衛教後安排檢查日期，2023 年起配合智慧醫療政策改採電腦排程。本研究探討不同排程系統對心肌血流灌注造影檢查未完成率、未完成原因及當日遞補情形之影響。

Method

本研究採回溯性研究，收集 2020 年至 2025 年心肌血流灌注造影檢查資料，包括總預約人數、未完成人數、未完成原因及當日人工遞補人數。「未完成」定義為已完成檢查預約，但因未到、取消或其他病人因素而未依原排程完成檢查者。比較 2020 至2022 年人工排程與 2023 至 2025 年電腦排程之未完成率、未完成原因及當日人工遞補率；另考量 2020 年為COVID-19疫情初期，可能影響病人就醫行為，排除 2020 年後再次進行比較。組間比例採卡方檢定或Fisher's exact test，以$p<0.05$為統計顯著。

Results

2020至 2022 年人工排程未完成率為 4.19%，2023 至 2025 年電腦排程未完成率為 4.14%，兩組無顯著差異（$p=0.897$）。排除 2020 年後，2021 至 2022 年人工排程共 4,256 人，未完成 123 人（2.89%）；2023 至 2025 年電腦排程共 7,121 人，未完成 295 人（4.14%），電腦排程期間未完成率顯著較高（$p<0.001$）。未完成原因中，當日無故取消比例由 13.82% 增至 23.73%（$p=0.023$），因病人不適取消由 36.59% 降至 24.07%（$p=0.009$），其餘原因無顯著差異。未完成後當日人工遞補率由 31.71% 提升至 50.85%（$p<0.001$）。

Conclusion

整體而言，人工與電腦排程之檢查未完成率無顯著差異；排除COVID-19疫情初期資料後，電腦排程期間未完成率較高，但當日人工遞補率亦顯著提升。結果顯示電腦排程未降低檢查未完成情形，未來除優化資訊化排程外，仍應強化檢查前提醒及未完成個案管理，以降低未完成率並提升檢查資源利用效率。

壁報論文 臨床組 **PC-065**

個案報告 臨床診斷

Pituitary Stalk Metastasis from Breast Cancer Presenting as Panhypopituitarism: The Role of 18F-FDG PET/MR

[1]李哲皓

[1]臺北榮民總醫院

Keywords 造影儀器 | 有趣影像

Background

Pituitary metastasis is rare and may mimic inflammatory pituitary disease. We report breast cancer metastasis to the pituitary stalk causing panhypopituitarism, central diabetes insipidus, and visual disturbance, with 18F-FDG PET/MR aiding recognition of metastatic disease.

Case report

A 55-year-old woman with a history of treated left breast cancer developed panhypopituitarism and central diabetes insipidus. MRI initially showed an enhancing pituitary stalk lesion suspected to represent hypophysitis. Despite steroid pulse therapy, the lesion enlarged, causing bitemporal hemianopia and diplopia. 18F-FDG PET/MR revealed a 3.1-cm intensely hypermetabolic hypothalamic/pituitary stalk mass (SUVmax 25.46) without other FDG-avid lesions. Endoscopic biopsy demonstrated metastatic carcinoma, with immunohistochemistry positive for CK7, GATA3, and TRPS1, supporting breast origin.

Conclusion

Pituitary stalk metastasis should be considered in patients with malignancy and rapidly progressive pituitary dysfunction. Progressive enlargement despite corticosteroid therapy and intense 18F-FDG uptake raised suspicion for metastasis. 18F-FDG PET may aid differentiation of indeterminate pituitary stalk lesions and detection of isolated metastatic disease.

壁報論文 臨床組 **PC-066**

統合分析 臨床診斷

Diagnostic Accuracy of 18F-FET PET in Brain Gliomas: A Meta-Analysis Stratified by Tumor Grade and Disease Status

[1]何宗穎, [2]郭心柔, [2]黃雅庭

[1]基隆長庚紀念醫院
[2]普瑞默生物科技
[3]羅東聖母醫院

發表者 何宗穎

Keywords 分子影像 | 18F-FET | Glioma

Background

Accurate diagnostic characterization of brain gliomas using O-(2-[18F]fluoroethyl)-L-tyrosine(18F-FET) PET imaging is vital for clinical management. We meta-analyzed the overall diagnostic accuracy of 18F-FET PET and evaluated performance differences across disease statuses and WHO tumor grades.

Method

A comprehensive and systematic search of the databases of PubMed/MEDLINE and Cochrane Library was performed to retrieve original articles published until June 25, 2026. Two authors independently reviewed the titles and abstracts of the retrieved articles based on the inclusion and exclusion criteria. Pooled sensitivity, specificity, positive predictive value (PPV), and negative predictive value (NPV) with 95% confidence intervals (CIs) were calculated using Wilson score methods across clinical subgroups.

Results

Twenty-five unique studies encompassing 1,212 patients (57 cohorts; cohort median age: 44.2 years [range across cohorts: 12.6–59.0 years]) were included. Overall performance of 18F-FET was a pooled sensitivity of 78.97% (95% CI: 76.84–80.97%), specificity of 83.18% (79.34–86.52%), PPV of 94.35% (93.05–95.42%), and NPV of 48.99% (45.64–52.36%). Subgroup analysis by status demonstrated higher sensitivity for recurrent glioma/treatment-related change (90.02%) than initial diagnosis (86.42%), with equivalent specificities (~83.5%) and superior NPV in recurrence (77.22% vs. 61.48%). Stratification by WHO grade revealed higher sensitivity and specificity in HGG (91.14% and 84.04%) than LGG (82.65% and 66.67%).

Conclusion

18F-FET PET provides robust diagnostic accuracy in brain gliomas. It exhibits higher sensitivity and NPV in evaluating tumor recurrence over initial diagnosis, as well as superior diagnostic performance in high-grade over low-grade gliomas.

壁報論文 臨床組　　**PC-067**

經驗分享　臨床治療或診療合一

同位素治療中心輻射廢棄物管理經驗分享

[1]吳忠順, [1]蘇詩琪, [1]諶鴻遠

[1]高雄榮民總醫院

發表者　吳忠順

Keywords　輻射防護 | 智慧醫療 (ML/DL/LLM)

Background

本科同位素治療中心於病患出院後先由輻射防護人員偵測四周環境輻射，將輻射廢棄物放置本科核廢室後，再由清潔人員進行環境整理。核廢室放置層架提供一般輻射廢棄物置放，另有一台大型冷凍冰箱提供廚餘及容易產生異味或病媒蚊等之輻射廢棄物置放，因空間有限，室內亦放置一台廢水排放控制系統，在核廢室內狹小的空間裡，如何減少輻射廢棄物堆積，是管理上的一大課題，本文分享近 2 年半來對於輻射偵測、輻射廢棄物之收集及丟棄等經驗，提供大家參考。

Method

病患入住前先以包膜或除汙紙黏貼於病患可能接觸的地方及浴室外地板及浴室內地面等處，垃圾袋則依照是否接觸體液分為一般及輻射廢棄物垃圾，並於入住時由護理師衛教。使用輻射偵測器背景值約為 0.1 微西弗 / 小時，偵測物表面大於 0.3 微西弗/ 小時視為汙染。廢棄物之偵測及收集步驟依序為: 將偵檢器放置於背景值區域 (例如前室)，先偵測一般垃圾桶，並依偵測結果分為無汙染 (小於 0.3 微西弗 / 小時)、低輻射汙染 (0.3-2 微西弗 / 小時) 及高輻射汙染 (大於 2 微西弗 / 小時) 作為後續收集廢棄物之依據，依序將病房內之包膜及除汙紙撕下後偵測，並依輻射強度放置在以上三個區域，最後於完成廢棄物收集打包後再做最後之偵測，並將偵測結果輸入計算表後計算可丟棄日期，再於廢棄垃圾袋上黏貼具有核種種類、封裝日期、輻射劑量值及預棄日期等資訊之貼紙，並按月份依序放置於層架及冷凍冰箱，並於隔月月中統一將上個月欲清除之輻射廢棄物偵測後交由清潔人員處理。

Results

偵測結果發現輻射廢棄物垃圾桶具輻射之比例高達 99.1%，誤將輻射廢棄物丟入一般垃圾桶之比例為 10.4%，另其他易汙染地方為浴室內馬桶和洗手台區域除汙紙 (56.8%)、枕頭上除汙紙 (5.4%)、書桌除汙紙 (4.2%)。進一步分析結果發現浴室內馬桶區域除汙紙高於 2 微西弗 / 小時之比例只有 7.6%，枕頭和書桌除汙紙則均未超過，輻射廢棄物垃圾桶和其他廢棄物之輻射強度平均為 84 微西弗 / 小時。小於 2 微西弗 / 小時之廢棄物需置放之時間不超過 3 個半衰期，84 微西弗 / 小時之廢棄物需置放之時間為 8.5個半衰期，I-131(半衰期 8 天) 或Lu-177(半衰期 6.65 天) 之置放時間需延長至少 5.5 個半衰期 (36-45 天)。

Conclusion

使用同位素治療中心之病患所產生之輻射廢棄物其輻射強度差異極大，病患入住前給予詳細之說明，可降低病患殘留之輻射汙染物。收集時若只依輻射強度是否大於0.3 微西弗 / 小時就將廢棄物統一打包，容易造成輻射廢棄物之體積及輻射強度過高而須放置時間延長，故於收集時若能再將輻射廢棄物區分出低輻射，可大量減少核廢室堆放之空間與時間。廢棄物置放時若依月份放置後再於隔月月中統一處理，可大幅降低輻防人員之處理時間及接觸時之輻射劑量，也可避免封裝時測量產生的誤差及降低廢棄物之輻射強度，達到合理抑低及管理之目的。

壁報論文 臨床組 PC-068

文獻綜述 臨床診斷

Diagnostic Accuracy of Tc-99m-MAG3 Renal Scintigraphy for Detecting Acute Rejection in Kidney Transplant Recipients: A Systematic Review

[1]吳俊昌, [1]張鈺婕, [1]馬郁庭

[1]台北馬偕醫院

發表者 吳俊昌

Keywords 分子影像 | 造影儀器

Background

Kidney transplantation is the top treatment for end-stage renal disease, but acute rejection still threatens long-term graft survival. While Banff-graded biopsy remains the gold standard, it is invasive and prone to sampling errors. This makes it hard to distinguish rejection from acute tubular necrosis (ATN) during early graft dysfunction. Dynamic Tc-99m-mercaptoacetyltriglycine(MAG3) scans offer a non-invasive solution. Because MAG3 is cleared efficiently through renal tubules, it provides precise curves and indices to track perfusion and clearance. Ideally, these metrics can catch early rejection before serum creatinine even rises. The logic is simple. Rejection reduces graft blood flow much more severely than ATN does, allowing doctors to tell them apart. Yet, despite forty years of clinical research, the diagnostic accuracy of MAG3 for rejection has never been systematically synthesized.

Literature review

Following PRISMA guidelines, we searched PubMed/MEDLINE, EMBASE, and the Cochrane Library to systematically evaluate the fragmented evidence on MAG3 scintigraphy for diagnosing acute rejection. In 1993, Carmody et al. found that sequential MAG3 scans flagged most rejection episodes early. However, this sensitivity came at a cost, as the scans were nonspecific and the perfusion index offered no diagnostic value. Other studies reported the opposite trade-off: one evaluation of the Hilson index found a sensitivity of only 26% against 82% specificity, failing to separate rejection from ATN. Even a newer 2-minute uptake parameter fared little better: abnormal scans yielded a positive predictive value of just 9%, again failing to distinguish rejection from severe ATN. Head-to-head tracer comparisons add further disagreement: Aktaş et al. (2006) found that MAG3 and DTPA performed differently in chronic cases, a divergence that may be technical rather than biological, since the classic perfusion index itself carries a 39% error rate on repeat testing and 53% between patients. Despite forty years of research, MAG3 lacks a unified diagnostic threshold, with interest now pivoting toward PET imaging.

壁報論文 臨床組 **PC-069**

文獻綜述 臨床診斷

Diagnostic Accuracy, Advantages, and Limitations of Brain Death Scintigraphy Compared to Computed Tomography Angiography in Confirming Death by Neurological Criteria: A Systematic Review

[1]吳俊昌, [1]蘇楚涵, [1]楊斯閔, [1]林劼

[1]台北馬偕醫院

Keywords 分子影像 | 造影儀器

Background

Clinical exam is the gold standard for determining death by neurological criteria (DNC). But ancillary blood-flow tests are needed when the apnea test is unsafe, or when sedation, hypothermia, or trauma limit the exam. Brain death scintigraphy (BDS) measures tissue-level blood flow via 99mTc-HMPAO or ECD SPECT, unaffected by sedatives. Computed tomography angiography (CTA) checks large-vessel flow instead and it is fast and widely available. Guidance is divided. The 2020 World Brain Death Project and 2023 AAN criteria accept scintigraphy and catheter angiography, but not CTA, citing weak evidence. However, many countries use CTA routinely. No review has compared their accuracy, craniectomy-related false negatives, and practical factors like transport time and donor kidney risk. This review fills that gap.

Literature review

Following PRISMA guidelines, we searched PubMed/MEDLINE, EMBASE, the Cochrane Library, and Web of Science from inception to 2026, without language restriction. HMPAO/ECD scintigraphy has long matched four-vessel angiography closely with pooled sensitivity is near 88% for perfusion SPECT and up to 98% for radionuclide angiography. False negatives mostly reflect scalp tracer activity, and SPECT is hard to perform in unstable patients. CTA accuracy is criterion-dependent. Sensitivity rises from about 67% to 96% as scoring scales shrink from 10-point to 4-point criteria (Sawicki et al., 2014). A 2014 meta-analysis of 12 studies found sensitivity between 85% and 99%, but specificity stayed poorly defined (Kramer & Roberts, 2014). Craniectomy often causes false-negative or unclear CTA results, since skull defects let some vessels stay faintly visible after arrest. Revised scoring adding infratentorial criteria has been proposed (Marchand et al., 2016) and direct comparisons are rare. One paired study found CTA reached 86% sensitivity and 100% specificity against scintigraphy, with disagreement confined to craniectomy patients and no clear renal harm (Berenguer et al., 2010); a later quantitative method raised sensitivity to 97% (Suarez-Kelly et al., 2015). Overall, evidence remains fragmented and single-modality, supporting the need for a pooled comparison.

壁報論文 臨床組 **PC-070**

個案報告 臨床診斷

18F-FDG PET/CT Findings of Heterotopic Ossification Mimicking Malignancy

[1]沈淑禎

[1]聖馬爾定醫院

Keywords 分子影像

Background

Heterotopic ossification (HO) is the formation of mature bone within soft tissues outside the normal skeletal system. During the active or immature phase, HO may demonstrate increased metabolic activity and tracer uptake on nuclear medicine imaging, potentially mimicking malignancy or metastatic disease. We present a case of 18F-FDG-avid HO detected on PET/CT in a patient with a history of metastatic lung cancer, highlighting the potential role of nuclear medicine imaging in differentiating HO from malignant lesions and assessing its maturity.

Case report

A 54-year-old woman with a history of lung cancer and multiple bone metastases involving the thoracic spine and sacrum developed progressive paraparesis that subsequently progressed to paraplegia. She received radiotherapy and targeted therapy. During follow-up, a bone scan demonstrated abnormal tracer uptake in the right hip suspicious of bone metastasis . She was subsequently referred to our PET center for 18F-FDG PET/CT to evaluate for possible recurrence or additional bone metastasis.

PET/CT demonstrated peripheral calcification within the soft tissues surrounding the right hip, accompanied by increased 18F-FDG uptake. The lesion was located outside the normal bony structures, and its imaging appearance was considered more compatible with heterotopic ossification than osseous metastasis. The increased uptake on both bone scintigraphy and ^18F-FDG PET/CT suggested active, immature HO, reflecting ongoing osteoblastic and inflammatory activity.

Conclusion

A hybrid SPECT/CT or PET/CT may help distinguish heterotopic ossification from bone or soft-tissue metastasis and prevent misinterpretation of an FDG-avid lesion as recurrent or metastatic malignancy. Furthermore, the combination of bone scintigraphy and 18F-FDG PET/CT may provide a noninvasive approach to evaluating the activity and maturity of HO, with higher tracer uptake reflecting an active or immature phase and decreasing activity while maturation.

壁報論文 臨床組 **PC-071**

個案報告 臨床診斷

Incidental Detection of Early-Stage Ovarian Cancer on 18F-FDG PET/CT During a Health Examination

[1]沈淑禎
[1]聖馬爾定醫院

Keywords 分子影像

Background

Ovarian cancer is difficult to detect at an early stage because there is no established population-based screening program for asymptomatic women, and early disease often produces few or nonspecific symptoms. Incidental malignancies may occasionally be identified during whole-body 18F-FDG PET/CT performed as part of a health examination. This case highlights an asymptomatic ovarian cancer detected incidentally by PET/CT despite a normal serum CA-125 level.

Case report

A 62-year-old asymptomatic woman underwent whole-body 18F-FDG PET/CT during a routine health examination. PET/CT revealed a large cystic adnexal mass with a hypermetabolic solid component, ovarian malignancy is highly suspected, R/O ovarian cystadenocarcinoma . Her serum CA-125 level was 7.3U/mL, within the normal range. Gynecologic ultrasonography subsequently demonstrated a pelvic mass measuring approximately 9.9 cm. Because of the suspicious imaging findings, further gynecologic evaluation was arranged. Approximately two weeks later, the patient underwent debulking surgery. Histopathological examination revealed high-grade serous carcinoma. The tumor was classified as pT1aN0, with no lymphovascular or perineural invasion. The final pathological stage was pT1aN0M0, corresponding to FIGO stage IA.

Conclusion

This case demonstrates the potential clinical value of incidental findings on 18F-FDG PET/CT during health examinations. Although PET/CT is not a stand-alone screening tool for ovarian cancer, the combination of a large cystic adnexal lesion and a hypermetabolic solid component can provide an important clue to an otherwise occult malignancy. Notably, the patient had no suggestive symptoms and a normal CA-125 level, underscoring the limitations of relying solely on clinical symptoms or serum tumor markers for early detection. Prompt recognition of the abnormal PET/CT finding led to further evaluation and definitive surgical diagnosis while the disease was still at an early pathological stage. Careful evaluation of incidental adnexal abnormalities on whole-body 18F-FDG PET/CT may facilitate the detection of clinically occult ovarian malignancy. In asymptomatic patients, particularly when a cystic adnexal mass contains a hypermetabolic solid component, appropriate gynecologic evaluation should be considered even when the CA-125 level is within the normal range. Early recognition may allow timely treatment before progression to advanced-stage disease.

壁報論文 臨床組 **PC-072**

統合分析 臨床診斷

Head-to-head Comparative Meta-analysis of 18F-FET PET vs. MRI and Other Imaging Modalities in Brain Gliomas

[1]鄭如伶, [2]黃雅庭, [1]張雁翔

[1]高雄長庚醫院

[2]普瑞默生物科技

發表者 鄭如伶

Keywords 18F-FET | Glioma | Recurrence

Background

Conventional imaging modalities often present diagnostic limitations in brain gliomas. We conducted a head-to-head comparative meta-analysis evaluating the diagnostic odds ratios (ORs) of PET against magnetic resonance imaging (MRI), PET, and 5-aminolevulinic acid (5-ALA) fluorescence.

Method

A comprehensive and systematic search of the databases of PubMed/MEDLINE and Cochrane Library was performed to retrieve original articles published until June 25, 2026. Two authors independently reviewed the titles and abstracts of the retrieved articles based on the inclusion and exclusion criteria. Pooled ORs and corresponding -values for sensitivity, specificity, PPV, and NPV were calculated using inverse-variance random/fixed-effects models.

Results

Paired head-to-head diagnostic studies evaluating 18F-FET PET alongside alternative modalities in glioma patients (15 studies, 507 patients; median age: 49 years [range: 37-59.0 years]) were synthesized. In direct comparison with MRI, 18F-FET PET demonstrated significantly higher overall diagnostic odds for sensitivity (pooled OR = 4.17 [95% CI: 2.61–6.66],), specificity (OR = 4.69 [1.50–14.70],), and NPV (OR = 4.09 [1.72–9.69],). Stratified analysis revealed remarkable sensitivity advantages of 18F-FET PET over MRI in non-enhancing low-grade gliomas (OR = 12.62,) and high-grade gliomas (OR = 5.67,), as well as superior specificity in differentiating tumor recurrence from post-treatment changes (OR = 6.04,).Compared with 18F-FEG PET, 18F-FET PET exhibited vast superiority in diagnostic sensitivity (OR = 7.65 [2.74–21.34],) and NPV (OR = 4.91 [1.38–17.41],), effectively overcoming high cortical background suppression. Additionally, 18F-FET PET achieved significantly superior sensitivity over 5-ALA fluorescence (OR = 3.80 [1.82–7.90],), while demonstrating equivalent diagnostic performance to other amino acid tracers 18F-FDOPA,11C-MET).

Conclusion

18F-FET PET offers statistically significant diagnostic superiority over MRI, 18F-FED, and 5-ALA. It represents a vital diagnostic tool for non-enhancing low-grade tumors and post-treatment recurrence differentiation.

壁報論文 臨床組 **PC-073**

個案報告 臨床診斷

Sternal Bone Metastasis from Prostate Cancer Mimicking Ectopic Parathyroid Tissue on Tc-99m-MIBI SPECT/CT

[1]丁意玲, [1]張雁翔

[1]高雄長庚醫院

發表者 丁意玲

Keywords 有趣影像 | 解剖學 /CT/MR | 造影儀器

Background

Technetium-99m methoxyisobutylisonitrile (Tc-99m-MIBI) scintigraphy is widely used for the preoperative localization of hyperfunctioning parathyroid tissue in patients with hyperparathyroidism. However, Tc-99m MIBI uptake is not specific to parathyroid tissue and may also occur in malignant lesions. We report an unusual case of a sternal bone metastasis from prostate cancer mimicking an ectopic parathyroid lesion on Tc-99m-MIBI scintigraphy, highlighting the diagnostic value of SPECT/CT.

Case report

A 73-year-old man with prostate cancer and known bone metastases was evaluated for hyperparathyroidism. Tc-99m-MIBI planar scintigraphy demonstrated persistent focal uptake in the left upper neck, suggestive of a parathyroid adenoma. Another focal area of MIBI uptake was observed in the upper chest, raising suspicion for ectopic parathyroid tissue. Subsequent Tc-99m-MIBI SPECT/CT localized the thoracic focus to the sternal manubrium rather than the mediastinum. Correlation with anatomical imaging and the patient’ s history confirmed the lesion as a sternal bone metastasis from prostate cancer.

Conclusion

This case demonstrates that non-parathyroid malignancies, including bone metastases, may show significant Tc-99m-MIBI uptake and mimic ectopic parathyroid tissue. SPECT/CT provides essential anatomical localization and facilitates differentiation between parathyroid lesions and other MIBI-avid abnormalities. Careful interpretation of MIBI scintigraphy in conjunction with SPECT/CT and clinical history can help prevent misinterpretation and unnecessary surgical intervention.

壁報論文 臨床組 **PC-074**

個案報告 臨床治療或診療合一

Feasibility and Personalized Dosimetry of [177Lu]Lu-DOTATATE Therapy in a Child with Relapsed High-Risk Neuroblastoma: The First Pediatric Case at Our Institution

[1]徐丞, [1]劉嘉儒, [1]盧孟佑, [1]陳怡潔, [1]羅美芳, [1]王淑貞, [1]鄭媚方

[1]臺大醫院

發表者 徐丞

Keywords 劑量學 (Dosimetry) | 定量分析 | 曝露劑量 (Exposure)

Background

Relapsed high-risk neuroblastoma carries a poor prognosis with limited therapeutic options. Somatostatin receptor (SSTR) expression provides a potential target for [177Lu]Lu-DOTATATE therapy. Although increasingly used in neuroendocrine tumors, its application in pediatric malignancy remains limited. We report our institution's first pediatric neuroblastoma case treated with [177Lu]Lu-DOTATATE, emphasizing treatment feasibility, renal protection, and post-therapy dosimetry.

Case report

A 9-year-old girl was diagnosed with stage M, MYCN non-amplified, high-risk left cervical neuroblastoma with bone and marrow metastases. Despite extensive multimodal therapy from 2022 to 2025 (including TPOG N2020 HR, proton therapy, anti-GD2, autologous stem cell transplantation, and DFMO), progressive disease persisted. In April 2026, [68Ga]Ga-DOTATATE PET revealed extensive SSTR-expressing osseous lesions (Krenning score 4). [177Lu]Lu-DOTATATE therapy was initiated on July 14, 2026, with an administered activity of 100 MBq/kg (total 2.53 GBq). LysaKare® (20 mL/kg) was co-infused for renal protection. The patient tolerated the therapy well, with transient fever on the first night post-infusion as the only adverse event; complete blood count at 2-week follow-up showed no evidence of hematologic toxicity. Dosimetry through serial post-therapy SPECT revealed a substantial mean tumor absorbed dose of 40.76 Gy. Mean absorbed doses were 18.95 Gy for kidneys (safely below the 23 Gy threshold), 6.02 Gy for bone marrow, 16.50 Gy for spleen, and 6.95 Gy for liver.

Conclusion

We demonstrated the feasibility of SSTR-targeted therapy for pediatric high-risk neuroblastoma. Integrating weight-based dosing, renal protection, and SPECT-based dosimetry enabled effective tumor irradiation with sparing critical organs. Patient-specific dosimetry remains essential to balance tumor control against marrow and renal toxicity, guiding subsequent treatment fractions.

壁報論文 臨床組 **PC-075**

個案報告 臨床診斷

Optimizing Tc-99m PYP Myocardial Imaging for ATTR-CM Diagnosis Through SPECT/CT Integration: A Case Report

[1]黃琪雯, [1]羅浚哲, [1]翁瑞鴻

[1]中山醫大附設醫院

發表者 黃琪雯

Keywords 造影儀器 | 解剖學 /CT/MR

Background

Technetium-99m pyrophosphate (Tc-99m PYP) myocardial scintigraphy has become an important noninvasive screening tool for transthyretin cardiac amyloidosis (ATTR-CM). However, planar imaging alone may be affected by residual blood-pool activity, rib overlap, soft-tissue attenuation, and differences in patient positioning, potentially leading to equivocal interpretation or false-positive findings. SPECT/CT provides three-dimensional anatomical localization and attenuation-corrected imaging, while quantitative analysis using the heart-to-contralateral lung (H/CL) ratio may provide additional objective support for visual interpretation. This case demonstrates the clinical value of integrating SPECT/CT with standardized quantitative analysis to improve the accuracy and consistency of Tc-99m PYP myocardial imaging.

Case report

A patient with heart failure with preserved ejection fraction (HFpEF) and left ventricular hypertrophy underwent Tc-99m PYP myocardial scintigraphy for evaluation of suspected cardiac amyloidosis. Three hours after tracer injection, anterior, left anterior oblique (LAO), and left lateral planar images were acquired, followed by SPECT/CT imaging with attenuation correction.

Visual interpretation was performed according to the Perugini grading system. For quantitative analysis, standardized regions of interest (ROIs) of identical size were placed over the myocardium and contralateral lung to calculate the H/CL ratio. The planar images demonstrated myocardial tracer uptake greater than rib uptake, corresponding to Perugini Grade 3, with an H/CL ratio of 1.77.

However, planar imaging alone was potentially confounded by overlapping structures and residual blood-pool activity. SPECT/CT demonstrated that the abnormal radiotracer accumulation was clearly localized within the myocardial wall, helping to exclude residual blood-pool activity and skeletal overlap. The agreement between SPECT/CT localization, visual grading, and quantitative H/CL analysis increased diagnostic confidence and improved the reproducibility of image interpretation.

Conclusion

This case demonstrates that technical optimization of Tc-99m PYP myocardial scintigraphy can substantially improve the assessment of suspected ATTR-CM. Integration of SPECT/CT with a standardized H/CL ratio measurement provides complementary anatomical and quantitative information, helping to reduce potential false-positive interpretations and interobserver variability. A standardized imaging and quantitative workflow may therefore enhance image quality control and diagnostic confidence in cardiac amyloidosis evaluation. These findings also highlight the important role of radiologic technologists in image acquisition, quality assurance, and quantitative analysis, as precise technical execution directly contributes to the quality of clinical decision-making.

壁報論文 臨床組 **PC-076**

個案報告 臨床診斷

18F-FDG PET/CT for Differentiating Hypopharyngeal and Cervical Esophageal Cancer: Two Case Reports

[1]黃琪雯, [1]羅浚哲, [1]翁瑞鴻

[1]中山醫大附設醫院

發表者 黃琪雯

Keywords 解剖學 /CT/MR

Background

Accurate identification of the primary tumor site is essential for cancer staging, treatment planning, and prognosis. Hypopharyngeal and cervical esophageal cancers are anatomically adjacent and may share similar histological features, making differentiation challenging when a tumor extends across both regions. Because the staging systems, treatment strategies, prognosis, and cancer registration differ between these two malignancies, accurate determination of the primary site is clinically important. 18F-FDG PET/CT provides both metabolic and anatomical information and may help delineate the extent of tumor involvement and identify the most likely primary site. This report presents two cases demonstrating the clinical value of 18F-FDG PET/CT in differentiating hypopharyngeal cancer from cervical esophageal cancer.

Case report

Case 1:

A 64-year-old man presented with dysphagia. Gastroscopy revealed an esophageal lesion, and biopsy demonstrated squamous cell carcinoma. 18F-FDG PET/CT was performed for pretreatment staging. The imaging demonstrated extensive hypermetabolic involvement of the posterior hypopharyngeal wall, postcricoid region, prevertebral fascia, and upper cervical esophagus, with multiple regional lymph node metastases. The extent of tumor involvement was greater in the hypopharyngeal region than in the esophagus, suggesting a hypopharyngeal primary with esophageal invasion. Subsequent direct laryngoscopic examination confirmed the diagnosis of hypopharyngeal cancer.

Case 2:

A 64-year-old man presented with throat pain and was pathologically diagnosed with hypopharyngeal carcinoma. 18F-FDG PET/CT was performed for pretreatment staging and demonstrated hypermetabolic tumor involvement extending from the hypopharynx through the postcricoid region, prevertebral fascia, and cervical esophagus, accompanied by multiple hypermetabolic right cervical lymph nodes consistent with nodal metastases. Although the tumor involvement of the hypopharynx and esophagus was similar in size, the imaging findings favored a hypopharyngeal primary with esophageal invasion. This distinction was clinically significant because classification as esophageal cancer would result in M1 disease in this setting, whereas classification as hypopharyngeal cancer corresponded to M0 disease, allowing consideration of potentially curative rather than palliative treatment.

Conclusion

These two cases demonstrate the important role of 18F-FDG PET/CT in differentiating hypopharyngeal cancer from cervical esophageal cancer when tumor involvement crosses anatomically adjacent regions. By integrating metabolic activity with anatomical localization, PET/CT can help identify the most likely primary site, define tumor extent, and assess lymph node involvement. Accurate interpretation is particularly important because the distinction between hypopharyngeal and esophageal cancer can substantially alter cancer staging and subsequent treatment options. 18F-FDG PET/CT therefore provides valuable information for multidisciplinary treatment planning in patients with tumors involving both the hypopharynx and cervical esophagus.

壁報論文 臨床組 **PC-077**

其他 | 非診療之臨床相關主題

台灣放射製藥專業人才核心能力與可信賴專業活動之建構:放射製藥人才之能力導向教育與EPA培育架構

[1,2]李庚穎, [1,2]張文議, [1,2]楊邦宏, [1]洪鈞澤, [1]林千愛, [1]陳世沛, [1]邱芯語

[1]臺北榮民總醫院
[2]陽明交通大學

發表者 李庚穎

Keywords 製藥 | 臨床前藥物研究 | 實驗室流程改善 | 教學

Background

隨著放射性藥物在精準醫療、影像診斷與治療領域的應用日益廣泛，放射製藥人才的培育已成為臨床與產業鏈中關鍵的一環。然而，目前國內在職訓練與教育內容缺乏一致性，尚未建立符合專業發展所需之能力架構與教學標準。

Method

為因應放射製藥專業角色多元化與高信賴度需求，本研究擬採用共識建立法（Delphi Method），建構一套以 ** 能力導向教育（Competency-Based Education, CBE）為核心，並結合可信賴專業活動（Entrustable Professional Activities, EPA）**的放射製藥教育模組。

Results

（1）建立三大專業領域之 EPA 清單，明確界定可觀察、可評量且可逐步授權之專業活動；(2）建構涵蓋知識、技能與態度（Knowledge–Skills–Attitude）之核心能力模組，包括放射化學、核種物理、製藥與品管技術、法規、安全、危機處理、溝通合作及專業態度等；(3）建立初階、進階與高階人員之能力進程圖（Milestone Framework），使專業能力、教育階段及工作授權程度得以相互對應；(4）發展教學評量工具原型與課程應用範例，並透過受訓人員及教師回饋評估其可行性；(5）完成放射製藥教育指引手冊草案及相關學術成果。

Conclusion

可建立台灣放射製藥專業人才之核心能力、EPA及能力進程共識架構，將傳統以課程時數或操作經驗為主的訓練方式，逐步轉化為以實際專業能力及可信賴程度為核心之培育模式。此架構可作為未來放射製藥人員教育訓練、能力評核、工作授權及職涯進階之共同依據，提升人才培育的一致性與專業信賴度。

壁報論文 臨床組 **PC-078**

個案報告 臨床診斷

Pulmonary Infarction Secondary to Lung Cancer Presenting with Concordant PET Rim Sign and CT Atoll Sign: A Case Report

[1]郭建瑋

[1]屏東榮民總醫院

Keywords 有趣影像

Background

Lung cancer can induce pulmonary infarction either through direct tumor compression of adjacent pulmonary vessels or via vascular occlusion of distal branches by thromboemboli. Herein, we report a case of lung cancer-induced pulmonary infarction that presented with characteristic imaging features on both positron emission tomography (PET) and computed tomography (CT).

Case report

A 40-year-old male presented with worsening cough and dyspnea. Subsequent diagnostic evaluation revealed lung cancer of the left upper lobe, invading the mediastinum and extending into the left lower lobe. Bronchoscopy showed tumor involvement at the orifice of the superior segmental bronchus of the left lower lobe (LB6). For initial tumor staging, F-18 FDG positron emission tomography/computed tomography (PET/CT) was performed. PET imaging demonstrated a peripheral ring of FDG uptake with a central photopenic region in the left lower lobe, characteristic of the "rim sign." On CT, the hypermetabolic ring corresponded to a circumferential rim of consolidation surrounding a central area of ground-glass opacity, consistent with the "atoll sign" (reversed halo sign). Subsequent computed tomography angiography (CTA) confirmed tumor invasion into the left pulmonary artery, left pulmonary vein, and left main bronchus, which resulted in total occlusion of the left pulmonary artery. Therefore, the lesion was considered consistent with pulmonary infarction secondary to vascular occlusion.

Conclusion

Although studies indicate that the incidence of pulmonary infarction in patients with central-type bronchogenic carcinoma is approximately 10–25%, it remains relatively uncommon in routine clinical practice. Our case was readily diagnosed due to the characteristic features of pulmonary infarction demonstrated on both PET and CT imaging.

壁報論文 臨床組 **PC-079**

病例系列 臨床診斷

治療後復發性神經母細胞瘤之 ^{18}F-FDOPA 與 ^{18}F-FDG PET/CT 影像表現不一致

[1]羅浚哲

[1]中山醫大附設醫院

Keywords 神經母細胞瘤 | 18F-FDOPA | 18F-FDG | PET/CT

Background

18F-FDOPA PET/CT 對神經母細胞瘤具有良好的病灶偵測能力，而 18F-FDG PET/CT 則反映腫瘤葡萄糖代謝活性。由於兩者呈現不同的腫瘤生物學特性，治療後可能出現不同的示蹤劑攝取表現。本病例探討復發性神經母細胞瘤治療後，18F-FDOPA 與 18F-FDG PET/CT 出現肝臟影像差異之臨床意義。

Method

一名 12 歲女童於 2017 年診斷左側腎上腺第 IV 期神經母細胞瘤，合併骨、骨髓、眼眶及腦部轉移，曾接受化學治療、腫瘤切除及自體周邊血幹細胞移植。2025 年底肝臟與骨髓復發，再次接受化學治療。

治療前後以 18F-FDG PET/CT 及 MRI 追蹤。2026/08/10 接受 18F-FDOPA PET/CT，兩天後再接受 18F-FDG PET/CT，比較治療後肝臟與骨骼之示蹤劑攝取表現。

Results

2025/12/17 18F-FDG PET/CT 顯示肝腫大及瀰漫性肝臟高代謝，SUVmax 4.8，並伴廣泛骨髓高代謝。化學治療後，2026/03/25 肝臟 SUVmax 降至 2.8。2026/06/29 MRI 顯示肝臟及骨病灶較前部分退縮，但仍存在治療後殘存異常。

2026/08/10 18F-FDOPA PET/CT 未見明確局灶性高攝取病灶，Curie score 與 SIOPEN score 均為 0，先前 MRI 所見之肝臟及骨病灶亦未清楚呈現。

2026/08/12 18F-FDG PET/CT 則顯示肝臟第 2、3、6、7 節有**中度、不均勻的代謝增加**，但未形成明確局灶性高代謝病灶；骨骼呈對稱性輕度 FDG 攝取增加，較傾向反應性骨髓變化及治療後修復。

兩種 PET/CT 因此呈現治療後肝臟示蹤劑攝取差異。

Conclusion

本病例顯示治療後復發性神經母細胞瘤可出現 18F-FDOPA 與 18F-FDG PET/CT 影像表現不一致。

18F-FDOPA PET/CT 未見明確活性病灶，而 18F-FDG PET/CT 僅呈現肝臟中度、不均勻代謝增加。目前缺乏同期病理檢查、後續 MRI 或其他明確參考標準，因此**無法判定 FDG所見代表殘存活性腫瘤，或為治療後相關代謝變化；同樣也無法認定 FDOPA 為偽陰性。**

本病例顯示，在治療後神經母細胞瘤評估中，不同示蹤劑結果應結合 MRI、臨床變化及後續影像進行判讀。由於本病例缺乏治療前 18F-FDOPA PET/CT，亦無法比較治療前後 FDOPA 攝取變化，為本病例的重要限制。

壁報論文 臨床組 PC-080

個案報告 臨床治療或診療合一

Acute Cholecystitis During Lu-177 PSMA-617 Radioligand Therapy: A Case Report

[1]柳侑昇, [1]侯景維, [1]王心怡, [1]蔡世傳, [1]林宜瀞

[1]臺中榮民總醫院

發表者 柳侑昇

Keywords Lu-177 PSMA-617

Background

Radioligand therapy (RLT) with Lu-177 PSMA-617 is delivered as a fixed-activity, multi-cycle regimen for metastatic castration-resistant prostate cancer (mCRPC). Current practical guidelines define no absolute contraindication to RLT but list acute infection among the relative contraindications, and provide no guidance for patients who require an invasive procedure during the treatment course. We report a patient in whom a scheduled cycle of RLT was administered during acute cholecystitis and followed two days later by percutaneous transhepatic gallbladder drainage (PTGBD).

Case report

A 79-year-old man with metastatic castration-resistant prostate cancer progressing under darolutamide (PSA 25.97 ng/mL) had PSMA-avid nodal and diffuse skeletal metastases on F-18 rhPSMA-7.3 PET/CT; comorbidities included cirrhosis with chronic thrombocytopenia. After two cycles of Lu-177 PSMA-617, he was admitted before the third cycle with right upper quadrant pain, fever (38.7 C), C-reactive protein (CRP) 6.53 mg/dL and platelets 77,000/microL; cholangiopancreatography showed gallbladder stones with wall thickening, confirming acute cholecystitis. After multidisciplinary assessment the infection was judged localized and drainable, without septic shock, organ failure or gangrenous change, and the third cycle was given on schedule with activity reduced to 160 mCi for thrombocytopenia. He met institutional release criteria four hours after infusion. With CRP rising to 17.27 mg/dL, percutaneous transhepatic gallbladder drainage was performed two days after infusion, without complication. Post-therapy whole-body and SPECT/CT imaging showed regressed nodal and skeletal uptake compared with the preceding cycle, compatible with treatment response; PSA declined to 9.78 ng/mL. He remained afebrile, was discharged four days after drainage, and CRP normalized to 0.13 mg/dL five weeks later; elective cholecystectomy was planned after platelet recovery.

Conclusion

This case illustrates that acute infection, listed as a relative contraindication for RLT in practical guidelines, permits individualized assessment and management.

壁報論文 臨床組 **PC-081**

個案報告 臨床診斷

Multimodality Nuclear Imaging for Intermittent Gastrointestinal Bleeding: A Case Report

[1,2]黃琪雯, [1,2]羅浚哲

[1]中山醫大附設醫院
[2]中山醫學大學

發表者 黃琪雯

Keywords 解剖學 /CT/MR

Background

Intermittent gastrointestinal (GI) bleeding can be difficult to diagnose and localize when conventional endoscopic examinations fail to identify the bleeding source. Tc-99m-labeled red blood cell (Tc-99m RBC) scintigraphy provides temporal information for detecting intermittent bleeding, while SPECT/CT can improve anatomical localization. This case demonstrates the complementary value of planar scintigraphy and SPECT/CT in the evaluation of obscure GI bleeding.

Case report

A 74-year-old woman presented with melena and progressive anemia. Both esophagogastroduodenoscopy (EGD) and colonoscopy were performed, but neither examination identified a definite bleeding source. Tc-99m RBC scintigraphy was subsequently performed using a modified in vitro labeling method, with a labeling efficiency greater than 95%.

Dynamic and serial planar images were acquired, followed by delayed imaging at 1, 4, and 7 hours after injection. The 7-hour delayed planar image demonstrated abnormal radiotracer accumulation in the right lower abdomen and pelvic region, suggesting intermittent active GI bleeding. The suspected bleeding site corresponded anatomically to the terminal ileum and ascending colon. SPECT/CT performed at 7 hours further localized the abnormal activity within the intestinal lumen and helped distinguish it from overlapping urinary bladder and vascular activity.

Conclusion

Tc-99m RBC scintigraphy with delayed planar imaging and SPECT/CT provides complementary temporal and anatomical information for the evaluation of intermittent GI bleeding. In this case, both EGD and colonoscopy failed to identify the bleeding source, whereas delayed planar imaging detected abnormal radiotracer accumulation and SPECT/CT provided more precise anatomical localization. These findings highlight the important role of SPECT/CT in nuclear medicine evaluation of obscure or intermittent GI bleeding.

壁報論文 臨床組 **PC-082**

經驗分享 非診療之臨床相關主題

比較使用不同微量吸管TSH檢驗結果之差異

[1]沈宜瑾, [1]張素雲, [1]黃筱崴, [1]廖建國, [1]游舜宇

[1]大林慈濟醫院

發表者 沈宜瑾

Keywords 放射免疫分析

Background

背景介紹: 微量吸管為放射免疫分析實驗室重要的設備，本實驗室TSH檢驗常用的微量吸管 (10-100μL)有兩支，兩支吸管每年實驗室都會進行外部校正。其中一支近期有輕微摔落，因可正常使用故未外送校正，但不知道是否已影響檢驗結果。本研究目的即為比較兩支常用微量吸管之TSH檢驗結果，以確認兩者的差異是否可接受。

Method

材料方法: 隨機收集 2026 年 7 月 1 日至 2026 年 7 月 31 日間例行TSH檢驗之檢體，進行分析。第一次實驗使用編號 148 的微量吸管，第二次使用編號 141 的微量吸管 (近期輕微摔落)。兩支微量吸管皆於 2025 年 10 月送外部校正實驗室 (康境科技公司) 校正合格，校正共測試 10、50、100μL等 3 個點，允收值分別為最大允許系統誤差：0.8μL、最大允許隨機誤差：0.3μL。TSH檢驗的方法依照原廠 (BECKMAN COULTER)的說明書，首先加入 100μl的病人血清，再加入 100μl的示蹤劑 (Tracer)，放在室溫下搖晃 1 小時 (轉速為大於 280rpm)，最後以清洗液 (wash solution)清洗共兩次後上機計數 (r-counter廠牌: MESSIAH)，依照機器所偵測的CPM換算濃度。因TSH實驗步驟中皆使用 100μL，故無特別測試較低量 (例如 50μL)之實驗是否有受到影響。檢測後，再使用Excel軟體計算不同微量吸管TSH檢驗結果之差異 (%)，並依此項目內部品管之最大允許誤差 (± 3倍CV值) 判定兩支微量吸管之檢驗值差異 (%) 是否是否可接受。

Results

結果：總計收集 35 件病人血清，分析比較常用的兩支微量吸管 (編號 141 及 148) TSH檢驗結果，發現兩支微量吸管的檢驗數值有高度的相關性 (R2 = 0.9962) (圖 1)，其中 33 件(佔 93.94%) 的檢驗結果落在最大允許誤差 (± 3 倍CV值) 內，顯示大部份的結果差異可被接受 (圖 2)。不過，仍有 2 件TSH檢驗結果未落在最大允許誤差 (± 3 倍CV值) 內，表示近期輕微摔落的第二支微量吸管 (編號 141) 可能仍會影響檢驗結果。因此，微量吸管**發生摔落或異常時，仍應**立刻**停止使用**，並進行維修與重新校正，才是正確的做法。

Conclusion

結論：本研究比較兩支常用微量吸管之TSH檢驗結果，雖顯示大部份檢驗結果的差異可被接受，但仍有少數結果不可接受，表示近期輕微摔落的第二支微量吸管 (編號141) 可能仍會影響檢驗結果。日常作業中透過與已知精準度的微量吸管進行檢驗結果的比對，僅可作為暫時評估微量吸管有無異常的手段，實驗室仍應透過設備校正才能了解微量吸管的準確度與精密度是否符合 ISO 8655 國際標準。

壁報論文 臨床組　　**PC-083**

個案報告　臨床診斷

全身骨骼掃描中膀胱 Donut Sign：兩病例報告

[1]張秀瑛, [1]廖建國, [1,2]莊紫翎

[1]大林慈濟醫院
[2]慈濟大學

發表者　張秀瑛

Keywords　有趣影像

Background

全身骨骼掃描為核醫學常用之影像檢查，廣泛應用於惡性腫瘤骨轉移、原發性骨腫瘤、骨折、感染及其他骨代謝異常之評估。Tc-99m MDP 經靜脈注射後主要由骨骼攝取，未被攝取之放射性示蹤劑則經腎臟及泌尿系統排泄，因此膀胱通常呈現相對均勻之高放射性活性。然而，膀胱充盈程度、尿液分布、膀胱解剖形態及鄰近骨盆腔器官等因素，均可能改變膀胱內放射性示蹤劑之分布，形成非典型影像表現。由於平面骨骼掃描屬二維投影影像，當膀胱出現局部相對低放射性活性區時，僅依平面影像不易判斷其實際來源。本文報告兩例全身骨骼掃描中出現膀胱 donut sign 之病例，並藉由 SPECT/CT 進一步評估其可能原因。

Case report

病例一為頸部軟組織鱗狀細胞癌男性患者，合併良性攝護腺肥大，接受全身骨骼掃描。影像顯示左側額骨、頸椎及右側第七肋骨異常放射性活性聚積，膀胱中央呈相對低放射性活性區，周圍呈環狀放射性聚積，即典型之甜甜圈徵象（donut sign）。SPECT/CT 除確認上述骨骼異常攝取外，膀胱中央可見明顯放射性缺損，考量攝護腺肥大所造成之膀胱形態改變，可能影響含放射性示蹤劑尿液之分布。病例二為攝護腺癌男性患者，由腫瘤科轉介接受全身骨骼掃描。影像顯示左側肱骨近端顯著異常放射性聚積，膀胱亦呈中央相對低放射性活性區，周圍呈環狀放射性聚積，形成donut sign。SPECT/CT 顯示左側肱骨近端伴有骨質破壞，並見攝護腺增大凸入膀胱，使膀胱後側向內凹陷。綜合平面影像與 SPECT/CT，考慮膀胱特殊放射性分布與攝護腺增大相關。

Conclusion

本報告呈現兩例全身骨骼掃描中出現膀胱 donut sign 之病例，兩位患者分別具有良性攝護腺肥大及攝護腺癌。雖臨床診斷不同，兩病例之 SPECT/CT 均顯示攝護腺相關之膀胱底部形態改變，可能影響放射性示蹤劑尿液分布，使中央區域呈相對低放射性活性，周圍呈較高放射性活性，進而於平面影像形成 donut sign。此特殊影像可能反映局部解剖構造與放射性尿液分布之交互影響，而非特定攝護腺疾病所專有。當全身骨骼掃描出現膀胱內中心放射性充填缺損或環狀放射性聚積時，除攝護腺增大外，亦應考量留置導尿管水囊（Foley balloon）、膀胱內血塊、膀胱結石及膀胱腔內或膀胱壁腫瘤等可能原因。判讀時應綜合患者病史、導尿管使用情形及影像表現，並利用 SPECT/CT 確認充填缺損之解剖位置及與鄰近構造之關係。男性可留意攝護腺增大，女性則可考量子宮等骨盆腔鄰近構造，以協助釐清影像來源並降低誤判。

壁報論文 臨床組 **PC-084**

個案報告 臨床診斷

全身骨骼掃描中 Arterial Hand Sign 之影像表現：病例報告

[2]張秀瑛, [2]許幼青, [2]廖建國, [1,2]莊紫翎

[1]慈濟大學
[2]大林慈濟醫院

發表者 張秀瑛

Keywords 有趣影像

Background

全身骨骼掃描為核子醫學常用之影像檢查，主要利用 Tc-99m methylene diphosphonate（Tc-99m MDP）評估骨骼代謝異常及惡性腫瘤骨轉移。正常情況下，示蹤劑經由靜脈注射後隨血液循環分布，並依骨骼代謝活性及局部血流情形由骨組織攝取，未被攝取之示蹤劑則主要經腎臟排泄。除了反映骨骼代謝情形外，放射性藥物的注射方式及體內分布亦可能影響影像表現。若注射過程發生非預期狀況，例如示蹤劑意外進入動脈系統，可能造成注射側肢體異常的放射性分布，形成 arterial hand sign（動脈手徵象）。此類影像表現雖少見，但具有辨識價值，可避免將注射相關異常分布誤認為骨骼病變或其他病理性攝取。

Case report

一位 57 歲男性肺癌患者，因標靶藥物事前審查所需接受全身骨骼掃描檢查，以評估是否存在骨骼異常代謝或轉移性病灶。影像顯示第四及第五腰椎椎體呈輕度至中度示蹤劑攝取，與前次骨骼掃描比較後，考慮為退化性變化；雙側上顎骨及下顎骨區域亦可見示蹤劑攝取，建議進一步由牙科醫師評估。此外，左前臂及手部出現不符合正常骨骼攝取模式之異常放射性分布，呈線狀及分支狀聚積，形成arterial hand sign，與典型 glove phenomenon 主要呈現手部瀰漫性手套樣放射性分布不同，本病例之異常分布由左前臂延伸至手部，且可見前臂骨骼及手部關節明顯攝取，呈現較為廣泛且具線狀、分支狀特徵的放射性分布。綜合注射紀錄（左側手肘部位注射）、注射側別及影像表現，推測此特殊放射性分布可能與注射過程中非預期進入動脈系統有關。然而，由於缺乏即時血管影像或其他直接證據，無法進一步確立為 intra-arterial injection，只是根據文獻報告影像比對及排除其他可能此為最佳鑑別診斷。

Conclusion

Arterial hand sign 為全身骨骼掃描中少見但具有代表性的注射相關影像表現，可能發生於 Tc-99m MDP等藥物，注射過程中意外進入動脈系統時順流吸收，該動脈所供應的下游骨骼與軟組織，會呈現較高濃度的放射性藥物累積，使注射側前臂及手部出現特異的放射性分布。由於此類影像表現可能與局部骨骼病灶、軟組織異常攝取或其他病理性變化混淆，如誤診為反射性交感神經失調等疾病，因此正確辨識其影像特徵相當重要。當全身骨骼掃描出現不符合正常骨骼攝取模式之局部異常放射性分布時，除考量可能的病理性變化外，亦應將注射相關因素納入判斷，並配合注射部位、注射紀錄及臨床資訊進行綜合判讀，以降低影像誤判及不必要的後續檢查。此外，辨識 arterial hand sign 亦具有檢查品質管理上的意義，可幫助改善注射技術及提升檢查品質。

壁報論文 臨床組 **PC-085**

個案報告 臨床診斷

三相骨掃描對於周邊軟組織發炎之特異性侷限與氟18葡萄糖正子電腦斷層掃描之輔助診斷：個案報告

[1]籃瑋承, [1]林致毅, [1]王婉酈, [1]孫鵬凱, [1]蘇淨儀, [1]林品秀, [1]周易賢

[1]臺大雲林分院

發表者 籃瑋承

Keywords 有趣影像 | 分子影像

Background

三相骨掃描（Three-phase bone scan）能夠透過局部血流供應情況，依照不同時相受檢部位對於放射性同位素攝取程度觀察血流、軟組織及骨骼代謝狀況。然而，其診斷特異性（Specificity）常因病患的局部狀況或骨骼本身疾病而有不同，甚至出現偽陽性結果。氟 18 葡萄糖正子電腦斷層造影（FDG PET/CT）則具備高解析度的解剖定位與代謝評估能力，可作為輔助診斷的重要利器。

Case report

一名 16 歲男性因發燒及右側大腿至膝蓋部位紅腫疼痛到本院急診就醫，此病人於一年前發生過車禍，右腳踝有骨折並且開過刀。至急診後接受下肢含顯影劑電腦斷層掃描，顯示右膝蓋滑囊內有明顯浸潤現象，伴隨可疑積液；血液報告顯示白血球和C-反應蛋白數值上升。結合其臨床狀況，臨床醫師考量疑似化膿性關節炎或蜂窩性組織炎所以收治住院。

住院期間，關節組織液分析顯示白血球計數和C反應蛋白濃度仍高，且培養結果為金黃色葡萄球菌，根據兒科感染性疾病指引依化膿性關節炎方案給予抗生素治療。並針對右膝關節進行三相骨掃描：於靜脈注射放射性同位素後立即進行每 4 秒一幀的血流相共搜集 32 幀、5 分鐘後的血池成像、3 小時後的全身及局部骨掃描影像。三相骨掃描影像中右膝蓋在血流相及血池相放射性增高，四小時後的全身及局部骨掃描呈現右側髕骨放射性藥物攝取量些微上升，無法確認是骨髓炎或是右側髕骨因周圍組織發炎導致的反應性攝取。所以在核醫科醫師的建議下，病人另外接受全身炎症掃描，採用FDG PET/CT：檢查前空腹六小時，靜脈注射放射性同位素 50 分鐘後進行顱頂至足底的全身造影。FDG PET/CT影像呈現右膝蓋軟組織有FDG攝取增加情形（SUVmax=5.2），而髕骨則無，顯示右膝只有軟組織處於感染及發炎狀態，在接受一共 20 天的抗生素治療後，病人情況穩定下出院。

Conclusion

三相骨掃描常用於區分細菌感染引起的骨髓炎和蜂窩性組織炎，兩者在血流及血池相皆有攝取增高現象。鑑別方法為骨髓炎的病患在藥物代謝一段時間後的骨掃描會呈現出骨骼攝取增加，但蜂窩性組織炎的病患則不會。另考量氟 18 葡萄糖正子電腦斷層造影相對於Ga-67炎症掃描具備優異的解剖定位能力與偵測細胞高活度異常代謝的特性，能更精確地劃分發炎病灶所在的解剖層次（軟組織或骨骼），因此採用FDG PET/CT做為輔助診斷工具。本個案凸顯了三相骨掃描在面對鄰近軟組織感染時，其特異性會常因鄰近骨骼的反應性攝取（Reactive uptake）而大幅降低診斷特異性（Specificity）。當骨掃描結果難以鑑別反應性攝取與真實骨髓炎時，結合FDG PET/CT能精準定位發炎層次，有效提升診斷特異性，避免不必要的臨床處置。

壁報論文 臨床組

PC-086

原著論文 臨床診斷

The Osteoporosis Paradox in Men with Benign Prostatic Hyperplasia: Metabolic Syndrome Severity Deceptively Elevates Lumbar Spine Bone Mineral Density

[1]陳保良, [2,3]王昱豐, [1]李政怡, [4,5]莊紫翎

[1]Department of Biomedical Sciences, National Chung Cheng University, Chiayi, Taiwan.
[2]Department of Nuclear Medicine, Taipei Veterans General Hospital, Taipei, Taiwan
[3]Department of Biomedical Imaging and Radiological Sciences, National Yang Ming Chiao Tung University, Taipei, Taiwan
[4]Department of Nuclear Medicine, Dalin Tzu Chi Hospital, Buddhist Tzu Chi Medical Foundation, Chiayi,Taiwan
[5]School of Medicine, Tzu Chi University, Hualien, Taiwan

發表者 陳保良

Keywords Bone Mineral Density

Background

Both benign prostatic hyperplasia (BPH) and metabolic syndrome (MetS) are prevalent in aging men, with recent evidence linking MetS components (e.g., hyperglycemia, obesity, low HDL) to prostate enlargement (Urgesa et al., 2026). However, the combined impact of MetS severity on bone health remains controversial. While cumulative evidence suggests men with MetS maintain bone mass due to higher body mass (Rył et al., 2023), the dose-response relationship between MetS accumulation and site-specific bone parameters needs clarification. This study investigated associations between MetS component accumulation and macro- and micro-structural bone parameters—specifically bone mineral density (BMD) and trabecular bone score (TBS)—in a large cohort of aging Taiwanese men, focusing on those with BPH.

Method

This retrospective study screened males aged 50–90 years at a southern Taiwan medical center (June 2014–April 2021). Cross-sectional analysis included 4,574 participants (1,518 BPH patients) after exclusions. Participants were stratified by MetScomponents (0–3). Crude parameters were compared via one-way ANOVA; analysis of covariance (ANCOVA) controlled for age and body mass index (BMI).

Results

Before adjustment, accumulating MetScomponents significantly increased lumbar spine BMD and T-scores (BPH group: –0.5 ± 1.3 for 0 components vs. 0.4 ± 1.6 for 3 components, $p < 0.001$). Conversely, bone microarchitecture quality (TBS) significantly decreased ($p = 0.007$). After adjusting for age and BMI, the trend for TBS vanished ($p = 0.754$), but adjusted lumbar spine BMD remained significant ($p = 0.023$), with a persistent difference between 0 and 3 component groups ($p < 0.050$).

Conclusion

This DXA study uncovers a critical diagnostic blind spot—the osteoporosis paradox—wherein MetS severity deceptively inflates areal BMD while masking microstructural deterioration in aging men. Central obesity is identified as the primary driver of this deceptive DXA elevation, significantly lowering apparent low bone density odds in BPH patients. Relying solely on conventional DXA-BMD severely underestimates true bone fragility in this metabolically compromised population, making routine TBS integration clinically imperative.

壁報論文 臨床組 **PC-087**

個案報告 臨床診斷

18F-rhPSMAPET/CT於攝護腺癌術後生化復發之診斷與術後追蹤：病例報告

[1]王雅萍, [1]曾能泉

[1]童綜合醫院

發表者 王雅萍

Keywords 18F-rhPSMA PET/CT | 生化復發 (BCR)

Background

根據最新統計，攝護腺癌為國人男性常見之泌尿道惡性腫瘤，國人在十大癌症死亡率攝護腺癌為排名第五名。攝護腺癌經治療後有復發或轉移時常伴隨 PSA 上升，攝護腺特異膜抗原（prostate-specific membrane antigen, PSMA）正子電腦斷層造影已廣泛應用於攝護腺癌復發及轉移評估。18F-rhPSMA為新一代PSMA標靶正子示蹤劑，可與攝護腺癌細胞表面高度表現之PSMA受體結合，提高病灶偵測率。18F-rhPSMA PET/CT對於低PSA值之生化復發患者具有較高敏感度，可協助偵測局部復發、淋巴結轉移及遠端轉移病灶，提供臨床治療決策及治療反應評估的重要依據。本病例藉由 18F-rhPSMA PET/CT成功偵測攝護腺癌術後骨盆腔淋巴結復發，並於骨盆腔淋巴結清除術後進行追蹤評估，展現其於術後監測及治療反應評估之臨床應用價值。

Case report

本病例是 64 歲男性攝護腺癌的患者，於 2024 年 8 月接受達文西輔助根除性攝護腺切除術（robot-assisted laparoscopic prostatectomy, RaLP）合併骨盆腔淋巴結清除術（bilateral pelvic lymph node dissection, BPLND）。

術後追蹤血清前列腺特異抗原（PSA）呈現上升趨勢，2024 年 9 月為 0.032 ng/mL，後續逐步上升至 2025 年 6 月 0.318 ng/mL，符合生化復發之表現。2025 年 6 月底電腦斷層報告顯示右側外髂區域有腫大淋巴結，至 2025 年 7 月初PSA進一步上升至 0.515 ng/mL。考量PSA持續上升及影像學發現，主治醫師 2025 年 7 月初安排 18F-rhPSMA PET/CT檢查，結果顯示右側外髂淋巴結呈高度PSMA攝取（SUVmax 16.28），高度懷疑淋巴結轉移，後續病人於 2025 年 7 月中接受進一步骨盆腔淋巴結清除術（pelvic lymph node dissection, LND）病理檢查證實為轉移性攝護腺癌。術後於 2025 年 9 月初PSA 一度下降至 0.239 ng/mL，惟後續仍呈波動性變化。2025 年 11 月隨後進行追蹤性 18F-rhPSMA PET/CT檢查，結果顯示原先右側外髂淋巴結病灶已無明顯攝取，呈現影像學上的局部治療反應，惟因 PSA 仍維持可測得，是否存在殘存疾病仍需持續追蹤。

Conclusion

18F-rhPSMA PET/CT能有效偵測攝護腺癌患者於根除性攝護腺切除術後發生生化復發時之骨盆腔淋巴結轉移病灶，並可作為治療後反應評估及疾病追蹤的重要影像工具。其在復發病灶定位及後續治療決策上具有重要臨床價值。

壁報論文 臨床組 **PC-088**

個案報告 臨床診斷

放射師Gallium-67發炎掃描判讀教學：以感染性關節炎偵測定位為例

[1]許幼青, [1]廖建國, [1]林昱璁, [1]陳薇璇, [1]莊紫翎

[1]大林慈濟醫院
[2]慈濟大學

發表者 許幼青

Keywords 教學 | 造影儀器

Background

Gallium-67全身發炎掃描是感染來源不明（Infection of Unknown Origin, IUO）患者的重要核醫檢查，其主要價值在於定位活動性發炎病灶，而非直接診斷病原菌。對放射師實習生及PGY學員而言，應建立系統化判讀流程，熟悉正常生理性攝取、辨識異常放射性聚積，並結合SPECT/CT及臨床資訊，提供有助於後續診斷與治療的影像資訊。

Case report

82歲女性，具腎病症候群病史，臨床懷疑微小病變腎病（minimal change disease），接受Prednisolone治療中。因持續全身倦怠及發炎指數升高住院，臨床無法確認感染來源，安排Gallium-67全身發炎掃描。影像發現胃部異常聚積，左膝關節明顯Gallium攝取增加，左肘及腕關節亦有輕度攝取，其中以左膝最具臨床意義；SPECT/CT進一步定位攝取位於關節腔內而非骨骼結構，表示關節腔感染 / 發炎病變。故臨床安排左膝關節液抽吸檢查。滑膜液（關節液）分析顯示：白血球計數為 32,076/dL，其中嗜中性球（PMNs）佔 80%，支持感染性關節炎（septic arthritis），雖然血液培養及滑液培養皆為陰性（culture negative），但病人接受抗生素治療後發炎指數明顯下降且臨床症狀改善，整體臨床表現仍支持感染性關節炎診斷，臨床改善加理學檢查，左肘及腕關節及胃部異常聚積的僅為非特異性的輕微發炎。本案例進一步建立 Gallium-67 發炎掃描之系統化判讀教學流程，供放射師實習生及 PGY 學員作為影像判讀 Check-list。判讀首先由辨識正常生理性分布開始，再進行全身性異常攝取搜尋，發現可疑病灶後利用 SPECT/CT 確認解剖位置，並進一步建立鑑別診斷，最後結合病史、臨床症狀、發炎指數及實驗室檢查進行整合判讀。本案例以左膝關節為例，學員可依「正常分布辨識 → 異常攝取偵測 →SPECT/CT 定位 → 鑑別診斷 → 臨床整合」五階段逐步判讀，從發現異常攝取進一步確認其位於關節腔，並思考感染性關節炎與其他類風濕性關節炎、退化性關節炎、結晶性關節病及骨髓炎等發炎性或退化性關節疾病之鑑別，最終理解影像結果如何引導關節液抽吸等後續臨床處置。透過此結構化流程，可將傳統病例影像描述轉化為具體、可重複應用的核醫影像判讀教學模式。

Conclusion

Gallium-67全身發炎掃描可有效協助感染來源不明患者定位病灶，並引導後續侵入性檢查與治療。本案例除呈現Gallium scan的偵測能力和SPECT/CT定位能力外，更作為放射師教導實習生及PGY學員的教學案例，強調建立標準化判讀流程、培養臨床整合能力及跨團隊溝通的重要性，使核醫影像真正成為臨床決策的重要依據。

壁報論文 臨床組 **PC-089**

病例系列 | 臨床治療或診療合一

胰島素內分泌腫瘤病人接受同位素治療之照護經驗從單一個案到病房照護常規之建立

[1]潘怡蓁, [1]呂季庭, [1]吳珈羽, [1]陳庭萱, [1]李明璇, [1]曾敏容, [1]陳怡潔, [1]呂惠敏, [1]劉嘉儒

[1]臺大醫院

發表者 潘怡蓁

Keywords 病人安全 | 輻射防護

Background

胰島素神經內分泌腫瘤 (Insulinoma) 接受LUTATHERA®胜肽受體放射性核種治療 (Peptide Receptor Radionuclide Therapy，PRRT)的藥物時，腫瘤細胞凋亡可能引發大量胰島素釋放，導致致命的低血糖危機。臨床統計，此類病人住院期間低血糖加劇的機率高達 19-47%。由於此類個案罕見，且LUTATHERA®治療需於同位素治療病房內進行，護理人員需同時應對高頻率血糖監測、低血糖急症處置以及輻射防護的多重臨床挑戰。面對此類罕見且高風險之治療，臨床團隊普遍缺乏相關照護經驗與信心。有鑑於此，本專案建立跨團隊照護準則並導入實境教育訓練，期能確保病人生命安全，同時達成醫療人員輻射劑量合理抑低（ALARA）之目標。

Method

建立跨科部（涵蓋核子醫學部、內科部代謝內分泌科、內科部胃腸肝膽科與護理團隊）的專屬照護準則。規範重點包含：確立高頻率血糖監測時機、低血糖緊急處置流程，以及規劃符合合理抑低 (ALARA) 原則之緊急重症轉送動線。

Results

為有效確保了病人於同位素治療期間的安全，並顯著提升整體照護品質。在臨床處置上，團隊依據病況進行動態調整：首次療程病人因餐間與清晨更易有低血糖狀況，治療過程採取預防性持續滴注 10% 葡萄糖水 (D10W)，成功避免低血糖危機；第二次療程因病人低血糖狀況改善，其治療當日血糖監測值為 82mg/dL，未予以預防性D10W持續輸注，然於治療隔日 (給予LUTATHERA®23小時後) 測得血糖降至 51 mg/dL。醫療團隊即刻介入指導，因病人意識清楚，基於 ALARA原則，請病人口服自備含糖食物，18 分鐘內血糖迅速回升至 121 mg/dL。護理人員的輻射暴露時間與劑量監測方面數據如下：**第一次同位素治療期間**：3 位護理師因抽血及更換點滴各 2 次進入病室，平均總時間分別為 20 分鐘、15 分鐘與 10 分鐘。光激發光劑量計 (OSLD)計讀結果為Hd:0.09mSv、Hs:0.10mSv（等於環境背景劑量），3 位護理師之電子式個人劑量計（EPD）總劑量約增加 0-0.003 mSv。**第二次同位素治療期間**：3 位護理師更換點滴進入病室，平均總時間分別為 5 分鐘、11 分鐘與 15 分鐘。光激發光劑量計 (OSLD)計讀結果同樣為 Hd:0.09 mSv、Hs:0.10 mSv（等於環境背景劑量）。

Conclusion

面對罕見且具高急處置風險之胰島素腫瘤治療，本團隊透過事前研擬照護準則與輻射防護實境演練，成功消除護理人員對疾病急症與輻射暴露之恐懼。客觀劑量監測數據顯示護理人員劑量皆維持於背景值，具體證實跨團隊標準作業流程（SOP）能有效兼顧病人安全與醫療人員之輻射防護，可作為未來推動相關特殊核醫同位素治療之標準範本。

壁報論文 臨床組

PC-090

其他 臨床診斷

乳癌術前插針定位對核醫前哨淋巴結定位檢查耗時之影響

[1]黃美瑩, [1]李佳鴻, [1]莊凱文, [1]吳雅嵐

[1]台北慈濟醫院

發表者 黃美瑩

Keywords 流程優化

Background

在乳癌的術前準備中，核醫前哨淋巴結定位 (Sentinel Lymph Node Mapping)為協助外科醫師尋找第一站淋巴結之重要檢查。於標準造影流程中，病人需將患側手臂上舉以充分暴露腋下淋在乳癌的術前準備中，核醫前哨淋巴結定位 (Sentinel Lymph Node Mapping)為協助外科醫師尋找第一站淋巴結之重要檢查。於標準造影流程中，病人需將患側手臂上舉以充分暴露腋下淋巴結區域並進行局部揉壓。然而，在臨床實務中部分病人會於核醫造影前先行完成細針定位 (Breast Needle Localization)，因患部已留置定位針具，為避免針具移位而會無法配合舉手姿勢與揉壓。本研究旨在透過量化分析，探討病人因留置定位針具而對核醫檢查耗時的影響。巴結區域並進行局部揉壓。然而，在臨床實務中部分病人會於核醫造影前先行完成細針定位 (Breast Needle Localization)，因患部已留置定位針具，為避免針具移位而會無法配合舉手姿勢與揉壓。本研究旨在透過量化分析，探討病人因留置定位針具而對核醫檢查耗時的影響。

Method

2025年 9 月 1 日至 2026 年 7 月 20 日間，於北部某醫學中心核醫科接受前哨淋巴結定位之病人，共計 114 例有效樣本。

- 對照組：未放置定位針，可配合標準流程造影者（N = 107）。
- 實驗組：已放置定位針，為避免定位針移位，無法舉手及進行局部揉壓者（N = 7）。

檢查耗時定義為自同位素藥物注射開始計時，至影像中出現可明確進行前哨淋巴結定位之時間。對照組照相時採雙手上舉姿勢，實驗組則因留置定位針而採雙手不上舉之姿勢。

紀錄完成該項檢查所花費之時間（分鐘）。採用獨立樣本 t 檢定 (Independent Two-Sample t-test) 直接比較兩組病人的平均檢查耗時，以評估其差異是否達統計顯著水準。

Results

對照組：平均檢查耗時為 8.6 分鐘。實驗組：平均檢查耗時為 19.3 分鐘。已放置定位針病人之平均檢查耗時為未放置定位針病人的 2.24 倍，增加約 124%。

經獨立樣本 t 檢定分析，兩組檢查耗時具有統計上顯著差異（$p < 0.001$）。結果顯示，放置定位針病人的前哨淋巴結定位檢查時間顯著較長。

Conclusion

本研究顯示，已放置定位針病人之核醫前哨淋巴結定位檢查耗時明顯增加，可能與無法進行注射部位揉壓，以及無法採雙手上舉姿勢而增加影像定位與擺位調整時間有關。

考量已放置定位針病人之平均檢查時間較長，臨床流程上可考慮針對此類病人適度調整第一次造影時間。現行第一次造影時間為同位素注射後約 5 分鐘，未來可進一步評估延後至約 10 分鐘是否能提供較充裕的自然引流時間，減少病人在造影機台上等待及維持固定姿勢的時間，並提升病人舒適度與檢查流程效率。

此流程調整建議仍需透過後續研究進一步驗證其實際效益。

壁報論文 臨床組

PC-091

原著論文　臨床診斷

Gallium-67狼瘡性腎炎造影於平面與SPECT/CT半定量分析之一致性比較

[1]陳彥榕, [1,2]龔瑞英, [3]曾智偉, [2]張振榮, [1,2]林宜瀞

[1]臺中榮民總醫院核子醫學科
[2]中臺科技大學醫學影像暨放射科學系
[3]臺中榮民總醫院內科部過敏免疫風濕科

發表者　陳彥榕

Keywords Gallium-67腎臟造影 | 狼瘡性腎炎 | 半定量分析

Background

狼瘡性腎炎為系統性紅斑狼瘡嚴重的併發症，臨床上透過侵入性腎臟切片評估發炎程度為其黃金指標。Gallium-67腎臟造影可提供非侵入性發炎評估，隨著SPECT/CT造影技術廣泛應用於臨床，本研究旨在比較平面影像與SPECT/CT半定量分析的一致性，並探討不同腎臟ROI分析方式所得半定量結果之差異。

Method

回顧性分析 206 例接受注射後 48 小時Gallium-67平面影像及SPECT/CT造影之狼瘡性腎炎患者影像。平面影像沿左右腎臟可辨識之輪廓繪製全腎ROI，並以鄰近脊椎ROI作為背景參考，計算腎臟／脊椎比值（kidney-to-spine ratio, K/S ratio）。SPECT/CT則於左右腎臟可辨識之腎實質區域及局部高攝取區繪製ROI，避開腎盂與集尿系統，其中局部高攝取區ROI大小約為 100 pixels（±10%）。兩種影像之脊椎ROI均選取鄰近腎臟之L1–L2區域，大小約為 500 pixels（±10%）。局部高攝取區／脊椎比值（hot-spot kidney-to-spine ratio, HK/S ratio）定義為腎臟局部高攝取區ROI平均計數除以脊椎ROI平均計數。採用Spearman等級相關係數、組內相關係數及Wilcoxon signed-rank檢定評估兩種分析方法的一致性與差異。

Results

左右腎平面影像K/S ratio中位數（IQR）分別為 0.97（0.88–1.08）及 1.04（0.94–1.17），斷層影像則分別為 0.95（0.87–1.10）及 1.04（0.94–1.17）。兩者展現良好一致性（左腎ICC＝0.809；右腎ICC＝0.752，均$p<0.001$）。等級相關性分析中，左右腎均呈高度正相關（左腎$r_s=0.843$；右腎$r_s=0.717$，均$p<0.001$）。SPECT/CT左右腎最高攝取熱點比值 (HLK/HRK)顯著升高，分別為 1.11（0.98–1.29）及 1.16（1.02–1.33）；其與平面影像K/S ratio之ICC降為 0.424-0.504。

Conclusion

Gallium-67腎臟造影提供狼瘡性腎炎的非侵入性影像評估。平面影像與SPECT/CT腎實質半定量結果呈顯著正相關，並具有良好一致性。SPECT結合CT解剖定位，能進一步呈現腎臟局部高攝取區，顯示其評估腎內攝取分布及異質性的潛力，為臨床提供更可靠的非侵入性影像工具。本研究主要為平面影像與SPECT/CT半定量分析之方法學比較，局部高攝取是否代表較活躍的局灶性發炎，仍需結合臨床、病理或預後指標進一步驗證。

壁報論文 臨床組 **PC-092**

個案報告 臨床診斷

Visualization of the Liver on Nuclear Bone Scan in a Case of Clopidogrel-Induced Hepatic Injury

[1]莊雅雯
[1]高雄醫學大學

Keywords 分子影像

Background

Clopidogrel (Plavix) plus aspirin is the first-line antiplatelet therapy for reducing cardiovascular events, with a relatively low occurrence of adverse side effects. However, reports about cases of hepatotoxicity due to clopidogrel are increasing in the last few years, after the increased use of this drug. Clopidogrel is a prodrug converted to its active form by various cytochromes in the liver, including cytochrome P 450 and CYP 4A3. These active metabolites are responsible for the antiplatelet effects as well as the hepatotoxic effects of the medication due to inhibition of cell glutathione. By affecting some isoenzymes in the cytochrome pathways, interactions between clopidogrel or certain statins may lead to liver damage. There are few of those cases and review of the literature in which nuclear medicine imaging obtained in the diagnostic workup.

Case report

The authors report the case a 50-year-old man who was admitted to the hospital for left lung tumor with neck lymphadenopathy found by image survey in Vietnem last month. He decided to come back to Taiwan for further management. He was referred to our department for detecting metastatic bone lesions. 99mTc methylene diphosphonate (MDP) scan demonstrated diffuse intense hepatic uptake accidentally. Impaired liver function with hyperbilirubinemia and coagulopathy was found by laboratory follow-up. In addition, clopidogrel usage due to unknown condition was told. This drug was held, and hepatoprotective agents with oral Silymarin, oral Uliden and intravenous Stronger were all prescribed, and the trend of liver function tests showed significant improvement and was even back within normal limit.

Conclusion

Drug-induced hepatotoxicity is a common cause of acute hepatitis, and the recognition of the responsible drug may be difficult. The diagnosis is strongly suggested by an accurate medical history and liver biopsy. Although no liver biopsy was performed in this case due to improvement of clinical condition, we believe that clopidogrel-related acute hepatitis seems most likely. Physicians should carefully consider the risk of drug-induced hepatic injury when clopidogrel is prescribed.

壁報論文 臨床組 **PC-093**

原著論文 臨床診斷

Normal-Organ [^{18}F]FDG Uptake in Metformin-Treated Patients with Type 2 Diabetes: An Exploratory Comparison Before and After Glucose Normalization

[1]葉信顯, [2]黃文盛, [3]謝栢滄, [3]Mai Thi Bach Tieu

[1]三軍總醫院
[2]彰濱秀傳醫院
[3]中台科技大學

發表者 黃文盛

Keywords 定量分析 | 分子影像

Background

To compare normal-organ [^{18}F]FDG uptake between metformin-treated patients with type 2 diabetes mellitus (T2DM) and non-diabetic controls, and to examine how glucose normalization affects these comparisons.

Method

This retrospective study included 33 metformin-treated patients with T2DM and diffuse bowel uptake and 25 non-diabetic patients with stage IA–IB lung cancer. PMOD was used to quantify body-weight-normalized SUVmean in the brain using a 70% SUVmax threshold, liver, gluteus medius muscle, and lung. Glucose-normalized SUV was calculated as SUVmean × blood glucose (mg/dL)/100. Exploratory lung-based normalization multiplied tissue SUVmean by the corresponding group mean lung SUVmean divided by individual lung SUVmean. Between-group comparisons used two-sided t-tests.

Results

Blood glucose was higher in the T2DM group (146.97 ± 31.48 vs. 114.24 ± 20.42 mg/dL). Uncorrected brain SUVmean was lower in this group (5.66 ± 1.53 vs. 7.66 ± 2.12, $p < 0.001$), whereas liver and muscle SUVmean did not differ significantly. After glucose normalization, the brain difference was no longer statistically significant (7.98 ± 1.65 vs. 8.50 ± 1.86, $p = 0.271$), while liver (3.51 ± 1.04 vs. 2.59 ± 0.50, $p < 0.0001$) and muscle (1.11 ± 0.35 vs. 0.89 ± 0.18, $p = 0.0035$) values were higher in the T2DM group. Combined lung and glucose normalization produced a similar pattern.

Conclusion

Glucose normalization altered the statistical interpretation of normal-organ [^{18}F]FDG uptake differences between these groups. The findings do not establish an independent metformin effect or demonstrate that glucose-normalized SUV reflects true tissue metabolism. Diabetes-related physiology, differences in cancer characteristics, and selection for diffuse bowel uptake limit causal inference and generalizability.

壁報論文 臨床組 **PC-094**

臨床診斷 傳統核醫

腦部多巴胺轉運體影像：人工 ROI 與自動量化分析之判讀一致性比較

[1]呂麗如, [1]陳世緯

[1]恩主公醫院

發表者 呂麗如

Keywords 定量分析

Background

Tc-99m TRODAT-1 腦部多巴胺轉運體（dopamine transporter, DAT）SPECT 可呈現紋狀體多巴胺轉運體之分布情形，影像判讀可透過視覺評估及定量分析進行。傳統人工ROI 圈選需由操作者依影像判斷紋狀體位置並設定 ROI，其圈選位置、範圍及背景區域可能因操作者而有所差異，進而影響定量結果。

自動量化分析軟體則可透過標準化影像處理、ROI 定位及定量計算流程取得 Specific Binding Ratio（SBR），並可與正常資料庫進行比較。因此，本研究著重於比較人工ROI 與自動量化分析在相同 Tc-99m TRODAT-1 SPECT 影像下，不同醫師間之判讀一致性及定量值變異，以評估自動量化分析於影像分析標準化上的應用價值。

Method

本研究為單一中心回溯性研究，納入 2024 年 7 月至 2025 年 12 月接受 Tc-99m TRODAT-1 DAT SPECT 檢查之 10 例受試者；影像品質不佳或資料不完整者予以排除。Tc-99m TRODAT-1 注射劑量為 25 mCi，於注射後 3.5 小時進行影像擷取。使用 Siemens Symbia SPECT 系統搭配 Fan Beam Collimator，影像矩陣為 128 × 128、Zoom 1，共 60 projections，每 projection 30 秒。影像以 OSEM 2D 進行重建（10 iterations、8 subsets、Gaussian filter 8.00），並進行 attenuation correction（$\mu = 0.12\ cm^{-1}$）。

由兩位核醫醫師於未知受試者臨床診斷及疾病狀態下獨立判讀。人工 ROI 分析於左右紋狀體頭核及尾核之最顯著四張影像進行圈選，背景 ROI 設於小腦，計算左右側及平均 Specific Binding Ratio（SBR）。自動量化分析則使用「鑠騰」核醫紋狀體分析軟體，依標準化流程進行腦部定位、紋狀體自動定位及背景參考區域分析，取得左右側及平均 SBR，並與正常資料庫比較。

Results

本研究將比較人工 ROI 與自動量化分析於兩位醫師間之判讀一致性，以及 SBR 定量值之變異程度。結果將以 κ 值、ICC、mean difference 及 absolute difference 呈現，以客觀評估兩種分析方法之醫師間一致性。

討論

人工 ROI 圈選可能受到 ROI 位置、大小及操作者判斷差異影響，而自動量化分析透過標準化 ROI 定位及計算流程，可降低人工操作造成之變異。此外，若軟體提供年齡配對正常資料庫，可提供年齡相關之參考資訊，作為影像判讀之輔助依據。

Conclusion

本研究以標準化影像擷取、重建及分析流程，比較人工 ROI 與自動量化分析之醫師間一致性。透過 κ 值、ICC 及定量值變異，可客觀評估兩種分析方式之差異。惟本研究僅納入 10 例，樣本數有限，研究結果之統計效力及推論性受到限制，後續仍需增加樣本數及進行多中心研究加以驗證。

壁報論文 臨床組

PC-095

原著論文 非診療之臨床相關主題

CT-Based Generation of Synthetic Bone Scintigraphy Images: A Proof-of-Concept Study

[1]許祐寬, [1]楊仁
[1]成大醫院

發表者 許祐寬

Keywords 影像處理 / 軟體

Background

Controllable bone scintigraphy synthesis could provide labeled training data for augmentation; simplified acquisition assumptions require evaluation. We evaluated parameter-dependent image variation, angular-response effects and reference-informed parameter selection.

Method

Forty thoracic CT volumes were converted into anterior and posterior synthetic images using HU-weighted activity within TotalSegmentator bone masks, variable kidney activity, and simplified acquisition models. Parameter sensitivity and angular-response effects were assessed against repeat-noise variation. A final setting was selected against 20 cases from BS-80K, a publicly available bone-scan dataset, by minimizing the mean standardized Wasserstein distance across five image features under common normalization; confidence intervals used case-level bootstrapping. Two physicians each classified 80 standardized images from 20 synthetic and 20 reference cases. Exploratory source comparisons used two-sided case-level permutation tests with Holm correction.

Results

Generation completed for 40/40 CTs, yielding 800 image observations. Increasing noise increased high-frequency power fraction by 0.0965 (95% CI, 0.0934–0.0995), whereas increasing resolution loss decreased it by 0.0610 (95% CI, 0.0555–0.0670). Under the tested angular-response approximation, image differences exceeded repeat-noise variation (mean within-CT NRMSE ratio, 1.56; 95% CI, 1.52–1.60). Among nine settings, the 6° acceptance-angle setting had the lowest aggregate feature-distribution distance to the reference, reducing it from 0.820 at baseline to 0.605. Entropy remained higher than the reference (difference, 0.289 bits; 95% CI, 0.157–0.419). Both readers classified all 40 real images as real. Synthetic images were judged real in 29/40 (72.5%; 95% CI, 57.5–87.5%) and 13/40 (32.5%; 17.5–47.5%) judgments, respectively, significantly less often than real images (adjusted $p=0.0012$ and $p<0.0001$).

Conclusion

This proof of concept integrates established models for controllable bone-mask-guided synthesis and reference-informed image-feature improvement; visual differences remain. CT-derived anatomy does not establish disease-related tracer uptake. Noise and resolution sensitivity do not establish physiological robustness: scatter, body habitus, injection-to-imaging interval and renal function were not systematically evaluated. Reusing reference cases for parameter selection and assessment limits independent validation. Future work includes bone-component and joint-region priors, controlled lesions and multi-view labels for anatomical localization and lesion-related learning; pathological fidelity and downstream training benefit remain unvalidated.

壁報論文 臨床組 **PC-096**

原著論文 非診療之臨床相關主題

核醫科品質指標分析工具P管制圖即時監控平台之開發與應用

[1]張添信

[1]台中慈濟醫院

Keywords 品管 | 流程優化 | 行政管理 | 主管單位查核

Background

在核子醫學科的臨床實務中，統計製程管制 (SPC) 是監控放射藥物、儀器妥善率與報告時效等關鍵指標的重要工具，傳統手動繪製管制圖的流程不僅耗費大量行政人力與時間，且容易產生人為計算誤差，靜態的圖表更缺乏即時風險預警機制，為解決這些痛點，醫療品質管理團隊自主開發了數位化、自動化的視覺圖表分析平台，期望透過即時的燈號警示與動態管制界限，在不良事件或流程異常發生前及早介入，落實預防性與主動性的醫療品質風險管控管理。

Method

本系統全面採用純前端網頁技術架構開發，運用HTML5與JavaScript進行SPC核心統計數學運算，打造專業的視覺化介面，在醫療資安防護上，系統運算皆於使用者瀏覽器端獨立執行，數據自動儲存於本機快取而不上傳雲端，同時整合支援Excel匯入匯出功能以降低登打負擔，計算模型方面，系統支援「計算歷史平均值」與「挑戰自訂目標值」雙軌模式，並能自動依據每個月的樣本數，動態精準計算當期中心線、標準差以及 2σ 與 3σ 的管制與警告界限。

Results

系統上線後成功將繁複的統計分析自動化，並內建了五大核醫核心品質指標監控，包含放射藥物浪費率（低好）、注射外滲率（低好）、住院報告 24 小時達成率（高好）、門診報告 72 小時達成率（高好）與核醫設備運轉率（高好）。此外，系統結合嚴格的判定規則提供即時脈衝動畫警示：數據超出 3σ 界限會顯示「失控」紅燈提示啟動根本原因分析；連續 3 點有 2 點落於同側 2σ 外顯示「快失控」橘紅燈；落於2σ 與 3σ 之間顯示「警告」橘燈；穩定落於 2σ 區間內則顯示「管制內」綠燈，大幅提升了臨床數據的可讀性與判讀效率。

Conclusion

製作核醫專屬數位化P管制圖即時監控平台，不僅確保了最高規格的醫療資安，有效降低第一線品管人員的操作門檻與學習成本，自動化的偵測規則與直觀的數據洞察，提升跨部門品質會議的溝通效率，強化臨床風險的早期預警能力，在實務推廣上，建議使用者仍需參與SPC相關教育訓練以避免臨床數據誤判，未來本平台也將利用前端架構的高靈活度，進一步擴充更多元的醫療品質指標模組，以滿足不同科室的臨床品管需求。

壁報論文 臨床組 **PC-097**

經驗分享 非診療之臨床相關主題

應用擬真情境演練提升核醫科急救應變技能之經驗分享

[1]陳薇璇, [1]許幼青, [1]廖建國, [1]游舜宇

[1]大林慈濟醫院

發表者 陳薇璇

Keywords 流程優化

Background

核醫科因檢查特性，病人常於造影過程中發生生命徵象變化，放射師需具備即時急救應變能力。然而現況分析發現團隊在基本救命術（BLS）訓練後，仍普遍缺乏臨場實戰經驗與團隊默契，加上電擊器操作不熟悉、急救現場口頭溝通聲音不明顯等問題，可能延誤急救時效與影響病人安全。有鑑於此，本科以「病安在心，急救在行」為主題，導入擬真情境演練，強化急救動作執行與團隊協作。

Method

1.設定改善目標為提升急救動作執行完整性、建立團隊合作流程。2. 擬定對策，包括建立擬真情境演練劇本、邀請急診醫師指導專業技術，並規劃年度模擬演練制度化。3. 依團隊資源管理（TRM）架構，逐年導入標準化急救流程：事前說明（Brief）→呼叫支援（Call-Out）→推電擊車（AED）、急救車 → 放置背板 → 高品質壓胸、確實給氧 → 貼AED貼片、AED電擊 → 閉環溝通（Closed-Loop Communication）→相互支援（Mutual Support）→事後檢視（Debrief）。

Results

透過持續導入擬真情境演練，急救流程逐年改善：2022 年著重於確實給氧與高品質壓胸；2023 年強化TRM Call-Out及確實放置背板；2024 年將傳統電擊器轉換為AED模式，並強化TRM相互支援；2025 年進一步導入TRM閉環溝通與擬真Debrief機制。成效評估以確實壓胸、確實給氧、放背板、拿腳凳及AED操作五項指標計算，每年演練 2 次，年度達成率為五項指標總執行次數除以應執行次數（10 次）。達成率由 2022 年10%，提升至 2023 年 50%、2024 年 60%，2025 年達 90%。此外，團隊亦代表醫院參與外部擬真競賽，於 2024 年放射全聯會擬真情境類獲核醫組金獎，2025 年於NCMEA國家臨床醫學教育獎擬真情境類競賽獲金獎，顯示團隊訓練成果和外部專業肯定。

Conclusion

導入擬真情境演練搭配TRM團隊資源管理，並逐年建立標準化急救流程，有助於提升放射師急救動作執行，與團隊分工配合之完整性。未來規劃進一步導入碘 131 病房急救演練，結合核醫科、加護病房（ICU）、輸送、新陳代謝科、急診護理師與急救小組等跨科別團隊，持續強化全院急救應變網絡與病人安全。

壁報論文 臨床組 **PC-098**

經驗分享 非診療之臨床相關主題

結合教學影片與情境模擬之核醫臺灣台語教學課程：實習生學習反應之初探

[1]王苡安, [1]廖建國, [1]莊紫翎

[1]大林慈濟醫院
[2]慈濟大學

發表者 王苡安

Keywords 衛教 | 教學

Background

核子醫學科服務對象以中高齡族群居多，且臺灣南部部分病人習慣以臺灣台語溝通。放射師實習生於核醫科實習期間，需執行病人引導、病史詢問、檢查說明及相關臨床作業，因此熟悉臨床常用臺灣台語表達具有實務意義。為協助實習生熟悉核醫檢查情境中的臺灣台語用語，本研究建置「核醫臺灣台語臨床教學」課程，並初步評估實習生的學習表現與課程反應。

Method

本研究採課程介入前後測之先驅性研究設計，研究對象為 2025 年至本院核子醫學科實習之醫學影像相關科系實習生。課程內容包含核醫檢查常用臺灣台語、病史詢問、檢查前準備及檢查說明，並結合翻轉教學、教學影片、情境模擬與臨床演練。課程介入前後以五題認知測驗評估學習表現，題目涵蓋病人身分確認、候診區病人引導與確認事項、特殊病史下的血壓測量、生理監視器數據判讀，以及心肌灌注檢查第一階段後的衛教注意事項。課程結束後，使用 10 題李克特五點量表進行教學滿意度調查，內容包含教學目標、教材與簡報、臨床案例運用及專業技能學習等面向。量表原始總分為 10 至 50 分，並換算為百分制呈現（(原始得分 /50)×100）；分數越高代表滿意度越高。

Results

本研究共收集 5 位實習生的教學資料。認知測驗前測結果為：1 位得分 60 分、1 位得分 80 分、3 位得分 100 分；後測結果為：1 位得分 80 分、4 位得分 100 分。整體而言，後測達滿分的人數由前測的 3 位增加至 4 位。教學滿意度換算為百分制後，1 位實習生得分 80 分，其餘 4 位得分 100 分。整體而言，實習生對課程的滿意度高，並回饋教學影片及情境式學習有助於理解核醫臨床情境，以及熟悉臺灣台語在病史詢問、檢查說明與病人互動中的應用。本研究未納入高齡病人，也未直接測量病人端結果，因此尚無法判定課程對實際病人溝通成效的影響。

Conclusion

本研究完成核醫臺灣台語臨床教學課程之初步建置，並觀察實習生認知測驗表現及教學滿意度。結果顯示，多數學生於前後測皆維持高分，且課程滿意度高，顯示此課程具教學可行性與推廣潛力。然而，本研究樣本數有限，評量工具以五題認知測驗及學生滿意度為主，尚不足以證實實習生臨床溝通能力已提升，也未評估高齡病人的溝通經驗或照護結果。未來可擴大研究樣本、建立更完整的情境式溝通能力評量，並納入病人端回饋，以進一步評估課程成效。

壁報論文 臨床組 **PC-099**

經驗分享 非診療之臨床相關主題

從擬真模擬競賽到臨床實踐：團隊資源管理與病人安全之經驗分享

[1]陳薇璇, [1]許幼青, [1]廖建國, [1]游舜宇

[1]大林慈濟醫院

發表者 陳薇璇

Keywords 擬真模擬競賽 | 病人安全

Background

擬真模擬訓練透過情境重現臨床事件，使人員進行判斷、溝通與處置，強化團隊合作及病人安全等非技術性技能。團隊於 2024 年「全國醫學影像暨放射科學臨床技能競賽」醫事放射擬真情境類核醫組，以及 2025 年「NCMEA 國家臨床醫學教育獎擬真情境類競賽」醫事放射組獲得金獎。兩次競賽準備過程中，透過情境演練與賽後檢討，發現競賽情境可將日常容易忽略的細節放大，促使團隊重新檢視臨床風險，並將角色分工、情境監測及結構化溝通等 TRM 概念帶回日常工作。核醫科各檢查環節皆存在潛在風險，小事應成為主動確認與預防的起點。

Method

本次以 2024、2025 年兩次擬真競賽訓練與參賽經驗為基礎，由核醫科參賽團隊（3名放射師＋1 名護理師）進行角色分工、情境演練、溝通訓練及賽後檢討，將臨床常見照護與突發狀況融入情境，並將演練後辨識的風險與應對方式帶回日常工作。訓練融入結構化溝通與 Cross Monitoring 等 TRM 技巧，並透過安全疑慮表達及重新評估強化團隊合作。情境亦強調及早辨識小異常，如病人空腹檢查後出現頭暈、無力，應評估低血糖並依流程處理；急救情境則熟悉 AED 操作與院內流程，在符合規範下及早啟動急救程序。

Results

參與模擬演練競賽後，團隊將訓練中建立的習慣帶回臨床，於日常工作中觀察到相關行為改變。以往工作多以任務完成為導向，檢查結束、報告產出即視為告一段落，病人出現輕微不適時也常歸因於緊張；回到臨床後，成員會更主動確認病人的安全狀態。例如面對疑似低血糖的病人，會主動詢問空腹時間、評估生命徵象，並依SOP 轉介護理人員處理。急救情境方面，過去多是被動等待急救團隊到場；經訓練熟悉 AED 操作與院內急救流程後，能在符合規範的前提下及早啟動急救程序，爭取處置時間。溝通方面，則由過去的口頭轉達、事後回報，轉為運用 SBAR、Call-Out 與Check-Back，使訊息傳遞更有結構，確認也更加確實。這些習慣也延伸到病人移位、檢查前評估及藥物注射後觀察等日常環節，團隊於臨床工作中持續運用相關技巧。

Conclusion

透過兩次競賽準備與擬真訓練，團隊重新檢視日常工作中容易被忽略的風險，並將訓練中的觀察、溝通與相互支援技巧應用於臨床工作。病人安全不只是正確完成影像檢查，更包含主動觀察、及時辨識異常，以及與團隊有效溝通合作。臨床越熟悉的流程越容易產生習慣性思考，因此面對異常應多一分觀察、多一次確認，必要時主動通報並尋求支援。從把事情做完，到把事情安全地做好，是本次經驗最重要的體會。未來將持續透過擬真訓練與流程檢視，強化團隊非技術性技能與病人安全文化。

壁報論文 臨床組 **PC-100**

原著論文 | 臨床治療或診療合一

轉移性去勢抗性攝護腺癌病人接受Radium-223治療之完成施打率探討

[1]張添信

[1]台中慈濟醫院

Keywords 流程優化 | 同位素治療 | 精準醫療

Background

Radium-223(Ra-223)是一種能發射α射線的標靶放射性同位素，能有效延長伴隨骨轉移之轉移性去勢抗性攝護腺癌（mCRPC）患者的整體存活期，標準療程為施打 6 劑，然而在真實世界臨床實務中，患者常因骨髓毒性或疾病快速惡化而被迫提早中斷治療，本研究目的探討單一機構 mCRPC 患者接受 Ra-223 治療的實際施打完成率，分析提早停藥的臨床原因，並評估完成標準療程與患者 40 週存活狀態之關聯性。

Method

本研究為回溯性觀察研究，共納入 13 位確診為 mCRPC 且接受Ra-223治療的男性患者，Ra-223以約每 4 週間隔靜脈注射，目標完成 6 劑療程，回溯追蹤患者總觀察期達 40週，記錄其實際施打劑數、提早中斷原因（包含疾病惡化或無法耐受之毒性），以及觀察期末的存活狀態，圖表視覺化採用游泳者圖（Swimmer Plot）呈現個別病患之治療時序與臨床事件。

Results

本研究世代共納入 13 位 mCRPC 病患 (平均年齡：77.2 歲)，分析結果顯示有 7 位順利完成 6 劑滿療程（完成施打率達 53.8%），而另外 6 位未滿 6 劑即提早中斷（佔 46.2%，中位數施打劑量為 3.5 劑），進一步分析提早中斷的原因，最主要為疾病惡化，共計 4 位（佔整體 30.8%），且多發生於第 3 至第 5 劑之間；另有 2 位（佔 15.4%）則是於施打 3 劑後因毒性不良反應而停止治療，在預後與存活狀態方面，經過 40 週的觀察期，共有 7 位存活（53.8%）及 6 位死亡（46.2%），值得注意的是，順利打滿 6 劑的完成施打組展現出較佳的存活優勢，高達 85.7%（6/7）的患者於觀察期末仍存活，相較之下未完施打組僅有 16.7%（1/6）存活，清楚顯示出療程完成施打率與否與患者的中短期存活狀態具有高度的關聯性。

Conclusion

本機構的經驗顯示，mCRPC 骨轉移患者接受 Ra-223治療的完成施打率約為 54%，且能夠順利完成 6 劑療程的患者，展現出較高的 40 週描述性存活比例，此結果凸顯了在臨床實務上，精準挑選合適病患及早期介入的重要性，未來有賴擴增樣本數，進一步探討影響完成施打率的基線血液與影像學預測因子。

壁報論文 臨床組　　**PC-101**

經驗分享　非診療之臨床相關主題

運用目視化管理優化核醫檢查交班流程之經驗分享

[1]陳薇璇, [1]廖建國, [1]游舜宇

[1]大林慈濟醫院

發表者　陳薇璇

Keywords　病人安全 | 流程優化

Background

核醫科病人完成全身骨骼掃描後，若經醫師判讀需進一步安排 SPECT/CT 加照，需先移至走廊等候，並將檢查單轉送至另一造影室，由該機台人員後續叫號。過去因中午輪替交班、人員忙碌分心或新進同仁尚未熟悉流程，偶有交班資訊中斷，導致等候加照病人未被即時掌握，甚至曾發生病人於完成全身骨骼掃描後逕自離開，直至另一機台準備叫號時才發現。此類情形雖可透過聯繫病人返回處理，仍屬應避免之流程疏失。有鑑於此，本單位導入精實醫療（Lean Healthcare）概念，運用低成本目視化管理（Visual Management）工具，將原本仰賴口頭交班與個人記憶的「待SPECT/CT 加照」資訊轉換為現場可辨識的視覺提示，以降低資訊斷點。

Method

本單位設有 2 台 Gamma Camera 及 1 台 SPECT/CT。針對病人完成全身骨骼掃描後至SPECT/CT 加照的交接期，團隊設計書寫「切 SPECT/CT」之標示紙，平時反面朝外貼於電腦螢幕後方，不影響作業；當醫師確認病人需加照後，工作人員即將標示紙翻至螢幕正面，並同步將檢查單移至另一造影室，使後續接手人員可直接辨識該病人尚有未完成的檢查，不必完全仰賴口頭交班或個人記憶。另以「已叫廁所」、「人在走道」等夾子標記作為延伸應用，協助團隊掌握病人當下位置與狀態，並結合TRM Cross Monitoring概念，提供成員間相互提醒與確認的視覺提示。

Results

導入目視化管理前，於 2025 年 10 月至 2026 年 4 月期間，曾發生 4 例病人完成全身骨骼掃描後，因交班資訊中斷而未完成SPECT/CT加照即離開；導入目視化管理後，於2026 年 5 月至 2026 年 8 月期間，未再發生類似事件（0 例）。導入後即使遇到中午輪替交班、跨班別交接或新進同仁初次接手，後續人員仍可透過「切 SPECT/CT」標示辨識尚有未完成之加照檢查，讓待加照資訊於交接過程中持續可見，減少對口頭交班及個人記憶的依賴。「已叫廁所」、「人在走道」等標記於日常作業中則可協助團隊辨識病人暫離檢查區域等狀態，作為病人流程管理之輔助。

Conclusion

本經驗顯示，針對全身骨骼掃描後 SPECT/CT 加照的交班資訊斷點，不一定需要高科技系統，透過簡單的紙本標記即可將「待加照」資訊轉為現場共同可見，有助於降低因人員輪替、忙碌或記憶遺漏造成的資訊斷點，並協助團隊掌握病人檢查進度。將精實醫療與 TRM Cross Monitoring 概念融入日常工作，工具具低成本、容易執行及可複製等特色，可作為核醫臨床流程改善與病人安全管理之參考。

壁報論文 臨床組 **PC-102**

經驗分享 | 臨床治療或診療合一

結合AI衛教短影片於放射碘-131治療：提升病人輻射防護安全認知與放射師衛教給藥流程優化

[1]段玟卉, [1]許文齡, [1]董芳妤, [1]林宛宣, [1]陳芓安, [1]蔡席晨

[1]土城醫院

發表者 段玟卉

Keywords 衛教 | AI | 數位化系統 | 輻射防護 | 碘病房

Background

針對分化良好型甲狀腺癌或復發轉移患者，接受大於 30 毫居里（mCi）高劑量放射性碘 -131 治療時依法須入住隔離病房。傳統衛教依賴大量紙本且耗時 70–90 分鐘，患者易因資訊過載限制認知成效。為此，本專案透過跨團隊合作，將核心輻射防護與標準化給藥流程導入AI影像生成技術（Topview AI）建構數位教材，藉由視覺化工具提升病人認知、精簡放射師與護理師衛教工時，並確保隔離病房之輻射防護管理品質。

Method

本研究依據臨床實務與長庚醫院《放射性碘 131 治療病人須知》，提煉出輻射防護、腮腺炎預防、體外劑量測量及給藥流程等核心要點建構標準腳本。經放射師、護理師與專科護理師跨團隊模擬拍攝，並運用AI技術生成標準化數位衛教影片。成效評估本研究採行病人問卷進行實證分析，主要針對入住 I-131 隔離病房之患者，系統性評估其觀看影片後之輻射防護認知、衛教認知提升度及滿意度，據以確立教材之臨床應用價值。

Results

本研究自 115/07/09 至 115/08/03 共納入 26 位入住I-131隔離病房之患者，未來會持續收案。問卷結果顯示，患者對AI衛教影片整體滿意度平均得分均高於 4.50 分（滿分 5 分）。在認知提升上，以「服藥前後 2 小時禁食規定」與「每日飲水 2000–3000 c.c.」得分最高（皆為 4.88 分），實證AI影片在傳達核心定量資訊上具顯著成效；此外，「正確服藥方式」、「給藥流程順暢度」及「減少反覆詢問時間」均高於 4.65 分，證實該模式能有效減輕一線放射師與護理師之衛教工時，從原本的 82.6±16.4 分鐘縮短至71.2±10.4 分鐘。在優化建議與分層分析方面，部分患者反映語速略快，未來可於系統增設語速調整功能，以提供更客製化的衛教體驗。依人口統計學特徵進行分層分析顯示，20–39 歲青年族群對AI科技接受度最高（4.81–4.86 分）；性別部分呈現顯著差異，女性之正面評價（4.83–4.97 分）明顯高於男性（4.22–4.43 分）。據此，未來臨床上可針對男性患者加強口頭引導，進一步探討不同性別群體的認知需求差異，並優化影片之視覺呈現與訊息傳達方式，以期全面提升不同特質患者之衛教成效。

Conclusion

本研究實證，AI數位化衛教教材能有效提升放射性碘 -131 治療患者之防護認知，並具高臨床接受度，有助於降低患者入住隔離病房之焦慮感。同時，此模式可顯著減少重覆性諮詢、優化臨床流程，兼具深化學習成效與減輕團隊負荷之雙重效益。綜上所述，該創新教材未來可作為核子醫學隔離病房之標準化數位衛教工具，並推廣至其他核子醫學及放射治療相關臨床衛教領域之應用價值。

壁報論文 臨床組

PC-103

原著論文 非診療之臨床相關主題

運用HFMEA改善造影作業流程之成效分析

[1]廖建國, [1]陳薇璇, [1]游舜宇

[1]大林慈濟醫院

發表者 廖建國

Keywords 行政管理

Background

醫療照護失效模式與效應分析 (Healthcare Failure Mode and Effects Analysis，簡稱HFMEA)是一種預防式的風險管理工具，主要透過檢視整個醫療照護流程，系統性的找出流程中可能潛在的錯誤並預先修正，以預防可能的異常發生。本研究目的即為分析比較近 2 年HFMEA之風險評估資料，以了解近 2 年進步與退步的情形，作為持續改進之參考。

Method

收集 2025 及 2026 年之HFMEA年度風險評估資料，其中涵蓋各作業流程之風險 (包括主流程與次流程項)，比較 2024 年 (2025 年 1 月評估) 與 2025 年 (2026 年 1 月評估) 之年度風險評估之危害指數，以探討 2025 年之改善成效。危害指數以發生頻率與嚴重度之乘積計算，發生頻率 (表 1) 與嚴重度 (表 2) 之分級皆依HFMEA風險評估之手法執行。由於HFMEA年度風險評估資料，皆是依據前一年的品質表現所建立，當危害指數大於或等於 8，或屬於單點失效時，即被判定為高風險，並需進入決策樹分析以採取改善行動，因此資料也包括各項異常發生後的改善措施。本研究不探討各項改善措施，僅比較近 2 年HFMEA風險評估之危害指數進步與退步的情形。

Results

近 2 年之風險評估結果，主流程合計 13 項，次流程合計 58 項。比較近 2 年結果，可得知 2025 年各項目之危害指數有降低者計 8 項 (危害指數皆低於 8)，包括注射或給藥疏失主流程 1 件 (放射性藥物漏針導致輻射污染); 造影前準備異常主流程 2 件 (病人辨識錯誤、病人未排尿); 影像品質不良主流程 4 件 (影像不完整 / 腳底影像未完全照完、儀器設備異常導致影像品質不良、病人造影中移動且放射師未發現影像有異常、影像日期標示錯誤); 報告疏失主流程 1 件 (報告逾時 / 漏發報告)。而 2025 年各項目之危害指數有升高者計 4 項 (危害指數為 8 者有 3 項)，包括檢查醫囑不當主流程 1 件 (核醫醫師審查檢查單後醫囑錯誤)、藥品或耗材異常主流程 1 件 (漏訂藥品)、注射或給藥疏失主流程 1 件 (多針注射造成病人抱怨)、影像品質不良主流程 1 件 (影像方向標示錯誤)，針對這些項目造影室皆已列入 2026 年的優先改善項目，進行重點監控與審查。另外，近 2 年危害指數不變 (即無進步也無退步) 之次流程項目，合計 46 項 (危害指數皆低於 8)，比例佔 79.3%，顯示大多數的次流程項目皆可維持在高風險以下。

Conclusion

比較近 2 年結果，總計 58 項次流程中大多數的項目 (佔 79.3%) 危害指數不變，危害指數有降低者 (計 8 項) 佔 13.8%，而危害指數有升高者 (計 4 項) 佔 6.9%，顯示 2025 年有進步的項目明顯較退步者多，且大多數的次流程項目皆可維持在高風險以下。針對少數退步的項目，造影室將繼續進行監控與改善，以持續提升造影品質。

壁報論文 臨床組 **PC-104**

原著論文 臨床診斷

運用根本原因分析(RCA)改善核醫肺灌注檢查之靜脈外滲與藥物殘留

[1]林至群, [1]張雁翔

[1]高雄長庚醫院

發表者 林至群

Keywords 流程優化 | 品管 | 行政管理

Background

根本原因分析（RCA）是一種系統性的回溯方法，針對已發生的醫療異常事件進行全面性的因果探討，找出隱藏在表象背後的潛在系統性失效、流程漏洞與組織因素。以預防再發生的角度，對引發危機的核心原因重新審視並建立多重防護屏障，能阻絕重複性重大危害錯誤的發生。本單位於 2024、2025 年間接連發生 3 件肺灌注檢查（Lung Perfusion）之放射性藥物（Tc-99m MAA）靜脈外滲與管路卡藥異常事件，除了造成檢查失敗，更可能導致患者皮下組織遭受非計畫性局部輻射曝露，並引發環境輻射污染，是核醫臨床作業與輻射防護的重大議題。本研究目的在以跨團隊合作方式，運用根本原因分析方法，深度溯源異常事件的潛在原因。並針對現行作業流程與防護機制進行檢視，研擬具體且可執行之改善措施，強化人員操作標準、查核機制，建立多重防護屏障，降低類似事件再次發生之風險。期望透過本研究之改善介入，提升作業安全與品質，並兼顧病人安全與輻射防護，作為核醫部門後續臨床作業改善及異常事件管理之參考。

Method

本專案由核醫科放射師、護理師及醫師組成跨團隊改善小組，針對異常事件依循根本原因分析程序進行系統性分析。分析過程包括「事件重建與資料收集」、「近端原因分析」、「根本原因判定」及「改善行動發展」四大階段，透過事件時間軸重建、流程檢視及跨團隊討論，釐清事件發生之直接原因、潛在原因與系統性因素。依據RCA所辨識之根本原因，跨團隊共同制定並執行兩項核心改善策略：（一）標準化作業流程（SOP）修訂：建立靜脈通路評估、確認及異常處置指引，強化注射前之通路安全確認機制；（二）管路注射方式改良：針對原有注射流程之潛在失效點進行改善，增加注射過程中的主動式安全防護屏障，具體作法為注射藥物前先將病人肺部置於偵檢器下，採取分段注射法，先注入微量 Tc-99m MAA與生理食鹽水，由即時影像確認藥物確實進入肺部微血管後，方將剩餘藥物注入完畢。

Results

本單位自 2024 至 2025 年間共執行 465 件肺灌注檢查，其中發生 3 件漏藥事件導致病人需要重照，顯著高於近年本單位整體重照率 0.02%。透過RCA的方法，大幅降低漏藥異常事件的發生，改善前發生率為 0.65%(N=3)，改善後截至 2026 年 7 月發生率為 0%(N=0)。

Conclusion

運用RCA根本原因分析能有效減少核醫肺灌注檢查之靜脈外滲與藥物殘留，降低檢查重照率，在確保患者輻射安全的同時，亦顯著提升核醫臨床診斷效能與跨團隊照護品質。

壁報論文 臨床組

PC-105

原著論文 非診療之臨床相關主題

醫事放射職類核子醫學領域可信賴專業活動(EPAs)於放射實習生之應用

[1]張嘉容, [1]楊邦宏, [1]陳奕倫, [1]陳孟穎, [1]姜振豪

[1]臺北榮民總醫院

發表者 張嘉容

Keywords 教學 | EPAs

Background

近年來醫事人員臨床教育的改革以勝任能力導向醫學教育（Competency-Based Medical Education, CBME）為主要發展方向，並架構建置醫事放射職類的可信賴專業活動（Entrustable Professional Activities, EPAs）作為職場的訓練與評估。因核子醫學領域的新進醫事放射師人數較少，導致臨床教師在可信賴專業活動評分經驗值不易累積。本研究目的為建置出符合放射實習生的EPAs的臨床相關主題及可觀察實務活動，促進臨床教學，並了解臨床教師與實習生之使用經驗及滿意度。

Method

以放射全聯會公告臺灣醫事放射職類核子醫學可信賴專業活動EPAs公版為依據，以正子電腦斷層造影檢查(PET/CT)及全身骨骼掃描檢查兩項作為放射實習生之EPAs主題。透過本院 13 位核醫資深醫事放射師，採用名義團體法與修正式德菲法共識會議建立放射實習生版之EPAs任務。本研究共有 18 位實習生，依本院實習分站安排，於正子電腦斷層造影檢查實習半週，於進行全身骨骼掃描檢查之儀器的第一週及第二週，由 8 位臨床教師進行評分。以李克特五點量表問卷收集臨床教師與放射實習生對可信賴專業活動 (EPAs)之成效。

Results

本研究在共識會議後，公版之任務評分項目中「異常事件」(100%) 及「病人相關訊息交班」(61.5%) 皆有半數以上同意刪除，故不列入評分。18 位實習生之正子電腦斷層造影檢查EPAs的信賴等級評分，其中「OPA1檢查前準備」評分為 2a/2b/3a/3b人數分布為 1/2/11/4，「OPA2執行造影檢查」評分為 2a/2b/3a/3b人數分布為 2/5/8/3，「OPA3 檢查後處置」評分為 2a/2b/3a/3b人數分布為 1/3/8/6；全身骨骼掃描檢查EPAs的信賴等級評分，第一周「OPA1檢查前準備」評分為 3a/3b/3/4人數分布為 1/5/11/1，「OPA2執行造影檢查」評分為 3a/3b/3/4人數分布為 1/9/6/2，「OPA3 檢查後處置」評分為 3a/3b/3/4人數分布為 2/7/5/4。第二周「OPA1檢查前準備」評分為 3b/3c/4人數分布為 3/12/3，「OPA2執行造影檢查」評分為 3b/3c/4人數分布為 8/8/2，「OPA3 檢查後處置」評分為 3b/3c/4人數分布為 8/6/4，其中第二周全身骨骼掃描檢查EPA的信賴等級評分較高的人數增加。臨床教師與放射實習生對EPAs的評分及教學滿意度之李克特五點量表結果分別為 4.50 及 4.56。

Conclusion

透過建置適合於核子醫學領域放射實習生之可信賴專業活動 (EPAs)的評估系統，有助於提升臨床教師的教學及評分與放射實習學生的學習。

壁報論文 臨床組 **PC-106**

個案報告 臨床診斷

攝護腺癌患者在骨頭掃描及 18F-PSMA掃描中的轉移性超級掃描分享

[1]許文齡, [1]張淑敏, [1]紀雅閔, [1]張晉銓, [1]莊雅雯, [1]王榛婷

[1]高雄醫學大學

發表者 許文齡

Keywords 有趣影像

Background

骨頭掃描是核醫常見用於癌症骨轉移的一項檢查，PSMA(prostate-specific membrane antigen)為一種攝護腺特定膜抗原，利用此特性，標記上同位素，能在攝護腺癌診斷中提高靈敏度，在PSA輕微上升或復發初期找到微小淋巴或骨頭病灶。正常的PSMA影像中，會見唾液腺、淚腺、腸胃道、腎臟泌尿系統、肝臟、脾臟的正常攝取。超級掃描 (Super scan)是骨頭掃描中一種特殊的表現，其骨骼活性遠高於軟組織，而泌尿系統活性微弱或沒有；在PSMA表現上為：骨骼瀰漫性放射性活性增高，而唾液腺、淚腺、肝脾臟、近端小腸和腎臟的放射性或性減少。

Case report

一位 76 歲攝護腺癌男性因私人因素從外院轉至本院核醫科先後進行骨頭掃描及F-18 PSMA檢查，分期：T3bN0M1b, 4B。PSA由 261.56ng/ml慢慢增加至 297.68ng/ml。骨頭掃描顯示：全身骨骼多處放射性活性增加，尤其以中軸骨及四肢近端為主，腎臟及全身軟組織放射性活性幾乎消失，為典型的Super scan表現。而 F -18 PSMA掃描顯示：唾液腺、淚腺、腎臟、肝、脾臟、小腸射性活性幾乎消失，骨骼呈現瀰漫性PSMA攝取，為典型的Super scan攝取。

Conclusion

Super scan是骨頭掃描中特殊的表現，常見於攝護腺癌、乳癌、肺癌的病人，因其容易造成廣泛性骨轉移，然而副甲狀腺機能亢進、腎性骨病發育不全或骨軟化症等，也可能造成其現象需謹慎評估。18F-PSMA因能及早發現微小的病灶，是目前公認偵測攝護腺癌淋巴結及遠端轉移的最佳檢查，搭配Lu-177同位素標靶治療，能在賀爾蒙治療或化療效果有限時，精準破壞癌細胞，有效延長病人整體存活時間、延後復發、減少骨骼相關併發症，然而當疾病進展到一定程度，是否能進行Lu-177治療則需臨床謹慎評估。

壁報論文 臨床組 **PC-107**

原著論文 臨床治療或診療合一

Predictive Value of PSMA PET Radiomics for PSA Progression-Free Survival After Metastasis-Directed Radiotherapy in Metastatic Prostate Cancer

[1,2]黃玉儀, [1]陳志成

[1]陽明交通大學

[2]和信醫院

發表者 黃玉儀

Keywords 分子影像 | 影像組學 (Radiomics)

Background

PSMA PET radiomics may predict PSA progression-free survival (PSA-PFS) after metastasis-directed radiotherapy, but whether ADT modifies this remains unclear.

Method

Retrospective single-institution study: 37 metastatic prostate cancer patients with pre-radiotherapy 68Ga-PSMA-11 PET/CT. PSA-PFS: time to PSA progression (Phoenix/Chicago criteria) or censored at last follow-up. We extracted 107 radiomics features from 128 PSMA-avid lesions, reduced to 8 representative features via variance and Spearman filtering, and mean-aggregated at patient level. Median radiomic score was used as the cutoff for risk stratification. A standardized LASSO-Cox model was developed with lambda selected by leave-one-out cross-validation. Bootstrap validation (1,000-resample, OOB C-index) assessed model discrimination.Subgroup and sensitivity analyses evaluated post-radiotherapy ADT status and patients with ≤5 lesions.

Results

Among 37 patients, 24 PSA-PFS events were observed; 18 patients received post-radiotherapy ADT, and 30 patients had five or fewer lesions. In this exploratory analysis, the radiomic score stratified PSA-PFS in the full cohort, with median PSA-PFS of 7.0 months (high-risk) versus 25.0 months (low-risk; log-rank p = 0.0006). However, the substantial gap between apparent C-index (0.717) and bootstrap out-of-bag C-index (0.555; 95% CI, 0.321-0.750) indicates considerable model overfitting. The OOB C-index of 0.555 suggests modest discriminative ability only marginally better than chance (0.5), highlighting the risk of overfitting in this small exploratory cohort (N=37) and the need for external validation in independent cohorts. Stratification persisted in ADT and no-ADT subgroups (ADT: 8.0 vs 25.0 months, p=0.0084). ADT-interaction was not significant (p=0.37). Oligo-only sensitivity analysis (n=30) showed similar patterns (8.0 vs 25.0 months, p=0.0063, OOB C-index 0.533). In contrast, a clinical model incorporating clinical risk factors, treatment history, and the number of PSMA PET-detected lesions did not significantly stratify PSA-PFS by Kaplan-Meier analysis (p = 0.284).

Conclusion

Exploratory results suggest pre-treatment 68Ga-PSMA-11 PET radiomics may stratify PSA-PFS, but optimism bias (0.717→0.555) and small sample size preclude clinical application without external validation.

壁報論文 臨床組 **PC-108**

個案報告 臨床診斷

Discovery of Diffuse Large B-Cell Lymphoma via Lymphoscintigraphy SPECT/CT in a Patient with Unilateral Limb Edema

[1]曾昶深, [1,2]陳昱宏, [1]何靜淳, [1,2]黃威翰, [1]黃想容, [1]劉淑馨

[1]花蓮慈濟醫院
[2]慈濟大學

發表者 曾昶深

Keywords 分子影像 | 有趣影像

Background

Unilateral lower limb edema in the elderly is often attributed to venous insufficiency, deep vein thrombosis (DVT), or lymphedema. However, secondary lymphedema caused by an underlying malignancy obstructing the lymphatic drainage is a critical differential diagnosis. While conventional lymphoscintigraphy evaluates lymphatic flow, the addition of single-photon emission computed tomography/computed tomography (SPECT/CT) provides additional anatomical information. Here, we report a case of diffuse large B-cell lymphoma (DLBCL) presenting initially as unilateral limb edema, which was discovered using lymphoscintigraphy SPECT/CT.

Case report

An 81-year-old woman presented with progressive left lower limb edema for four months, accompanied by poor appetite and generalized weakness. She reported no fever, night sweats, or significant weight loss. Initial lower extremity vascular ultrasonography showed no DVT but revealed enlarged lymph nodes in the left inguinal region. To evaluate the lymphatic function, Tc-99m phytate lymphoscintigraphy with SPECT/CT was performed. The planar images demonstrated proximal and distal dermal backflow in the left lower limb with visualization of inguinal lymph nodes but no visible lymphatic ducts, confirming lymphedema. Furthermore, the transmission CT component incidentally revealed multiple enlarged, confluent lymph nodes in the retroperitoneal and bilateral inguinal regions, highly suggestive of malignancy. Lymph node biopsy confirmed DLBCL, and the patient was treated with Rituximab and Lenalidomide.

Conclusion

DLBCL rarely presents with isolated unilateral lower limb edema, mimicking benign venous or lymphatic obstruction. This case underscores the importance of investigating secondary causes of lymphedema in older adults, even when classic B symptoms (fever, night sweats, weight loss) are absent. Furthermore, it demonstrates the clinical benefits of hybrid imaging with lymphoscintigraphy SPECT/CT. By simultaneously confirming the physiological impairment of lymphatic drainage and mapping the underlying structural etiology, SPECT/CT enabled early biopsy and timely medical intervention.

壁報論文 臨床組 **PC-109**

個案報告 臨床診斷

Clinical Utility of 18F-FDG PET/CT in Head and Neck Squamous Cell Carcinoma: Case Analysis and Exploration of Incidental Uptake

[1]許雅晴, [1]許友齡

[1]嘉義基督教醫院

發表者 許雅晴

Keywords 有趣影像

Background

18F-FDG PET/CT is crucial for staging, treatment selection, response assessment, and prognosis in oral cancer due to its high accuracy in detecting nodal involvement and distant metastasis. However, false positives from physiological or inflammatory uptake (e.g., in the tongue) remain a major diagnostic challenge.

Case report

A 57-year-old male with upper gingival SCC underwent FDG PET/CT for post-chemotherapy evaluation, showing primary tumor, pulmonary metastasis, and incidental prostatic FDG uptake. Over 10 months, stable PSA levels (1.1 ng/mL) and complete resolution of prostatic uptake on follow-up PET/CT confirmed the finding was transient/non-specific rather than a second malignancy.

Conclusion

A retrospective review shows incidental FDG PET/CT findings occur in ~35% of patients, with non-prostate cancer populations exhibiting incidental prostatic uptake in 1.6%–2.83% of cases. Because oral squamous cell carcinoma primarily metastasizes to the lungs and rarely to the prostate, such findings should be managed as non-specific incidental uptake rather than presumed metastasis.

Although malignant lesions typically exhibit higher SUVmax, studies have confirmed a significant overlap in SUVmax between benign conditions (such as BPH or prostatitis) and malignant tumors; thus, SUVmax alone is insufficient for a definitive diagnosis. Compared to diffuse uptake, focal uptake located in the peripheral zone carries a higher risk of malignancy (approximately a 5-fold increase), yet its positive predictive value remains only about 25%, serving merely as a risk modifier. Within clinical management algorithms, serum PSA levels are a more robust differential indicator than SUVmax. As demonstrated in this case, the patient’s stable PSA levels (1.1 ng/mL) and the complete resolution of uptake in subsequent follow-up imaging strongly support that the initial finding was a transient, non-specific inflammatory or physiological response rather than a malignancy.

When encountering such incidental findings, that should detailly describe the uptake pattern (focal vs. diffuse) and CT morphology. If the uptake is focal and accompanied by persistently elevated PSA, referral to urology for multiparametric MRI (mpMRI) or biopsy evaluation should be recommended. In deciding whether to proceed with invasive procedures, the prognosis of the patient’s primary cancer (e.g., oral cancer) and whether diagnosing a second primary cancer would substantially alter the treatment strategy must be carefully weighed.

In conclusion, combining 18F-FDG PET/CT with PSA levels and serial imaging prevents overdiagnosis and unnecessary invasive interventions.

壁報論文 臨床組 **PC-110**

原著論文 臨床診斷

Code-less, LLM-Assisted Development of a Cross-Platform, HIS-Interoperable Structured Reporting Tool for 18FDG PET/CT Lymphoma with Integrated Deauville Criteria, Lugano Classification, and Richter Transformation Red-Flag Alerting

[1]李碧芳

[1]彰化基督教醫院
[2]高雄秀傳紀念醫院
[3]成大醫院

Keywords 數位化系統 | 分子影像 | 智慧醫療 (ML/DL/LLM)

Background

Lymphoma staging and response evaluation rely heavily on 18F-fluorodeoxyglucose positron emission tomography/computed tomography (F18-FDG PET/CT) imaging utilizing standardized frameworks such as the Lugano classification and the five-point Deauville criteria. Identifying aggressive transformation, such as Richter Transformation (RT) in chronic lymphocytic leukemia, is critical for clinical decision-making. However, conventional PET/CT lymphoma reports are typically narrative free-texts lacking systematic integration, structured scoring, and prompt clinical red-flag recognition. Existing structured solutions often demand cumbersome IT involvement or expensive commercial licensing, hindering deployment across fragmented hospital information systems (HIS). We describe a clinician-developed, self-contained structured reporting tool for FDG PET/CT lymphoma evaluation, integrating automated Deauville scoring, Lugano staging assistance, and RT red-flag detection.

Method

Using iterative natural language prompting with an LLM, a single-file HTML/JavaScript application was constructed without software engineering support. The tool features an 8-step workflow: (1) Demographics with RT red-flag screening (B-symptoms, LDH, cytopenias); (2) Technical parameters; (3) Comparison study; (4) Anatomical findings across four regions with dynamic lesion descriptors and Deauville scoring (1–5, X); (5) Impression compiler; (6) Rule-based Lugano staging logic mapping nodal/splenic/extranodal sites to Stages I–IV (with IE/IIE suffixes); (7) Standardized recommendations; and (8) Plain-text report generator. To address data privacy, all processing occurs entirely client-side without external network transmission. Browser LocalStorage provides auto-save protection against accidental browser reloads, while an explicit human-in-the-loop review interface enables clinicians to verify and edit all generated text prior to final HIS copy-pasting.

Results

The single-file architecture operates locally in any standard web browser without database installation or vendor lock-in. The rule-based staging engine accurately maps anatomical distribution to Lugano criteria. The integrated RT checklist facilitates prompt documentation of disease transformation. Client-side local execution guarantees complete patient data privacy, while the review interface ensures 100% human verification of AI-assisted outputs before HIS integration.

Conclusion

Clinician-directed LLM development enables independent creation of secure, zero-cost, HIS-interoperable structured reporting tools. Combining rule-based staging logic, Deauville criteria, and RT red-flag detection with privacy-preserving client-side execution enhances reporting standardization and decision support without software engineering resources. Formal quantitative clinical validation (e.g., time-motion studies, completeness rates, or multi-reader comparisons) was beyond the scope of the present work and is planned for subsequent studies in the near future.

壁報論文 臨床組 **PC-111**

統合分析 臨床治療或診療合一

Comparative Safety and Real-World Survival Outcomes of 177Lu-PSMA-617 versus 177Lu-PSMA-I&T Radioligand Therapy in Metastatic Castration-Resistant Prostate Cancer: A Systematic Review and Meta-Analysis

[1]諶鴻遠, [2]陳力瑜, [2]郭心柔, [2]黃雅庭

[1]高雄榮民總醫院
[2]普瑞默生物科技

發表者 諶鴻遠

Keywords Radioligand Therapy | PSMA | mCRPC

Background

PSMA-targeted radioligand therapy (RLT) is established for metastatic castration-resistant prostate cancer (mCRPC). 177Lu-PSMA-617 (VISION/TheraP) and 177Lu-PSMA-I&T share the PSMA-binding motif but differ in chelator (DOTA vs DOTAGA) and pharmacokinetics, and are used interchangeably despite limited head-to-head evidence. We compared their efficacy and safety in mCRPC.

Method

A comprehensive and systematic search of the databases of PubMed/MEDLINE and Cochrane Library was performed to retrieve original articles published until June 25, 2026. Two authors independently reviewed the titles and abstracts of the retrieved articles based on the inclusion and exclusion criteria. To ensure independent observations, overlapping institutional cohorts were carefully de-duplicated. Primary outcomes evaluated were the PSA≥50% decline rate and median overall survival (OS).

Results

Five studies involving 593 patients were included. Regarding biochemical responses, the primary pooled analysis for PSA decline ≥50% showed no statistically significant difference between 177Lu-PSMA-I&T and 177Lu-PSMA-617 (OR = 0.84, 95% CI: 0.44–1.59). In contrast, any PSA decline was more frequent with 177Lu-PSMA-617 than with 177Lu-PSMA-I&T with a modest but statistically significant difference (OR for I&T vs. 617 = 0.63, 95% CI: 0.41–0.98). Safety analyses showed greater reductions in leukocyte and platelet counts with 177Lu-PSMA-617, whereas Grade 1–2 nephrotoxicity was more frequently observed with 177Lu-PSMA-I&T. Grade ≥3 hematologic and renal toxicities were uncommon in both groups.

Conclusion

177Lu-PSMA-I&T and 177Lu-PSMA-617 showed similar PSA50 response and overall survival, but differed in biochemical response and toxicity profiles. 177Lu-PSMA-617 was associated with a higher rate of any PSA decline and greater reductions in leukocyte and platelet counts, whereas low-grade nephrotoxicity was more frequent with 177Lu-PSMA-I&T. Whether these differences are attributable to the radioligands themselves remains uncertain because treatment protocols and dosimetry assessment were not standardized across studies. Prospective, randomized head-to-head studies using standardized treatment protocols and patient-specific dosimetry are warranted.

壁報論文 臨床組　　**PC-112**

原著論文　非診療之臨床相關主題

臺灣五十年核子醫學研究發展：以 Web of Science Core Collection 收錄文獻為基礎之書目計量分析

[1]郭之凡, [1]洪光威, [2]黃怡璇, [3,4]楊盈盈, [1,4]黃信彰

[1]彰濱秀傳醫院
[2]振興醫院
[3]臺北榮民總醫院
[4]陽明交通大學

發表者　郭之凡

Keywords　分子影像 | 核子醫學 | 書目計量分析 | Web of Science | 引用分析

Background

書目計量分析（bibliometric analysis）可量化評估研究生產力、學術影響力及國際合作。本研究旨在分析 1973–2025 年臺灣核子醫學研究於 Web of Science Core Collection 收錄之文獻，探討其發展趨勢、學術表現及國際合作網絡。

Method

自 Web of Science Core Collection（SCI-Expanded 及 SSCI）檢索作者地址含「Nuclear Medicine」且國家／地區為 Taiwan、出版年 1973–2025 之文獻（檢索日期 2026 年 6 月 21日），即以核子醫學單位參與發表之文獻為分析母體。分析年度發表篇數、引用次數、H-index、期刊影響因子（IF）、研究領域、機構、作者、期刊、研究經費及國際合作情形；期刊舊刊名併入現刊名，作者姓名之索引變體（如全名與縮寫）經人工檢視合併，並以 VOSviewer 進行國際合作網絡分析。

Results

共納入 4,783 篇文獻（全球第 17 位），累積引用 147,304 次，平均每篇 30.8 次，H-index為 121。年發表量自 1990 年代中期快速成長，於 2015 年達高峰（311 篇），其後回落；年度平均 IF 於研究期間維持穩定。主要研究領域為「放射學、核子醫學與醫學影像」、腫瘤學及一般內科學；中國醫藥大學及長庚紀念醫院為最具生產力之機構。

17.7% 之文獻具國際合作，其發表期刊之平均 IF 顯著高於無國際合作者（7.76 vs. 4.96，$p < 0.001$）。

Conclusion

過去五十餘年間，臺灣核子醫學研究累積可觀產出並涵蓋多個醫學領域；2015 年後產出回落之成因仍待探討。國際合作與較高之期刊 IF 相關，可能為提升臺灣核子醫學研究影響力之重要途徑，可供學術發展與合作規劃參考。

SPONSORS

贊助廠商

感謝以下廠商支持本次年會（依贊助順序排列）

NOVARTIS

Reimagining medicine, together.

台灣諾華股份有限公司

奇異亞洲醫療設備股份有限公司

GMS GLOBAL MEDICAL SOLUTIONS TAIWAN, LTD. 臺灣新吉美碩股份有限公司

臺灣新吉美碩股份有限公司

普瑞默生物科技股份有限公司	恩典科技股份有限公司	台灣璞氏健康發展有限公司
元新儀器股份有限公司	輝瑞大藥廠股份有限公司	艾拉倫股份有限公司
巨研科技股份有限公司	吉晟生技股份有限公司	富特茂股份有限公司
常捷生醫科技股份有限公司	西門子醫療設備股份有限公司	貝克西弗股份有限公司
台灣禮來股份有限公司	泰歷藥品儀器股份有限公司	財團法人中華民國輻射防護協會
愛樺企業股份有限公司	冷泉港生物科技股份有限公司	昶洋貿易股份有限公司
台灣拜耳股份有限公司	法商益普生股份有限公司台灣分公司	龍霆科技企業有限公司

PLUVICTO® 鐳必妥 注射液
lutetium(177Lu)vipivotide tetraxetan 1,000 MBq/mL

全方位的治療武器

PSMA+ mCRPC 兼顧療效及安全性的治療選擇



產品名稱: 鐳必妥®注射液 1000百萬貝克/毫升 PLUVICTO® 1,000 MBq/mL (衛部藥輸字第R00106號)
適應症:Pluvicto適用於治療曾接受雄性素受體途徑抑制(ARPI)療法之攝護腺特異性膜抗原(PSMA)陽性之轉移性去勢抗性攝護腺癌(mCRPC),且具以下情況的成人病人:適合延後以紫杉醇為基礎(taxane-based)的化學治療,或曾接受以紫杉醇為基礎(taxane-based)的化學治療。禁忌:無警語:放射線暴露風險、骨髓抑制、腎毒性、胚胎-胎兒毒性、不孕風險。副作用:疲倦、口乾、噁心、貧血、減少胃口、便祕、嘔吐、腹瀉、白血球減少症、淋巴球減少、尿道感染、腹痛、體重下降。
使用前請詳閱說明書、警語及注意事項
僅限醫療專業人士參閱
詳細資訊請掃QR code參閱完整仿單
FA-11366101_20270301

NOVARTIS 台灣諾華股份有限公司
10480 台北市中山區民生東路三段 2 號 8 樓
諾華網站：www.novartis.com.tw
電話：(02) 2322-7777
傳真：(02) 2322-7328

使用前請詳閱產品說明書之警語及注意事項，詳細處方資料備索
北市衛藥廣字第 115040174 號

PLUVICTO® 鐳必妥 注射液
lutetium(177Lu)vipivotide tetraxetan 1,000 MBq/mL

FA-11657466_20260420-20280420

LUTATHERA®

鎦住新希望

為神經內分泌腫瘤病患
精準擊殺腫瘤的新希望



鎦癌平® 注射液 LUTATHERA® (衛部藥輸字第 R00104 號)

適應症： 用於治療成人無法手術切除或轉移性，分化良好 (G1及G2) 且經體抑素類似物 (somatostatin analogue) 治療無效之體抑素受體 (somatostatin receptor) 陽性的胃腸道胰腺神經內分泌腫瘤（Gastroenteropancreatic neuroendocrine tumors, GEP-NETs）。

禁忌： 本品為具放射線藥品，確定或疑似懷孕，或尚未排除懷孕的情況下請勿使用。

警語： 放射線暴露風險、骨髓抑制、繼發性骨髓增生不良症候群及白血病、腎毒性、肝臟毒性、神經內分泌荷爾蒙危象、胚胎-胎兒毒性、不孕風險、與胺基酸溶液相關的高血鉀症、心臟衰竭與代謝性酸中毒。

副作用： 噁心、嘔吐、疲倦、腹痛、腹瀉、高血壓、背痛、腎衰竭、淋巴球減少症、貧血、白血球減少症、血小板減少症、肌酸酐增加、高血糖、GGT 增加、鹼性磷酸酶升高、AST 增加、ALT 增加、高血糖、高尿酸血症、低血鉀症。

▶ 詳細資訊請掃 QR code 參閱完整仿單

NOVARTIS 台灣諾華股份有限公司
10480 台北市中山區民生東路三段 2 號 8 樓
諾華網站：www.novartis.com.tw
電話：(02) 2322-7777
傳真：(02) 2322-7328

使用前請詳閱說明書、警語及注意事項
僅限醫療專業人士參閱

北市衛藥廣字第 114090073 號
FA-11499290_20270829

GE HealthCare

Built on Trust
Focused on Hearts

MYOVIEW™
(KIT FOR THE PREPARATION OF TECHNETIUM [99mTc] TETROFOSMIN)
衛部藥輸字第 R00110 號

“邁優影” 心臟造影試劑

適應症：心肌灌注造影，以診斷及定位心肌梗塞及心肌功能之評估



GE HealthCare

Integrated Precision Medicine Solutions

從全身腫瘤負荷量化到個人化吸收劑量評估

MIM 核醫診療整合方案

01 治療前影像評估

MIM LesionID™ Pro

AI 協助病灶勾勒

全身腫瘤負荷量化

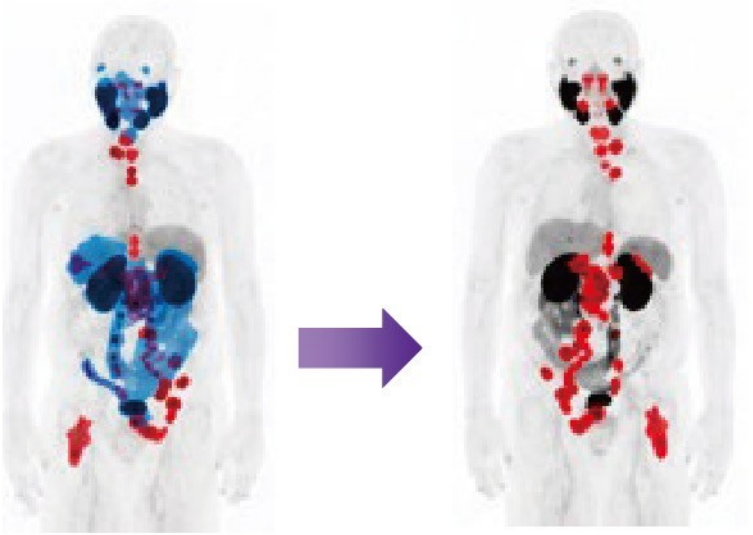

AI 協助分析　　全身腫瘤

自動勾勒病灶、協助排除生理攝取、量化腫瘤負荷

02 治療影像劑量評估

MIM SurePlan™ MRT

整合 SPECT 量化影像

AI 協助器官勾勒與影像融合

評估腫瘤與器官吸收劑量

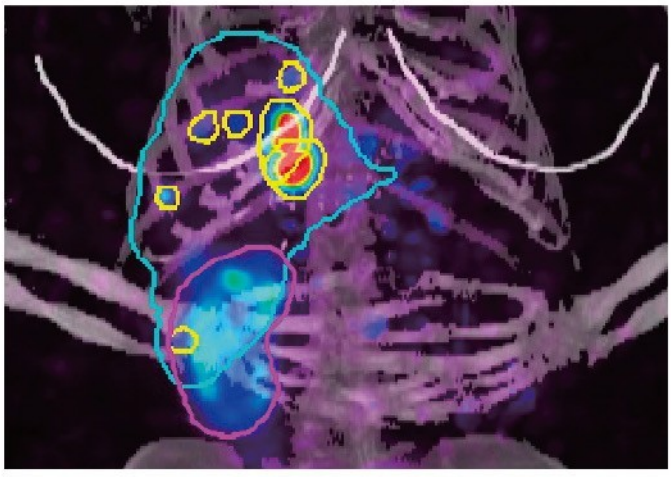

器官與腫瘤劑量分布示意圖

整合影像量化與劑量評估，支持核醫治療

歡迎洽詢 GE HealthCare，了解 MIM 核醫整合方案

產品功能與銷售依當地核准資訊為準。影像示意。